

UNIVERSITÉ DU QUÉBEC À MONTRÉAL
BY EXTENSION FROM
THE UNIVERSITÉ DU QUÉBEC À CHICOUTIMI

HYPOGENE ZINC SILICATES, OXIDES AND SULFIDES IN MESOPROTEROZOIC
GRENVILLE SUPERGROUP MARBLES OF THE BRYSON-RENFREW REGION
(QUEBEC AND ONTARIO): DISTRIBUTION AND GENETIC SIGNIFICANCE

THESIS PRESENTED TO
UNIVERSITÉ DU QUÉBEC À CHICOUTIMI
AS A PARTIAL REQUIREMENT OF THE
DOCTORAT EN RESSOURCES MINÉRALES

BY
JEAN-FRANÇOIS LARIVIÈRE

OCTOBER 2012

UNIVERSITÉ DU QUÉBEC À MONTRÉAL
Service des bibliothèques

Avertissement

La diffusion de cette thèse se fait dans le respect des droits de son auteur, qui a signé le formulaire *Autorisation de reproduire et de diffuser un travail de recherche de cycles supérieurs* (SDU-522 – Rév.01-2006). Cette autorisation stipule que «conformément à l'article 11 du Règlement no 8 des études de cycles supérieurs, [l'auteur] concède à l'Université du Québec à Montréal une licence non exclusive d'utilisation et de publication de la totalité ou d'une partie importante de [son] travail de recherche pour des fins pédagogiques et non commerciales. Plus précisément, [l'auteur] autorise l'Université du Québec à Montréal à reproduire, diffuser, prêter, distribuer ou vendre des copies de [son] travail de recherche à des fins non commerciales sur quelque support que ce soit, y compris l'Internet. Cette licence et cette autorisation n'entraînent pas une renonciation de [la] part [de l'auteur] à [ses] droits moraux ni à [ses] droits de propriété intellectuelle. Sauf entente contraire, [l'auteur] conserve la liberté de diffuser et de commercialiser ou non ce travail dont [il] possède un exemplaire.»

UNIVERSITÉ DU QUÉBEC À MONTRÉAL
EN EXTENSION AVEC
L'UNIVERSITÉ DU QUÉBEC À CHICOUTIMI

GÎTES DE SILICATES, D'OXYDES ET DE SULFURES DE ZINC DANS LES
MARBRES MÉSOPROTÉROZOÏQUES DU SUPERGROUPE DE GRENVILLE DE LA
RÉGION DE BRYSON-RENFREW (QUÉBEC ET ONTARIO) :
DISTRIBUTION ET SIGNIFICATION

THÈSE PRÉSENTÉE À
L'UNIVERSITÉ DU QUÉBEC À CHICOUTIMI
COMME EXIGENCE PARTIELLE
DU DOCTORAT EN RESSOURCES MINÉRALES

PAR
JEAN-FRANÇOIS LARIVIÈRE

OCTOBRE 2012

ACKNOWLEDGMENTS

Firstly, I wish to thank my thesis supervisor, Michel Gauthier, for his patience, his confidence and his continuous support throughout the project. His passion for mineral deposits, his ingenuity and his strong scientific competence enabled me to successfully complete this study. It was an honor to have such a supervisor.

I also thank professor André-Mathieu Fransolet (Université de Liège, Belgium) for his help, his advices and the access to his mineralogy laboratory. His strong knowledge in mineralogy was appreciated. Thanks to Frédéric Hartert (U. Liège, Belgium) for his help with X-Ray diffraction in Belgium.

I thank Serge Perreault (MRNF), Damien Gaboury (UQAC) and Luc Harnois (UQAM) for their advice and for their presence on the scientific committee.

I thank my thesis committee Francis Chartrand, Réal Daigneault (UQAC) and Normand Goulet (UQAM) for their constructive advice on the manuscript.

I thank Richard A. Volkert from the New Jersey Geological Survey for the excellent field-trip he prepared during our visit to the Franklin and Sterling Hill deposits. My thanks also go to Robert W. Megster, former Sterling Hill mine geologist, for our discussions about the Sterling Hill deposit.

A special thanks to Michelle Laithier (UQAM) for her advice, expertise and help with figure creation from poster to individual figures, to Michel Preda (UQAM) for his help and deep experience in X-Ray diffraction and for the many years I worked with him, to Raymond Mineau (UQAM) and Shi Lang (McGill) for the MEB and microprobe analyses and to Frédéric Toupain (UQAM) for his computer support and discussions.

This project was made possible with financial support from NSERC and FQRNT grants. The project has also benefited from financial support from DIVEX.

I thank Gino Roger from Midland Exploration Inc. for his support and for granting me the time necessary to complete this project.

Special thanks to my good friend and field-assistant Éric Hébert for our many discussions and for his help throughout the project.

Finally, I wish to thank to my wife, family and family in-law who supported me all along this project. It is their continuous help and encouragement that motivated me to complete such a project. Again, thank you.

TABLE OF CONTENT

| | |
|--|------|
| ACKNOWLEDGMENTS | i |
| LIST OF FIGURES | vii |
| LIST OF TABLES | xii |
| RÉSUMÉ | xiii |
| ABSTRACT | xiii |
| INTRODUCTION | 1 |
| GENERAL SEDEX-TYPE DEPOSIT REVIEW | 6 |
| GEOLOGICAL CONTEXT OF THE GRENVILLE SUPERGROUP | 9 |
| SECTION I | |
| HYPOGENE SULFIDE ZINC DEPOSITS: BALMAT-TYPE SEDEX..... | 11 |
| CHAPTER I | |
| BALMAT-EDWARDS SEDEX ZINC SULFIDE DEPOSITS | 12 |
| Introduction | 12 |
| Geological Context..... | 12 |
| Zinc Mineralization..... | 15 |
| Stable Isotope Studies | 15 |
| Conclusion | 16 |
| CHAPTER II | |
| MANIWAKI-GRACEFIELD SEDEX ZINC SULFIDE DEPOSITS..... | 17 |
| Introduction..... | 17 |
| Geological Context..... | 17 |
| Zinc Mineralization..... | 18 |
| Chemin-Piché Iron Formation..... | 19 |
| Conclusion | 20 |
| CHAPTER III | |
| CADIEUX SEDEX ZINC SULFIDE DEPOSIT..... | 21 |
| Introduction..... | 21 |
| Geological Context..... | 21 |

| | |
|---|----|
| Zinc Mineralization..... | 22 |
| Stable Isotope Studies | 22 |
| Conclusion | 23 |
| CHAPTER IV | |
| DISCUSSION OF GRENVILLE SUPERGROUP SEDEX ZINC SULFIDE DEPOSITS..... | 24 |
| SECTION II | |
| HYPOGENE STRATIFORM NON-SULFIDE ZINC DEPOSITS: FRANKLIN- TYPE SEDEX..... | 27 |
| CHAPTER V | |
| FRANKLIN AND STERLING HILL DEPOSITS..... | 28 |
| Introduction..... | 28 |
| Geological Context..... | 28 |
| Zinc Mineralization..... | 32 |
| Genetic Model..... | 36 |
| Stable Isotopic Studies | 38 |
| Discussion of the Depositional Environment..... | 40 |
| Conclusion | 41 |
| SECTION III | |
| ZINC SILICATES, OXIDES AND SULFIDES IN THE MESOPROTEROZOIC GRENVILLE SUPERGROUP MARBLES OF QUEBEC AND ONTARIO, CANADA | 43 |
| CHAPTER VI | |
| INTRODUCTION | 44 |
| CHAPTER VII | |
| HISTORICAL GEOLOGICAL WORK..... | 47 |
| CHAPTER VIII | |
| THE BRYSON-RENFREW REGION | 49 |
| Introduction..... | 49 |
| Location and Geological Context..... | 49 |
| Methodology | 51 |
| 8.3.1 Outcrop Characterization | 51 |
| 8.3.2 Sampling for Age Determination of the Calumet Deposit | 54 |
| 8.3.3 Geological Data Compilation and Treatment..... | 55 |
| Results..... | 56 |

| | |
|---|-----|
| 8.4.1 Geological Map of the Bryson-Renfrew Area | 56 |
| 8.4.2 General Geological Map | 57 |
| 8.4.3 General Structural Features..... | 61 |
| 8.4.4 Characterization of Marbles Units | 65 |
| 8.4.5 Other Significant Mineral Occurrences..... | 68 |
| 8.4.6 Zinc Metallogeny | 75 |
| 8.4.7 Age Results for the Calumet Mine Sequence..... | 81 |
| Discussion of the Bryson-Renfrew Region Results | 82 |
| 8.5.1 General Geological Features | 83 |
| 8.5.2 Marbles Features | 85 |
| 8.5.3 Zinc Sulfide Mineralization | 89 |
| 8.5.4 Grenville Supergroup Age Determination..... | 90 |
| 8.5.5 Bryson-Renfrew Geological Environment..... | 92 |
| Conclusion | 93 |
| CHAPTER IX | |
| BRYSON ZINCIAN MAGNETITE OCCURRENCE | 95 |
| Introduction..... | 95 |
| Description of the Bryson Zincian-Magnetite Showing | 95 |
| Conclusion | 96 |
| CHAPTER X | |
| THE BRYSON AREA..... | 97 |
| Introduction..... | 97 |
| Location and Geological Context..... | 97 |
| Methodology | 98 |
| Results..... | 99 |
| 10.4.1 Geological Map..... | 100 |
| 10.4.2 Geological and Structural Features | 101 |
| 10.4.3 Marble Features..... | 103 |
| 10.4.4 Non-Sulfide Zinc Mineralization | 105 |
| Discussion | 114 |
| 10.5.1 The Bryson Geological Environment..... | 115 |
| 10.5.2 Non-Sulfide Zinc Mineralization | 116 |

| | |
|--|-----|
| Conclusion | 116 |
| CHAPTER XI | |
| MINERALOGICAL PROPERTIES OF ZINC SILICATES AND OXIDES FROM THE BRYSON AREA..... | 118 |
| Introduction..... | 118 |
| Methodology | 118 |
| 11.2.1 Sample Selection..... | 119 |
| 11.2.2 Microscope Petrologic Studies..... | 119 |
| 11.2.3 X-Ray Diffraction Studies..... | 119 |
| 11.2.4 Microprobe Studies | 120 |
| Results..... | 120 |
| 11.3.1 Magnetic Zincian Spinel | 120 |
| 11.3.2 Zinc Silicate and Oxide | 122 |
| Discussion | 142 |
| 11.4.1 Magnetic Zincian Spinel | 142 |
| 11.4.2 Zinc Silicate and Oxide | 142 |
| Interpretation of the Bryson Non-Sulfide Zinc Paragenesis | 143 |
| Conclusion | 144 |
| SECTION IV | |
| DISCUSSION OF SEDEX ZINC SULFIDE AND NON-SULFIDE MINERALIZATION IN THE BRYSON-RENFREW REGION..... | 146 |
| CHAPTER XII | |
| GENERAL DISCUSSION | 147 |
| Introduction..... | 147 |
| Bryson: Franklin-Type Mineralization | 147 |
| Bryson-Renfrew: Balmat-Type SEDEX Geological Environment..... | 148 |
| Bryson: The Missing Link Between SEDEX Sulfide and Non-Sulfide Deposits..... | 149 |
| Relationship Between Both End-Members of SEDEX Deposits..... | 151 |
| CONCLUSION..... | 158 |
| APPENDIX A | |
| GEOLOGICAL FEATURES OF BALMAT-TYPE AND FRANKLIN-TYPE SEDEX DEPOSITS | 159 |

| | |
|---|-----|
| APPENDIX B | |
| LOCATION OF DIAMOND DRILLING HOLES USED FOR THE U-PB GEOCHRONOLOGY OF THE NEW CALUMET MINE | 161 |
| APPENDIX C | |
| U-PB GEOCHRONOLOGY OF A SAMPLE FROM THE NEW CALUMET MINE | 163 |
| APPENDIX D | |
| GEOLOGICAL CHARACTERISTICS OF THE BRYSON-RENFREW REGION SEDEX ZINC SHOWINGS | 168 |
| APPENDIX E | |
| DETAILED GEOLOGICAL MAPS OF THE BRYSON-RENFREW SHOWINGS | 171 |
| APPENDIX F | |
| OUTCROP LOCATION AND DESCRIPTION DATABASE..... | 181 |
| REFERENCES | 201 |

LIST OF FIGURES

| Figure | Page |
|---|------|
| 1.1: Classification of Non-Sulfide Zinc deposits by Hitzman et al. (2003)..... | 1 |
| 1.2: Map showing the location of SEDEX sulfide and non-sulfide zinc deposits located in Mesoproterozoic Grenville Supergroup or equivalent marbles in the Grenville Province. Similar terranes localized on this figure and discussed in this thesis are the Maniwaki-Gracefield area in Quebec and the Bryson-Renfrew region (Qc and Ont). Modified from Johnson and Skinner (2003). | 5 |
| 1.3: Distribution of SEDEX zinc sulfide deposits throughout the Grenville Supergroup marbles of the southwestern Grenville Province. The most important example is the Balmat-Edwards district located in the southeastern part of the Grenville Supergroup. The Maniwaki-Gracefield area and the Cadieux deposit are discussed in this thesis and are localized here on this map. Stratiform meta-evaporites associated with these SEDEX deposits (i.e. anhydrite, tourmaline and siderite/magnesite) are reported on this map. Modified from Gauthier and Chartrand (2005)..... | 10 |
| 1.4: Stratiform lavender anhydrite bed observed underground at Balmat-Edwards district. Typical Balmat-type stratiform massive sphalerite is also present on this figure. Zinc mineralization at Balmat-Edwards often occurs in close spatial association with evaporite deposition, as seen on this figure. | 14 |
| 5.1: Distribution of the marble-hosted Franklin and Sterling Hill SEDEX non-sulfide zinc deposits in the New Jersey Highlands Mesoproterozoic terrane after Johnson and Skinner (2003) and Volkert (2004). Modified from Gauthier and Chartrand (2005)..... | 29 |
| 5.2: Stratiform non-sulfide zinc mineralization (willemite-franklinite-zincite) observed along the wall of the Sterling Hill open-pit. | 32 |
| 5.3: Franklin and Sterling Hill ore assemblage of willemite (Si_2O_4) and franklinite ($((\text{Zn}, \text{Mn}^{2+}\text{Fe}^{2+})^{+}(\text{Fe}^{3+}, \text{Mn}^{3+})_2\text{O}_4)$)..... | 33 |

| | |
|---|----|
| 5.4: Franklin and Sterling Hill ore assemblage of zinc silicates and oxides observed under ultraviolet (UV) light. Willemite (Si_2O_4) is characterized by a green fluorescence while manganese-calcite is red. | 34 |
| 5.5: Microscopic features of Franklin and Sterling Hill willemite-franklinite zinc ore observed under a) natural reflected light and b) natural transmitted light. | 35 |
| 5.6: Prograde metamorphic dissociation of a dolomitic mud containing variable proportions of zinc, iron and manganese into willemite, franklinite and zincite. Modified from Squiller and Sclar (1980). | 38 |
| 6.1: Location of the Bryson-Renfrew region in the black rectangle, relatively to the Mesoproterozoic Grenville Supergroup marble belt. Gauthier et al. (1987) discovered zincian magnetic spinel of the franklinite-magnetite solid-solution near the town of Bryson (Qc) and identified on this map by a star. Modified from Gauthier and Chartrand (2005). | 45 |
| 8.1: General geological map compilation of the Bryson-Renfrew region showing the dominance of marbles. Marbles are un-differentiated on this map. Map compiled from our field data combined with those of Lumbers (1982), Osborne (1944) and Katz, 1976). | 58 |
| 8.2: Contact between the gabbro and the marble belt on the Island along the Cadieux dam, near Portage-du-fort. The metasomatic effect of the gabbro intrusion is characterized and restricted to a 10 centimeter-thick pink calcite and calc-silicate fringe. | 59 |
| 8.3: Calcitic marble fragment isolated inside the gabbro intrusion showing the pink calcite metasomatic rim. Picture taken from the Cadieux dam near Portage-du-Fort. | 60 |
| 8.4: Structural map of the Bryson-Renfrew region showing linear trend interpretation from satellite imagery. | 62 |
| 8.5: Example of structural style of polyphase deformation in calcitic marbles of the Bryson-Renfrew area. P1 (blue) isoclinal folds are refolded by P2 (orange). Observed along the Ottawa River at the Chenaux dam, near Portage-du-Fort. View towards the northeast. | 63 |
| 8.6: Classification of the marble units in the Bryson-Renfrew area based on relative proportions of dolomite, calcite and silicates (diopside-forsterite-tremolite): M01: Dolomitic marble, M02: Calcareo-dolomitic marble, M03: Calcitic marble, M04: Silicated calcitic marble, M05: Silicated calcareo-dolomitic marble, M06: Silicated dolomitic marble, M07: Silicate marble. | 65 |
| 8.7: Metallogenic map of the Bryson-Renfrew region showing the distribution of SEDEX mineralization and marble-type. | 68 |

| | |
|---|----|
| 8.8: (a) The road to the Timminco magnesium plant at Haley (Ont), showing the abundance of magnesium in the area. (b) Panoramic view of Timminco's dolomite quarry at Haley viewing to the south. Picture clearly shows the pure dolomitic horizon from which magnesium metal is extracted..... | 69 |
| 9.9: Pure dolomitic marble mined at Haley's Timminco dolomite quarry. Notice the purity of the sample with no traces of silicates..... | 70 |
| 8.10: Panoramic view of Dolomex's rehabilitated dolomite quarry at Portage-du-fort where a silicate-poor dolomitic marble was exploited for industrial mineral and fertilizers purposes. Demonstrate the abundance of pure dolomitic marbles in the Bryson-Renfrew area. | 71 |
| 8.11: Pure dolomitic marble that was exploited at Portage-du-Fort's Dolomex dolomite quarry..... | 72 |
| 8.12: a) The Maxwell stratiform brucitic dolomitic marble quarry at Bryson (Qc). b) Brucitic dolomitic marble sample showing brucite nodules (white) in a silicate-poor dolomitic marble. Surface alteration dissolves brucite and leaves behind cavities indicating where brucite was present. This can be observed on the top-left corner of the figure. | 73 |
| 8.13: Lavender coloured anhydrite in a deep drill hole from the Swamp zone of the Cadieux zinc deposit by Noranda Exploration Inc. | 74 |
| 8.14: Typical semi-massive to disseminated stratiform sphalerite mineralization hosted by a tremolite-forsterite-rich dolomitic marble unit at the Cadieux deposit near Renfrew (Ont). Brown mineral is disseminated sphalerite..... | 76 |
| 8.15: Portage-du-Fort zinc sulfide showing discovered along the dolomite quarry. Disseminated stratabound sphalerite hosted by a silicate dolomitic marble unit. Red coloration is due to the application of Zinc Zap (highlighted in a red dashed line)..... | 77 |
| 8.16: Disseminated stratabound sphalerite mineralization hosted by a silicate-rich dolomitic marble unit in the trenches south of the New Calumet Mine on the Grand-Calumet Island..... | 78 |
| 8.17: Another example of disseminated stratiform sphalerite mineralization hosted by a silicate-rich dolomitic marble unit in the trenches south of the New Calumet Mine on the Grand-Calumet Island..... | 79 |
| 8.18a: Fragmented amphibolite sampled at the New Calumet Mine for radiometric zircon dating. | 81 |

| | |
|---|-----|
| 8.18b: Zircon U-Pb dating results are distributed along a regressed lines. The intersection of this line with Concordia yield an age of $1232.8 \pm 3.9/-2.7$ (Appendix C) (David, 2009)..... | 82 |
| 10.1: Geological map of the immediate area around the town of Bryson(Qc) showing the distribution of non-sulfide zinc occurrences reported. Name and sample number of reported showings is shown on this map..... | 100 |
| 10.2: Magnetic zinciferous spinel and serpentine nodules from Gauthier's et al. (1987) discovery outcrop. Silicate-rich dolomitic marble sample from the road-cut outcrop near the bridge to Grand-Calumet Island at Bryson. | 106 |
| 10.3: Positive Zinc-Zap reaction of the zincian magnetite (Mt) and zinciferous serpentine (Serp) in a pyroaurite-bearing silicate-rich dolomitic marble. Zinc-Zap only applied inside red-dashed lines. Sample from the Bryson bridge to Grand Calumet Island road-cut..... | 107 |
| 10.4: Stratiform zincian magnetic spinel and zinciferous serpentine-bearing dolomitic marble. The one-meter thick horizon is represented by the red dashed-line. Showing located at Bryson's hydroelectric dam. | 108 |
| 10.5: a) Bryson hydroelectric dam stratiform zincian magnetic spinel and zinciferous serpentine-bearing dolomitic marble horizon (Sample 065-B1). b) Zinc Zap reaction of this non-sulfide zinc showing inside the red-dashed line. | 109 |
| 10.6: Close-up of the area near the Bryson hydroelectric dam stratiform zincian magnetic spinel and zinciferous serpentine dolomitic-marble horizon. The horizon was intercepted, along strike, 300 meters to the south behind Hydro-Quebec's gate near the dam. | 110 |
| 10.7: Stratiform zincian magnetic spinel and zinciferous serpentine-bearing dolomitic marble. Extension along strike of Bryson's hydroelectric dam showing, about 300m behind Hydro-Quebec's gate. The green and/or red colourations is due to application of Zinc Zap (green no zinc red zinc is present)..... | 111 |
| 10.8a: Positive Zinc-Zap reaction of the zinciferous serpentine (Serp) in a silicate-rich dolomitic marble devoid of magnetite from the Bryson water treatment plant showing (Sample 013-8A). Zinc-Zap only applied inside red-dashed lines..... | 112 |
| 10.8b: Dolomitic silicate-rich marble horizon from the Bryson water treatment plant showing. A zinc silicate is reacting with Zinc Zap. Sprayed area is outlined in a red dashed line..... | 113 |
| 10.9: Dolomitic silicate and oxide-rich marble horizon from a road-cut outcrop along route 148 near the Bryson's Cadieux power station (Sample 008-9). Zinc Zap sprayed area outlined in a red-dashed line..... | 114 |

| | |
|---|-----|
| 11.1: Aggregate of fine dendritic wurtzite/sphalerite exsolutions in magnetite from the Bryson hydroelectric dam showing (Sample 065-B1). Photo taken under polarized reflected light. | 121 |
| 11.2: Aggregate of fine dendritic wurtzite/sphalerite in a magnetite-bearing dolomitic marble unit from the Bryson hydroelectric dam showing (Sample 065-B1). Photo taken under natural reflected light. | 124 |
| 11.3: X-Ray powder diffractogram of the zincian magnetic spinel from the Bryson hydroelectric dam showing (Sample 065-B1). XRD confirms that the spinel is a magnetite and all the peaks position and intensity relatively match those of the mineralogical database (green lines) (Deer et al., 1992). Data from this diffractogram was used to calculate the cell parameter of this magnetite. | 125 |
| 11.4: Back-scatter microprobe imagery showing dendritic wurtzite/sphalerite exsolutions in a magnetite from the Bryson hydroelectric dam showing (Sample 065-B1). | 126 |
| 11.5: Back-scatter microprobe imagery showing a second example of dendritic wurtzite/sphalerite exsolutions in a magnetite from the Bryson hydroelectric dam showing (Sample 065-B1). | 127 |
| 11.6: a) A relic zincian spinel, of the spinel-gahnite solid-solution, inside a zinciferous serpentine nodule from outcrop 003-1. Observed under natural transmitted light. b) Pyrophanite exsolutions inside the zincian spinel is revealed by observation under natural reflected light. c) Close-up of the zincian spinel relic inside the zinciferous serpentine nodule. | 128 |
| 11.7: Back-scatter microprobe imagery showing zincian serpentine without pyrophanite inclusions from the Bryson water treatment showing (Sample 013-8A). | 129 |
| 11.8: Back-scatter microprobe imagery of a zincian serpentine from the road-cut near the Bryson Cadieux power plant (Outcrop 008-9). The serpentine is zinciferous and also contains inclusions of fine zincian pyrophanite (transitory composition between ecandrewsite-pyrophanite solid-solution). | 130 |
| 11.9: Back-scatter microprobe imagery showing a coarser zincian pyrophanite from the road-cut near the Bryson Cadieux power plant (Outcrop 008-9). | 131 |
| 11.10: Back-scatter microprobe imagery showing a coarser zincian pyrophanite hosted in a zincian serpentine from the road-cut near the Bryson Cadieux power plant (Sample 008-9). | 132 |
| 11.11: Back-scatter microprobe imagery of the zincian spinel (Sample 003-1) confirms the presence of fine pyrophanite exsolutions. | 133 |

LIST OF TABLES

| Table | Page |
|--|------|
| 4.1: Comparaison of the major geologic features of McArthur and Selwyn-subtype SEDEX deposits | 25 |
| 10.1: Geochemical Rock Analyses | 110 |
| 11.1: XRD Data for Lattice Parameter Calculation | 134 |
| 11.2: Electron Microprobe Analyses of Magnetite | 135 |
| 11.3: Electron Microprobe Analyses of Wurtzite/sphalerite..... | 136 |
| 11.4: Debye-Scherrer Camera Data | 137 |
| 11.5: Electron Microprobe Analyses of Serpentine | 138 |
| 11.6: Electron Microprobe Analyses of Serpentine | 139 |
| 11.7: Electron Microprobe Analyses of Pyrophanite | 140 |
| 11.8: Electron Microprobe Analyses of Spinel | 141 |

RÉSUMÉ

Dans une perspective d'avenir pour le développement durable, les gisements de zinc non-sulfurés seront favorisés relativement aux gisements sulfurés conventionnels. Les marbres mésoprotérozoïques du Supergroupe de Grenville ainsi que leurs équivalents dans les terrains grenvilliens exposés au New Jersey contiennent deux types de minéralisations zincifères SEDEX : (1) Les gisements plus communs et compris de zinc sulfuré SEDEX (i.e. district de classe-mondial de Balmat-Edwards, New York), et (2) les gisements hypogènes et stratiformes rares, et moins compris, de zinc non-sulfuré (i.e. gisements de classe-mondial de Franklin et Sterling Hill, New Jersey). La rareté et la localisation isolée des gisements de Franklin et Sterling Hill ne permettent pas d'imaginer une relation entre les gisements SEDEX sulfurés et non-sulfurés de zinc. Cependant, un horizon de marbre contenant un oxyde de zinc est présent près du village de Bryson (Québec), à environ 30 kilomètres au nord du gisement SEDEX de zinc sulfuré de Cadieux (Renfrew, Ontario). La région de Bryson-Renfrew nous offre conséquemment l'opportunité d'étudier la relation pouvant exister entre les deux pôles de minéralisation zincifère SEDEX.

La région de Bryson-Renfrew est caractérisée par (1) une abondance de marbres dolomitiques pures, (2) par la présence d'horizons stratiformes d'anhydrite ainsi que (3) par des niveaux riches en magnésium (i.e. brucite). De telles caractéristiques indiquent une précipitation de carbonates dans un environnement évaporitique peu profond. Ce type d'environnement est typique des gisements SEDEX de zinc sulfuré du type McArthur (i.e. district de Balmat-Edwards). La région de Bryson-Renfrew contient plusieurs indices de zinc sulfuré, associés aux unités de marbres dolomitiques riches en minéraux silicatés. Elle contient aussi plusieurs indices de zinc non-sulfuré également encaissés dans des marbres dolomitiques riches en silicates. Ainsi, les minéralisations SEDEX zincifères non-sulfurés et sulfurés de zinc se forment dans un environnement géologique similaire. Les études pétrographiques sur l'assemblage zincifère non-sulfuré révèlent des exsolutions dendritiques de wurtzite/sphalerite dans des grains de magnétite. De plus, des analyses de diffraction aux rayons-X et à la microsonde révèlent que le silicate zincifère est une serpentine contenant jusqu'à 4.31% de ZnO. D'autres serpentines sont plutôt caractérisées par la présence d'inclusions fines de pyrophanite zincifère ((Fe,Mg,Zn,Mn)TiO₃), une ilmenite zincifère rare mais connue aux gisements de Franklin et Sterling Hill. Les exsolutions dendritiques de wurtzite/sphalerite sont interprétés comme résultant de la déstabilisation rétrograde de la franklinite. De plus, le produit d'altération de la willémitte (Zn₂SiO₄), le principal minéral de zinc aux gisements de Franklin et Sterling Hill, résulte en une serpentine lors d'une déstabilisation métamorphique rétrograde.

Des minéralisations zincifères non-sulfurées de type-Franklin sont ainsi confirmées. Un lien entre les gisements SEDEX zincifères sulfurés et non-sulfurés existe donc puisqu'ils se présentent dans le même environnement géologique. La présence de minéralisations SEDEX zincifères non-sulfurées pourrait de ce fait être expliquée et indiquer la présence d'un système exhalatif à haute température plutôt qu'un système à température moyenne déposant des sulfures de zinc.

Mots-clés: Supergroupe de Grenville, sulfures de zinc, silicates de zinc, oxydes de zinc

ABSTRACT

In a sustainable development perspective, environmentally-friendly non-sulfide zinc deposits will possibly be favored relative to conventional sulfide types. Mesoproterozoic Grenville Supergroup marbles of the Canadian Shield and adjacent outliers in Appalachian uplifted terranes (New Jersey) are characterized by hosting two end-members of hypogene zinc deposits: (1) The better understood and widely distributed SEDEX zinc sulfide deposits (i.e. world-class district of Balmat-Edwards, New York), and (2) the less well understood and much rarer stratiform hypogene non-sulfide zinc deposits (i.e. world-class Franklin and Sterling Hill deposits in New Jersey). The paucity of examples and location of Franklin-Sterling Hill away from other deposits does not permit relationship studies between non-sulfide and SEDEX sulfide zinc deposits to be easily studied. However, the presence of a marble-hosted zinc oxide occurrence near the town of Bryson (Qc), 30 kilometers north of the Cadieux (Renfrew, Ont) SEDEX zinc sulfide deposit, affords a unique opportunity to determine if a relationship exists between both end-members of zinc deposits.

The Bryson-Renfrew region is characterized by (1) an abundance of pure dolomitic marble units, (2) the presence of stratiform anhydrite beds and (3) magnesium-rich (brucite-rich) horizons. Such features are characteristic of a shallow-water, evaporitic and oxidized, carbonate platform geological environment. Such an environment hosts the McArthur-subtype SEDEX zinc sulfide deposits (i.e. Balmat-Edwards district). Stratiform zinc sulfide occurrences and deposits reported in the Bryson-Renfrew region are associated with a silicate-rich dolomitic marble unit. Several new non-sulfide zinc occurrences are also reported around the town of Bryson. Here, stratiform zinc silicates and oxides are associated, once again, with silicate-rich dolomitic marble units. SEDEX zinc sulfide and non-sulfide mineralization thus occurs in the same geological environment.

Ore-microscopy of the non-sulfide zinc assemblage reveals dendritic wurtzite/sphalerite exsolutions inside magnetite grains. X-Ray diffraction and microprobe analysis reveal that the zinc silicate is a serpentine containing up to 4.31% weight ZnO. Other zincian serpentine nodules present fine inclusions of zincian pyrophanite ((Fe,Mg,Zn,Mn)TiO₃), a rare zincian ilmenite also known to occur in the Franklin-Sterling Hill camp. Bryson pyrophanite contains up to 8.91% ZnO. Such assemblages are observed at Franklin and Sterling Hill deposits. Dendritic wurtzite/sphalerite exsolutions are interpreted as retrograde destabilization of granulite-facies franklinite. Moreover, the alteration of willemite (Zn₂SiO₄), the main zinc ore mineral in the Franklin and Sterling Hill deposits, produces a serpentine during retrograde metamorphism.

Franklin-type non-sulfide zinc mineralization is thus confirmed to exist in a marble belt hosting SEDEX zinc sulfide deposits and occurrences. A relationship therefore exists between both end-members of SEDEX deposits because they occur in the same geological environment. SEDEX non-sulfide zinc deposits could indicate the presence of a hot exhalative system operating in a shallow-water evaporitic carbonate environment, rather than a warm one which would rather deposit zinc sulfides.

Keywords: Grenville Supergroup, zinc sulfides, zinc silicate, zinc oxides

INTRODUCTION

New environmental and social considerations have a direct impact on zinc exploration strategy, as reviewed by Sangster (2003). With the continuous need for low-cost zinc resources, environmentally-friendly non-sulfide zinc deposits will be favored relatively to conventional sulfide ones. With advances in hydrometallurgical techniques (i.e. acid-leaching, solvent extraction and electrowinning technology), the economic potential of non-sulfide ores has been greatly enhanced allowing these ores to be possibly envisaged as a major source for zinc in the twenty-first century (Hitzman et al., 2003; Heffernan, 2006). Non-sulfide zinc deposits are generally poor in lead, sulfur and other environmentally deleterious elements and their grades can be higher (>20% Zn) than the majority of their sulfide counterparts.

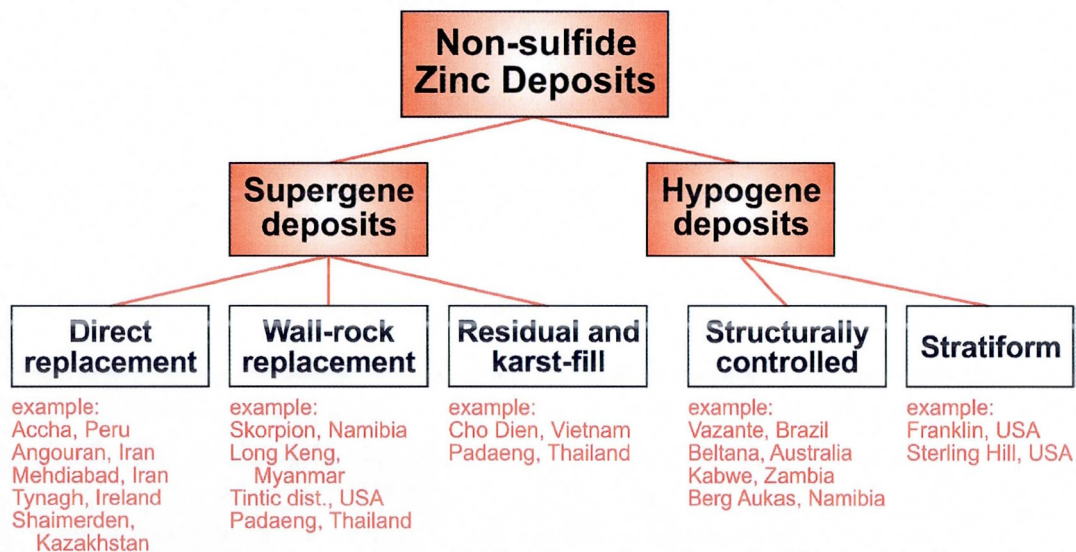


Figure 1.1: Classification of Non-Sulfide Zinc deposits by Hitzman et al. (2003).

A recent classification of non-sulfide zinc mineralization recognizes two major deposit types (Fig. 1.1): (1) The widely distributed and common supergene deposits and (2) the uncommon hypogene deposits (Hitzman et al., 2003). The most important examples of the hypogene-type are Franklin (21.8 Mt at 19.5% Zn) and Sterling Hill (10.9 Mt at 19% Zn) located in marbles of the Grenville Province in New Jersey (Fig. 1.2) (Johnson and Skinner, 2003). The Grenville Supergroup marbles of the Canadian Shield share the same characteristics as those in New Jersey (Johnson and Skinner, 2003).

In this perspective, Mesoproterozoic Grenville Supergroup marbles of the Canadian Shield and correlative adjacent outliers in Appalachian uplifted terranes are of interest because they are characterized by hosting two end-members of hypogene zinc deposits : (1) the more understood and widely distributed sedimentary exhalative (SEDEX) zinc sulfide deposits (e.g. world-class district of Balmat-Edwards (N.Y.) 40.8 Mt at 9% Zn) (deLorraine, 2001) and (2) the more controversial and much rarer stratiform hypogene non-sulfide zinc deposits (e.g. Franklin and Sterling Hill deposits (N.J.)) (Hitzman et al., 2003). The latter group constitutes the world's largest hypogene stratiform non-sulfide zinc-type district with a total of 34Mt of ore grading 20% Zn, 9% Mn and 17% Fe (Fronde! and Baum, 1974; Johnson et al., 1990, Johnson and Skinner, 2003; Hitzman et al., 2003).

The paucity of examples and isolated location of Franklin and Sterling Hill non-sulfide zinc deposits in New Jersey does not permit a clear relationship to be established with conventional SEDEX sulfide zinc deposits (Fig 1.2). Is Franklin and Sterling Hill non-sulfide mineralization an exceptional anomaly in the Grenville Province? Is there a link between non-sulfide and sulfide SEDEX deposits?

Unmetamorphosed carbonate-hosted Zn-Pb sulfide deposits occur throughout the world and geological time, from the Proterozoic SEDEX zinc belt in Australia (McArthur River) (Cooke et al., 2000), to the Paleozoic Irish-type deposits of Ireland (Hitzman and Beaty 1996), and up to the Atlantis II Deep hydrothermal deposits currently in operation in the Red Sea (Pottorf and Barnes, 1983). Unmetamorphosed carbonate-hosted hypogene non-sulfide zinc deposits examples also occur across geological time, from the Proterozoic

Vazante deposit in Brazil (Monteiro et al., 1999), to the Cambrian Beltana deposit in Australia (Brugger et al., 2003), and also under the form of hydroxides exhalites in the Red Sea Atlantis II Deep modern hydrothermal system (Pottorf and Barnes, 1983). Metamorphism of SEDEX zinc sulfide is well documented by Vokes (2000) and Cartwright and Oliver (2000), while metamorphism of hypogene non-sulfide zinc deposits is well studied by Frondel and Baum (1980), Johnson et al. (1990), Johnson and Skinner (2003) and Hitzman et al. (2003). Recent research on stratiform carbonate-hosted Zn-Pb sulfide SEDEX deposits, that contain more than 50 percent of the world's resources of zinc, resulted on a better understanding of the ore forming hydrothermal brines and the subdivision of the SEDEX-type into two sub-types (Cooke et al., 2000). In parallel, new research by Brugger et al. (2003) on the stability of willemite, the main ore mineral of hypogene non-sulfide zinc deposits, suggests that willemite is capable of direct precipitation from hydrothermal brines similar to those found in SEDEX environments. The observation of a willemite-sphalerite intergrowth at the Vazante deposit in Brazil (Monteiro et al., 1999) supports this affirmation and suggests that a continuum could exist between the two types of zinc mineralization. Therefore, could hypogene stratiform non-sulfide zinc mineralization exist in the geological environment of the Grenville Supergroup SEDEX zinc sulfide deposits?

To determine whether or not a relationship between hypogene stratiform non-sulfide and sulfide zinc deposits exists we need to confirm that both types exist in the same marble belt and geological environment. The first part of this study will present a review of the marble-hosted Grenville Supergroup SEDEX zinc sulfide deposits in the light of recent scientific advances in our understanding of the SEDEX deposit-type. We then present a review for the unconventional Franklin and Sterling Hill hypogene non-sulfide zinc deposit-type. These reviews are necessary to properly understand and place each deposit-type in its geological context. The next part of the study presents field work data for the Bryson(Qc)-Renfrew(Ont) area. This data is used to characterize the geological environment and the SEDEX zinc mineralization of this area to permit comparison studies with the Balmat-Edwards district. Further field work, petrologic and geochemical around the town of Bryson, where a non-sulfide occurrence is known, is presented to characterize the mineralogical characteristics of stratabound non-sulfide zinc mineralization. Results are then compared to Franklin and Sterling Hill non-sulfide mineralization. The final section discusses the

significance of the acquired data to determine if a relationship exists between Franklin and Sterling Hill non-sulfide zinc mineralization and Balmat-Edwards SEDEX zinc sulfide deposits.

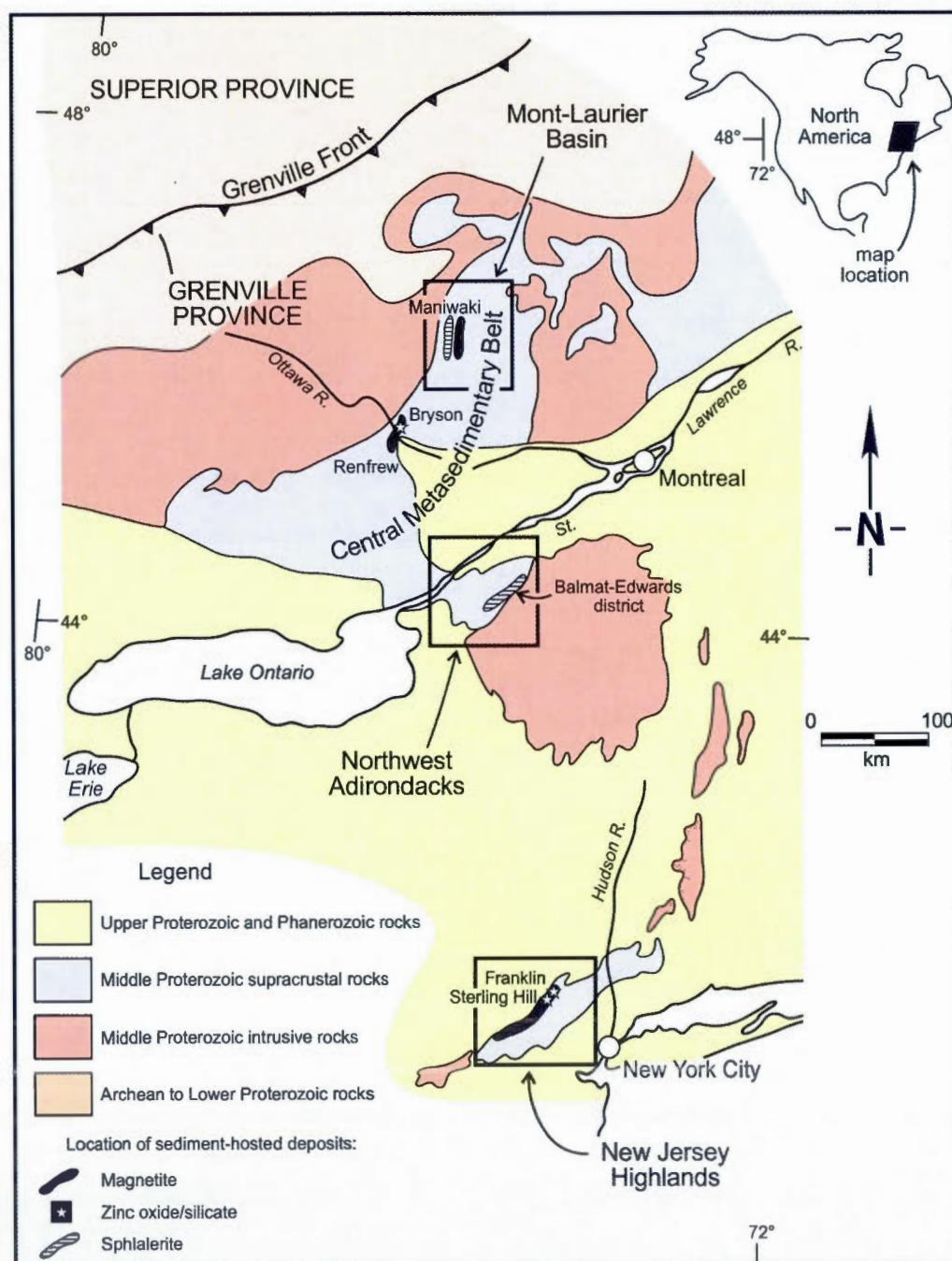


Figure 1.2: Map showing the location of SEDEX sulfide and non-sulfide zinc deposits located in Mesoproterozoic Grenville Supergroup or equivalent marbles in the Grenville Province. Similar terranes localized on this figure and discussed in this thesis are the Maniwaki-Gracefield area in Quebec and the Bryson-Renfrew region (Qc and Ont). Modified from Johnson and Skinner (2003).

GENERAL SEDEX-TYPE DEPOSIT REVIEW

Discovery and acceptance of plate tectonics and sea-floor hydrothermal vents deposits in the 1960s led to the recognition of sedimentary exhalative deposits (Large, 1980). The acronym "SEDEX" was proposed by Carne and Cathro (1982) for these deposits. SEDEX deposits can be simplified as fault-driven metalliferous hydrothermal brines exhaling into sea-floor local sub-basins where the metals precipitation occurs as chemical sediments (Large, 1980; Goodfellow et al., 1993; Lydon, J.W., 1996). Sub-basins in extensional tectonic regime are important for the control of where fluid mixing (i.e. hydrothermal fluid with seawater for example) occurs because it initiates metal deposition (Cooke et al., 2000; Hitzman et al., 2003). SEDEX deposits are known to be hosted by turbiditic shales and also carbonates (Cooke et al., 2000).

Shale-hosted SEDEX deposits are well known in Canada with those of the Selwyn basin in northwestern Canada (total of about 174.1 Mt at 5.6% Zn) and also the Sullivan deposit (170 Mt at 5.5% Zn and 5.8% Pb) in British Columbia (Goodfellow et al., 1993; Lydon, 1996). Carbonate-hosted SEDEX deposits examples are found in the Grenville Supergroup marbles of the Grenville Province (i.e. Balmat-Edwards district). Although the Grenville Supergroup SEDEX zinc sulfide deposits were metamorphosed up to granulite-facies, the SEDEX nature of the deposits is still recognizable (Gauthier and Brown, 1986; Easton, 1992; deLorraine, 2001; Gauthier et al., 2004).

Unmetamorphosed and undeformed Proterozoic equivalents for the Grenville Supergroup SEDEX deposits are the Proterozoic carbonate-hosted SEDEX zinc sulfide deposits in the McArthur River basin (237 Mt at 9.2% Zn and 4.1% Pb) in central northern Australia (Cooke et al., 2000). With the stratigraphically equivalent Mount Isa basin, they host most of the world's known Proterozoic SEDEX deposits (i.e. McArthur River (HYC), Mount Isa, Hilton, George, Fischer, Century, Dugald River and Lady Loretta deposits) and are part of the Australian Proterozoic zinc belt (Cooke et al., 2000). An unmetamorphosed

Paleozoic analogue would be the Irish-type stratabound carbonate-hosted zinc deposits exemplified by the world's major zinc district of the Irish Zinc-Lead Orefield (including the world-class Navan deposit with over 70Mt of ore grading 10% Zn and 2.6% Pb, and also Lisheen, Silvermines, Galmoy and Tynagh deposits) (Hitzman and Beaty, 1996). A modern example of a SEDEX zinc sulfide ore is the Red Sea Atlantis II Deep that is still operating today (Pottorf and Barnes, 1983). There, metalliferous brines pools in axial rifts are depositing zinc ore mainly under its sulfide form, sphalerite. The Atlantis II Deep contains 1.8Mt of ore at 2.06% Zn (Pottorf and Barnes, 1983; Nawab, 1994; Scholten et al., 2000).

Hypogene non-sulfide zinc deposits are represented by a small number of deposits recognized throughout the world (i.e. Vazante in Brazil, Beltana in Australia, Berg Aukas in Namibia, Franklin and Sterling Hill, etc.) and these deposits dominantly contain willemite or a willemite-franklinite-zincite assemblage (Hitzman et al., 2003). While only Franklin and Sterling Hill are stratiform hypogene deposits in the above examples, they share certain genetic features with the other deposits that are structurally controlled. It is more a matter of where the hydrothermal zinc bearing fluid mixed with another fluid and/or rock unit (Hitzman et al., 2003; Brugger et al., 2003). Franklin and Sterling Hill deposits were affected by granulite-facies metamorphism (Johnson et al., 1990) but unmetamorphosed non-sulfide zinc deposits examples exists. Notably, the Vazante deposit in Brazil (28.5 Mt at 18% Zn), currently the nation's main zinc producer, consists mainly of hypogene willemite hosted by an unmetamorphosed Proterozoic carbonate sequence (Montiero et al., 1999; Montiero et al., 2006). Willemite is intergrown with sphalerite at Vazante suggesting that they coprecipitated (Monteiro et al., 1999). This feature is shared among other non-sulfide zinc deposits such as Berg Aukas (Namibia) and Kabwe (Zambia) with mineral assemblage ranging respectively from willemite-(sphalerite) to sphalerite-(willemite) (Hitzman et al., 2003). This suggests that a mineralogic and geochemical continuum may exist between the deposit types (Hitzman et al., 2003). A Cambrian unmetamorphosed hypogene non-sulfide zinc deposit example is the Beltana deposit in southern Australia. The Beltana epigenetic deposit occurs within a dolomite rock unit and is willemite dominant (no sulfides) (Groves et al., 2003; Brugger et al., 2003; Hitzman et al., 2003). Hitzman et al. (2003) suggests that the closest analogue for stratiform non-sulfide mineralization could be the Langban stratiform manganese and iron deposit in Sweden. This deposit-type is believed analogue to stratiform mixed oxide-sulfide

submarine accumulations of the Atlantis II Deep deposits in the Red Sea (Pottorf and Barnes, 1983; Hitzman et al., 2003).

So, unmetamorphosed SEDEX zinc sulfide and non-sulfide zinc deposits examples are known and are well documented in the literature. However, high grade metamorphism is present in the Grenville Supergroup and adjacent outliers in New Jersey.

Metamorphism of SEDEX zinc sulfide deposits is documented (Vokes, 2000 and references therein) from subgreenschist to granulite facies. In central northern Australia, adjacent to the McArthur basin, the stratigraphically equivalent Mount Isa basin has a strong southeast-trending metamorphic gradient from subgreenschist to amphibolite facies which permitted to study the metamorphism of carbonate-hosted SEDEX zinc deposits (Pietsch et al., 1991; Cooke et al., 2000). The Studies by Cartwright and Oliver (2000) on the Mount Isa and Broken Hill zinc-lead deposits (Australia) indicates that the formation of massive zinc-lead deposits, such as those in Australia, during regional metamorphism should be rare because of the moderately low salinities of most metamorphic fluids. Therefore, while secondary zinc-lead concentration during metamorphism may occur, evidence points toward a premetamorphic syngenetic or diagenetic origin for the zinc ores, such as observed at the Broken Hill and Mount Isa orebodies (Large et al., 1996).

Metamorphism of non-sulfide zinc deposits is discussed by Hitzman et al. (2003), Squiller and Sclar (1980) and Johnson et al. (1990). Willemite is the dominant mineral present in hypogene non-sulfide zinc deposits (i.e. Vazante, Beltana, etc.) and has been commonly associated with metamorphism (Hitzman et al., 2003). However, recent research on SEDEX deposits ore forming fluids (Cooke et al., 2000) and on willemite stability in hydrothermal environments (Brugger et al., 2003) brings new insights on the formation of sulfide and non-sulfide zinc deposits and raises the possibility that a relationship between the two deposits could exists.

GEOLOGICAL CONTEXT OF THE GRENVILLE SUPERGROUP

Mesoproterozoic Grenville Supergroup marble-hosted zinc deposits are part of the Grenville Province which forms the southeastern part of the Canadian Shield. The Grenville Province can be considered as an orogenic belt that developed on the southeastern margin of Laurentia during the Proterozoic (Rivers, 1997). Replacing the original expression "Grenville Series" described by Logan (1863), the Grenville Supergroup represents the metasedimentary and metavolcanic units which characterize the Central Metasedimentary belt (CMB) as defined by Wynne-Edwards (1972). This Mesoproterozoic supracrustal sequence occupies the southwestern part of the Grenville Province (Fig. 1.2) and consists mainly of a succession of gneisses and marbles with minor amphibolites, metavolcanics, quartzites and calc-silicate rocks (Easton, 1992). Marbles are an important constituent of the Grenville Supergroup (Davidson, 1998). High metamorphic grades (from local greenschist up-to granulite facies) and polyphase deformation characterize the Grenville Supergroup (Easton, 1992) and resulted from a continent-continent type collision during the Grenvillian orogeny at about 1.1 Ga (Rivers et al., 2002).

The northwestern margin of the Grenville Supergroup, where SEDEX zinc sulfide zinc deposits occur, is characterized by thick sequences of dolomitic and calcitic marbles dominating the stratigraphy with abundant quartz arenites and minor metavolcanics (Easton, 1992). Dolomitic marbles locally contain preserved stromatolites (where deformation such as shearing was limited) which imply a shallow-water depositional environment (Easton, 1992). Moreover, meta-evaporites are locally observed and are characterized by thick stratiform anhydrite beds (Brown and Engel, 1956; Brown, 1973). Sulfur isotope studies on anhydrite occurrences, notably in the Balmat-Edwards district and in Ontario, confirm the evaporitic nature (δS^{34} consistently highly positive) and thus an origin from direct precipitation of marine sulfate (Brown, 1973; Whelan et al., 1990). The dolomitic marble units also host the numerous stratiform SEDEX zinc sulfides of the Grenville Supergroup (e.g. Balmat-Edwards district, Cadieux and Maniwaki) (Fig. 1.3) (deLorraine, 2001; Easton, 1992; Gauthier and

Brown, 1986). The depositional environment is therefore characterized by a metamorphosed shallow-water evaporitic carbonate platform. More detailed geological setting for the zinc deposits will occupy the following sections of the paper.

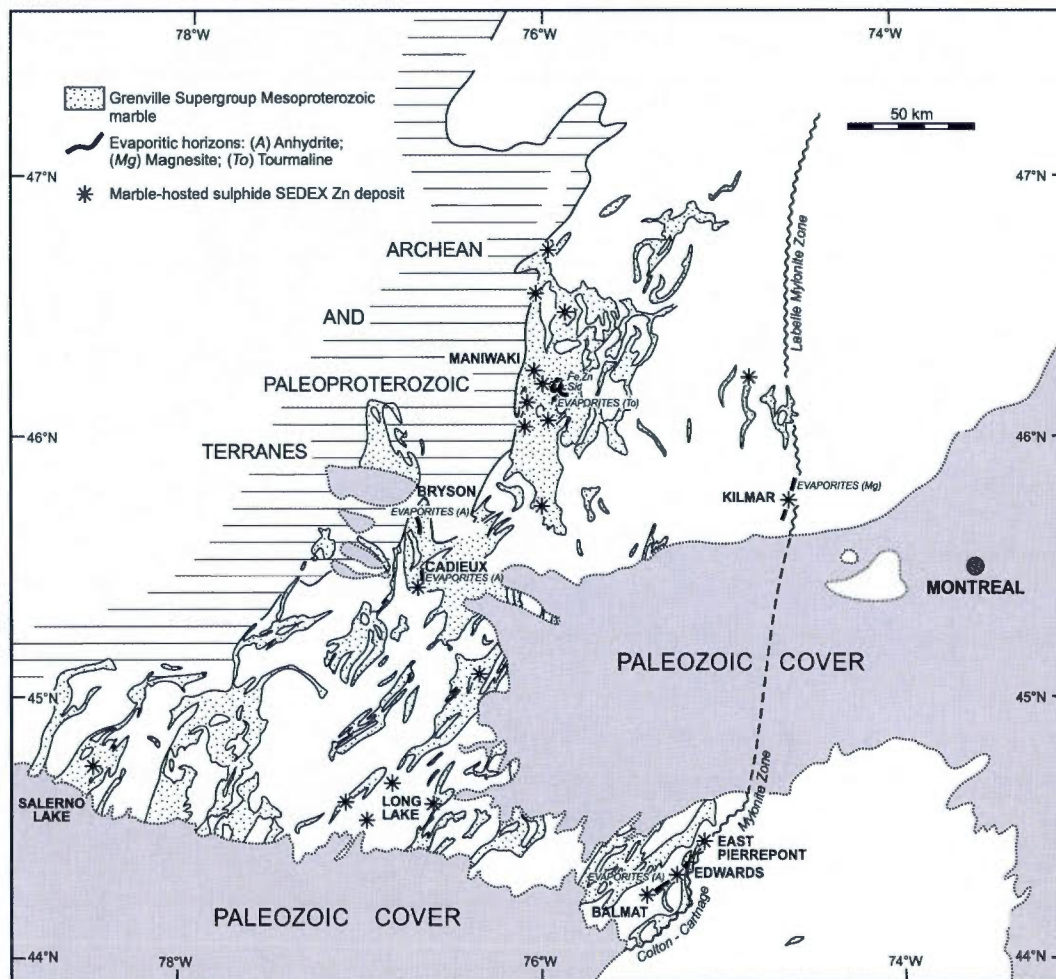


Figure 1.3: Distribution of SEDEX zinc sulfide deposits throughout the Grenville Supergroup marbles of the southwestern Grenville Province. The most important example is the Balmat-Edwards district located in the southeastern part of the Grenville Supergroup. The Maniwaki-Gracefield area and the Cadieux deposit are discussed in this thesis and are localized here on this map. Stratiform meta-evaporites associated with these SEDEX deposits (i.e. anhydrite, tourmaline and siderite/magnesite) are reported on this map. Modified from Gauthier and Chartrand (2005).

SECTION I

**HYPOGENE SULFIDE ZINC DEPOSITS:
BALMAT-TYPE SEDEX**

CHAPTER I

BALMAT-EDWARDS SEDEX ZINC SULFIDE DEPOSITS

1.1 INTRODUCTION

As mentioned earlier, the best known, the most important and longest commercially producing SEDEX zinc sulfide mines in the Grenville Supergroup are the Balmat-Edwards zinc orebodies with past production and reserves totaling 40.8 metric tonnes (Mt) at grades of 9.4% zinc (deLorraine, 2001). This zinc mining district began production at the Edwards mine in 1908 and continued on other zinc deposits until 2008.

1.2 GEOLOGICAL CONTEXT

The Balmat-Edwards district is located in the Adirondack Lowlands. The Adirondack lowlands form part of the southern extension of the Grenville Province and the Grenville Supergroup of Canada and are underlined by marbles, calc-silicate rocks and subordinate paragneiss and metavolcanic rocks of upper amphibolite grade (deLorraine, 2001). Although the Adirondack Lowlands are transected by several major lineaments and fault zones, detailed mapping revealed that specific stratigraphic markers exist among the fault-bounded-panels, thus permitting construction of a regional sequence (deLorraine, 2001). Regarding this regional sequence, deLorraine (2001) points out that apparent structural discontinuities exists between some of the major formations and proposes that the section may reflect lithotectonic stacking rather than a true stratigraphic sequence.

The basement of the Adirondack Lowlands, and the structurally lowermost recognized rock unit, is a leucogranitic gneiss named the Hyde School Gneiss that has been reinterpreted as intrusive in origin by McLelland et al. (1992). Overlying this basement is the

Lower Marble Formation composed mainly of calcitic, locally graphite-bearing, marbles. The Popple Hill Gneiss, a migmatitic gneiss of overall dacitic composition structurally overlies these marbles (Carl, 1988, deLorraine, 2001). The Upper Marble Formation, also referred to as the Balmat-Edwards marble belt, occurs at the stratigraphic top. The zinc deposits occur in this marble belt which is characterized by Mesoproterozoic pure dolomitic and siliceous dolomitic marble units, including meta-evaporites and stromatolitic-bearing strata (deLorraine, 2001).

The Grenvillian orogeny (1130 to 1170 Ma) resulted in polyphase deformation of the metasedimentary rocks of the Adirondack Lowlands with metamorphic grades reaching upper amphibolite facies. At Balmat, temperatures reached 640°C based on calcite-dolomite geothermometry (Whelan et al., 1984). At least four phases of deformation are recognized. First-phase deformation occurred at metamorphic peak conditions, defining the dominant regional foliation. It is characterized by intrafolial isoclinal folds with a well-developed axial planar foliation. The second phase of deformation produced the region's dominant northeast-trending fold structures (deLorraine, 2001). It is characterized by isoclinal folds refolding early isoclines and their axial-planar foliation. The best example of second-phase folds is the Sylvia Lake syncline between Balmat and Edwards where the zinc deposits of this district occur (deLorraine, 2001). Third-phase folds are more or less coaxial with second phase folds and locally produced crescent-and hook-shaped interference patterns. Finally, phase four is characterized by regional-scale inflections of northwest trending folds. Although polyphase deformation occurred in the Balmat-Edwards district, the presence of intercalated stratigraphic marker beds enabled Brown and Engel (1956) to decipher the detailed stratigraphic column of the Upper Marble formation, and revealing the stratiform nature of the zinc deposits.

In the Balmat-Edwards district area, marbles have a thickness of approximately 1000 meters (Brown and Engel, 1956; deLorraine, 2001). The detailed stratigraphic column for the Upper Marble Formation or Balmat Marble belt is characterized by a dominance and alternation of nearly pure dolomitic marbles with siliceous dolomitic marbles distributed throughout 16 units (Brown and Engel, 1956). These 16 units will not be individually described in this thesis. Coarse-grained grey to white dolomitic marble containing more than

95% dolomite characterizes approximately half of the units. They are generally not mineralized and silicate poor. Four units are characterized by dolomitic marbles rich in fine diopside-forsterite layers (Brown and Engel, 1956), and these silicate-rich marbles host the zinc mineralization (deLorraine, 2001). Noteworthy is the fact that stromatolites were identified in the Balmat-Edwards stratigraphic sequence (Isachsen and Landing, 1983). Stratiform anhydrite layers are present through the dolomitic marble and siliceous dolomitic marble units. Medium-to coarse-grained lavender anhydrite forms from 50 and up to 100% of these horizons and were demonstrated to be meta-evaporite layers (Whelan et al., 1990). Anhydrite thickness varies from 1 to 60 meters (Brown and Engel, 1956; Whelan et al., 1990).

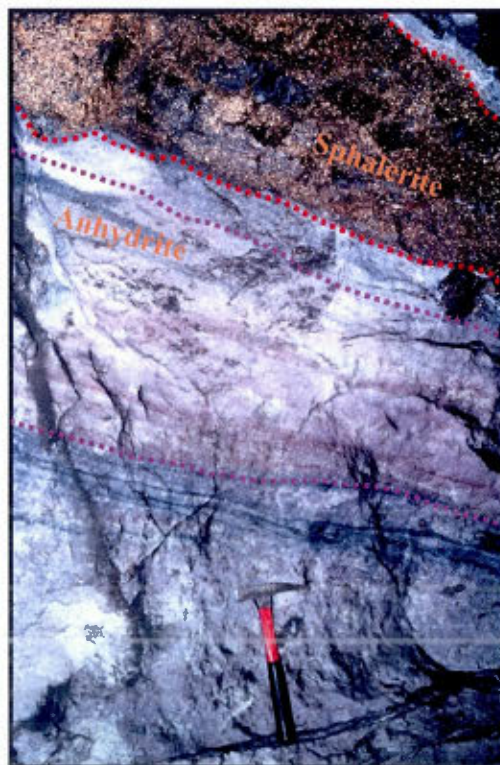


Figure 1.4: Stratiform lavender anhydrite bed observed underground at Balmat-Edwards district. Typical Balmat-type stratiform massive sphalerite is also present on this figure. Zinc mineralization at Balmat-Edwards often occurs in close spatial association with evaporite deposition, as seen on this figure.

1.3 ZINC MINERALIZATION

Zinc sulfide mineralization is present as stratiform massive to semi-massive lenses hosted by silicate-rich dolomitic marble units (Fig 1.4). While non-stratiform zinc mineralization is also present, it is known that these correspond to structural features due to Grenvillian deformation and that the pre-metamorphic nature of the deposit is stratiform (deLorraine, 2001). These cross-cutting sulfide remobilizations are explained by the "Mother-daughter" model of deLorraine (2001), where "daughter" remobilizations are linked to a "Mother" source bed (stratiform sphalerite deposit). This led deLorraine (2001) to conclude that three primary ore forming cycles are present in the Balmat sequence, rather than six or eight. Meta-evaporites are also spatially associated with the ore forming cycles (Fig 1.4) (Whelan et al., 1990). Zinc mineralization consists mainly of coarse-grained sphalerite grains deposited and is in close spatial association with an evaporitic layer (Fig. 1.4) (deLorraine, 2001).

1.4 STABLE ISOTOPE STUDIES

Stable oxygen and sulfur isotopic data from the Balmat-Edwards district reveal key features for the geological environment in which the hydrothermal brines were deposited.

A stable oxygen isotopic study of the carbonates hosting the Balmat-Edwards deposits was conducted by Whelan et al. (1990). Oxygen isotopes were preferred because in a restricted basin, evaporation fractionates the two stable oxygen isotopes O^{16} and O^{18} because it is easier to evaporate the lighter O^{16} isotope rather than the heavier O^{18} . With time and following this fractionation pattern, the basin seawater is gradually enriched in O^{18} because O^{16} is taken out of the system by evaporation (Rollinson, 1993). Therefore, high O^{18}/O^{16} ratios indicate an arid evaporitic environment. The stable oxygen isotopic signature of the dolomitic marbles hosting the Balmat-Edwards deposits is O^{18} -enriched with values ranging from 22.6 to 26.6 per mil (Whelan et al., 1990). This records an arid climate and evaporation in a restricted shallow-water basin.

The sulfur isotopic data of anhydrite indicates that anhydrite layers were deposited in an isolated evaporation basin that was the site of accumulation of highly saline brines and extensive bacterial sulfate reduction (Whelan et al., 1990). The stratigraphic isotopic record

at Balmat shows a significant increase in δS^{34} from the bottom to the top of the anhydrite lenses (Whelan et al., 1990). Brine formation results from the evaporation of seawater at basin surface. As evaporation proceeds, the denser brine settles at the bottom of the restricted basin, stagnates and becomes anoxic. These conditions are ideal for bacterial sulfate reduction. Isotopic fractionation occurs during bacterial sulfate reduction; sulfate reduction of S^{32} demands less energy and is faster than the reduction of S^{34} in the conversion of sulfate H_2SO_4 (oxidized state) to H_2S (reduced state) (Whelan et al., 1990). Therefore S^{32} is preferably converted in H_2S relatively to the isotope S^{34} . This results in brines enriched in S^{34} relatively to S^{32} because S^{34} is preferably left in the brine. Anhydrite precipitated from such hypersaline brines will be enriched in S^{34} and have a high δS^{34} isotope signature. Sulfides (i.e. sphalerite and pyrite) are formed by the combination of metal (iron and/or zinc) with reduced sulfur (H_2S) and are brought in the system by hydrothermal activity. Thus, the more metals are available, the more H_2S is combined to form sulfides and the less S^{32} stays in the system. This is the effect of rising the δS^{34} ratios of the deposited anhydrite and sulfides because the system becomes more and more enriched in S^{34} , resulting from a restricted evaporation basin.

Hydrothermal activity can thus amplify and/or accelerate the increase of S^{34} of the sulfate in the dense brine by providing metals for the extraction of bacterially produced H_2S . Hydrothermal activity might also promote anhydrite precipitation by slightly rising the basin water temperature (Whelan et al., 1990).

Stable isotopic data demonstrates that the Balmat-Edwards deposits were formed in a shallow-water evaporitic carbonate platform environment. The high δO^{18} signature of carbonates and the high δS^{34} signature of anhydrite and sulfides from the Balmat-Edwards district record such an environment.

1.5 CONCLUSION

Balmat-type SEDEX zinc deposits can therefore be characterized by zinciferous hydrothermal brines deposited in a shallow water evaporitic carbonate platform environment. The zinc mineralization consists in sphalerite. The mineralization is stratiform and spatially associated with anhydrite beds. Dolomitic silicate-rich marble (diopside and forsterite) hosts the zinc mineralization.

CHAPTER II

MANIWAKI-GRACEFIELD SEDEX ZINC SULFIDE DEPOSITS

2.1 INTRODUCTION

SEDEX zinc sulfide deposits also occur in Grenville Supergroup marbles of the Mont-Laurier basin in southwestern Quebec. These deposits were studied and considered to be comparable to Balmat-type deposits by Gauthier and Brown (1986) and have been historically the target of many exploration companies. A significant deposit is the Leitch deposit with 75 000 t of ore grading 8% zinc (Gauthier and Brown, 1986). Even today, high grade zinc deposits are actively being explored for in the sector, thus demonstrating the continuing potential for Balmat-type deposits in this marble belt. The deposits and showings are located in the northwestern extension of the Grenville Supergroup along its western boundary, more than 300 km north of the Balmat-Edwards district (Fig. 1.3). This marble belt is Mesoproterozoic in age and directly comparable to the marble belt present at the Balmat-Edwards district (Gauthier et al., 1986).

2.2 GEOLOGICAL CONTEXT

In this area Balmat-type stratiform SEDEX zinc sulfide mineralizations occur in a 50 by 30 square kilometer area around the town of Maniwaki (Quebec) (Gauthier and Brown, 1986). The geological environment of the Maniwaki-Gracefield SEDEX deposits consists of calcitic and dolomitic marbles that form part of the Median Marble Formation, as defined by Gauthier and Brown (1986). The marbles are underlain by a locally rusty and graphitic quartzitic paragneiss, itself in contact with amphibolites (Gauthier and Brown, 1986). Biotite

paragneiss overlay the Median Marble Formation (Gauthier and Brown, 1986; Gauthier et al., 1987). Polyphase deformation and granulite-facies metamorphic conditions affected the Maniwaki area (Indares and Martignole, 1984). While, most primary features of the country rocks were obliterated by dynamo-metamorphic effects, primary bedding is still preserved in the marble units (Gauthier et al., 2004). Polyphase deformation resulted in isoclinal P1 folds being refolded by P2 open fold plunging towards the northeast (Gauthier and Brown, 1986). Thickening at fold hinges and stretching of fold flanks are characteristic structural features of the area.

The Maniwaki-Gracefield SEDEX zinc deposits are hosted by silicate-rich dolomitic marbles. Marble units with low silicate content are zinc-poor or not mineralized. In fact, the zinc deposits are closely associated with an increase in silicate content in the dolomitic marble (Gauthier and Brown, 1986). Mineralization occurs in coarse grained diopside-forsterite (up-to 40%) dolomitic marbles. While calcitic marbles dominate the Grenville Supergroup in Quebec and Ontario, dolomitic marbles constitute an important part of the Maniwaki area stratigraphy. This abundance of thick dolomitic marble sequences reflects that it resulted from the metamorphism of dolostone formed in a pre-metamorphic magnesian shallow water depositional environment (Gauthier and Brown, 1986). Moreover, tourmaline horizons, rich in boron, are sporadically found throughout the area. Stable isotopic studies conducted on these tourmalines confirm that they formed in an evaporitic environment (Nantel, 1994).

2.3 ZINC MINERALIZATION

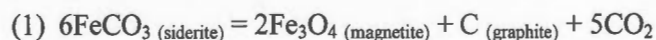
Zinc sulfide mineralization in the Maniwaki area is stratiform and consists of massive, semi-massive and disseminated coarse-grained sphalerite found at the contact between silicate-rich dolomitic marbles and a quartzitic-diopsidic rock unit. The zinc mineralization is characterized by an increase in silicate and magnesium in the dolomitic marble unit. An increase in the diopside-forsterite content is an exploration guide towards greater concentrations of sphalerite (Gauthier and Brown, 1986). There is a vertical zoning profile that characterizes the Maniwaki-Gracefield area mineralizations as follow: The mineralized contact grades from a silicate-rich dolomitic marble containing disseminated sphalerite devoid of iron sulfides into a massive sulfide horizon, followed by massive

sphalerite mineralization which is then overlain by a pyrrhotite-pyrite-rich diopside bearing quartzite (hanging wall) (Gauthier and Brown, 1986). Therefore, massive SEDEX zinc sulfide mineralization of the Maniwaki area is restricted to the contact between a dolomitic carbonate platform and a thick pelitic sequence as suggested by the presence of biotite paragneiss.

2.4 CHEMIN-PICHÉ IRON FORMATION

However, where zinc and iron mineralization occurs without the reduced overlying clastic rock unit, an iron formation is observed instead. In fact, magnetite-graphite-breunnerite (iron-rich magnesite)-forsterite zinc sulfide bearing iron formations are regionally present and associated with the SEDEX zinc deposits (Gauthier et al., 2004). Named the Chemin Piché iron formation, this lithology forms a continuous stratiform 50 centimeter-thick horizon hosted by dolomitic marble (Gauthier et al., 2004). Zinc is present as a disseminated sphalerite horizon in an adjacent underlying dolomitic bed. The geochemical profile of this iron formation shows an enrichment in magnesium and silica towards the top of the stratigraphic sequence (Gauthier and Brown, 1986; Gauthier et al., 2004), as demonstrated by the appearance of diopside and forsterite resulting from the addition of silica in the pre-metamorphic environment. During metamorphism at granulite facies, dolomite reacts with quartz to form diopside and forsterite (Pomeral et al., 2000; Winter, 2001). The Chemin Piché iron-formation is interpreted to be a stratigraphically equivalent distal horizon to the SEDEX sulfide zinc deposits of the Maniwaki area (Gauthier et al., 2004). The iron formation and SEDEX deposits are therefore related.

The pre-metamorphic nature of this iron formation would be a siderite-rich carbonate bed. With granulite facies metamorphism, magnesium-rich siderite reacts with silica to form the magnetite-breunnerite-forsterite-graphite assemblage observed today. The prograde dissociation reaction is as follow:



The presence of iron formation as a distant equivalent to the SEDEX zinc sulfide deposits indicates that an iron halo surrounds the deposits.

2.5 CONCLUSION

The Maniwaki-Gracefield SEDEX zinc sulfide deposits units are in many ways comparable to those observed at Balmat-Edwards. Like those of Balmat-Edwards district, the zinc deposits in Quebec are stratiform, grade from disseminated to massive and consist of sphalerite-rich ore which is poor in other metals such as copper and lead. Furthermore, zinc mineralization occurs in siliceous dolomitic marble units that deposited in a shallow-water evaporitic carbonate platform environment. The high magnesium content of the marble and the presence of tourmaline-rich layers is suggestive of formation in an evaporitic basin. Therefore, the Maniwaki-Gracefield zinc sulfide deposits are SEDEX in origin and are hosted by a similar to Balmat-Edwards geological environment.

CHAPTER III

CADIEUX SEDEX ZINC SULFIDE DEPOSIT

3.1 INTRODUCTION

In the Bryson-Renfrew area, another SEDEX zinc sulfide deposit is known to occur. The Cadieux deposit is located in Mesoproterozoic Grenville Supergroup marbles south of the Maniwaki-Gracefield SEDEX zinc sulfide deposits (central-western part of the CMB) 7 kilometers south of the town of Renfrew (Ont) (Fig. 1.3). The Cadieux deposit was first discovered in 1922 and sporadically worked by various companies including Breakwater Resources Ltd. Later exploration work by Noranda Exploration in the 90s increased resources from 750 000t of ore grading 10% zinc to 1.5 Mt of ore grading 9% zinc (Roger and Lapointe, 1998). The Cadieux deposit is the most important SEDEX zinc sulfide deposit in the southeastern part of the Grenville Supergroup of Ontario (Easton, 1992).

3.2 GEOLOGICAL CONTEXT

The geological environment of the Cadieux deposit is characterized by a dolomitic-calcitic marble belt bounded by siliceous clastic metasedimentary rocks to the northwest and granitic rocks to the southeast (Lumbers, 1982; Easton, 1992; Roger and Lapointe, 1998). The Grenville Orogeny produced polyphase deformation with metamorphic grades reaching upper greenschist to amphibolite in the Renfrew region (Easton, 1992). As is the case in the Maniwaki-Gracefield area, while metamorphism and deformation obliterated the primary features of most lithology-types, bedding can still be observed in the marble sequence due to the reactive nature of marbles during prograde metamorphism (Gauthier and Brown, 1986).

Regional-scale variations of sedimentary and diagenetic facies appear to be easier to recognize than local features which have been obliterated by anatexis, folding, boudinage and transposition (Easton, 1992).

The Cadieux deposit is hosted in dolomitic marbles in a similar way to the Balmat-Edwards SEDEX zinc deposits (Soever and Meusy, 1987; Easton and Fyon, 1992). Mineralization is hosted in a tremolite-diopside-rich dolomitic marble, which corresponds to a metamorphosed siliceous dolostone unit. Tremolite and diopside are coarse-grained (millimetric to centimetric) and represent up to 40% of the volume of the marble unit. Dolomite crystals are also coarse-grained and enclose minor amounts of interstitial calcite (less than 2%). A key feature of the stratigraphic column at Cadieux is the presence of a lavender anhydrite layer associated with the deposit. This anhydrite layer is stratiform, metric in scale and interpreted as a meta-evaporite layer. This anhydrite layer at the Cadieux deposit can only be observed in drill cores completed by Noranda Exploration Inc. because of the rapid dissolution of meta-evaporites by surficial waters (Roger and Lapointe, 1998). Thus, the depositional environment of the Cadieux deposit is a dolomite-dominated carbonate evaporitic platform shelf, like the one found in the Balmat-Edwards district.

3.3 ZINC MINERALIZATION

The zinc mineralization at the Cadieux deposit is closely associated with the silicate-rich (tremolite-diopside) dolomitic marble unit. The Cadieux zinc deposit is characterized by stratiform disseminated zinc sulfide mineralization which consists of coarse-grained dark colored sphalerite (ZnS) crystals. Noteworthy is the fact that iron sulfides (i.e. pyrite and pyrrhotite) are not abundantly associated with the mineralization, rendering the geophysical characterization of the deposit difficult (Chouteau et al., 2005).

3.4 STABLE ISOTOPE STUDIES

Stable sulfur isotopic studies were conducted on the Cadieux deposits in the 90s. Results have shown that δS^{34} isotopic data from sphalerite varies from -2.5 per mil to high (>10 per mil) δS^{34} values (Easton, 1992). High δS^{34} values are characteristic of a few zinc sulfide deposits, most notably those of the Balmat-Edwards district (Brown, 1973; Easton, 1992; Whelan et al., 1984).

3.5 CONCLUSION

The Cadieux deposit features are consistent with those of a SEDEX zinc sulfide deposit. Zinc sulfide mineralization is stratiform, hosted by a silicate-rich dolomitic marble unit, stratigraphically associated with meta-evaporites and has a stable sulfur isotopic signature typical of Grenville Supergroup SEDEX deposits. Thus, the Cadieux deposit is considered to be a SEDEX zinc sulfide deposit similar to those of the Balmat-Edwards district. Furthermore, the pre-metamorphic depositional environment of the deposit consists of a shallow water evaporitic carbonate platform environment, similar to the environment proposed for the Balmat-Edwards district.

CHAPTER IV

DISCUSSION OF GRENVILLE SUPERGROUP SEDEX ZINC SULFIDE DEPOSITS

The marble-hosted stratiform zinc sulfide deposits of the Grenville Supergroup are SEDEX-type. They are characterized by stratiform sphalerite mineralization hosted in silicate-rich dolomitic marbles deposited in a shallow water evaporitic carbonate platform. However, these are not the features of classic SEDEX deposits which are hosted by siliclastic turbidites. The genetic model used to characterize these zinc sulfide deposits was based on shale-hosted deposits such as those of the Selwyn Basin in northwestern Canada or Rammelsberg in Germany (Large, 1980). Exploration guidelines and the genetic model for the SEDEX zinc sulfide deposits of the Grenville Supergroup were designed accordingly (Gauthier and Brown, 1986; de Lorraine, 2001). Since the 1990's, the Australian Proterozoic zinc belt has emerged as the world's largest SEDEX district, an ore deposit type that now represents more than 50% of the world's reserve of lead and zinc (Cooke et al., 2000). Recent research by the Australian Mineral Research Association (AMIRA) resulted in a division of the SEDEX deposits into two subtypes: Selwyn-type deposits and the new McArthur subtype, exemplified by the McArthur deposit in Australia (Cooke et al., 2000) (Table 4.1). Which type of SEDEX corresponds to the zinc deposits found in the Grenville Supergroup?

Selwyn sub-type SEDEX deposits are characterized by deep-water basin and are dominated by carbonaceous siliclastic turbidites. The best example for this sub-type is the Selwyn basin in northern Canada (Cooke et al., 2000). Selwyn-type SEDEX are also characterized by reduced high temperature ($>200^{\circ}\text{C}$) brines deposited in a reduced basin and are not associated by a distal iron halo. On the other hand, McArthur-type SEDEX deposits are characterized by warm ($<200^{\circ}\text{C}$) oxidized hydrothermal brines deposited in an oxidized

shallow water carbonate evaporitic platform. Furthermore, a distal iron halo is associated with the zinc deposits (siderite-rich beds) (Cooke et al., 2000).

Table 4.1: Comparison of the major geologic features of McArthur and Selwyn-subtype SEDEX deposits¹

| | McArthur-subtype | Selwyn-subtype |
|-----------------------------------|---|---|
| Basin stratigraphy | Broad carbonate evaporite platforms (shallow marine to lacustrine) | Dominated by carbonaceous siliclastic turbidites |
| Carbonates | Commonly underlie the deposits; carbonate is also an important component in the mineralized environment | Mostly absent |
| Redox state of the fluid | Oxidized ($\text{SO}_4^{2-} > \text{H}_2\text{S}$) | Reduced ($\text{H}_2\text{S} > \text{SO}_4^{2-}$) |
| Temperature | Moderate to low ($>200^\circ\text{C}$) | Moderate to high ($>200^\circ\text{C}$) |
| Depositional mechanisms | Reduction, interaction with H_2S reservoir | Temperature decrease, pH increase, dilution |
| Fe carbonate halo (i.e. siderite) | Present | Absent |

¹ Modified from Cooke et al. (2000).

Grenville Supergroup SEDEX zinc sulfides deposits are hosted by metamorphosed carbonates that were deposited in a shallow water, evaporitic, carbonate platform-shelf environment. The following features support this affirmation: (1) the presence of anhydrite (meta-evaporite) layers at the Balmat-Edwards district and the Cadieux deposit, (2) the

omnipresence of dolomitic marbles associated with these deposits, (3) the presence of evaporitic boron in tourmalines of the Maniwaki-Gracefield area and (4) the results of stable oxygen and sulfur isotope studies on anhydrite and sulfides at the Balmat-Edwards district. Moreover, stromatolites were identified and described at the Balmat-Edwards district, thus confirming a shallow water environment. Finally, a distal magnetite-magnesite iron-formation, interpreted as the remnant of a metamorphosed breunnerite (magnesium-rich siderite) horizon (iron halo), is associated with the Maniwaki-Gracefield SEDEX deposits. These features are all characteristics of the McArthur subtype SEDEX deposits and are summarized in Appendix A.

The Grenville Supergroup SEDEX zinc sulfide deposits can therefore be considered to be of the McArthur subtype. Thus, for the purpose of this thesis, Balmat-type SEDEX zinc sulfide deposits are defined as hydrothermal brines deposited in a shallow water evaporitic dolomitic carbonate platform environment. The brines are warm (about $<200^{\circ}\text{C}$) and deposited in an oxidized environment. This carbonate platform was later metamorphosed to granulite facies forming the mineral assemblages described herein throughout the Grenville Supergroup SEDEX deposits.

SECTION II

HYPOGENE STRATIFORM NON-SULFIDE ZINC DEPOSITS: FRANKLIN-TYPE SEDEX

CHAPTER V

FRANKLIN AND STERLING HILL DEPOSITS

5.1 INTRODUCTION

The most important examples of Hitzman's et al. (2003) non-sulfide zinc deposit classification for the hypogene stratiform non-sulfide zinc deposit subtype are the Franklin and Sterling Hill zinc-manganese-iron deposits located in New Jersey (Fig 1.1). These deposits constitute the world's largest known stratiform non-sulfide zinc district with a total of 34Mt of ore grading 20% zinc, 9% manganese and 16% iron (Fronde! and Baum, 1974; Megster et al., 1958; Johnson et al., 1990; Hitzman et al., 2003).

The Franklin and Sterling Hill deposits are also famous among mineral collectors because they host a great diversity of different minerals species. More than 300 minerals were described at both deposits and of these, 65 were first recognized at the deposits and 33 currently have no other known occurrences (Dunn, 1985; Johnson, 1990).

Franklin and Sterling Hill were mined from the beginning of American colonial times (around 1640) until 1954 and 1987, respectively. The Franklin and Sterling Hill deposits were mined to a depth of 370 (Fronde! and Baum, 1974) and 564 meters (Megster, 2001), respectively. A combined total of 6.5 million metric tons (Mt) of zinc was produced by both mines (Johnson and Skinner, 2003). Thus, Franklin and Sterling Hill constitute a world-class zinc deposit district.

5.2 GEOLOGICAL CONTEXT

Franklin and Sterling Hill are located in the New Jersey Highlands, an uplifted tectonic window of a Grenvillian basement outlier exposed in the Appalachian orogenic belt

of the eastern coast of North America (Fig 5.1). The Highlands are therefore part of the Grenville orogenic belt that developed along the southeastern margin of Laurentia during the Proterozoic (Rivers, 1997; Johnson and Skinner, 2003; Volkert et al., 2004). The New Jersey Highlands are located more than 500 kilometers south of southernmost extension of the Grenville Province in New York State (Fig 1.2). The basement of this Grenvillian terrane consists of a remnant of a calc-alkaline magmatic arc which was later deformed, metamorphosed and partially melted during the Grenvillian Orogeny to form leucocratic gneiss, charnockite gneiss and amphibolites (Volkert, 2001; Johnson and Skinner, 2003). These rock units form the Losee metamorphic suite and constitute the oldest rocks of the New Jersey Highlands (Puffer and Volkert, 1991). Overlying the metamorphic basement is a metamorphosed and isoclinally folded supracrustal metasedimentary sequence. This metasedimentary sequence was affected by polyphase deformation and granulite-facies metamorphism from 1.06 to 1.03 Ga (Volkert, 2001). Approximately 2 kilometers thick, the supracrustal sequence dominates part of the New Jersey Highlands (Volkert, 2001).

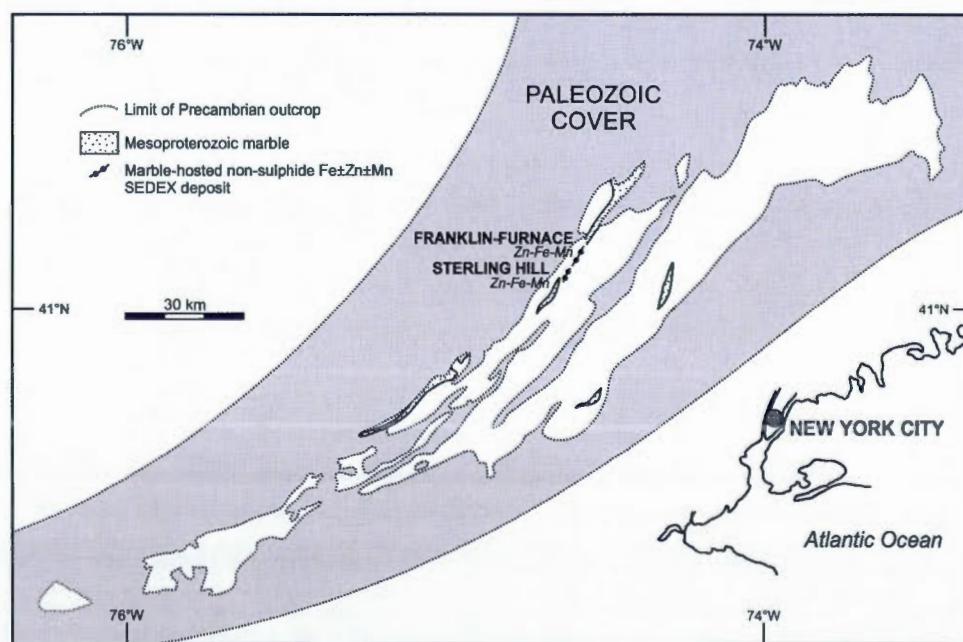


Figure 5.1: Distribution of the marble-hosted Franklin and Sterling Hill SEDEX non-sulfide zinc deposits in the New Jersey Highlands Mesoproterozoic terrane after Johnson and Skinner (2003) and Volkert (2004). Modified from Gauthier and Chartrand (2005).

The stratigraphic sequence of the metasedimentary supracrustal belt can be simplified as a (1) basal quartzofeldspathic metasediment-metavolcanic section overlain by an important series of (2) calc-silicate gneisses and marbles and finally an uppermost section characterized by a (3) quartz-feldspathic metasediment-metavolcanic section. Noteworthy is the fact that the middle series of marbles contains stromatolites and also probable evaporitic horizons (Volkert and Drake, 1999; Volkert, 2001). Differences between the basal and the uppermost metasedimentary-metavolcanic sections are that the sediments of the latter section are less mature and also that the proportion of mafic metavolcanic rock units are higher (Volkert and Drake, 1999). A transition from a shallow-water evaporitic basin to an immature clastic sequence and mafic metavolcanic rock is thought to reflect initiation of basin closure (Johnson and Skinner, 2003). Although no anhydrite-bearing units have been recognized, Kearns (1975;1977) has described boron-rich zones within the marble belt. Such a horizon has also been described in Grenville Supergroup marbles of the Balmat-Edwards district where their interpretations with evaporites is strengthened with the presence of stratiform anhydrite in the sequence (Fronde! and Baum, 1956). Spry et al. (2000) also points out that nearly all boron and tourmaline associated with stratiform deposits are formed by evolved seawater and of marine origin (Swihart and Moore, 1989; Palmer and Slack, 1989).

This supracrustal metasedimentary belt is comparable to the Grenville Supergroup present in Northwestern Adirondacks and in southwestern Quebec, where clastic and carbonate metasedimentary units are observed. As described earlier in section 1, a world-class stratiform SEDEX zinc sulfide district is known to occur in the dolomitic marbles units of northwestern Adirondacks. At Balmat-Edwards, it has been suggested that the sedimentary protoliths were deposited between 1.3 to 1.25 Ga (Rivers, 1997; Hanmer et al., 2000) while ages between 1.18 and 1.10 Ga have been suggested for the New Jersey sequence (Volkert, 2001). This implies a somewhat younger depositional age for the New Jersey Highlands metasedimentary sequence. Nevertheless, the New Jersey metasedimentary belt shares many similarities with the Grenville Supergroup and is considered a distal equivalent (Johnson and Skinner, 2003).

The Franklin and sterling Hill deposits are located within the Franklin marble, a distinctive unit contained in the middle series of the metasedimentary supracrustal sequence

described above. The Franklin marble is subdivided into two units, (1) the Lower Franklin Band, with thickness of 335 to 457 meters, hosts the Franklin and Sterling Hill zinc deposits, and the 91 meter-thick upper un-mineralized Wildcat Band (Hague et al., 1956). The Franklin marble is medium-to coarse-grained, white to light-gray and is calcitic to locally dolomitic. Common accessory minerals include graphite, phlogopite, chondrotite, amphibole and pyroxene (Volkert, 2001). The Franklin deposit occurs in the upper part of the Franklin band while the Sterling Hill deposit occurs in the lower part. Both deposits were subjected to multiple folding events. The Franklin deposit is folded in a hook-shaped synform that plunges 25° to the northeast (Fronde! and Baum, 1974). The Sterling Hill deposit is folded in a similar way, as a hook-shaped synform that plunges 45° to the northeast (Megster, 2001).

The Franklin marble becomes thinner and progressively interlayered with pelitic clastic metasedimentary units towards the east of the New Jersey Highlands. This indicates basin deepening from shallow water to deeper water to the east (Volkert, 2001).

The Franklin marble belt shares many similarities with the marble belts of the Grenville Supergroup in Canada and northwestern New York State. Both marble belts were subjected to polyphase deformation and granulite-facies metamorphism. Furthermore, both marble belts exhibit shallow-water features as well as the presence of evaporitic horizons. However, both marble belts are isolated by more than 500 kilometers of Paleozoic cover. The Franklin marble belt is dominated by calcitic marbles whereas the Balmat-Edwards district is dominated by dolomitic marbles. Now that the geological environment of Franklin and Sterling Hill was summarized and shown to be similar in many ways to the one present at Balmat-Edwards district, the characteristics of the unusual ore will be described in the following sub-section.

5.3 ZINC MINERALIZATION

The Franklin and Sterling Hill deposits are noteworthy because the zinc ore is composed of zinc silicates and oxides rather than sulfides. The uncommon and exotic ore mineral assemblage is composed of willemite (Zn_2SiO_4), franklinite ($((\text{Zn}, \text{Mn}^{2+}, \text{Fe}^{2+}) + (\text{Fe}^{3+}, \text{Mn}^{3+}))_2\text{O}_4$) and zincite (ZnO) (Fig. 5.2, 5.3, 5.4, and 5.5) rather than sphalerite (ZnS), which is the common and well-known constituent of zinc deposits. Moreover, the Franklin and Sterling Hill deposits are zinc-rich and poor in lead and copper (Johnson et al., 1990), which also seems to be a feature of the Grenville Supergroup SEDEX

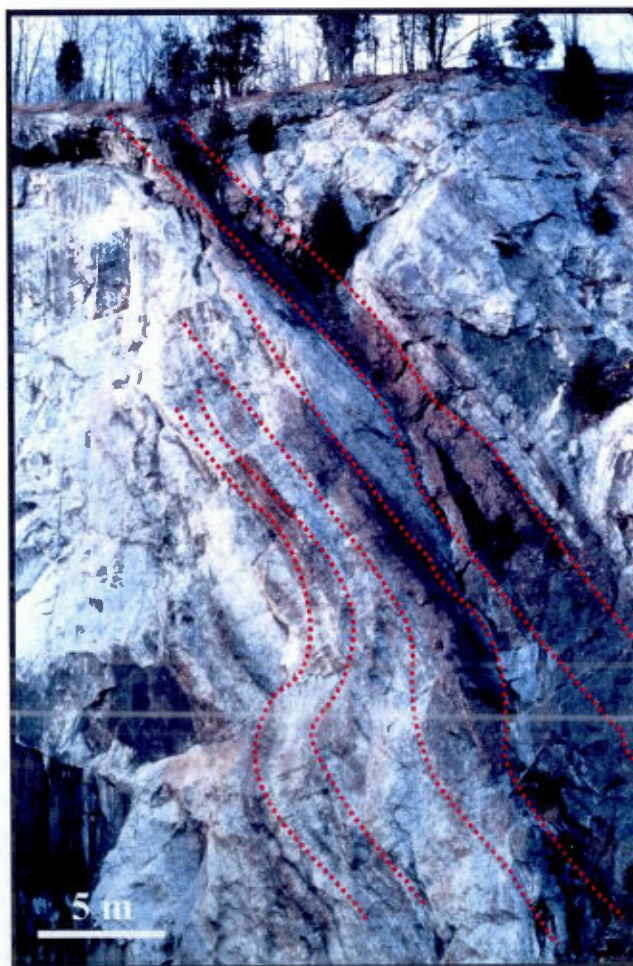


Figure 5.2: Stratiform non-sulfide zinc mineralization (willemite-franklinite-zincite) observed along the wall of the Sterling Hill open-pit.

zinc deposits (i.e. Balmat-Edwards, Maniwaki, etc.; Gauthier and Brown, 1986; deLorraine, 2001).

Layers rich in willemite-franklinite-zincite that characterize both deposits are stratiform (Fron del and Baum, 1974; Megster, 2001; Johnson et al., 1990; Johnson and Skinner, 2003). The evidence for the stratiform nature of the deposits comes from detailed structural studies which indicate that the ore bodies were composed of a continuous strata characterized by the same isoclinal folding pattern and mineral lineation (Fron del and Baum, 1974; Megster, 2001). Furthermore, mineralogical studies indicate that high temperature minerals characteristic of granulite-facies metamorphism are present. The Franklin and Sterling Hill deposits were metamorphosed to granulite-facies conditions before undergoing retrometamorphism (Johnson, 1990). Finally, geochemical studies on minerals have shown that there were little or no variations in composition along the strata while important chemical differences occur across the bedding (Squiller and Sclar, 1980).



Figure 5.3: Franklin and Sterling Hill ore assemblage of willemite (Si_2O_4) and franklinite ($((\text{Zn}, \text{Mn}^{2+}\text{Fe}^{2+})(\text{Fe}^{3+}, \text{Mn}^{3+})_2\text{O}_4)$).

Although the Franklin marble contains graphite as an accessory mineral, there is no graphite present near the zinc ore. In fact, a two meter thick graphite-free halo surrounds the

zinc deposits. This phenomenon was also observed at the Ducktown stratiform exhalative massive copper sulfide deposit in southeastern Tennessee (Nesbitt and Kelly, 1980). During prograde metamorphism, which reached granulite facies, sulfide ore bodies interact with their surroundings as oxidizing agents, which is the opposite of what workers would intuitively think. While it is true that sulfides form in a reducing environment, during metamorphism they can act as an oxidizing mass and oxidize any near graphite grains (Nesbitt and Kelly, 1980). The same phenomenon is observed at Balmat-Edwards where graphite-free zones envelope the massive sulfides ore horizons.

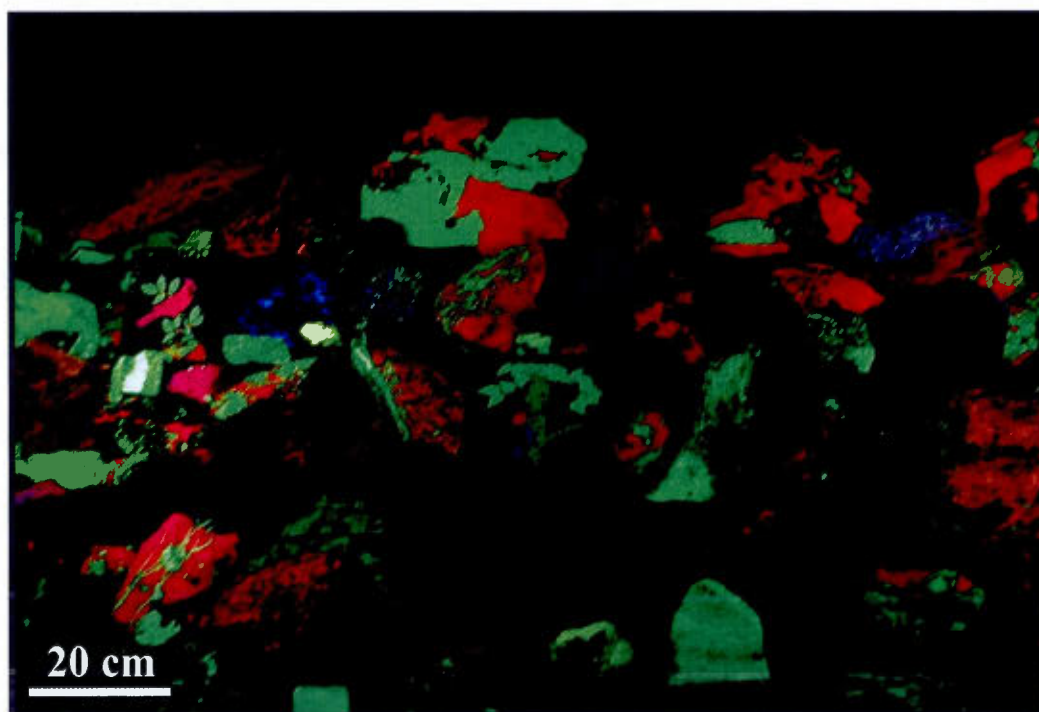


Figure 5.4: Franklin and Sterling Hill ore assemblage of zinc silicates and oxides observed under ultraviolet (UV) light. Willemite (Si_2O_4) is characterized by a green fluorescence while manganese-calcite is red.

Franklin and Sterling Hill deposits can therefore be considered as stratiform marble-hosted willemite-franklinite-zincite layers that occur in a Grenville Supergroup equivalent supracrustal belt. The stratiform and geochemical features of the deposits suggest a premetamorphic origin for the zinc ore. Moreover, the depositional environment for these non-sulfide zinc deposits is a shallow water carbonate platform environment with probable

evaporitic boron-rich layers. The origin and genesis of Franklin and Sterling Hill will be discussed in the following section.

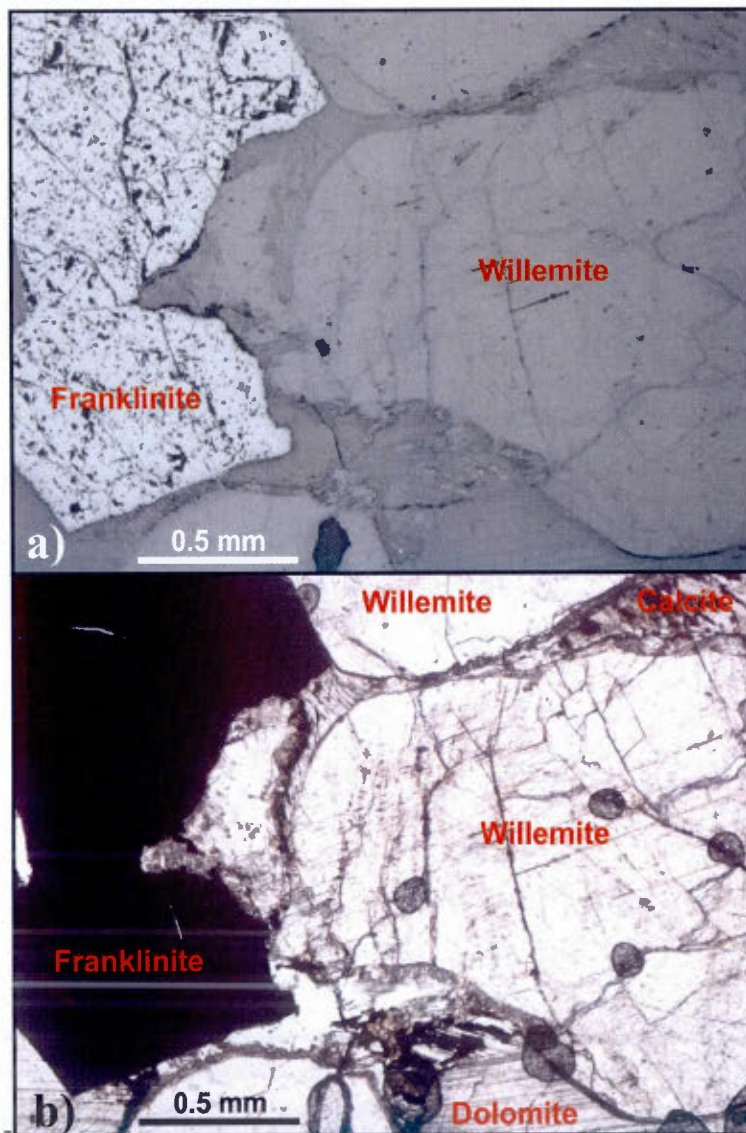


Figure 5.5: Microscopic features of Franklin and Sterling Hill willemite-franklinite zinc ore observed under a) natural reflected light and b) natural transmitted light.

5.4 GENETIC MODEL

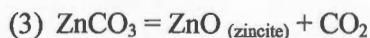
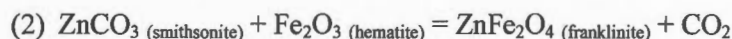
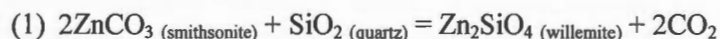
The origin of Franklin and Sterling Hill stratiform non-sulfide zinc deposits is very controversial and has been extensively debated for many years. A genetic model has to explain the many features observed at the deposits, such as the exotic zinc ore mineralogy which can reach very high zinc grades (average of 20% and reaching locally up to 40% (Fron del and Baum, 1974; Megster 2001)) relatively to classic SEDEX zinc sulfide deposits. Moreover, the metal assemblage ($Zn > Fe > Mn$) is quite uncommon when compared to other deposits. Until recently, Franklin and Sterling Hill were the only locality where willemite-franklinite-zincite stratiform deposits were known. Willemite mineralization is known to occur at the Vazante deposit in Brazil, while it is not stratiform in character but rather structurally-controlled, similarities exists between the deposits (Section V) (Monteiro et al., 1999).

Arguments for the origin of Franklin and Sterling Hill varied considerably from epigenetic and syngenetic hypotheses. The first evidence of discussion on the topic goes back to Rogers (1836). Before the discovery and acceptance of plate tectonics, some workers argued that favorable horizons of the Franklin marble were replaced with non-sulfide ore following a reaction with magmatic fluids (Spencer, 1908; Ries and Bowen, 1922; Pinger, 1950; Ridge, 1952). Others favored a syngenetic model in which the metals were deposited on an ancient sea-floor, or in shallowly buried sediment, in the form of sulfides which were later subjected to oxidization (Wolff, 1903; Tarr, 1929; Palache, 1935) or even under the form of zinc-manganese-iron rich sediments (Callahan, 1966; Megster et al. 1969; Squiller and Sclar, 1980). Fron del and Baum (1974) even suggested that the zinc was volcanically derived.

Johnson and Skinner (2003) states that, following the discovery of sea-floor hydrothermal vents and systems and their associated deposits, in the 1960's, opinion has increasingly swung to the view that Franklin and Sterling Hill deposits were syngenetic in origin and formed by hydrothermal systems operating beneath the floor of the Middle Proterozoic sea (Callahan, 1966; Megster et al. 1969; Squiller and Sclar, 1980). In this case, metal emplacement was either syngenetic or diagenetic. In both cases, because of intense deformation and metamorphism, the primary features required to distinguish both types were

obliterated. Whether the metaliferous brines settled from the water column or whether they formed diagenetically by replacement reactions in shallowly buried sediments remains an open question (Johnson and Skinner, 2003). Either way, the ore would be pre-metamorphic and hypogene in origin.

The most accepted model for the genesis of Franklin and Sterling Hill (Johnson et al., 1990; Johnson and Skinner, 2003) was proposed by Squiller and Sclar (1980). The model would later be further confirmed and adjusted with detailed geochemical and isotopic studies (Johnson et al., 1990; Johnson and Skinner, 2003). It is now mostly accepted by the scientific community that Franklin and Sterling Hill are sedimentary exhalative (SEDEX) deposits. Squiller and Sclar (1980) and Johnson et al. (1990) explain that oxidized hydrothermal brines would have deposited zinc, manganese and iron-rich sedimentary beds mostly in the form of carbonates, clays and hydroxides (Fig. 5.6). Zinc ore was deposited in an oxidized form. Therefore, the main zincian mineral was originally a zinciferous dolomitic carbonate containing various proportions of magnesium, iron and manganese (Squiller and Sclar, 1980; Johnson, 1990). With prograde metamorphism reaching granulite-facies conditions, the smithsonite (zinc carbonate) particule contained in solid-solution in the dolomite grains dissociates into zinc oxide (ZnO). Whether willemite, franklinite or zincite was formed depends of the on-site availability of silicon, manganese and iron. Where silica gel was available and manganese and iron virtually absent, the zinc oxide particle would combine with silica (SiO₂) to form willemite (Zn₂SiO₄)⁽¹⁾. If manganese and iron was abundant on site comparatively to silica gel, franklinite ((Zn,Mn²⁺Fe²⁺)+(Fe³⁺,Mn³⁺)₂O₄) would form⁽²⁾. Finally, if no silica, manganese or iron were present, zincite (ZnO) would form⁽³⁾ (Squiller and Sclar, 1980).



Therefore, the exotic mineralogy which characterizes Franklin and Sterling Hill deposits was formed during granulite-facies prograde metamorphism and subsequent retrometamorphism. Franklin and Sterling Hill are therefore considered of SEDEX origin, like the more common SEDEX zinc sulfide deposits occurring in the Mesoproterozoic Grenville Supergroup marbles, but with zinc silicates and oxides rather than sulfides.

5.5 STABLE ISOTOPIC STUDIES

Stable carbon and oxygen isotopic studies were conducted at Franklin and Sterling Hill deposits and the host Franklin marble belt. The isotopic signature for the deposits and marbles enabled the characterization of the depositional environment for the zinc deposits and to further refine the genetic model.

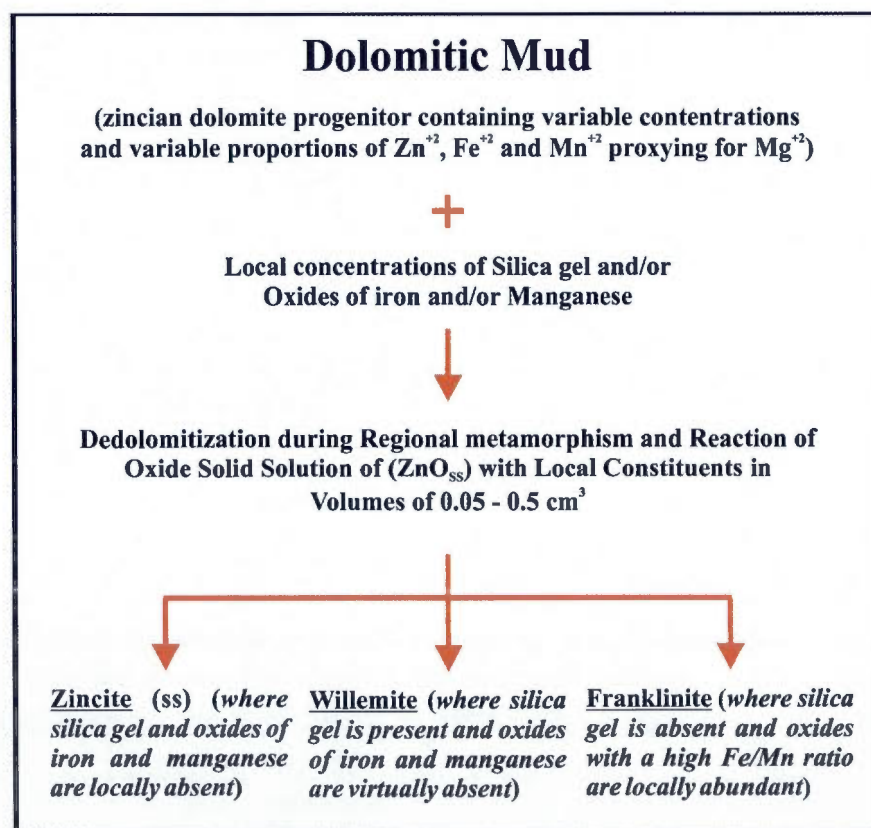


Figure 5.6: Prograde metamorphic dissociation of a dolomitic mud containing variable proportions of zinc, iron and manganese into willemite, franklinite and zincite. Modified from Squiller and Sclar (1980).

An important characteristic of the Franklin and Sterling Hill deposits is that, as stated above for geochemical layer compositions, the isotopic composition of individual minerals varies between lithologic strata while compositions within a stratum are uniform (Johnson et al., 1990). This further confirms the stratiform nature of the non-sulfide zinc ore layers and the syngenetic model.

Stable oxygen and carbon isotopes conducted on the Franklin marble hosting the Franklin and Sterling Hill deposits yielded $\delta^{18}\text{O}$ and $\delta^{13}\text{C}$ signatures comparable to average Mesoproterozoic marine compositions (Veizer and Hoefs, 1976). Thus, the Franklin marble is thought to have accumulated in a marine environment (Johnson and Skinner, 2003). Such an assumption was also inferred for the Grenville Supergroup marbles which also originated from Mesoproterozoic marine environment. Moreover, stromatolites and fluoborite-rich layers probably representing evaporite were also observed near the Franklin and Sterling Hill deposits (Kearns, 1977; Volkert, 2001; Johnson et al., 1990). This is strong evidence of a shallow-water evaporitic carbonate platform environment.

Whole-rock chemical and oxygen isotope compositions completed at the Sterling Hill deposit results consistent with a model protolith composed of carbonate, clay and hydroxide minerals that formed at a temperature of about $150\pm 50^\circ\text{C}$ (Johnson et al., 1990). Some authors suggested that Franklin and Sterling Hill could also have originated from the oxidizing of a pre-existing SEDEX zinc sulfide orebody. Results of oxygen isotopes on the zinc ore revealed a signature enriched in $\delta^{18}\text{O}$ for the hydrothermal fluid (Johnson et al., 1990). With these results, Johnson et al. (1990) argued that the estimated 150°C temperature for the ore bearing fluids was too high for sub-aerial weathering or seawater oxidation. This implies that sulfur-poor zinciferous mineral assemblages precipitated directly from warm metal-bearing hydrothermal brines in a sulfur (H_2S) depleted oxidizing environment (Johnson and Skinner, 2003). The paucity of sulfides minerals within the Franklin and Sterling Hill deposits is strong evidence that the ore bearing fluids were oxidized and H_2S poor. In such an environment, sulfur is rather stable in its oxidized sulfate form and dissolved in seawater.

Another feature present in the Franklin marble, near the non-sulfide zinc deposits, is the presence of stratiform magnetite. Johnson and Skinner (2003) propose that this represents

small iron formations associated with the zinc deposits. These iron formations could be distal equivalent to the zinc deposits, as it has been described at the Maniwaki-Gracefield SEDEX zinc deposits. Johnson and Skinner (2003) propose a similar genetic model for the formation of this distal iron formation. Prograde dissociation of a siderite into magnetite and graphite is discussed by Johnson and Skinner (2003). Results of isotopic studies reveal that metamorphism of a iron oxide-calcite assemblage rather than a decarbonation of siderite would better explain the observed isotopic signature. The evidence supporting this assumption is that prograde dissociation of siderite in magnetite-graphite would shift the oxygen isotopic ratios. In fact, the measured isotopic ratios on the iron formations (Franklin Furnace bed) do not vary according to the dissociation model but are rather consistent with a nearly isochemical metamorphism of a iron-oxide-rich layer (Johnson and Skinner, 2003). The iron formation thus resulted from seawater oxidation of hydrothermally transported iron near a brine conduit and/or on the basin floor at the interface between anoxic deep waters and oxygenated surface waters (Johnson and Skinner, 2003). The presence of an iron-rich halo surrounding a zinc deposit was also a feature described earlier for the McArthur-subtype SEDEX zinc sulfide deposits of the Grenville Supergroup.

Stable oxygen and carbon isotopic studies at the Franklin and Sterling Hill deposits confirmed the hypogene characteristic of the deposit. They also permitted a shallow-water evaporitic carbonate platform environment to be proposed in which a iron-rich halo surrounds the sedimentary exhalative zinc deposits.

5.6 DISCUSSION OF THE DEPOSITIONAL ENVIRONMENT

The depositional environment for the Franklin-type SEDEX non-sulfide zinc deposits shares many features with the McArthur SEDEX sub-type depositional environment (Cooke et al., 2000), describe earlier in this paper. Grenville Supergroup SEDEX zinc sulfides deposits (i.e. Balmat-type) were previously reinterpreted as being of McArthur-subtype rather than Selwyn-subtype. McArthur SEDEX zinc deposits are characterized by warm hydrothermal brines deposited in an oxidized shallow-water evaporitic carbonate platform environment.

Evidence brought forward at Franklin and Sterling Hill describes the depositional environment as a shallow-water evaporitic carbonate platform environment. The hydrothermal ore forming fluids were H_2S poor and oxidized. An iron-rich halo is also present around the zinc deposits (Johnson and Skinner, 2003). These are all features of the McArthur-subtype SEDEX zinc deposits.

Franklin and Sterling Hill are formed by sulfate-stable oxidized metalliferous brines similar to those that form the McArthur-subtype sediment-hosted zinc deposits. Oxidized brines such as these develop in sedimentary dominants by carbonates, evaporates and hematitic sandstones (Cooke et al., 2000). Sulfate-stable brines are characteristically poor in gold, barium and tin owing to the inability of sulfate-bearing brines to transport these metals. This could explain the zinc-rich metal content for the Franklin and Sterling Hill deposits (Johnson and Skinner, 2003). Thus, a key feature of the Franklin and Sterling Hill zinc ores is that metals were deposited in an oxidizing environment where sulfate was stable rather than in a reduced H_2S -stable environment. In contrast, H_2S -stable environments characterize the depositional environment for McArthur-subtype SEDEX zinc sulfide deposits, such as those of the Balmat-Edwards district.

5.7 CONCLUSION

The Franklin and Sterling Hill deposits are therefore hypogene stratiform non-sulfide SEDEX zinc deposits which we will refer to as Franklin-type SEDEX deposits for the purpose of this paper. Franklin-type deposits are characterized by oxidized, sulfate-bearing hydrothermal brines depositing zincian carbonates-clays-hydroxides in an oxidized environment, rather than a H_2S -rich environment which would form zinc sulfides. With prograde metamorphism reaching granulite-facies, the smithsonite particle in the carbonate dissociates into zinc oxide and combines with silica, manganese and iron to form the exotic willemite-franklinite-zincite ore assemblage present at Franklin and Sterling Hill (Fig. 5.6).

The New Jersey Highlands Franklin marble belt shares many characteristics with the Mesoproterozoic Grenville Supergroup marbles. Both are similar in age and formed in a similar tectonic setting. Both marbles belts are shallow-water, evaporitic, carbonate platform environments.

Furthermore, the hydrothermal fluids that form Franklin-type SEDEX deposits share many similarities with Balmat-type McArthur-subtype SEDEX zinc sulfide deposits. Oxidized sulfate-stable brines are deposited in a shallow-water evaporitic carbonate platform. Johnson and Skinner (2003) propose that a difference could be the redox state of the depositional site. Franklin-type deposits would be deposited in an oxidized environment rather than a H_2S stable environment in which SEDEX zinc sulfide deposit are formed.

Further relationship studies between Balmat-type and Franklin-type SEDEX deposits are difficult because they are separated by more than 500 kilometers of Paleozoic cover. Franklin-type deposits are scarce and were only known to occur in New Jersey where they represent the biggest example of hypogene stratiform non-sulfide zinc deposit-type (Hitzman et al., 2003). To facilitate the relationship study between the two end-members of SEDEX deposits (i.e. non-sulfide and sulfide SEDEX zinc deposits), both types have to occur in the same marble belt. The Grenville Supergroup marbles of Quebec and Ontario are similar to those found at Franklin and Sterling Hill and also at Balmat-Edwards district. Moreover, the discovery by Gauthier et al. (1987) of a zincian magnetite in Quebec suggests that there is a potential for Franklin-type deposit in the Grenville Supergroup.

SECTION III

ZINC SILICATES, OXIDES AND SULFIDES IN THE MESOPROTEROZOIC GRENVILLE SUPERGROUP MARBLES OF QUEBEC AND ONTARIO, CANADA

CHAPTER VI

INTRODUCTION

Mesoproterozoic Grenville Supergroup marbles and their widespread zinc sulfide deposits were discussed in section 1 (i.e. Balmat-Edwards district, Cadieux, Maniwaki-Gracefield, etc). This SEDEX zinc deposit-type is characterized by stratiform sphalerite mineralization hosted by a silicate-rich dolomitic marble deposited in a shallow-water evaporitic carbonate platform environment (i.e. McArthur sub-type SEDEX deposit). Grenvillian marbles are also known to host hypogene stratiform non-sulfide zinc deposits (i.e. Franklin and Sterling Hill deposits), as outlined in section 2 and referred to as Franklin-type. The almost unique Franklin-type deposit is characterized as being SEDEX in origin with stratiform zinc silicate and oxides hosted by dolomitic marbles deposited in a shallow-water evaporitic carbonate platform environment.

While Balmat and Franklin-type deposits are both SEDEX in origin, no relationship has ever been proposed to exist between these two types of deposits. However, as reviewed in sections 1 and 2, both end-members of SEDEX deposits occur and form in a similar geological environment (i.e. in a shallow water evaporitic carbonate platform environment). These similar features bring forward the possibility that a relationship could exist between Balmat sulfide and Franklin-type zinc deposits. However, Franklin-type mineralization has only ever been reported to exist in the New Jersey Highlands. This isolated occurrence of exclusively non-sulfide zinc mineralization, more than 500 kilometers south of the Grenville Supergroup, has hindered the study of possible relationship between both types of SEDEX deposits.

However, in a publication about Precambrian iron formations, Gauthier et al. (1987) report the unusual existence of a zincian magnetite horizon near the village of Bryson, in Quebec. This occurrence seems to have mineralogical similarities with Franklin-type mineralization. The Bryson area is located in Grenville Supergroup marbles near the frontier between Quebec and Ontario. This Mesoproterozoic marble belt, which extends from southeastern Ontario and southwestern Quebec, is known to host Balmat-type SEDEX

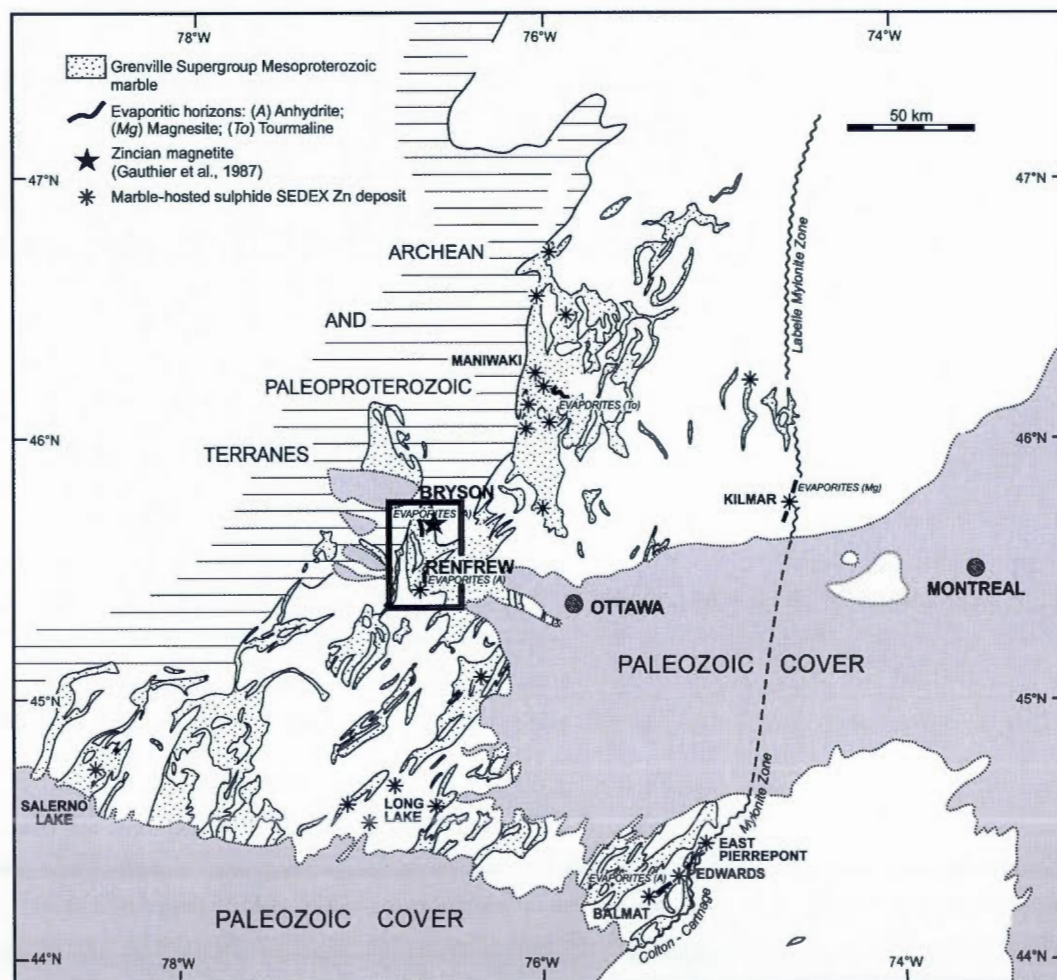


Figure 6.1: Location of the Bryson-Renfrew region in the black rectangle, relatively to the Mesoproterozoic Grenville Supergroup marble belt. Gauthier et al. (1987) discovered zincian magnetic spinel of the franklinite-magnetite solid-solution near the town of Bryson (Qc) and identified on this map by a star. Modified from Gauthier and Chartrand (2005).

deposits (i.e. Cadieux and Maniwaki-Gracefield) (Fig. 6.1). The existence of this mineralization in the Bryson area raises the possibility that there is potential for other Franklin-type deposits outside the New Jersey Highlands.

The discovery by Gauthier et al. (1987) discovery of the Bryson occurrence affords us an opportunity to study (1) the existence of Franklin-type SEDEX non-sulfide zinc deposits in the Grenville Supergroup of Quebec and Ontario, and (2) the relationship between both end-members of SEDEX deposits. Moreover, the Cadieux SEDEX zinc sulfide deposit lies about 30 kilometers south of the town of Bryson. The Bryson-Renfrew region is therefore a unique opportunity to study the possible link between sulfide and non-sulfide SEDEX zinc deposits. Study of this occurrence and its regional geological context is required to conclude if both types of SEDEX deposits occur in the same environment and this is the main objective of the present thesis.

To constrain and establish the coexistence of both end-members of SEDEX deposits in the Bryson-Renfrew region, we will: (1) review available data from previous studies for the Bryson-Renfrew region, (2) report upon geological mapping data for the Bryson-Renfrew region which characterizes the occurring zinc sulfide mineralization and the geological environment hosting them, (3) review, visit and present geological mapping data in the area near Gauthier's et al. (1987) zincian magnetite discovery, and (4) present petrologic and geochemical data used to characterize the Bryson non-sulfide zinc occurrence and demonstrate this mineralization as Franklin-type.

CHAPTER VII

HISTORICAL GEOLOGICAL WORK

Franklin-type non-sulfide zinc deposits are frequently considered to be “exotic” because of their uncommon mineralogy and genesis (Squiller and Sclar, 1980; Johnson and Skinner, 2003). Furthermore they were never considered, nor studied, in another geological environment in relation with other deposit-types, because of the isolated location of its most important examples (i.e. Franklin and Sterling Hill). Therefore, Franklin-type deposits have not been studied, associated and linked with other deposits in past scientific literature. Balmat-type SEDEX zinc-sulfides deposits, on the other hand, are widely spread, common and well understood (DeLorraine, 2001). The objective of this thesis is to complete this “missing link” by finding a new non-sulfide zinc occurrence and to describe its hosting environment and metallogeny.

The Bryson-Renfrew region has never been studied in this regard. The state of geological mapping and data is heterogeneous in the area, due in part to its position straddling the provinces of Quebec and Ontario. Each side of the border were mapped by the respective Provincial government survey during regional mapping campaigns and compilation. The Ontario portion of the area has seen much more geological mapping work (Lumbers, 1982) than the Quebec side, which was surveyed, relatively speaking, at a more regional scale and mostly limited to road/riverside outcrops (Osborne, 1944; Katz, 1976). However, Grand-Calumet Island in Quebec has been mapped in more detail due to the presence of the New Calumet Mine, a volcanogenic polymetallic massive sulfide deposit that will be briefly discussed below (Osborne, 1944). With the greater level of detail available in Ontario, dolomitic marbles were broadly differentiated from calcitic marbles (not the case for the Quebec side), but the silicate mineral phases and the dolomite-calcite ratios of the

marbles were not characterized (Lumbers, 1982). Exploration for zinc deposits also remains very limited in the Bryson-Renfrew area, and was concentrated near the Cadieux zinc sulfide deposit (as described in section 1). Finally, although Noranda Exploration Inc. and Gauthier et al. (1987) rapidly examined the area in the 80s and 90s in the search for zinc deposits, only Gauthier's et al. (1987) Bryson discovery was reported and not considered further because it was not a zinc sulfide occurrence. Therefore, one can easily conclude that from a metallogenic point of view, the area has not been intensively studied.

Thus, the available level of geological data in the Bryson-Renfrew area was inadequate and incomplete for the purpose of this study. A detailed geological mapping campaign was therefore required to refine and unify the geology between Bryson (Qc) and Renfrew (Ont).

CHAPTER VIII

THE BRYSON-RENFREW REGION

8.1 INTRODUCTION

Since the Bryson-Renfrew region provides a unique opportunity to study the relationship between SEDEX zinc and non-sulfide deposits, the first step that must be undertaken is to characterize the pre-metamorphic geological environment of the area and to characterize its zinc mineralization. This will enable us to compare and relate the Bryson-Renfrew region geological environment with the one associated with Balmat-type and Franklin-type deposits.

In order to accomplish this, we will (1) geographically locate the studied area and present its regional geological context, (2) explain the methodology used during the geological campaign, (3) present and discuss the results in order to demonstrate that the Bryson-Renfrew region is characterized by a typical SEDEX geological environment similar to Balmat and Franklin-type.

8.2 LOCATION AND GEOLOGICAL CONTEXT

The Bryson-Renfrew area is located approximately 75 kilometers northwest of the city of Ottawa (Ont). The region extends from the small town of Bryson, in Quebec, to the town of Renfrew (Ontario), 30 kilometers to the south (Fig. 6.1). The region is covered by good ground transportation infrastructures (roads and railways) and crosses the provincial border between Quebec and Ontario. Rugged low to medium topography characterizes the area with small hills and valleys. Flat fields with a thick sediment cover are also present in the central portion of the area where outcrops are scarce.

The Bryson-Renfrew area is located within the Grenville Supergroup which extends from Quebec and Ontario towards northwestern New-York State where the Balmat-Edwards district is located. The studies area is more precisely located in the southwestern portion of the Grenville Supergroup, partly in Quebec. The geological context of the Grenville Supergroup has been discussed in a previous section and can be summarized as a marble-dominated metasedimentary belt that was metamorphosed to granulite-facies and affected by polyphase deformation during the Grenvillian orogeny (1.0 Ga). The Grenville Supergroup rock units covering the regional Bryson-Renfrew region are Mesoproterozoic in age, and is estimated at ~1290-1250 Ma (Rivers and Corrigan, 1999). However, the only available radiometric age available to characterize the upper age bracket for the Grenville Supergroup marble belt of our studied region, comes from the Chenaux gabbro, a stock that intruded the marbles of the Bryson-Renfrew region at about 1100 Ma (Lumbers, 1982).

Known marble-hosted mineral deposits in the area include the Cadieux SEDEX zinc sulfide deposit (Balmat-type) located near the town of Renfrew. Two dolomite quarries were also operational during the early 2000s. A first dolomite quarry, at Haley in Ontario, has been operated by Timminco Metals Inc. since 1944 to extract magnesium metal directly from pure dolomite layers (Easton, 1992). The second quarry, which was located at Portage-du-Fort in Quebec, was mainly used as agricultural fertilizers and as industrial mineral. This quarry was operated by Dolomex and later closed in the mid 2000's by Placer Dome when they acquired the company. There are also broad references to a historical small scale brucite quarry near the town of Bryson (Osborne, 1939). Moreover, Gauthier et al. (1987) discovery of a zincian magnetite is located near the bridge crossing the Ottawa River at the town of Bryson. Other non-marble-hosted mineral deposits occur in the area. An amphibolite-hosted metamorphosed volcanogenic polymetallic massive sulfide deposit, the Calumet Mine, occurs on the western part of the Grand Calumet Island, in the Ottawa River west of the town of Bryson. The discovery of the mine dates to 1893 and it was exploited by New Calumet Mines Limited from 1942 to 1968. A total of 3.8 million tons with an average grade of 5.8% zinc, 1.6% lead, 65 grams-per-ton (g/t) silver and 0.4 g/t gold was extracted during this period (Sangster, 1967). A later re-evaluation of this mining property in 1985 by Lacana Mining Corp. demonstrated that gold mineralization was present in the wall-rock of the deposit mined by the New Calumet Mines Limited (Bishop and Villeneuve, 1987). This gold

mineralization shares many similarities with the Montauban Mine deposit (Bernier et al., 1987; Bishop and Jourdain, 1987; Villeneuve, 1987; Jourdain, 1993), which is located in the Grenville Province of Quebec several hundred kilometers northeast of the Bryson-Renfrew region. However, as opposed to the Montauban deposit, the Calumet deposit is associated with a thin calcsilicate marble horizon hosted by a biotite quartzo-feldspathic gneiss and amphibolite sequence. Although the Montauban volcano-sedimentary sequence was dated at $\sim 1.45 - 1.39$ Ga (Nadeau and Van Breeman, 1994), and the Calumet deposit sequence never dated, Gauthier et al. (2004) assumed that they were of the same age. This hypothesis implies that the Calumet deposit would be much older than the marbles of the adjacent Grenville Supergroup marbles (see above) and would thus represent an underlying basement not associated with the zinc mineralization. Apart from these occurrences and deposits, no other notable mineralization is reported in the Bryson-Renfrew area.

The geological context of the Bryson-Renfrew area is thus similar to the one observed for Balmat-type SEDEX zinc sulfide mineralization. However, further geological data is required to refine and characterize the geological environment of the Bryson-Renfrew zinc deposits. The next section presents our methodology used to achieve this goal.

8.3 METHODOLOGY

The geological environment of the Bryson-Renfrew region was characterized following detailed outcrops description. For this study, a total of more than 500 different outcrops (Appendix F) were studied, enabling us to refine (1) the general stratigraphic column of the area, (2) the general structural characteristics, (3) differentiate seven marbles units and (4) report on known and new occurrences of zinc sulfide mineralization in the study area. Selected samples were collected for the purpose of obtaining a radiometric age for the rock units hosting the Calumet deposit.

8.3.1 Outcrop Characterization

General geological and structural data were collected during field traverses. Road-side and inland traverses were first concentrated in areas where marbles were regionally thought to be present and then extended throughout the Bryson-Renfrew study area. Each outcrop was first systematically described following these steps: (1) Each outcrop was

precisely located using a Global Positioning System (GPS) device and physically described (i.e. width, length and type of outcrop). Aerial photographs and topographic maps were routinely used to verify outcrop positions. (2) The main rock lithology was then macroscopically identified and the overall rock texture was thoroughly described. Classic field equipment (such as a magnifying lens, magnet-pen, ceramic plate, etc.) was used to identify the main lithology and to describe each mineral phase (i.e. mineral type, abundance, grain size, structure). Typical unaltered samples representing a specific lithotype were carefully chosen and brought back to camp for future reference. (3) Structural characteristics were also systematically measured when outcrop quality was adequate. Acquired structural data included stratigraphic plane, foliation, fold hinge plane and plunge, fault plane and shear zone plane when these were available. High metamorphic grades and intense deformation characterizes the Grenville Supergroup in the studied region and it was shown by Gauthier and Brown (1986) and Gauthier et al. (2004) that most primary sedimentary features were obscured. However, extensive geological mapping work in the Balmat-Edwards district by Brown and Engel (1956) has shown that bedding may be recorded by laminated and persistent layers of quartz + diopside. In a similar way, bedding has also been preserved locally inside marbles units of the Maniwaki-Gracefield area (Gauthier and Brown, 1986). A more regional perspective is required to see through the metamorphic overprint. This phenomenon is explained by the plastic and malleable nature of anhydrite ("soap layers") units at high metamorphic grades and the high reactivity of carbonates with other minerals during prograde metamorphism (i.e. prograde reaction of dolomite + quartz = diopside). The best example of salt layer decollement is the Jura decollement where Triassic evaporates accommodates all the deformation (Pomerol et al., 2000). This phenomenon is also observed at Balmat where primary features are locally preserved because the thick anhydrite layers absorb the most of the deformation (Whelan et al., 1990). In fact, this permitted the conservation of Proterozoic stromatolites are observed in the Balmat stratigraphy (Isachsen and Landing, 1983). So, primary stratigraphic structural data was measured inside qualifying marble outcrops. These systematic steps enabled us to characterize the outcrops in the Bryson-Renfrew area and were used to refine the stratigraphic sequence of the region and its structural style. What we observed in the Bryson-Renfrew area is conform to what is observed to the north in the Maniwaki area (Gauthier and Brown, 1986) and to the south by

Lumbers (1982). Furthermore, the general stratigraphy of the area is well established by Lumbers (1982) because metamorphism decreases (to sub-greenschists facies) towards the south in the Ontario Grenville Supergroup. There, primary features are still present (Lumbers, 1982; Easton, 1992). Following metamorphic isograds, as defined by Barrow (1893) in Scotland, from the low metamorphic area up to the studied area in Ontario permitted Lumbers (1982) to define the regional stratigraphy which we used in our study.

Marble units are the rock type that hosts SEDEX zinc sulfide and non-sulfide zinc deposits in the Grenville Supergroup and equivalent outliers. Therefore, marble units were our priority and were thus investigated in greater detail when encountered. As mentioned above, differences in marble composition were never mapped and reported in past studies of the Bryson-Renfrew area. This data is necessary and will enable us to characterize the geological and depositional environment of the marble-hosted SEDEX mineralization identified therein. When marble units were present, special attention was given to the dolomite-calcite ratio of the marble unit to characterize its dolomitic or calcitic nature. We evaluated the most effective way of systematically determining this ratio. Hydrochloric acid (HCl) (specifically diluted to 10%) proved to be successful and practical for determination of the dolomite-ratio directly on the field. Acid tests were systematically conducted on clean, fresh cuts, marble samples from each marble outcrop encountered. At ambient temperatures, calcite actively reacts to 10% HCl acid as opposed to dolomite which must be grinded up. Dolomite-calcite ratio was estimated by observation of the acid reaction under an magnifying lens. To ensure precision of this method we regularly conducted a carbonate coloration test¹ (calcite turns red, dolomite remains uncolored and siderite turns blue) on the field and also x-ray diffraction analyses which confirms the hydrochloric acid method. The presence of other mineral phases and their proportions were also systematically evaluated and reported using classic field equipment. The presence of key indicative minerals, used for characterization of the geological environment associated with the marbles was reported on qualifying outcrops. Typical, unaltered samples representing a specific marble unit type were carefully chosen for

¹ A 0.2 g of Alzarin red ($\text{CO}_6\text{H}_4\text{CO}_6\text{H}(\text{OH})_2\text{SO}_3\text{Na} + \text{H}_2\text{O}$) in 100cc of 1.5% HCl mixed in equal proportion with 2 g of potassium ferricyanide ($\text{K}_3\text{Fe}(\text{CN})_6$) dissolved in 100cc of 15% HCl (Evamy, 1983; Dickson, 1965).

future reference. This more detailed study of the marble outcrops enabled us to divide the marble belt into seven distinct units.

Finally, since the objective of this thesis includes the study of SEDEX zinc mineralization, all encountered outcrops, were prospected for the presence of zinc sulfides, silicates and/or oxides. Observation under magnifying lens and the use of classic field identification equipment was carried out on all outcrops to identify any mineralization. Due to the varying physical properties of certain zinc silicates (i.e. willemite) and oxides and because zinc sulfides, silicates and oxides can be present as finely disseminated mineralization, we used a chemical reactant that reacts when zinc is present to aid us in the prospection for zinc. This zinc reactant, called "Zinc-Zap²" among mineral prospectors, gives a bright red coloration after a couple of seconds of application on rock sample or outcrop (Landry et al., 1995). Its chemical recipe is given at the bottom of this page. Zinc-Zap is most effective on zinc silicate and oxide mineralization but it will also react when disseminated zinc sulfide mineralization is present on an altered rock/outcrop surface. Noteworthy is the fact that direct application of Zinc-Zap on freshly-cut massive zinc sulfide mineralization does not yield conclusive results. Zinc silicates and oxides of the Franklin-Sterling Hill district are known for their ultraviolet luminescence. The zinc silicate willemite can be brightly fluorescent (green to orange) when observed with a UV light (Fig 5.4). Therefore, night prospecting using a UV lamp was conducted in areas where zinc silicates and oxides were identified and at other areas we judged pertinent. When marble-hosted zinc mineralization was encountered, a unaltered and representative sample was collected to conduct more in-depth laboratory studies. Systematic prospecting and the use of Zinc-Zap enabled us to identify new zinc mineralization occurrences throughout the Bryson-Renfrew region.

8.3.2 Sampling for Age Determination of the Calumet Deposit

The volcano-sedimentary sequence hosting the Calumet deposit has never been dated. However, the Calumet deposit is referred to share several characteristics with the Montauban deposit which is dated to be older than the Grenville Supergroup (Jourdain, 1993;

² A 3% potassium ferricyanide ($K_3Fe(CN)_6$) solution mixed in equal proportion with a 3% oxalic acid solution containing 0.5% dissolved diethylaniline (Landry et al., 1995).

Nadeau and Can Breeman, 1994). In order to determine if this deposit is older or part of the Grenville Supergroup we had to collect samples for radiometric studies. This date will also be used to determine the bottom age bracket for the Grenville Supergroup marbles of the Bryson-Renfrew region.

Two attempts were made to successfully obtain a valid sample. Sample selection was based on the quality of the outcrop/diamond drilling core. Only unaltered and representative samples were collected for zircon radiometric studies. The first attempt at dating the Calumet deposit volcano-sedimentary sequence was made in 2004 and the sample consisted in a biotite quartzo-feldspathic gneiss constituting the deposit's wall-rock (Jourdain, 1993). However, insufficient zircons were recovered from the samples. Resampling in 2005 of the fragmented amphibolite unit, this time, was successful in obtaining four zircons. The fragmented amphibolite is interpreted by Jourdain (1993) has a detritic volcanic rock unit (deformed intermediate tuf) and hosts the Calumet volcanic exhalative mineralization. This rock unit is thus directly related to the deposit and consists of an aerial volcanic rock deposited in a sedimentary context. The fragmented amphibolite samples were collected from diamond drilling core completed by Lacana Mining Corporation in 1987 (Jourdain, 1993; Bishop, 1987). The amphibolite layer from drilling holes 87-25 and 87-26 were sampled (Bishop, 1987). While the drilling core is available on site at the Calumet Mine, the location of the diamond drilling holes can be observed in Appendix B. The radiometric zircon dating was performed by M. Jean David at the GEOTOP laboratory, located at the Université du Québec a Montréal, using established methods. Detailed methodology and results of David (2009) are presented in Appendix C.

8.3.3 Geological Data Compilation and Treatment

In order to achieve a global understanding of the geological environment of the Bryson-Renfrew region, it was necessary to process all the geological data acquired throughout the campaign. This processing and compilation were successful in establishing geological maps and a better comprehension of the geological environment. The steps used for data compilation includes (1) database treatment and (2) the use of Geographical Information System (GIS) software.

All geological data acquired during outcrop descriptions were entered into a computer database. The database was programmed using SQL language and Visual Basic, on a Microsoft Access platform. All the location, geological, structural and mineralization data was entered and classified in the database. Specific compiled tables were extracted from the main database and organized under a specific theme, to be incorporated into a GIS system. The GIS software used was Mapinfo Professionnal. All data were georeferenced into the GIS environment permitting various spatial analyses to be performed. All general geological units were thus defined and linked together on a geological map. All defined marble units were also traced following the same procedure. All mineral mineralization were located as well. Again, spatial analyses of their relations with a specific lithology were conducted.

The final product of this database compilation is the building of a compiled geological and metallogenic map for the Bryson-Renfrew area.

8.4 RESULTS

8.4.1 Geological Map of the Bryson-Renfrew Area

As cited above, areas of the Bryson-Renfrew region were mapped at different scales by past government geological campaigns and by mining companies. For instance New Calumet Mine Ltd. and Lacana Mining Corp. mapped the Calumet deposit while the Cadieux SEDEX zinc deposit was worked by Noranda Exploration Inc. (Roger and Lapointe, 1998). The objective of our campaign was not to completely re-map the Bryson-Renfrew region. Our goals were to (1) consolidate the geological data across the provincial border, (2) refine the geological data and description of the marble belt, and (3) investigate zinc metallogeny and its depositional environment. Once this has been done, the Bryson-Renfrew region can then be compared to the Balmat-Edwards and Franklin-Sterling Hill districts.

The result of this work is the publication of a geological compilation of the Bryson-Renfrew that is focused on the region's zinc metallogeny and its depositional environment. A total of three maps are presented in this study. The first map represents the general geological compilation of the Bryson-Renfrew area, based on previous cartography and our work (Fig. 8.1). The geology of the Quebec and Ontario are linked and the marbles are undifferentiated on this map. The second map shows the structural data measured on outcrops and traced on

aerial photographs used, in part, to trace lithological contacts (Fig. 8.4). Finally the third map produced concentrates on the different marble units identified during the field campaign (Fig. 8.7). This map also synthesizes the wide range of SEDEX zinc mineralization and mineral occurrences encountered.

Results will be presented in the following order: (1) The general geological map and its geological units, (2) the structural features of the area, (3) the identified and differentiated marble units, (4) description of non-zinc particular mineral occurrences and features observed in the region, and (5) the description of the newly discovered and known zinc occurrences encountered during the campaign.

8.4.2 General Geological Map

The Bryson-Renfrew region has a wide range of lithologies. Since marbles were our priority the other lithologies were not described in equivalent detail. The lithologic descriptions of Lumbers (1982) were used for non-marble lithologies. Overall the Bryson-Renfrew area is characterized by an important marble belt that can be continuously traced from Bryson, to the north, to Renfrew to the south. Observed and compiled lithologies include a sequence of basal amphibolites, metavolcanic rocks and quartz-feldspar gneisses. Marbles dominate the area. Pure to diopside-bearing (up to 35% with a grain size of 2 millimeter) quartzite is observed near the town of Bryson, in the central-eastern and southern part of the Bryson-Renfrew region (Fig. 8.1). Biotite paragneiss units containing up to 30% medium-grained biotite (2 to 4 millimeters) are mostly present to the south-southwest of the town of Renfrew.

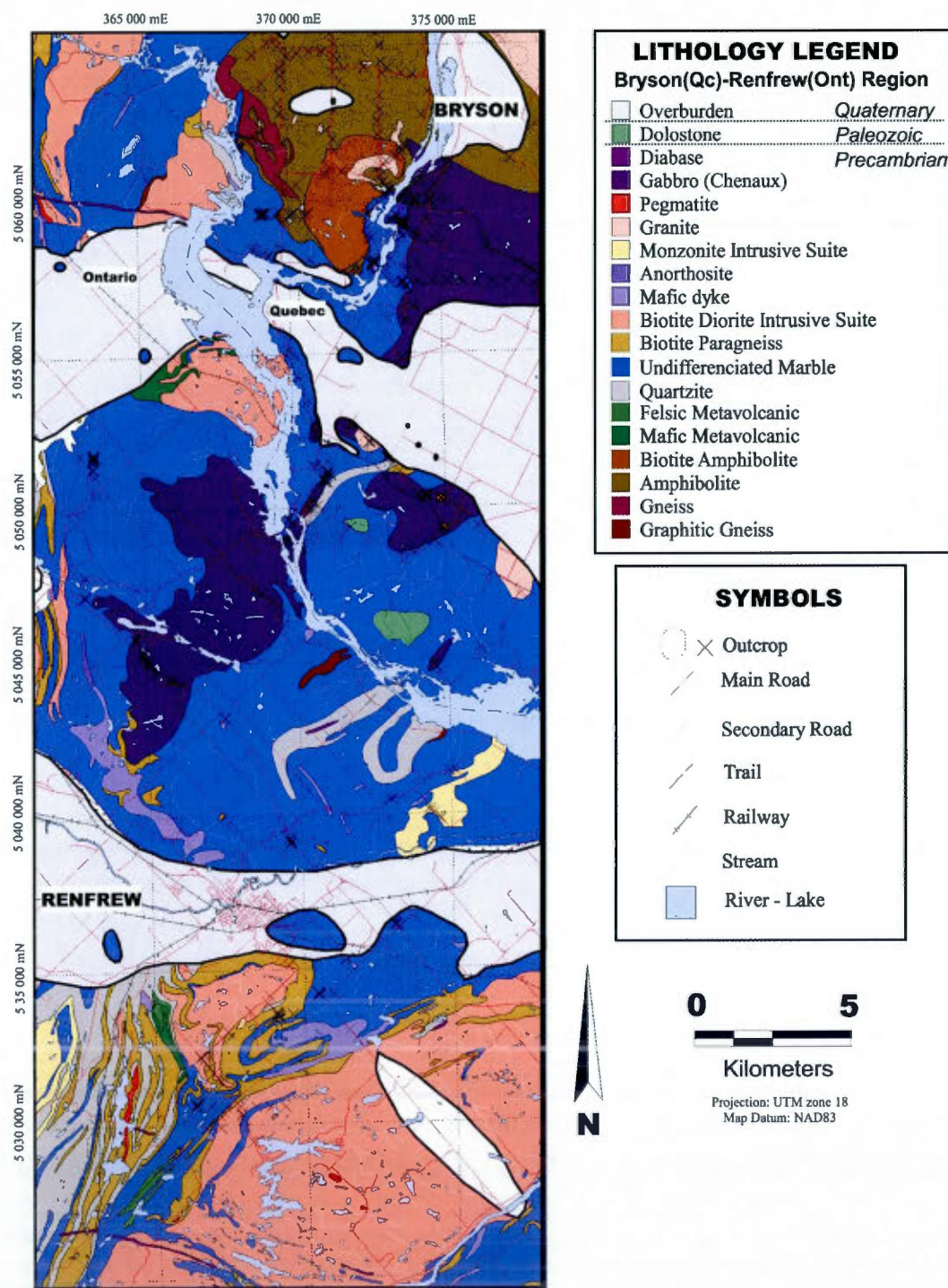


Figure 8.1: General geological map compilation of the Bryson-Renfrew region showing the dominance of marbles. Marbles are un-differentiated on this map. Map compiled from our field data combined with those of Lumbers (1982), Osborne (1944) and Katz, 1976).

The Bryson-Renfrew region was partly intruded by the Chenaux gabbro intrusion. This gabbro stock cross-cuts the marble sequence in the central area of the studied region and also east of the town of Bryson (Fig. 8.1). Outcrops showing the contact between the marbles and the Chenaux gabbro were observed on the islands in the middle of the Ontario Chenaux dam at Portage-du-Fort. The contact aureole between the marble and the gabbro is 3 to 10 centimeters thick and characterized by a reddish-pinkish color due to metasomatic addition of manganese inside calcite (Fig. 8.2 and 8.3) (Deer et al., 1992). The contact between the gabbro and the marble belt is un-mineralized and contains calc-silicate minerals such as fine grained diopside.

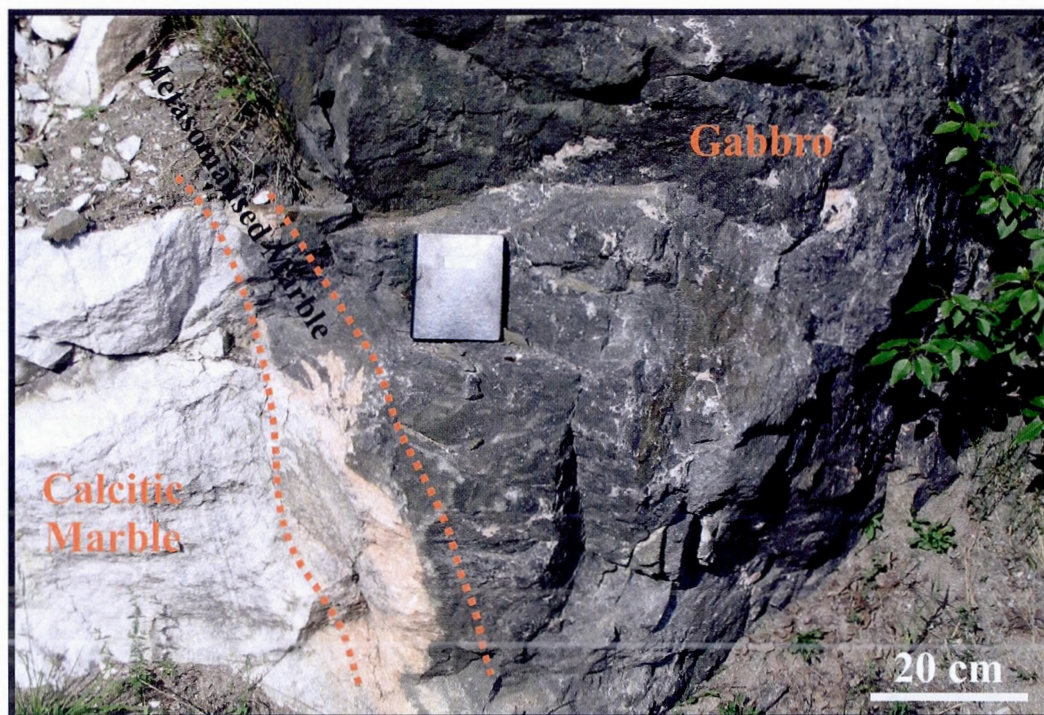


Figure 8.2: Contact between the gabbro and the marble belt on the Island along the Cadieux dam, near Portage-du-fort. The metasomatic effect of the gabbro intrusion is characterized and restricted to a 10 centimeter-thick pink calcite and calc-silicate fringe.

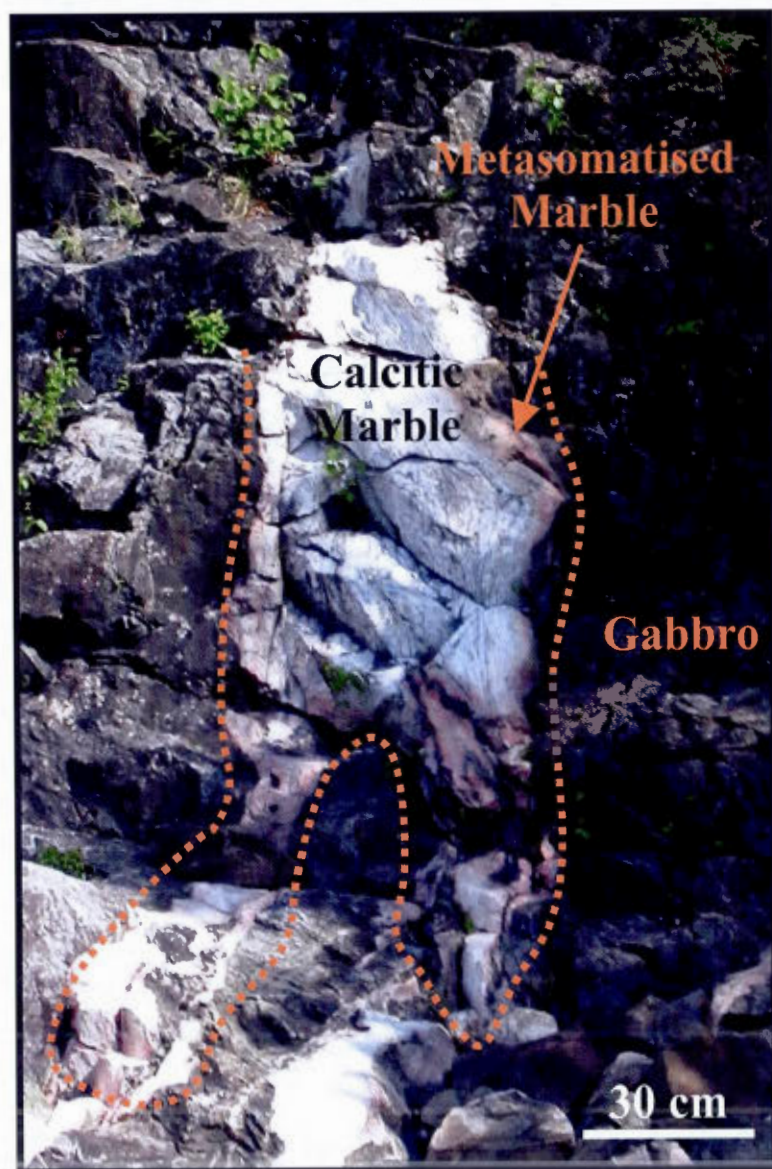


Figure 8.3: Calcitic marble fragment isolated inside the gabbro intrusion showing the pink calcite metasomatic rim. Picture taken from the Cadieux dam near Portage-du-Fort.

8.4.3 General Structural Features

Structural measurements throughout the Bryson-Renfrew area were compiled and shown on figure 8.4. This map was produced by positioning outcrops structural measurements onto a interpreted aerial photograph background. The local detail structural analysis confirms that the rocks units of the area were subject to strong metamorphism and polyphase deformation. It is why we mostly refer to the work of Lumbers (1982) were the lithologic units could be traced from low metamorphic grades to granulite facies in our area. The structural interpretation is a compilation from the work of Lumbers and our outcrops in the area. Because zinc mineralization in the Grenville Supergroup is stratiform (Gauthier and Brown, 1986), more attention was regarded to the mineralogy of the marbles and the structure within than the regional structural study. The results in support of this statement are presented below.

The gneissic and amphibolitic rock units of the Bryson-Renfrew stratigraphic sequence are characterized by a well-developed foliation that is often parallel to their stratigraphic contact. Primary structural features in these units were mainly obliterated during metamorphism. However, local features in the amphibolitic rock units, such as fragmented facies, provide additional clues regarding the primary structures of the rock units. Mafic and felsic intrusions present in the area are characterized by strong linear trends visible on aerial photographs and exhibit foliation structures when they are pre-metamorphic in nature.

Marble units, on the other hand, are characterized by silicate mineral layering which may represent the original stratigraphic plane, as used by Brown and Engel (1956) in the Balmat-Edwards district and Gauthier and Brown (1986) in the Maniwaki area. This phenomenon, as mentioned earlier, is explained by the high reactivity of carbonates with nearby minerals during prograde metamorphism and by the presence of anhydrite layers that absorb most of the deformation (Pomerol et al., 2000; Gauthier et al., 2004). Thin clastic sedimentary layers interlayered with carbonates will react to form calc-silicate minerals along that specific horizon. The primary bedding inside the marble belt is thus generally presumed preserved.

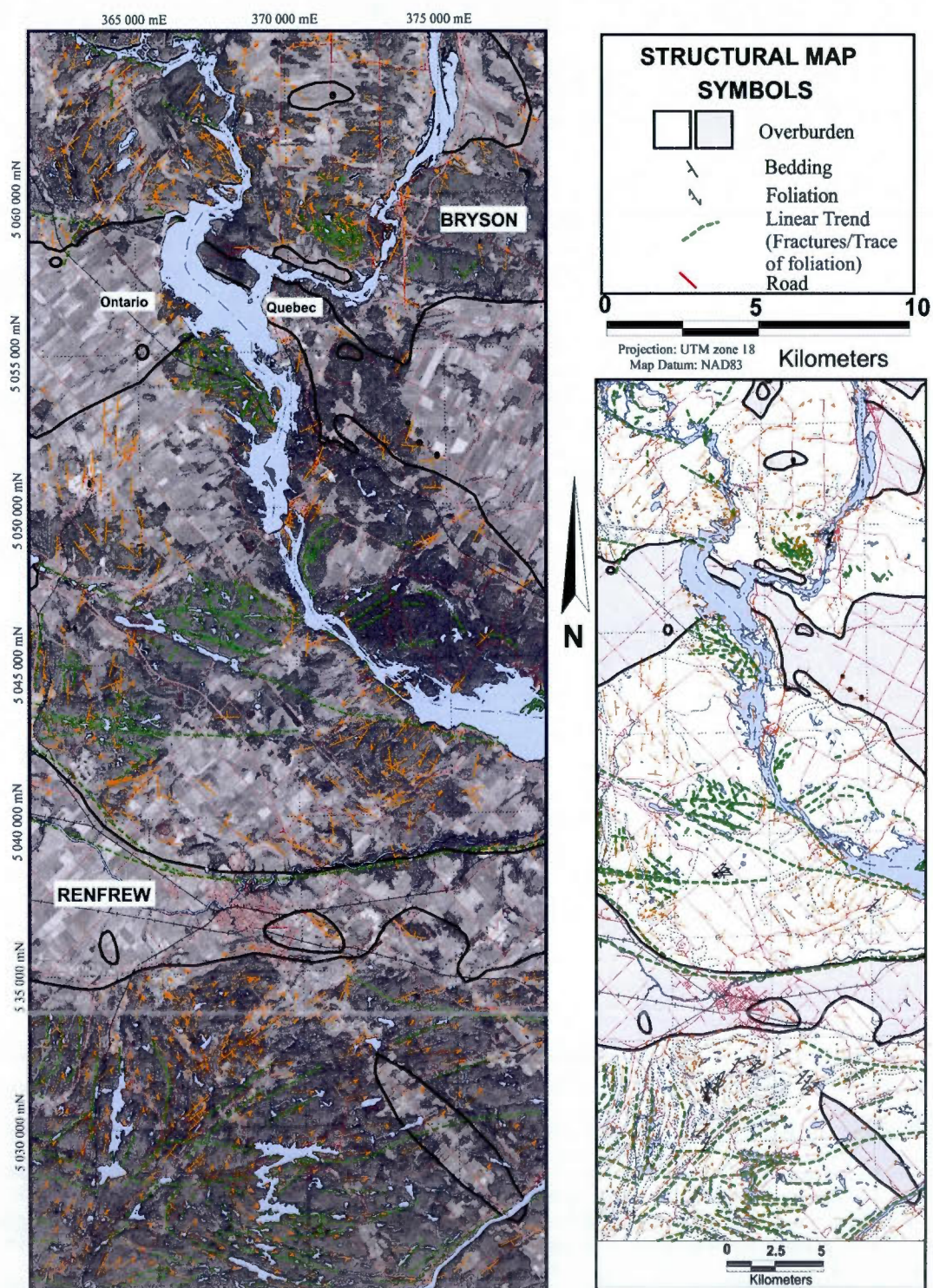


Figure 8.4: Structural map of the Bryson-Renfrew region showing linear trend interpretation from satellite imagery.

Local structural study of the marble outcrops in the Bryson-Renfrew region reveals that there are at least two phases of deformation evident. The detailed study of the Maniwaki region, north of the Bryson-Renfrew area, by Gauthier and Brown (1986) was used to understand and interpret what was locally observed in our outcrops. The first phase of deformation is characterized by tight isoclinal folds which thicken the sequence. The second phase is characterized by northeast-plunging open to tight folds that refold the first phase isoclinal folds (Fig 8.5). These two major deformational events produced structural interference patterns (hook-shaped folds) and also flow and fold-hinge thickening. This type of folding occurs at high metamorphic grades where the marbles flow plastically. More competent horizons, such as quartzite and calc-silicate layers respond to the intense deformation and stretching caused by the dynamo-metamorphic processes by boudinage. This boudinage was observed at a centimeter-scale but also at a plurimetric-scale and indicates the unit's resistance to flow during tectonic deformation.

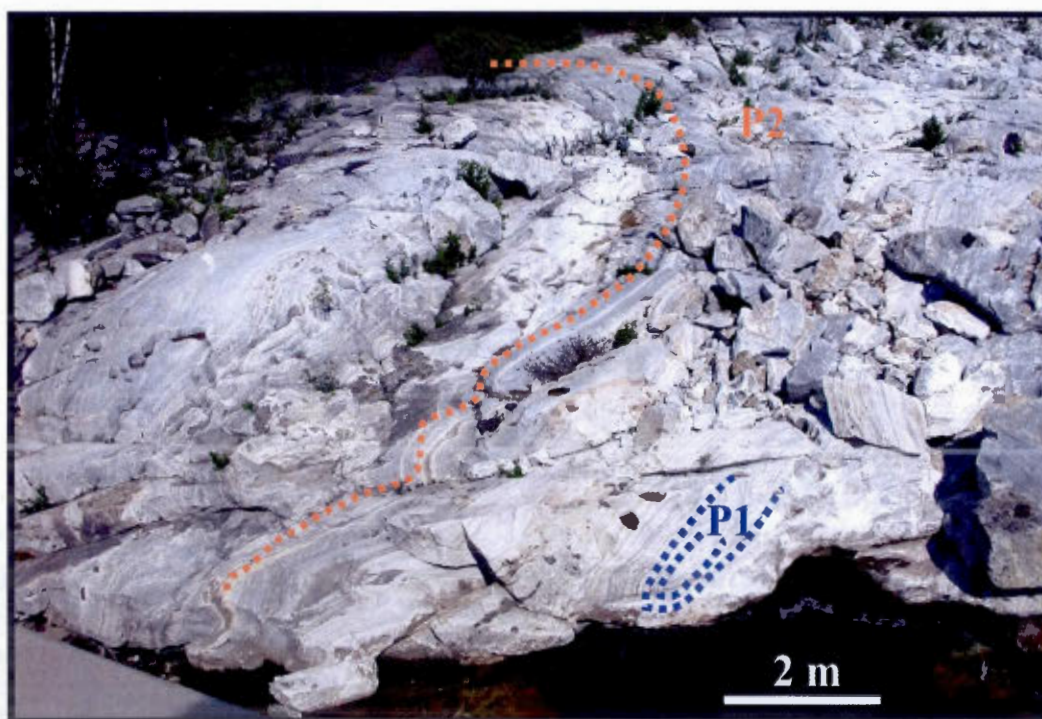


Figure 8.5: Example of structural style of polyphase deformation in calcitic marbles of the Bryson-Renfrew area. P1 (blue) isoclinal folds are refolded by P2 (orange). Observed along the Ottawa River at the Chenaux dam, near Portage-du-Fort. View towards the northeast.

The Bryson-Renfrew region was therefore subject to polyphase deformation and high grade metamorphism with development of a foliation in respective units. Primary structures were mostly obliterated by the high metamorphic grade and deformation. However, primary stratigraphic layering was considered preserved in the marble units allowing correlation of marble units throughout the region.

8.4.4 Characterization of Marbles Units

Detailed study of the marbles of the Bryson-Renfrew region is important to characterize its geological environment and associated zinc mineralization. Our field campaign was successful in identifying seven distinct marbles units. These marbles units are represented on figure 8.7 throughout the entire marble belt between the town of Bryson and Renfrew. The marble units were distinguished on the basis of the relative proportion of three common features which are (1) the proportion of dolomite, (2) the proportion of calcite and (3) the proportion of the silicate minerals diopside, forsterite and tremolite. A ternary diagram that illustrates the identifying criteria for each marble unit was constructed and used for classification (Fig. 8.6). The seven marbles units are described in detail in the following paragraphs.

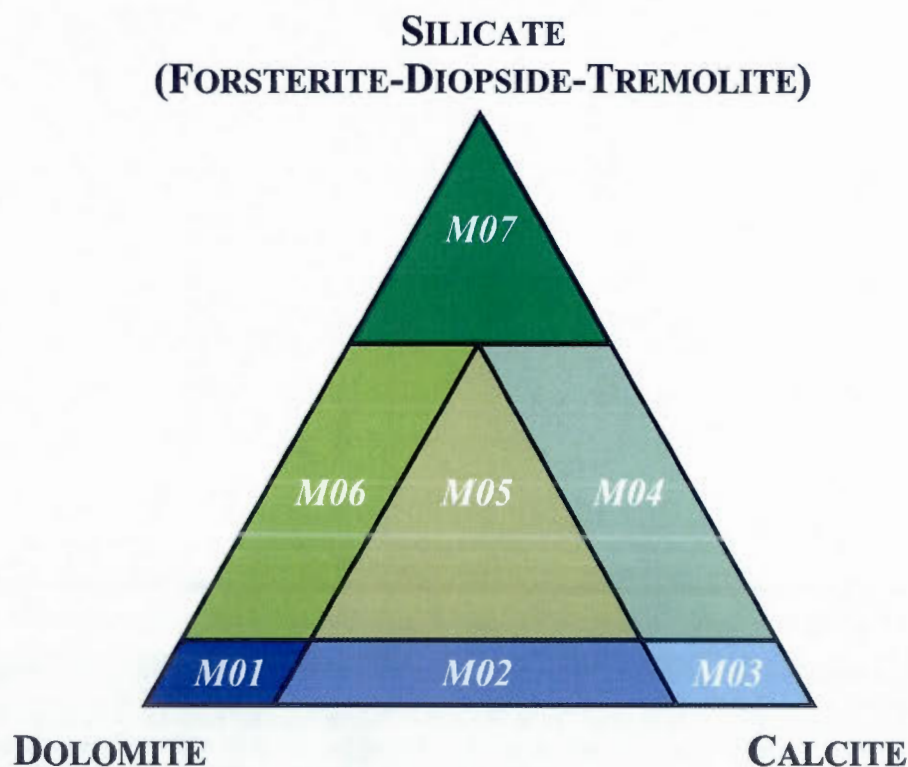


Figure 8.6: Classification of the marble units in the Bryson-Renfrew area based on relative proportions of dolomite, calcite and silicates (diopside-forsterite-tremolite): M01: Dolomitic marble, M02: Calcareo-dolomitic marble, M03: Calcitic marble, M04: Siliceous calcitic marble, M05: Siliceous calcareo-dolomitic marble, M06: Siliceous dolomitic marble, M07: Siliceous marble.

Dolomitic Marble (M01): This rock unit can be recognized in the field by its dark grey alteration color on exposed surfaces. Fresh cuts of the rock are of a pure white color. The unit does not directly react with 10% HCL acid, except locally between grains. The dolomitic marble unit consists of more than 80% dolomite and less than 10% calcite and 10% silicate. Traces of millimeter-scale disseminated pyrite were observed locally. Pure dolomitic marble (more than 99% dolomite) was recognized throughout the Bryson-Renfrew region and also near the two dolomite quarries described earlier. The presence of diopside-forsterite-tremolite is scarce in this unit. This unit is coarse-grained with an average grain size of 4-6 millimeters.

Calcaro-Dolomitic Marble (M02): This rock unit is a transitional unit towards the calcitic marble end-member. It is medium grey on altered surfaces and white on a fresh surface. This unit reacts moderately with HCl acid. This unit is composed of 20 to 80% dolomite, 20 to 80% calcite and up to 10% silicate. Locally, traces of pyrite are observed. This unit is coarse-grained with an average grain size of 4-6 millimeters.

Calcitic Marble (M03): The calcitic marble unit is characterized by a whitish-grey alteration color on weathered surfaces. The color of the marble on a fresh surface tends towards the grey. The unit reacts strongly with direct application of 10% HCl acid. More than 80% calcite composes this unit and up to 10% silicates are present. The grey color of the calcitic marble unit is due in part to the presence of millimetric disseminated graphite flakes. Disseminated phlogopite is observed locally. Grain size is smaller relative to the dolomitic marbles with an average of 2-4 millimeters.

Siliceous Calcitic Marble (M04): This unit is a pale greenish color when fresh, and is characterized by a grey color with a weathered surface. Also, because of differential erosion between carbonates and silicate, the silicate minerals stand out in relief in outcrops. The unit produces a strong reaction to the HCl solution and is composed of more than 10-30% silicate minerals, less than 20% dolomite and 50-70% calcite. Disseminated fine-grained graphite flakes (traces to 1%) are present in this marble unit. Grain size is, again, smaller than the dolomitic marble unit with an average of 2-4 millimeters.

Siliceous Calcareo-Dolomitic Marble (M05): This unit is a pale greenish-white color on a fresh surface. Dolomite and silicate stand out in relief relative to calcite in outcrops due to calcite's more soluble nature. The weathered surface color is a pale grey. The unit produces a moderate reaction to cold application of 10% HCl acid. The unit is mainly composed of 10-30% silicate minerals (diopside, forsterite and/or tremolite), 20-50% dolomite and 20-50% calcite. Grain size averages 2-4 millimeters.

Siliceous Dolomitic Marble (M06): The fresh surface is green and white in color whereas the weathered surface is medium to dark grey due to the higher abundance of dolomite. The weathered surface is rough because dolomite and silicate minerals are more resistant to erosion. This unit is characterized by less than 20% calcite, 20-60% silicate and 80% dolomite. White to pale-orange chondrodite is common locally and can represent up to 15% volume of the unit. Forsterite grains are frequently altered into serpentine throughout the region.

Siliceous Marble (M07): This unit is dark greenish colored on fresh surfaces and dark brown-grey-green color on altered surfaces. This rock unit is composed of more than 70% silicate minerals and by 30% calcite-dolomite. Diopside with lesser forsterite are the main minerals present in this lithological unit. Pyrite is common around diopside nodules and is associated with phlogopite. Grain size is generally in the 2-4 millimeter range but can locally be up to 1 cm.

Forsterite is commonly retrograded to serpentine nodules throughout the Bryson-Renfrew area. To recapitulate, the Bryson-Renfrew marble belt is divided into seven distinct lithological units based on the relative abundance of dolomite, calcite and silicate minerals. The next section presents mineral particularities that occur in the studied area.

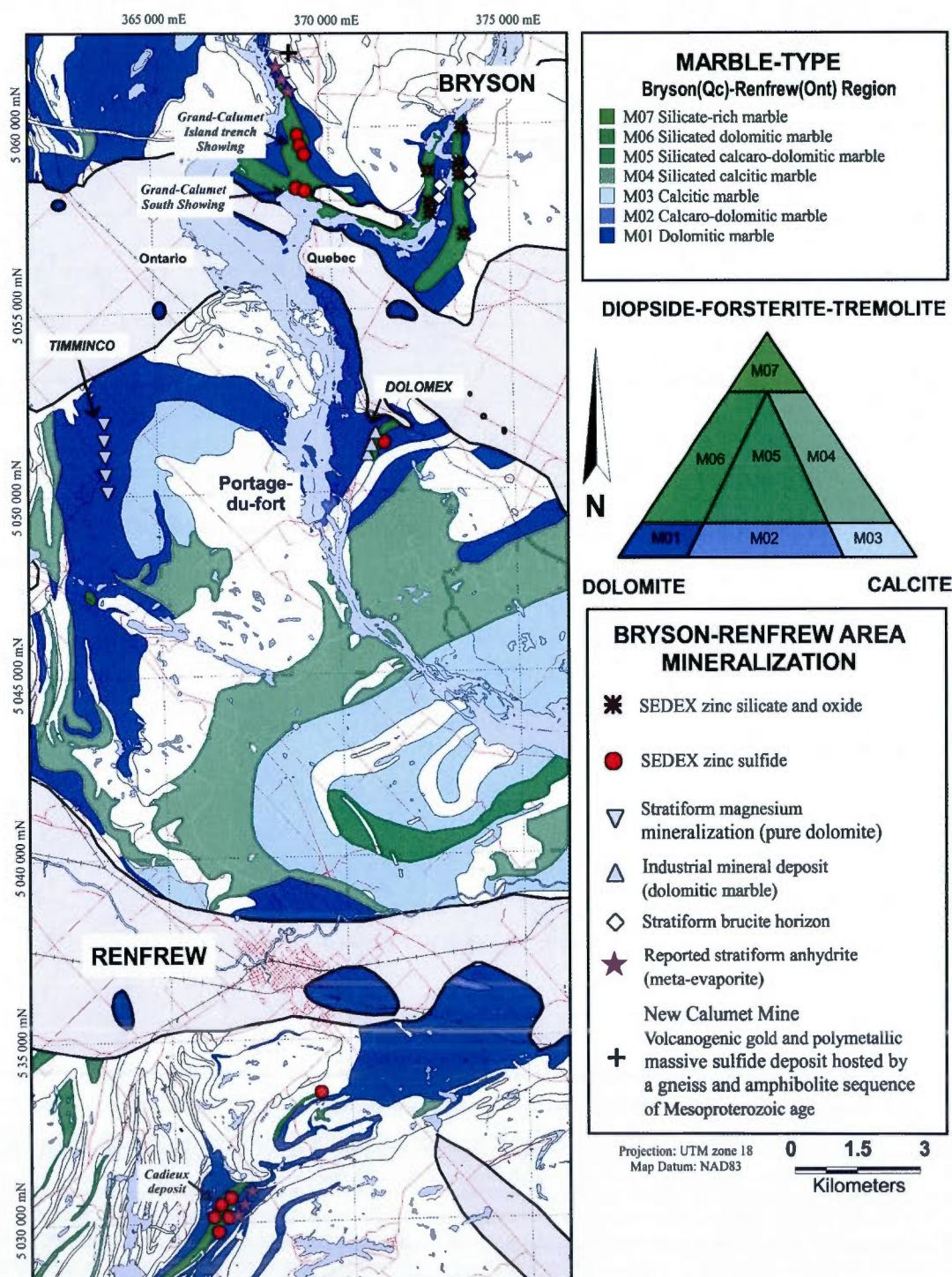


Figure 8.7: Metallogenic map of the Bryson-Renfrew region showing the distribution of SEDEX mineralization and marble-type.

8.4.5 Other Significant Mineral Occurrences

Significant non-zinc mineral occurrences that were encountered during the field campaign are discussed below. The presence of these occurrences provides additional information regarding the geological environment of the Bryson-Renfrew region. They include the presence of (1) pure dolomitic marbles, (2) brucite-rich horizons and (3) anhydrite layers.

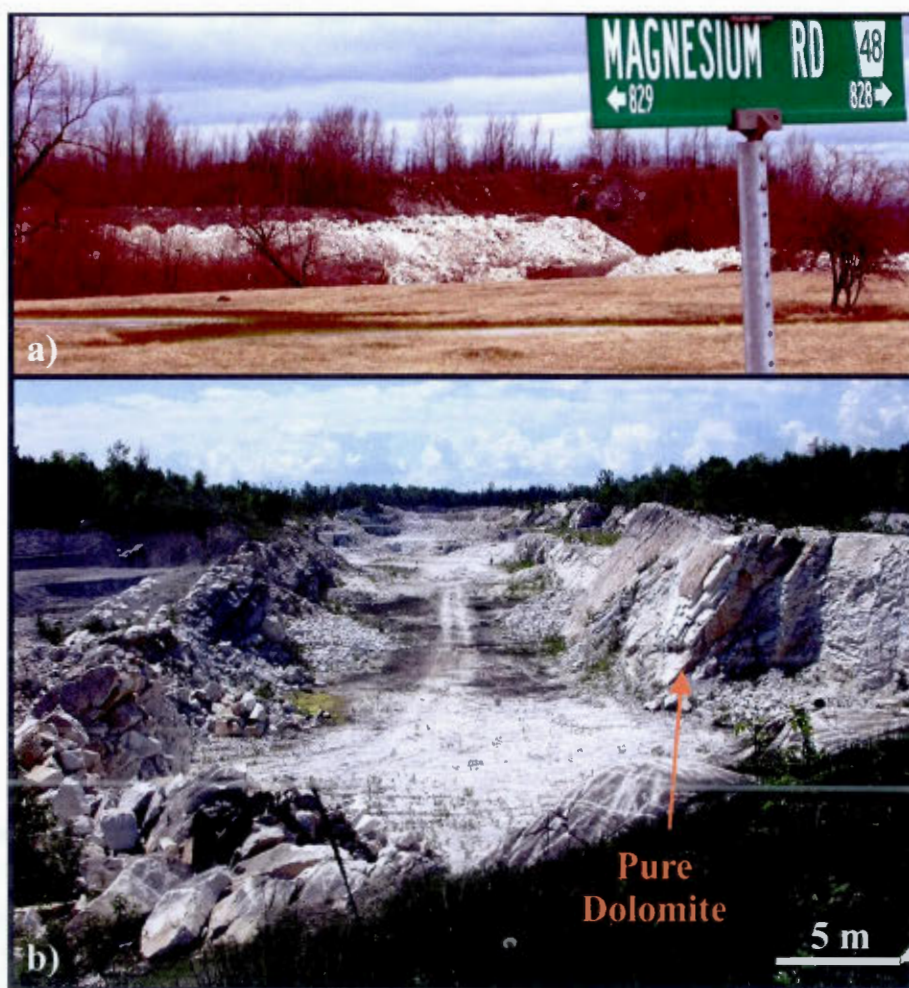


Figure 8.8: (a) The road to the Timminco magnesium plant at Haley (Ont), showing the abundance of magnesium in the area. (b) Panoramic view of Timminco's dolomite quarry at Haley viewing to the south. Picture clearly shows the pure dolomitic horizon from which magnesium metal is extracted.

Thick pure dolomitic marbles are mostly encountered in the western-central portion of the Bryson-Renfrew region. These marbles are coarse grained and extremely pure in the Haley area allowing Timminco Metals Inc. to extract magnesium metal directly from the dolomite in a nearby quarry (Fig. 8.7). The quarry is 300 meters long and 50 meters thick and

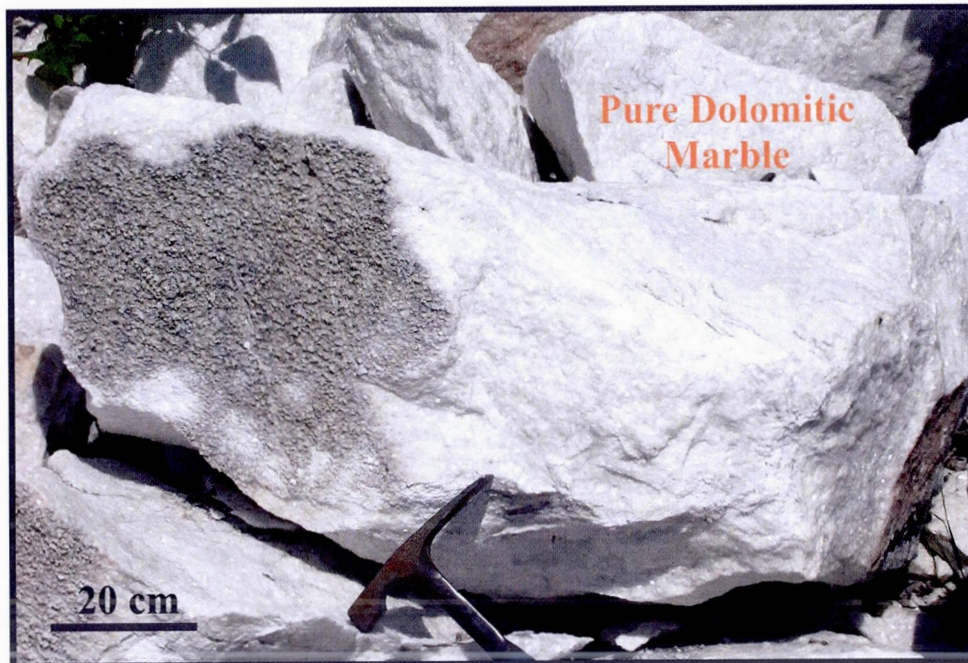


Figure 8.9: Pure dolomitic marble mined at Haley's Timminco dolomite quarry. Notice the purity of the sample with no traces of silicates.

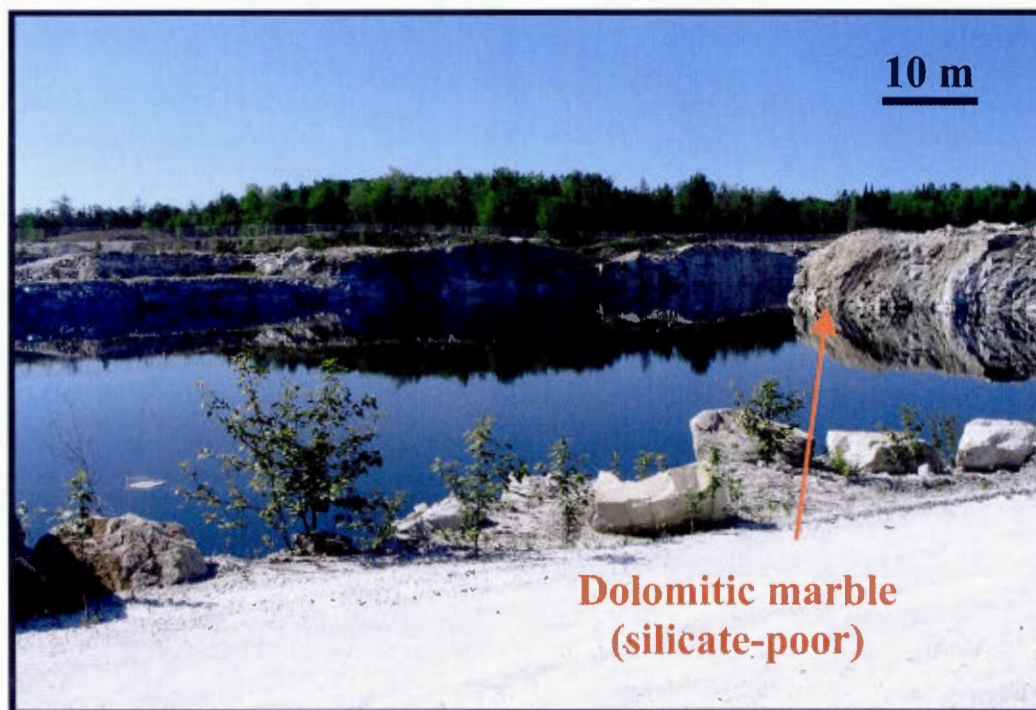


Figure 8.10: Panoramic view of Dolomex's rehabilitated dolomite quarry at Portage-du-fort where a silicate-poor dolomitic marble was exploited for industrial mineral and fertilizers purposes. Demonstrate the abundance of pure dolomitic marbles in the Bryson-Renfrew area.

follows a stratiform horizon of pure dolomitic marble (Fig. 8.8). This layer dips steeply towards the east and is about 50 meters thick. This horizon can be traced for several hundred meters in the area around Haley. Pure white dolomite is the only mineral present in this unit (Fig. 8.9). Grain size averages around 4-6 millimeters.

Another dolomite quarry was exploited by Dolomex Inc. near Portage-du-Fort (Fig. 8.7). In this quarry, dolomite constitutes the main component but up to 10% diopside can be present throughout (Fig. 8.10 and 8.11). Outside the quarry diopside can locally constitute up to 20% of volume of the unit and is concentrated in centimetric bands that define stratigraphy. Like the quarry at Haley, dolomite units strike roughly north-south and dips towards the east. Grain size again is coarse and averages from 4 to 6 millimeters. The impure nature of the dolomite explains why the Portage-du-Fort quarry supplied industrial minerals and fertilizers instead of magnesium metal extraction.

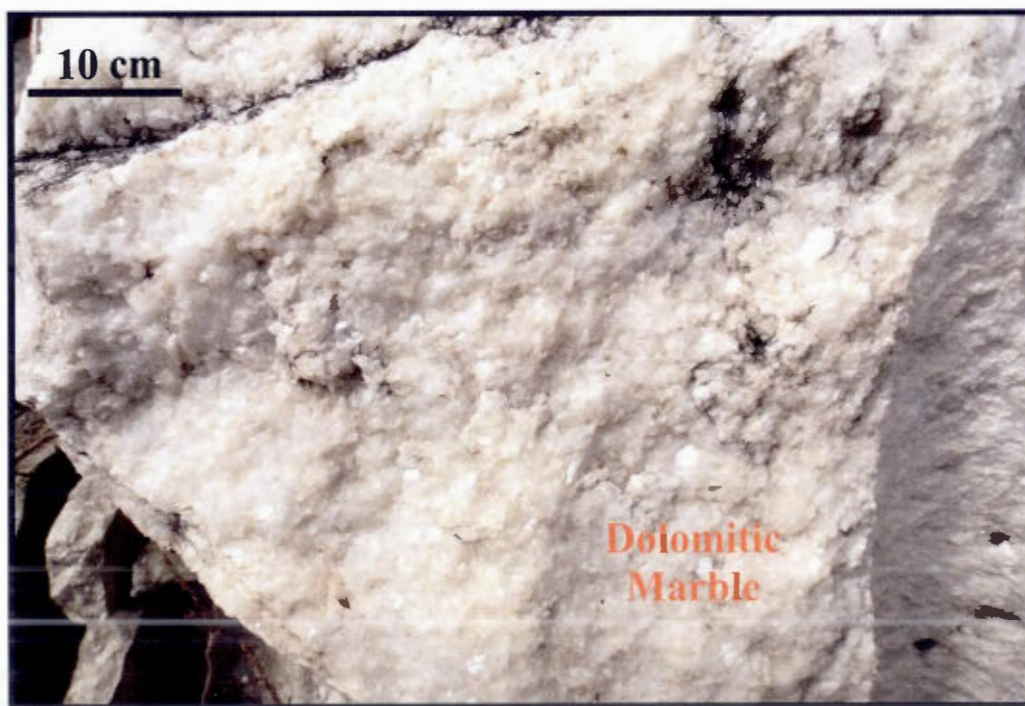


Figure 8.11: Pure dolomitic marble that was exploited at Portage-du-Fort's Dolomex dolomite quarry.

Brucite is also encountered in the Bryson-Renfrew area. Brucite is a magnesium hydroxide derived from the alteration of magnesium-rich silicate and carbonate. Brucite is magnesium-rich and was once mined for magnesium. In the vicinity of the Bryson area,

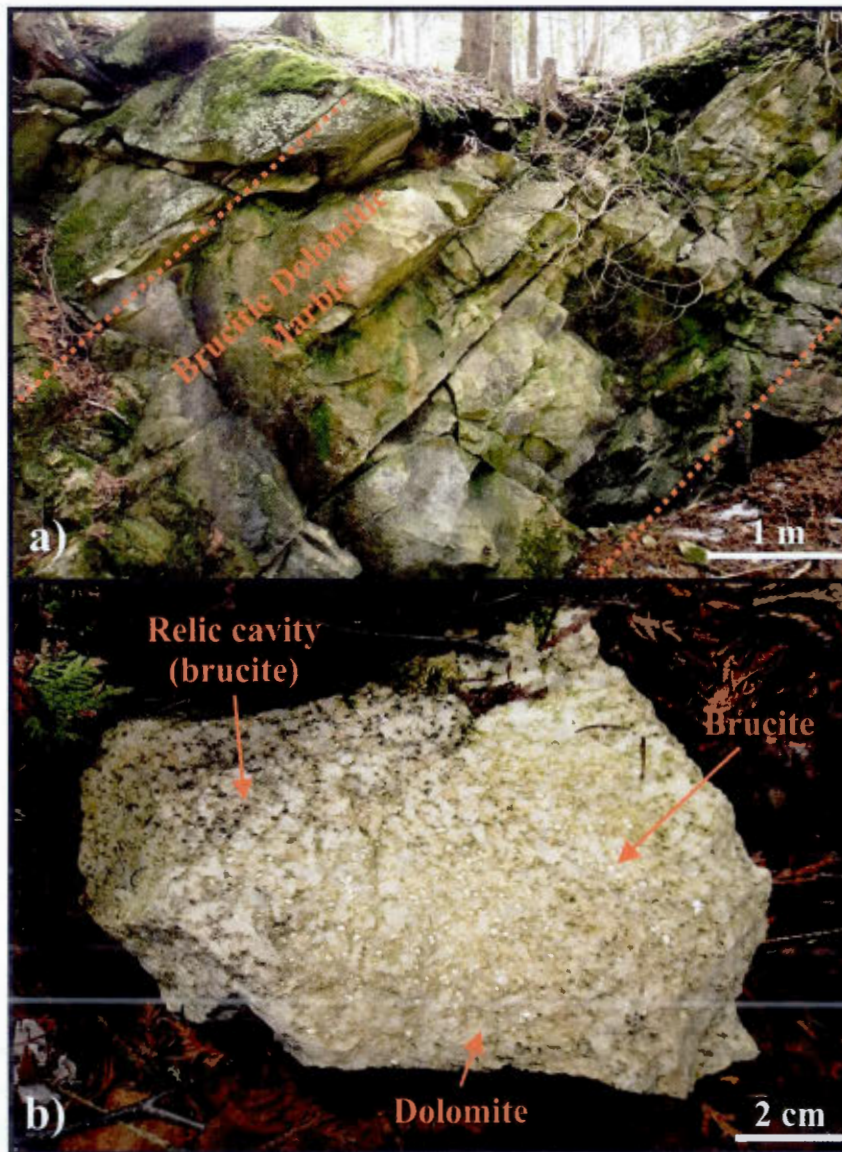


Figure 8.12: a) The Maxwell stratiform brucitic dolomitic marble quarry at Bryson (Qc). b) Brucitic dolomitic marble sample showing brucite nodules (white) in a silicate-poor dolomitic marble. Surface alteration dissolves brucite and leaves behind cavities indicating where brucite was present. This can be observed on the top-left corner of the figure.

historical records indicate a small-scale extraction of brucite from a quarry (Osborne, 1939). This brucite occurrence was located in the southern part of the Bryson village in two old quarries (30 meters wide/long) (Fig. 8.7). Here, stratiform disseminated white millimetric to centimetric brucite nodules are present in a dolomitic marble unit (Fig. 8.12). The silicate content of the marble is mostly composed of brucite. The alteration surface is characterized by negative relief because of differential erosion resistance between brucite (soft) and dolomite (harder). The brucite nodules can constitute up to 50% of the rock unit. The host marble is a dolomitic marble containing residual silicate minerals such as forsterite and diopside. Another brucite occurrence was discovered during the course of our study, this time on the other side of the Ottawa River, west of the old Bryson brucite quarry. This new showing is stratiform and contains up to 50% brucite nodules by volume. The nodules are white and their grain sizes vary from 4 millimeters to 1 centimeter.

Finally, another feature identified in the Bryson-Renfrew region is the presence of

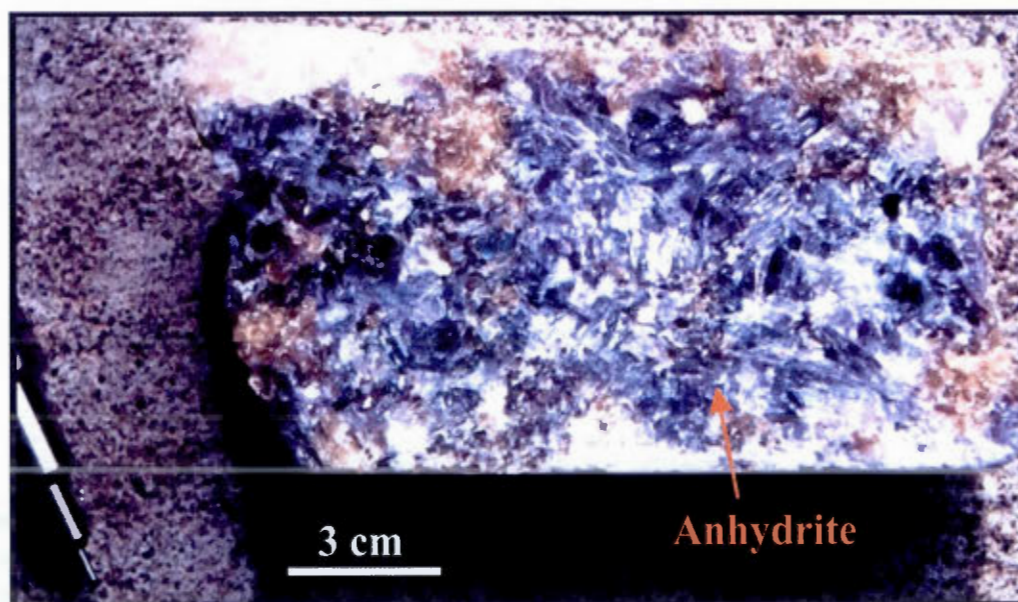


Figure 8.13: Lavender coloured anhydrite in a deep drill hole from the Swamp zone of the Cadieux zinc deposit by Noranda Exploration Inc.

anhydrite layers. However, anhydrite layers are easily dissolved by surface water, so anhydrite does not normally occur on surface outcrops and can only be observed in diamond

drill core and new fresh unaltered exposures. Therefore the unit could not be uniformly traced over the Bryson-Renfrew region because of the scarcity of diamond drilling holes available. In fact, available drill holes are only available on the Cadieux SEDEX zinc deposit, near Renfrew, and on the Calumet Mine, west of Bryson (Roger and Lapointe, 1998; Osborne, 1941; Osborne, 1944). This irregular distribution of drill data hindered the regional study of anhydrite complicated. Even though drill holes are scarce throughout the area, anhydrite layers are reported in New Calumet Mine logs from the Calumet Mine deposit (Osborne, 1944). Anhydrite was also reported in drill logs and observed at the Cadieux deposit (Fig. 8.13). Anhydrite layers in the Bryson-Renfrew area are stratiform, occurring in association with the dolomitic and silicate dolomitic marble units. The total thickness of the horizon is hard to estimate with the available data. Anhydrite composes from 80% to 100% of the unit. Grain size varies between 4 to 6 millimeters.

To summarize, results show that the marble units of the Bryson-Renfrew region are characterized by pure dolomitic marbles, stratiform brucite horizons and by the presence of anhydrite in the stratigraphic sequence.

8.4.6 Zinc Metallogeny

The known and newly discovered SEDEX zinc sulfide deposits were investigated during this study. As mentioned above, although the Cadieux and Calumet Mine deposits were known to exist, the Calumet Mine deposit is a volcano-sedimentary hosted massive sulfide deposit that was thought to be older (Gauthier et al., 2004) than the marble-hosted SEDEX deposit, so it was not firstly investigated in depth. Zinc metallogeny was first studied at the Cadieux deposit and then the region was prospected to the north towards Bryson. In this sub-section, we first report (1) geological data from the review of the Cadieux zinc sulfide deposit and the surrounding areas, then (2) geological data from the newly discovered Portage-du-Fort zinc occurrence and then (3) geological data from newly-discovered and historical work from the western part of the Grand-Calumet Island. Gauthier's and al. (1987) discovery of a zinciferous magnetite will be reviewed and investigated later in chapter 9.

The Cadieux SEDEX zinc sulfide deposit, located 5 kilometers south of the town of Renfrew, was reviewed in detail in section 2 (Fig. 8.7). Outcrops and samples studied from the deposit revealed the following: The deposit is hosted by silicate-rich dolomitic marbles. Coarse-grained tremolite with a grain size of 4 millimeters to 1 centimeter constitutes up to 40% of the rock composition (Fig. 8.14). Zinc mineralization is stratiform and can be traced for hundreds of meters along old trenches excavated in the 1990s. Zinc mineralization is in the form of sphalerite which is coarse-grained, dark colored “blackjack” sphalerite due to its high iron content. The mineralization is disseminated and represents up to 60% of the rock unit. Mineralization is several meters thick and lacks the presence of iron sulfides, such as pyrite or pyrrhotite, and galena. Only zinc sulfide is present at the Cadieux deposit.



Figure 8.14: Typical semi-massive to disseminated stratiform sphalerite mineralization hosted by a tremolite-forsterite-rich dolomitic marble unit at the Cadieux deposit near Renfrew (Ont). Brown mineral is disseminated sphalerite.

Another zinc sulfide occurrence was identified 3 kilometers northeast of the Cadieux deposit and named Renfrew North (Fig. 8.7). This occurrence is characterized by

disseminated sphalerite hosted by a siliceous dolomitic marble. Sphalerite forms from 1 to 2% of the rock unit and averages 2 millimeters in size. Mineralization is stratiform, one centimeter thick, and can be followed for 5 meters in an exposed outcrop along a small stream. The narrow marble belt in this area did not permit extension of the mineralized zone at surface.

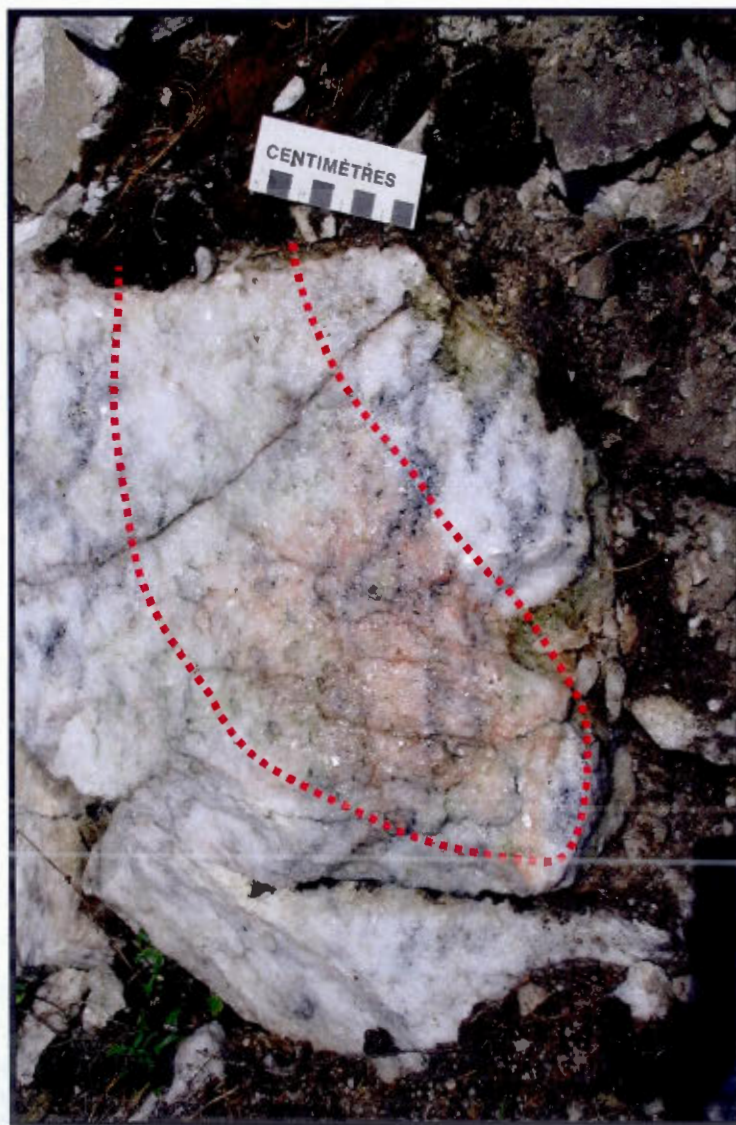


Figure 8.15: Portage-du-Fort zinc sulfide showing discovered along the dolomite quarry. Disseminated stratabound sphalerite hosted by a silicate dolomitic marble unit. Red coloration is due to the application of Zinc Zap (highlighted in a red dashed line).

A new zinc sulfide occurrence was discovered in the central section of the Bryson-Renfrew area, near the town of Portage-du-Fort. The Portage-du-Fort zinc sulfide occurrence was observed along the eastern flank of Dolomex's quarry and discovered using Zinc-Zap (Fig. 8.7 and Fig 8.15). The showing is hosted by a siliceous dolomitic marble unit present in the southern wall of the dolomite quarry. The dolomitic marble contains 20% diopside and 15% forsterite, 55% dolomite and less than 5% calcite. Average grain size is 4 to 6 millimeters for the carbonates and silicates. Forsterite grains are altered into greenish serpentine nodules. Sphalerite grains are about 2 millimeters in size and are disseminated in the marble unit where they form up to 3% of the rock. The mineralized horizon follows the stratigraphic bedding measured in the marbles and is about 30 centimeters thick. To summarize, the Portage-du-Fort zinc sulfide showing is stratiform in nature and was stratigraphically followed for 10 meters along the edges of the quarry.

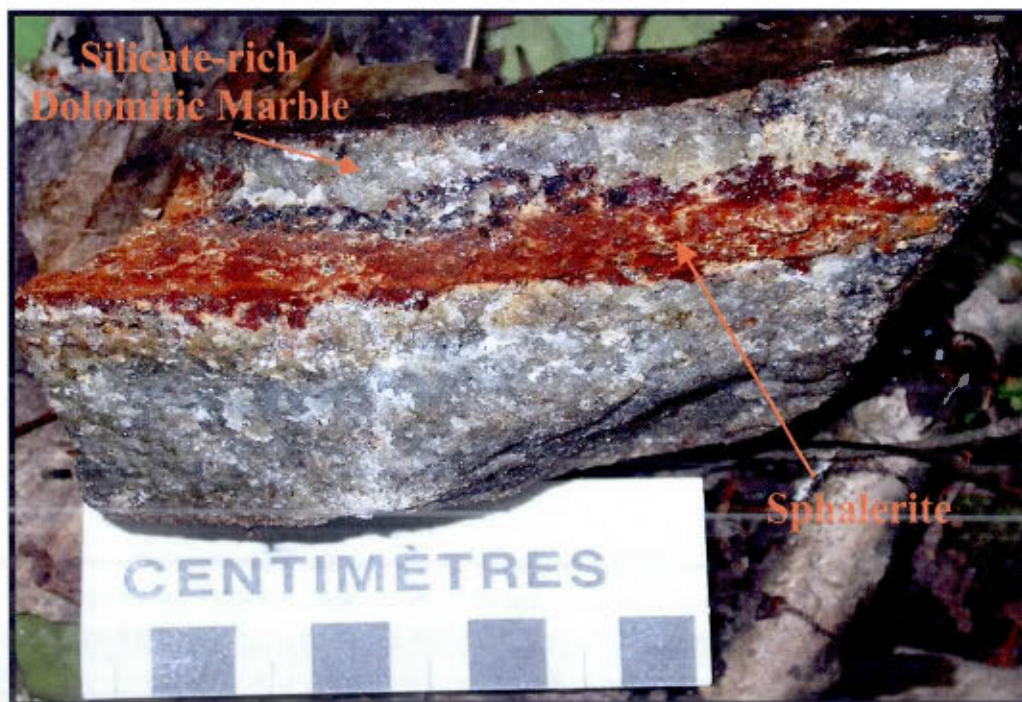


Figure 8.16: Disseminated stratabound sphalerite mineralization hosted by a silicate-rich dolomitic marble unit in the trenches south of the New Calumet Mine on the Grand-Calumet Island.

On Grand-Calumet Island west of the town of Bryson, the marble belt present west and south of the Calumet Mine along the Ottawa River were prospected for zinc mineralization. New Calumet Mines Ltd. archives revealed that the company explored the area immediately around the mine for zinc mineralization. In their search they excavated 3 trenches reported south of the mine site. No further work on these occurrences is reported in the company's archives, which were preserved and consulted at the original mine office building present on the mine site, which is now converted into a house. We undertook a search for these old small trenches and were successful in locating them about 2.5 kilometers south of the Calumet mine (Fig. 8.7). The trenches were overgrown by vegetation, partially covered by sediments and filled with water. The three trenches are a meter-wide and tens of meters long and separated by tens of meters. A particular feature of these trenches is that they occur in the marble rather than in a volcano-sedimentary sequence like the one present at the Calumet deposit. Mineralization in these trenches is also different from Calumet in that they



Figure 8.17: Another example of disseminated stratiform sphalerite mineralization hosted by a silicate-rich dolomitic marble unit in the trenches south of the New Calumet Mine on the Grand-Calumet Island.

are not polymetallic and zinc dominant. Re-investigation of these trenches revealed the following features. The trenches are located in a siliceous dolomitic marble horizon containing up to 25% diopside and 15% forsterite and less than 5% calcite. The marble unit is characterized by a typical coarse grain size (average of 4-6 millimeters). Disseminated and semi-massive sphalerite mineralization occurs within this dolomitic marble where coarse-grained sphalerite (up to 4 millimeter in size) locally forms up to 40% of the unit by volume (Fig. 8.16 and 8.17). The meter-thick sphalerite mineralization occurs along a specific horizon along the stratigraphic bedding observed in the marble and intercepted along strike by the three trenches. The Calumet-Trenches showing is thus an occurrence of stratiform zinc sulfide mineralization hosted by a siliceous dolomitic marble.

Further prospecting in the area brought forward the discovery of a new zinc sulfide showing (Southern Calumet Island showing), to the south (Fig. 8.7). This new occurrence, located west of Bryson and 1.5 kilometers south of the Calumet Trenches showing consists of a roadside (6 by 3 meters) vertical outcrop of silicate-rich dolomitic marble. This showing was discovered by the use of the Zinc-Zap chemical indicator. The dolomitic marble unit is characterized by coarse-grained diopside (25%) and forsterite (10%) grains and less than 5% fine-grained interstitial calcite. Disseminated medium-grained sphalerite mineralization occurs along a 20 centimeter-thick horizon and is characterized by an average of 2 millimeter-thick grains, which can represent up to 6% of the rock by volume. The mineralized zone is concordant with the stratigraphic bedding observed on the outcrop and is traced along the entire length of the exposed outcrop (6 meters). The Southern-Calumet-Island showing is therefore characterized by stratiform disseminated zinc sulfide mineralization hosted by a silicate-rich dolomitic marble unit.

Geological mapping and prospecting along the Bryson-Renfrew area revealed the presence of several stratiform zinc sulfide occurrences throughout the entire area. A total of five discovered and newly-discovered zinc sulfide occurrences were described and investigated during the study. They are summarized in Appendix D. This data will be used to characterize the geological environment of the zinc deposits of the Bryson-Renfrew region.

8.4.7 Age Results for the Calumet Mine Sequence

Sampling from the fragmented amphibolite rock unit (Fig. 8.18a) hosting the Calumet Mine exhalative volcano-sedimentary massive-sulfide deposit was successful in extracting 4 zircons adequate for isotopic radiometric dating (Appendix C). Analyses of these zircons yielded an age of $1232 \pm 3.9/-2.7$ Ma (Fig. 8.18b) (Appendix C). This age is Mesoproterozoic and refines the age bracket of the Grenville Supergroup marbles of the Bryson-Renfrew area as discussed below.

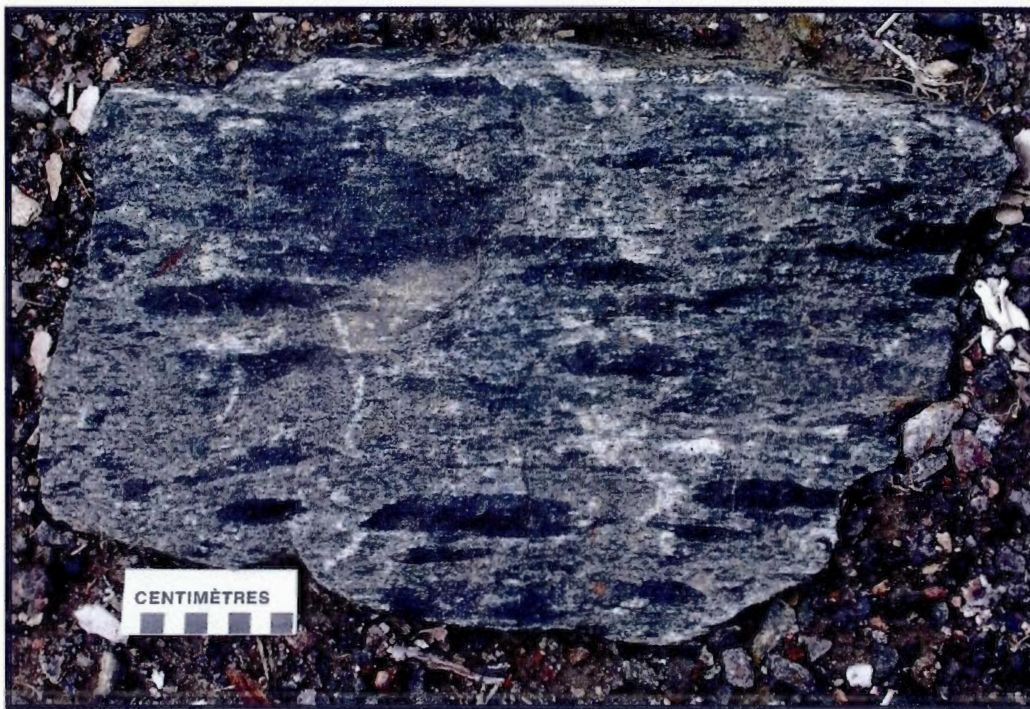


Figure 8.18a: Fragmented amphibolite sampled at the New Calumet Mine for radiometric zircon dating.

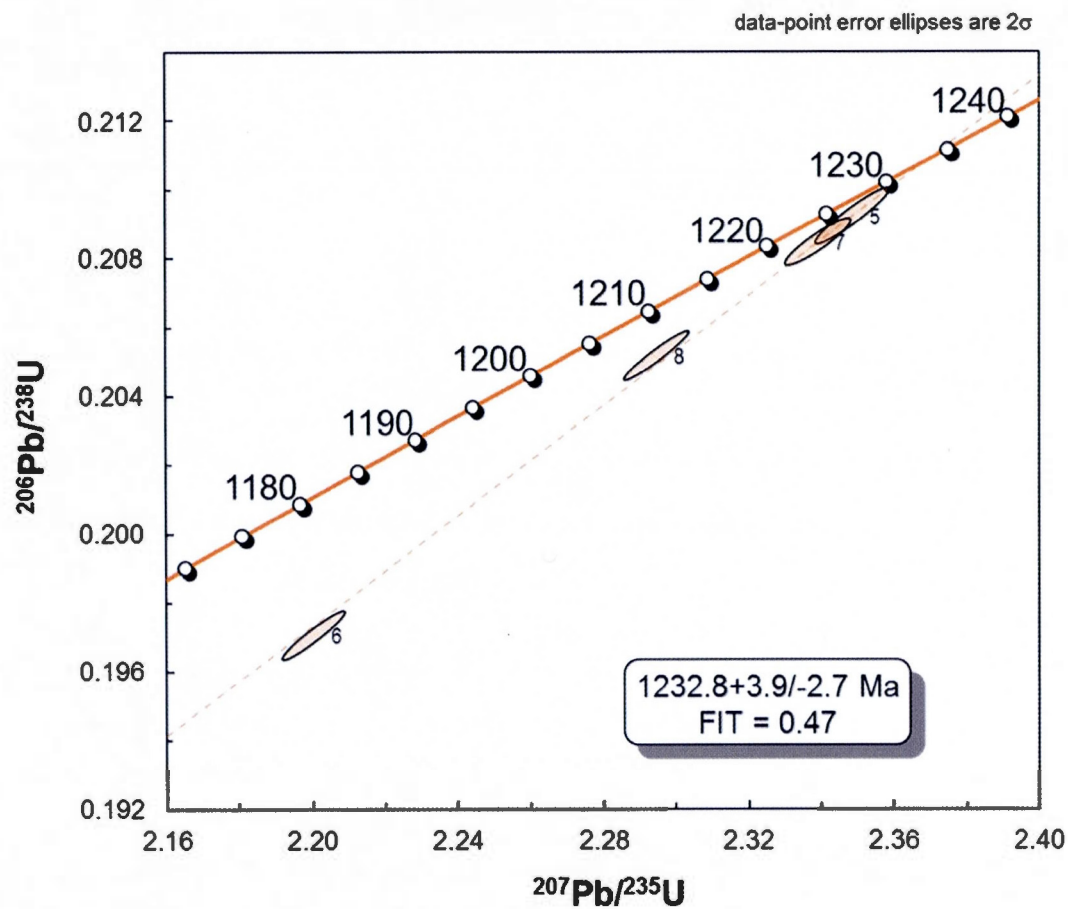


Figure 8.18b: Zircon U-Pb dating results are distributed along a regressed lines. The intersection of this line with Concordia yield an age of 1232.8+3.9/-2.7 (Appendix C) (David, 2009).

8.5 DISCUSSION OF THE BRYSON-RENFREW REGION RESULTS

The detailed field investigation and compilation of the Renfrew-Bryson region has produced important new information regarding the geological environment. The data described in sub-section 8.4 will be used to discuss and define the geological environment. The data also enables us to compare the Bryson-Renfrew region and its zinc sulfide mineralization with the mineralization present in the Balmat-Edwards district.

The following subjects will be discussed in this section. We will first present the general geological features resulting from the compilation and field data acquired during the study. We will then discuss the geological environment from the data acquired during our marble mapping campaign. Specific mineral occurrences will also be discussed in a regional overview of the Bryson-Renfrew marble belt. The zinc sulfide occurrences present in the area will be discussed and compared to Balmat-type SEDEX zinc mineralization, followed by discussion of the newly acquired radiometric age and its consequence on our understanding of the area.

Finally, all key features from the above discussions will be presented and reviewed in a geological environment perspective to determine if the Bryson-Renfrew area has a similar to the Balmat-type geological and depositional environment.

8.5.1 General Geological Features

The results from the general field campaign yields interesting features for the Bryson-Renfrew region. The geological sequence will firstly be discussed and compared to the geological environment of Balmat-type deposits. The structural features will then briefly be compared to the ones observed for the Balmat-Edwards district and the Maniwaki-Gracefield area.

The stratigraphic sequence of the area is characterized by amphibolites, which overlies a quartzo-feldspathic gneissic basement. The sequence is then overlain by quartzite and marbles. On top of the marbles lies a biotite paragneiss unit. The sequence was later intruded by granitic and anorthositic intrusions and also by the Chenaux gabbroic stock in the central and northern part of the Bryson-Renfrew region. The pre-metamorphic interpretation

for this sequence is a mafic volcanic basement deposited on an older gneiss basement (paleo-basement). The sequence is then overlain by quartz-rich pelitic sediments. With basin deepening, the sequence then grades into carbonates and finally black shales. This environment is typical of a local rift milieu with opening of an ocean basin. Variations in marble units in the area will be discussed in the following section. The same stratigraphic sequence was defined for the Balmat-Edwards district and for the Maniwaki-Gracefield SEDEX zinc sulfide deposits (deLorraine, 2001; Gauthier and Brown, 1986). Balmat-type SEDEX deposits form in a carbonate platform environment and such an environment is present in the Bryson-Renfrew area. Furthermore, like at the Balmat-Edwards district, the Bryson-Renfrew was affected by a strong regional metamorphism.

The Bryson-Renfrew region is characterized by polyphase deformation where at least two clearly phases of deformation have occurred. This type of deformation is observed throughout the Grenville Supergroup of Quebec, Ontario and northern New York state (Gauthier et al., 2004; Roger and Lapointe, 1998; deLorraine, 2001). For example, the Balmat-Edwards mining camp and the Maniwaki-Gracefield area are both characterized by a first phase of isoclinal folding which was later deformed and folded by a second deformation event. The folds observed at the exposed bedrock under the Portage-du-Fort dam represent an example of the regional folding pattern of the region (Fig. 8.5). In terms of deformation, what is observed at the outcrop scale usually reflects what is observed at a regional scale. While the structural deformation of the marble can locally be complicated, it is interesting from a metallogenic point of view because the type of folds observed in the region can concentrate and even thicken massive sulfide mineralization at folds hinges as is the case in the Balmat-Edwards district (deLorraine, 2001) and the Maniwaki-Gracefield area (i.e. Leitch deposit) (Gauthier et al., 2004). In conclusion, the Bryson-Renfrew structural features are in all ways similar to the type of deformation observed for Balmat-type SEDEX zinc sulfide deposits.

A feature that characterizes the Bryson-Renfrew area, when observing the geological map, is the abundance of marbles. Moreover, the marble belt can be continually traced between Bryson and Renfrew. This abundance of marbles, the typical stratigraphic sequence, the structural features and metamorphic grades are all similar and point towards Balmat-type

SEDEX zinc deposits geological environment. Detailed studies of the marble belt provide further evidence in favor of this hypothesis and are discussed in the next section.

8.5.2 Marbles Features

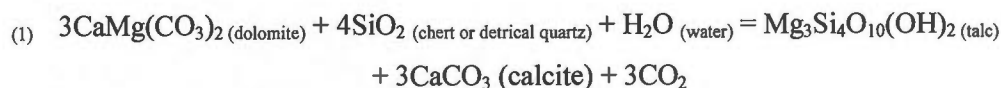
Results from our classification of the marbles into seven distinct units, and their distribution throughout the Bryson-Renfrew region, yields further key features to define the geological environment. Moreover, the mineral occurrences and particularities encountered in the marble belt provide evidence that will be discussed in the paragraphs below. General features of the marble belt will be discussed first, followed by the special features observed throughout the region. Finally, the environment will be compared to the Balmat-Edwards district.

Although, in general, calcitic marbles predominate in the Grenville Supergroup (Easton, 1992), the region under study is remarkable by the abundance of dolomitic marble units. The distribution of the different marble units is presented in figure 8.7. The established marble stratigraphic sequence grades from pure dolomitic marbles to siliceous dolomitic marbles. The sequence then grades to calcaro-dolomitic marbles and finally to calcitic marbles. Dolomitic and silicate dolomitic marbles units dominate the western northern, central and southern part of the studied region. Towards the central eastern section of the region, the marble sequence gradually grades to calcaro-dolomitic marbles to calcitic marbles on the eastern part of the map. An increase of the presence of calcite towards the east characterizes the region.

Prograde metamorphic reaction between carbonates and other minerals during metamorphism is used to characterize the pre-metamorphic characteristics of the defined marble sequence. At high metamorphic grades, dolomite reacts with quartz to form diopside and at higher temperatures, forsterite (reactions are presented below). Therefore the relative abundance of diopside-forsterite in the marble unit reflects the pre-metamorphic presence of pelitic quartz-rich sediments interlayered with the carbonates and/or the addition of silica in the system by hydrothermal activity. This relative abundance of diopside-forsterite, at a regional scale, also reflects the depth at which the sediments were deposited. A shallow-water

carbonate environment is more likely to have pelitic sediments (sand layers) eroded from the mainland interlayered with carbonates.

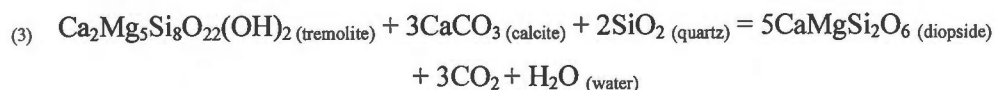
Prograde metamorphism of pure dolostone in the area does not result in mineral transformation and dolomite is simply recrystallized with increasing metamorphism. The prograde metamorphic reactions responsible for the mineral assemblage observed in the Bryson area are as follow (Winter, 2001). During prograde metamorphism of an impure dolostone, dolomite will react with quartz to form talc at temperatures from 150° to 250°C, following the reaction (1):



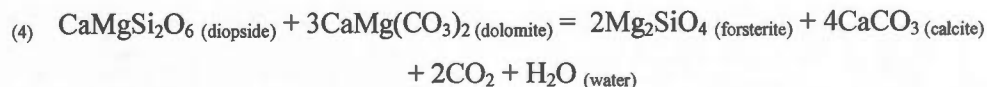
With increasing metamorphism and abundance of calcite the following reaction forms tremolite which occurs between 250° and 450°C:



At medium-high metamorphic grades, tremolite is replaced by diopside as further dehydration occurs. Note the loss of CO_2 and H_2O with prograde metamorphism. The following (3) reaction occurs from 450° to 600°C:



At higher metamorphic grade there is formation of a forsterite-bearing dolomitic marble which is characterized by the progressive dehydration of diopside to form forsterite (magnesium olivine). Reaction (4) highlights this prograde transformation:



The Bryson-Renfrew area was later affected by retrometamorphism which retrograded the granulite-facies mineral paragenesis. Rehydration of forsterite and diopside into serpentine nodules by retrometamorphic fluids was extensive in the region. This intense

retrometamorphism can be related to the Cambrian rifting episode association with the Ottawa-Bonnechère graben after the Grenvillian orogeny (Easton, 1992). This graben follows the Ottawa River where Paleozoic cover and glacial-lacustrine sediments can be observed as it is the case just north of Renfrew along highway 17 (Lumbers, 1982).

The pre-metamorphic characteristics of the Bryson-Renfrew marble sequence indicates that dolomite was initially precipitated in a shallow water basin. Sand layers were also deposited at the edge of the basin. The pre-metamorphic environment of the Bryson-Renfrew area indicates that the water basin was shallow to the west with direct dolomite precipitation and became progressively deeper to the east with the transition to calcite precipitation. The abundance, thickness and purity of the dolomitic marble unit in general are in agreement with this assumption. As the basin deepened, calcite precipitation became dominant. The marble sequence in the Bryson-Renfrew region is therefore characterized by deposition in a shallow-water environment, with typical calcite precipitation as the basin deepens towards the central-east of the region. Furthermore, the presence of pure dolomitic marble units, stratiform brucite and anhydrite layers enables us to further refine the geological environment as discussed below.

As mentioned above, not only dolomitic marble dominate the Bryson-Renfrew region, but their extreme purity also permitted exploitation of pure dolomitic marbles for magnesium metal, by Timminco in Haley (Ont) (Fig. 8.8 and 8.9). The presence of these highly pure dolomitic marble units strongly suggests an evaporitic environment. Further evidence of such an environment is given by the presence of meta-evaporites in the Bryson-Renfrew marble belt. These meta-evaporites consist of stratiform brucite and anhydrite layers.

Brucite is a magnesium hydroxide ($\text{Mg}(\text{OH})_2$) produced from the alteration of magnesium-rich minerals (Deer et al., 1992). Advanced serpentinisation and further alteration of forsterite, for example, can form brucite. Brucite is also commonly the alteration product of periclase (MgO), a commonly found mineral in marble produced by metamorphism of dolomitic limestone or dolostone. At near surface conditions, periclase readily alters into brucite (Deer et al., 1992). Brucite is therefore a mineral that directly indicates an abundance of magnesium. The stratiform brucite layers of the Maxwell deposit (12 million tons of

brucitic marble; Osborne, 1939), south of the town of Bryson, are particularly rich in brucite and generally devoid of silicate minerals. This paucity of silicate minerals and almost exclusive presence of brucite nodules strongly suggests that these layers were derived from the alteration of periclase-rich dolomitic marbles formed during the metamorphism of magnesium-rich dolomite limestone. The presence of stratiform brucite layers at Bryson therefore indicates that the area was characterized by a certain level of magnesium saturation during metamorphism. Moreover, this abundance of magnesium is characteristic of an evaporitic environment. Modern analogues can be found along the Persian Gulf where sabkhas-type environments are present (Pomerol et al., 2000). Evaporation of seawater in a restricted basin or sabkha environment will initiate precipitation of gypsum ($\text{CaSO}_4 + 2\text{H}_2\text{O}$), a hydrated anhydrite. This precipitation gradually enriches seawater with magnesium with progressive removal of calcium forming a magnesium-rich brine (Pomerol et al., 2000).

Anhydrite, an anhydrous calcium sulfate (CaSO_4), is also occurs in the Bryson-Renfrew area. We noted its presence in drill core near the Calumet Mine west of the town of Bryson, and near Cadieux south of Renfrew (Osborne, 1944; Roger and Lapointe, 1998). We explained earlier that because of the rapid dissolution of anhydrite by surface waters, anhydrite could only be observed in core from deep diamond drilling holes. This feature rendered the study of the presence of anhydrite difficult when no drilling data was present. Nevertheless, anhydrite layers do occur in the Bryson-Renfrew area and they are stratiform and probably stratiform (Brown, 1973). Stratiform anhydrite forms in an evaporitic environment (Whelan et al., 1990; Pomerol et al., 2000). Direct precipitation of primary anhydrite can occur from evaporitic brines rich in dissolved calcium and sulfate (SO_4^{2-}) when certain chemical conditions are met (for example, when the brine contains an excess of sodium or potassium chloride with temperatures above 40° Celsius) (Deer et al., 1992; Pomerol et al., 2000). Hydrated calcium sulfate, gypsum ($\text{CaSO}_4 + 2\text{H}_2\text{O}$) also precipitates from sulfate stable evaporitic brines (Deer et al., 1992). With prograde metamorphism and its dehydration of hydrous minerals, gypsum is dehydrated into anhydrite at granulite-facies condition. Because polyphase deformation and prograde metamorphism obliterated the primary sedimentary features of these anhydrite layers, we cannot determine whether anhydrite or gypsum was the primary mineral without more geochemical work. However, for the purpose of this study, it does not matter because both anhydrite and gypsum are indicative

of an evaporitic environment. Sulfate-stable evaporitic brine also points out that the environment is oxidized. If sulfate in dissolved water were to be introduced into a reducing anoxic environment, the sulfate (SO_4^{2-}) would convert into its reduced form H_2S by the action of sulfate-reduction bacteria (Whelan et al., 1990; Pomerol et al., 2000). The stratiform nature of the layers makes us conclude that anhydrite is characteristic of the regional depositional environment and not an exclusive local phenomenon.

The marble belt of the Bryson-Renfrew region is therefore characterized by the dominance of dolomitic marbles. The presence of pure dolomitic marbles and stratiform meta-evaporites both strongly indicate that the geological environment of the northern, western and southern part of the studied region was a shallow-water, oxidized (sulfate-stable) evaporitic carbonate platform environment. Such an environment is in many ways similar to the one proposed for Balmat-type SEDEX zinc deposits. Balmat-type SEDEX deposits were defined and characterized by hydrothermal brines deposited in a shallow-water, oxidizing and evaporitic carbonate platform environment. The same depositional environment prevails in the Bryson-Renfrew region. The next section presents a discussion on the zinc sulfide occurrences encountered during the mapping campaign and their association with specific marble lithologies and facies.

8.5.3 Zinc Sulfide Mineralization

The systematic reconnaissance of the marble facies of the Bryson-Renfrew region and their associated zinc mineralization enables us to study the association between them. In this section, we will summarize all known and newly-discovered zinc sulfide mineralization and link them to a particular stratigraphic position. They will then be classified by deposit-type and compared to Balmat-type SEDEX deposits.

Geological marble mapping and zinc prospecting in the Bryson-Renfrew area reveals the following features: All zinc sulfide mineralization is stratiform, consists of disseminated to semi-massive coarse-grained sphalerite mineralization, is generally poor in iron and lead sulfides, is associated with dolomitic marble horizons, and is characterized by the presence of nearby stratiform anhydrite in the stratigraphic sequence. Moreover, finely-disseminated sphalerite mineralization presents an affinity with silicate-poor dolomitic marble units while

higher sphalerite concentrations are associated with silicate-rich dolomitic marbles. Siliceous dolostones are then the pre-metamorphic host unit for this zinc sulfide mineralization. These features confirm the particular lithological associations (i.e. disseminated sphalerite in dolomitic marbles and higher concentrations in silicate dolomitic marbles) that have been first described by Sangster (1970) and later by Gauthier and Brown (1986) for SEDEX zinc sulfides deposits and occurrences.

Thus, the Bryson-Renfrew zinc sulfide mineralizations are SEDEX-type and are hosted by a siliceous dolomitic marble unit. These features are similar in many way to those observed for Balmat-type SEDEX zinc sulfide deposits. Our geological marble reconnaissance mapping and zinc prospecting campaign was successful in tracing the different marble units and their zinc sulfide mineralization throughout the entire Bryson-Renfrew region.

8.5.4 Grenville Supergroup Age Determination

The Grenville Supergroup of Quebec and Ontario is Mesoproterozoic in age (Easton, 1992). Until the present study, the Bryson-Renfrew area only had an upper age bracket as determined from the timing of the Chenaux gabbro stock in the central region. The Grenville Supergroup marbles of the area do not contain abundant favorable lithologies for radiometric age determination (i.e. marbles do not contain zircons). We reported about that the Chenaux gabbro which crosscuts the marble belt was dated at about 1100 Ma (Lumbers, 1982). We also pointed out that the region is host to an amphibolite-hosted massive polymetallic sulfide of unknown age. A radiometric age determination of the fragmented amphibolite horizon from the Calumet deposit was undertaken to determine the lower age bracket of the region's marble belt and determine the age of the Calumet mineralization.

Results confirm that the Bryson-Renfrew marble belt is Mesoproterozoic. The age bracket from the underlying amphibolite unit and from the Chenaux intrusion yields 1232.8 ± 3.9 – 2.7 Ma (Appendix C) and 1100 Ma (Lumbers, 1982)) respectively.

Two hypothesis exist for the age of the Calumet Mine (refer to chapter 2): (1) Calumet is an older basement for the Grenville Supergroup like the Montauban gold deposit, or (2) the Calumet deposit is Grenville Supergroup age. The radiometric datation results

yielded $1232.8 \pm 3.9/-2.7$ Ma (Appendix A). This confirms that the polymetallic Calumet deposit belongs to the metallogenic epoch of the Grenville Supergroup rather than the epoch of the Montauban Group (~ 1.45 - 1.39 Ga). The first hypothesis as proposed by Gauthier et al. (2004) can therefore be rejected. This conclusion forces us to consider the exhalative event at the origin of the Calumet deposit as contemporaneous to the SEDEX zinc sulfide deposits and occurrences present in the marbles of the Bryson-Renfrew region. This has important considerations on our study and we therefore must include the Calumet volcanic exhalative Zn-Pb-Au-Ag mineralization in our metallogenic interpretation.

Our objective with this study is not to re-evaluate the Calumet deposit because it is extensively well studied and is the main subject of a memoir and two theses: A.L. Sangster (1967; 1970) and later Jourdain (1993). However the Calumet deposit was never considered in a regional context before and it is why we decided to obtain a radiometric age determination for the mineralization. Jourdain (1993) compared the Calumet and Montauban deposits and proposed that they are similar, which incited Gauthier et al. (2004) to propose that both deposits belong to the same metallogenic epoch and represent an older basement on which the Grenville Supergroup rests. The work of Nadeau and Van Breeman (1994) on the metamorphosed mafic pyroclastic rock unit hosting the Montauban deposit determined the age of 1.45 - 1.39 Ga for the mineralization, which is older than the Grenville Supergroup marbles. The metallogenic epoch for the deposition of grenvillian polymetallic exhalative zinc-lead-gold-silver mineralization was thus considered to be around 1.45 - 1.39 Ga. But our determined age for the Calumet mineralization ($1232.8 \pm 3.9/-2.7$ Ma) now suggests that there is a second event of deposition of volcanogenic massive sulfide deposits in the Grenville, a first one at 1.45 - 1.39 Ga and a second episode at 1.23 Ga.

The Calumet volcanic exhalative massive sulfide deposit (VMS) can now be included in a regional context and depositional environment with the deposition of SEDEX zinc deposits. This indicates that the age of hydrothermal exhalative activity for the VMS and SEDEX deposits in the area is post emplacement of the Chenaux intrusion and therefore not related with it. So along the same chronostratigraphic horizon there is simultaneous deposition of mafic volcanic and carbonate rock units and with the presence of an active VMS hydrothermal system, regional zinc-dominant exhalites are also deposited. Gauthier and

Brown (1986) and Gauthier et al., (1987) demonstrated the formation of Zn-Fe meta-exhalites in the extensions of the SEDEX massive sulfide deposits in the Maniwaki-Gracefield area. In the same matter, distal exhalites issuing from the Calumet VMS deposit could precipitate zinc-dominant horizons such as those observed on the Grand-Calumet Island zinc sulfide showing.

Our study is focused on the marble-hosted SEDEX zinc deposits but further discussion in section 4 will put the Calumet VMS and SEDEX deposits in its regional geological context.

8.5.5 Bryson-Renfrew Geological Environment

Our study of the Bryson-Renfrew region enabled us to characterize its geological environment for the first time. Marble lithology differentiation and the in-depth study of its zinc mineralization were conducted to identify the key evidence required to characterize such an environment. This section will summarize the geological environment of the Bryson-Renfrew region and compare all the discussed features with those of Balmat-type SEDEX zinc sulfides deposits.

The Bryson-Renfrew is characterized by a stratigraphic sequence dominated by marbles, underlain by amphibolites and quartzo-feldspathic gneiss and overlain by diopsidite, quartzite and paragneiss units. Similar stratigraphic sequences were first described by Brown and Engel (1956) for the Balmat-Edwards district and later by Gauthier and Brown (1986) for the Maniwaki-Gracefield area. Both areas are characterized by Balmat-type SEDEX zinc mineralization. Moreover, the Bryson-Renfrew region was affected by metamorphic grades reaching granulite-facies and polyphase deformation resulting in refolded isoclinal fold. Such features are also present at the Balmat-Edwards district and the Maniwaki-Gracefield area (Brown and Engel, 1956; Gauthier and Brown, 1986). However, deLorraine (2001) demonstrate that zinc mineralization was premetamorphic in origin. Furthermore, Cartwright and Oliver (2000) argue that the formation of massive Zn-Pb deposits by metamorphic fluids during regional metamorphism is not likely. The marble mapping campaign revealed that the Bryson-Renfrew region is dominated by dolomitic marble units and by the presence of meta-evaporite. These features enabled us to propose that the Bryson-Renfrew region formed in a

shallow-water, oxidizing and evaporitic, carbonate platform environment. Cooke et al. (2000) described a similar environment for the McArthur SEDEX deposits in Australia (McArthur-subtype SEDEX). In section 1, we reviewed and further classified the Balmat-Edwards and Maniwaki-Gracefield SEDEX deposits as McArthur subtype SEDEX deposits, because of the similar geological environment. We can then conclude that the Bryson-Renfrew region geological environment is similar to the depositional environment for Balmat-type SEDEX zinc sulfide deposits. Moreover, the Bryson-Renfrew region does not only possesses a similar environment, but similar to Balmat-type SEDEX zinc sulfide occurrences (Calumet Island, Calumet Trenches, Portage-du-Fort and Renfrew) and deposits (Cadieux) were encountered in the area. Sangster's (1970) and Gauthier's and Brown (1986) lithologic association of disseminated sphalerite hosted by dolomitic marbles and higher concentration of sphalerite associated with silicate-rich dolomitic marbles is confirmed in the Bryson-Renfrew region. The stratiform nature of the mineralization with the presence of nearby meta-evaporites in the stratigraphic sequence are all features characteristic of Balmat-type SEDEX mineralization.

The comparison of the Bryson-Renfrew region with the well-understood and widely distributed Balmat-type SEDEX zinc sulfide mineralization reveals that they are both similar. The Bryson-Renfrew region can therefore for the first time be classified as a common Balmat-type SEDEX zinc sulfide environment.

8.6 CONCLUSION

The Bryson-Renfrew region was selected for our study because of the unique opportunity it afforded to study the relationship between SEDEX zinc sulfide and non-sulfide deposits (i.e. Balmat-type versus Franklin-type). In order to do this, the first step was to confirm that the Bryson-Renfrew region geological milieu was similar to the Balmat-type geological environment. The main reason for this step is, as previously stated, that Balmat-type SEDEX zinc sulphide deposits genesis and formation are well understood, widely distributed and common throughout the Grenville Supergroup. On the other hand, Franklin-type SEDEX non-sulfide zinc deposits are less well understood, scarce and restricted to the New Jersey Highlands more than 500 kilometers south of the Grenville Supergroup. Therefore, studying Franklin-type mineralization in the well understood geological

environment of the Balmat-type SEDEX zinc mineralization could propose that they can occur outside the New Jersey Highlands associated with SEDEX mineralization.

Our study revealed that the Bryson-Renfrew region is similar to the Balmat-type geological environment. The region's SEDEX zinc sulfide mineralization was deposited in a shallow-water, oxidized and evaporitic, carbonate platform environment. The first part of our study is thus successfully completed: The Bryson-Renfrew region is characterized by a conventional geological environment typical of Balmat-type SEDEX mineralization.

CHAPTER IX

BRYSON ZINCIAN MAGNETITE OCCURRENCE

9.1 INTRODUCTION

To study the relationship between Balmat and Franklin-type SEDEX deposits, two conditions, that were never previously met, were required: 1) The Balmat-Renfrew region must contain Balmat-type zinc mineralizations in a Balmat-type SEDEX geological environment. 2) Franklin-type SEDEX non-sulfide zinc mineralization must be confirmed in the same area. The first condition was addressed and answered in the previous chapter 3. The second step consists in confirming the presence of Franklin-type mineralization outside the New Jersey Highlands. Gauthier's et al. (1987) discovery of a zincian magnetite near the town of Bryson raised the possibility that other Franklin-type deposits could be found elsewhere. However, the Bryson occurrence was never studied further and determined to be a Franklin-type mineralization. The Bryson-Renfrew region was thus selected to solve our problem, specifically is there a relationship between both end-members of SEDEX deposits?

To resolve this issue, we firstly need to find evidence of non-sulfide zinc mineralization in the Grenville Supergroup marbles of the Bryson-Renfrew region. We will therefore review the Bryson zincian magnetite occurrence (Gauthier et al., 1987).

9.2 DESCRIPTION OF THE BRYSON ZINCIAN-MAGNETITE SHOWING

In a review of Precambrian iron deposits, Gauthier et al. (1987) present a synthesis of marble-hosted iron formations present in the Maniwaki region (Quebec). This iron formation called the Chemin-de-Piché iron formation was described in section 1. As mentioned above, this magnetite-breunnerite-fosterite horizon is interpreted to be a metamorphosed iron-rich

siderite halo enveloping and related to the SEDEX zinc sulfide deposits. Local disseminated sphalerite is present along this iron formation. With prograde metamorphism, the iron-rich siderite dissociates to form magnetite and graphite. In their synthesis, Gauthier et al. (1987) also noted the presence of a magnetite horizon near the village of Bryson, Quebec, 90 kilometers to the southwest of the town of Maniwaki. However, further analysis revealed that this iron formation was different than the Chemin-de-Piché iron formation.

Microprobe analysis of the Bryson occurrence revealed the presence of a zinciferous magnetite (Gauthier et al., 1987). Analyses revealed that up to four percent ZnO occurred in the magnetite grains (Gauthier et al., 1987). The pre-metamorphic nature of this horizon was interpreted as a zincian and iron rich carbonate "mud" (Gauthier et al., 1987). Prograde granulite-facies metamorphism dissociated zinc and iron from the carbonate "mud" which then combined to create the zinciferous magnetite. Gauthier's et al. (1987) interpretation is in many ways similar to that of Squiller and Sclar (1980) for the origin of Franklin-type deposits. This suggests that the Bryson zincian magnetite occurrence could be related to Franklin-type SEDEX mineralization.

9.3 CONCLUSION

The discovery of the Bryson zincian magnetite shown by Gauthier et al. (1987) raises the possibility that Franklin-type mineralization might occur outside the Franklin-Sterling Hill district. However, a reinvestigation of the Bryson occurrence is required at the original site of discovery and the surrounding area to unequivocally demonstrate the presence of Franklin-type mineralization in the Grenville Supergroup marbles near Bryson.

To accomplish this task, additional geological mapping and prospecting in the vicinity of the Bryson zincian magnetite occurrence was undertaken. The next section describes the data collected in the Bryson area and its significance.

CHAPTER X

THE BRYSON AREA

10.1 INTRODUCTION

The discovery at the town of Bryson (Qc) of a magnetite occurrence containing 4 percent franklinite component (ZnFe_2O_4) suggest that there could be a potential for other Franklin-type deposits. The objective of our thesis is to determine if a relationship exists between SEDEX zinc sulfide and non-sulfide deposits, and goes without saying that the Bryson area was selected because of its potential for this mineralization type, as identified by Gauthier et al. (1987). The Bryson area is part of the Bryson-Renfrew region, described previously in chapter 8, which is characterized by a shallow-water evaporitic carbonate platform environment hosting SEDEX zinc sulfide deposits (Balmat-type). Thus, as mentioned earlier, this area affords us a unique opportunity to study the relationship between both end-members of SEDEX deposits. Reinvestigation of the Bryson non-sulfide occurrence and surrounding area should enable us to conclude if the Bryson occurrence is a Franklin-type mineralization.

In order to accomplish this we will firstly briefly present the Bryson occurrence location area and geological context, obtained by our regional Bryson-Renfrew study. We then explain the methodology used for the geological mapping and prospecting campaign around the town of Bryson. We will then present and discuss the geological data obtained during the campaign in order to demonstrate that the Bryson region hosts non-sulfide zinc mineralization.

10.2 LOCATION AND GEOLOGICAL CONTEXT

The Bryson area is located in the northern part of the Bryson-Renfrew region (chapter 8), 30 kilometers north of the Cadieux SEDEX zinc sulfide deposit near the town of Renfrew (Ont). The area around the town of Bryson is characterized by medium topography characterized by hills and valleys.

The Bryson area, as mentioned in chapter 8, is located in Mesoproterozoic Grenville Supergroup marbles. The Bryson-Renfrew area is characterized by a metamorphosed shallow-water evaporitic carbonate platform environment where SEDEX zinc sulfide deposits were deposited. High metamorphic grade and polyphase deformation characterizes the Bryson-Renfrew region. The Bryson area is characterized by an abundance of dolomitic and silicate-rich dolomitic marbles units (Fig. 8.7). The Calumet Mine amphibolite-hosted polymetallic volcanogenic massive sulfide deposit is located approximately 6 kilometers west-northwest from the town of Bryson. SEDEX zinc sulfide occurrences (Calumet Island and Calumet Trench) occur 5 kilometers west of the town of Bryson. The Bryson zincian magnetite discovery is located along a roadside outcrop 30 meters east of the bridge between the town of Bryson and Grand Calumet Island.

The Bryson area, like the Bryson-Renfrew region, was mapped at a regional (1: 125 000) scale by the government of Quebec (Katz, 1976). Osborne (1944) compiled a geological map of the Grand-Calumet Island around the Calumet polymetallic deposit at a scale of about 1:40 000. However, the available data in the Bryson area was inadequate and incomplete for the purpose of evaluating the presence of Franklin-type mineralization. Thus, further geological data is required to refine and characterize the geological environment of the Bryson non-sulfide zinc occurrence around the Bryson zincian magnetite discovery. The next section presents our methodology used to achieve this goal.

10.3 METHODOLOGY

The geological context of the Bryson area was characterized following detailed outcrops description. For this study, a total of more than 120 different outcrops (Appendix F) were mapped, enabling us to define (1) the local general stratigraphic column of the Bryson area, (2) the local structural characteristics, (3) identify the different marble units present in the area, and (4) report on known and new occurrences of non-sulfide zinc mineralization in

the studied area. Selected outcrop samples were collected for the purpose of obtaining further mineralogical data for a detailed laboratory mineralogical study which will be discussed in chapter 11 below.

The same approach used for the geological mapping of the Bryson-Renfrew region was used for the mapping campaign conducted at a higher level of detail around the town of Bryson. Outcrops were described along the roadside and then along traverses following favorable marble lithology. Each outcrop was studied as described in chapter 8.3.1 (site description, localization, lithology, marble type, structural measurements, etc.). When marbles were present, a more detailed description was made (dolomite/calcite ratio, mineralogy, structural measurements of the stratigraphic horizon, etc.). The objective of this campaign was to characterize and resample the Bryson zincian magnetite occurrence and to uncover new non-sulfide zinc occurrences in the nearby surroundings. Therefore, special attention was given to zinc prospecting. As in chapter 8.3.1, the use of the Zinc-Zap (Landry et al., 1995) reactant proved useful in identifying zinc mineralization. Disseminated zinc silicates and/or oxides are more difficult to distinguish from other minerals (exotic uncommon mineralogy) when they are fine-grained and mixed with carbonates and silicates. While we previously explained that Zinc-Zap is more effective on disseminated sphalerite than massive sulfides, the reaction is even stronger on zinc silicates and oxides. Chapter 8.3.1 presents in further detail the methodology used for the geological mapping and zinc prospection of the Bryson area. All collected data were compiled into a computer database and spatially analyzed with the use of GIS software (refer to chapter 8.3.3 for more details).

In summary, systematic geological mapping and prospecting with the use of Zinc-Zap enabled us to identify several new non-sulfide zinc occurrences in the surrounding area of the town of Bryson. The following section presents the data collected during our study.

10.4 RESULTS

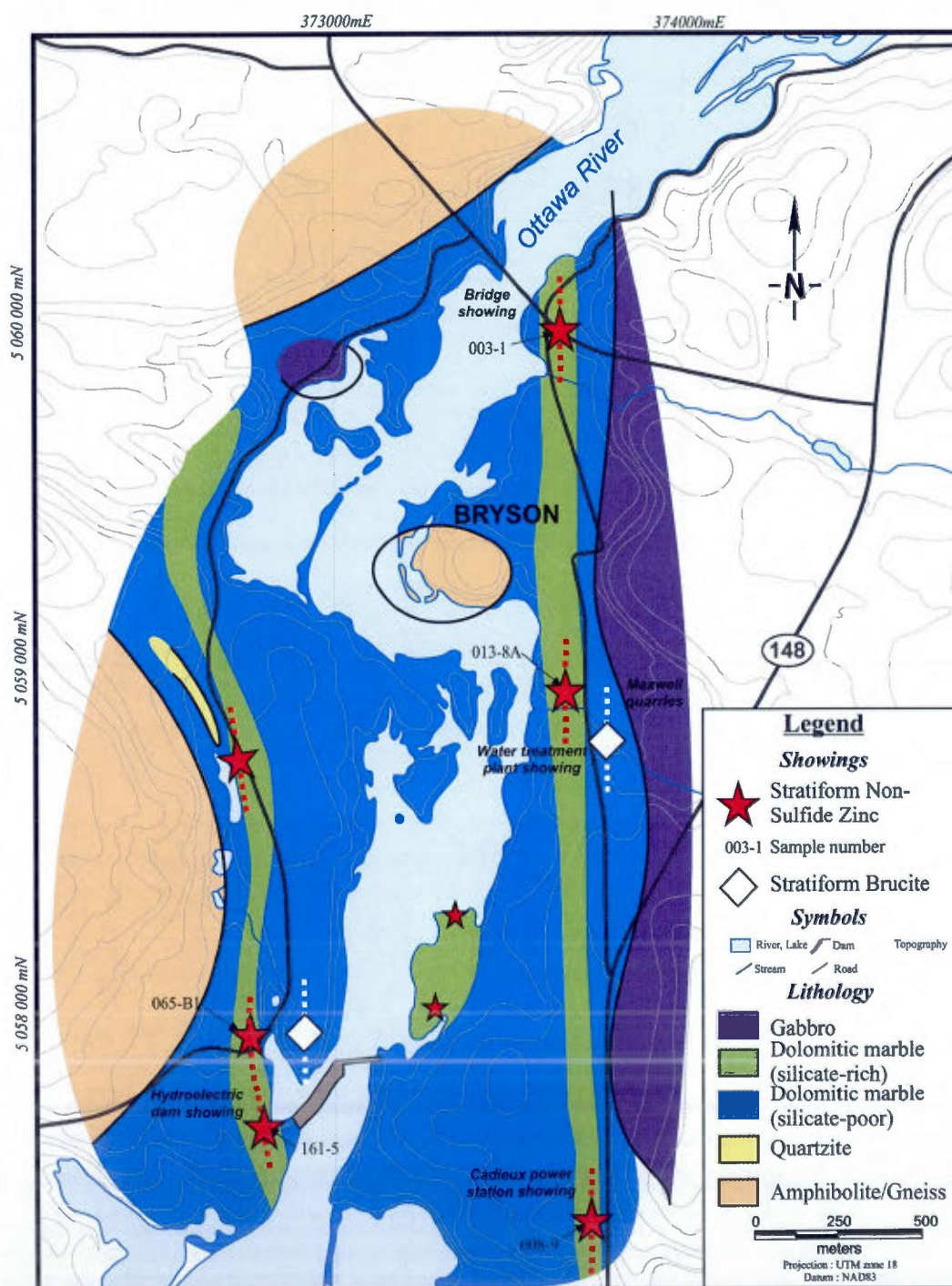


Figure 10.1: Geological map of the immediate area around the town of Bryson(Qc) showing the distribution of non-sulfide zinc occurrences reported. Name and sample number of reported showings is shown on this map.

10.4.1 Geological Map

To determine if the Bryson occurrence area can be related to Franklin-type non-sulfide zinc mineralization, we must characterize the local geologic features and identify and map zinc occurrences. These steps required us to conduct a detailed geological mapping and zinc prospecting campaign around the Bryson zincian magnetite occurrence. The main result of this study is the publication of a geological map of the Bryson area (Fig. 10.1) showing marble lithology and its zinc mineralization.

Systematic mapping, at a 1:10 000 scale, in a 6 km² area surrounding the original discovery site the Bryson zincian magnetite showing has provided us the required geological data necessary to identify the deposit-type of the region's zinc mineralization. The data will be presented in the following order: (1) The general geological and structural features of the area, (2) lithological characteristics of the marble belt present at Bryson and its non-zinc particular mineral occurrences, and (3) observations made on the known and newly discovered non-sulfide zinc mineralization.

10.4.2 Geological and Structural Features

Description and compilation of outcrops provided the necessary data to establish the stratigraphic column of the Bryson area. Lithological units were differentiated and structural measurements were used to trace the units throughout the Bryson area. The lithological units will be described in the following paragraphs and then their structural features will be briefly described.

The established stratigraphic column for the Bryson area includes a amphibolite/gneiss unit overlain by quartzite and then by marble. Finally, a gabbro intrudes the sequence in the western part of the area. Each unit is described below:

Gneiss/amphibolite: This unit is characterized by medium-to fine-grained quartzofeldspathic gneiss with inclusions of black biotite-amphibole-rich layers. Biotite and amphibolite typically represent up to 40% by volume with an average grain size of 1 to 2 millimeters. Quartz, plagioclase and potassic feldspars are equally distributed and possess a grain size of 1 to 2 millimeters. The unit is generally not magnetic (weakly locally when

amphibolite is present). The amphibolite layers are characterized by 20% biotite and 40% dark amphibole. Mafic minerals are concentrated in millimetric melanosomes along the developed foliation and grain size averages 1 to 2 millimeters.

Quartzite: Quartzite layers are locally present along the west shore of the Ottawa River west of Bryson. Medium-to fine-grained quartz is the main constituent of this unit. Quartz grain size averages 2 millimeters. Quartz represents more than 85% of the rock unit. Other accessory minerals include white diopside, forsterite grains altered to serpentine nodules, tremolite and feldspar locally.

Marble: Marble units and their facies will be described in more detail in the following section. However, marble is the main lithologic constituent of the Bryson area and characterizes the central portion of the map.

Gabbro: A coarse-grained gabbro intrusion is present in the western part of the Bryson area. This gabbro contains 35% pyroxene, 35% amphibole and 30% plagioclase with an average grain size of 2 to 4 millimeters. This unit is magnetic and is in cross-cutting relationship with the marble belt. This gabbro belongs to the Chenaux intrusive also present in the Bryson-Renfrew region near Portage-du-Fort. Contact between the marble belt and the gabbro is not well exposed in the area and does not reveal an intensive metasomatic event in the Bryson area. However, the metasomatic effect of the Chenaux gabbro has been observed at the Portage-du-Fort Island road-cut. There, as described in chapter 8, a ten-centimeter thick metamorphic contact aureole was observed. Chemical metasomatic manganese exchanges between the marble and the gabbro resulted in a red-colored marble and were limited to a couple of centimeters at most (Fig 8.2).

Structural measurements were made in the Bryson area. The gneiss/amphibolite unit is characterized by a well-developed foliation. Primary stratigraphic features, such as bedding, are therefore not preserved in this unit because of the effects of dynamo-metamorphic processes. However, as presented in a previous section, bedding was preserved and observed in the marble units. Again, this feature, first described by Gauthier and Brown (1986) and later by Gauthier et al. (2004), is explained by the high reactivity of carbonates with silicate minerals during prograde metamorphism and the presence of evaporitic

decollement that absorbs the deformation (Pomerol et al., 2000). Because primary bedding is preserved, we can characterize the stratiform nature of the zinciferous beds. Our structural study of the marble outcrops indicates that the first phase of deformation is characterized by isoclinal folding. A second phase of deformation refolds the first phase into wider open folds (i.e. observed near Portage-du-fort, figure 8.5). Such features are identical to the ones observed throughout the Bryson-Renfrew area, and therefore typical of other marble-hosted SEDEX environments in the Grenville Supergroup (i.e. Balmat-Edwards, Maniwaki-Gracefield, Franklin-Sterling Hill district).

Because the marble sequences host the Bryson zircon magnetite showing and that there is potential for others, marbles were more studied. Therefore, less attention was given to the description of the other lithological units. The next section presents our results and observations for the Bryson marble belt.

10.4.3 Marble Features

The Bryson marble belt yields particular features that are presented in this section. The marble belt of the Bryson area is characterized by two marble units. These two marble units will be described as well as the particular presence of brucite horizons (outlined during the regional Bryson-Renfrew compilation in chapter 8).

Marbles units were distinguished into seven different marble units by our mapping in the Bryson-Renfrew area (Fig. 8.6). This marble classification system was applied to the Bryson area. Field data show that dolomitic marbles (pure and silicate-rich) dominate the Bryson area where they are also exclusive. Two different marble units were encountered during the systematic mapping around the town of Bryson; common and abundant relatively silicate-poor and dolomite-rich dolomitic marble and local layers of silicate-rich dolomitic marble horizons.

The major marble unit present in the Bryson area is a crystalline coarse-to medium-grained dolomitic marble. This unit generally contains more than 85% euhedral to idiomorphic dolomite grains with a varying grain size between 3 to 9 millimeters. Interstitial fine-grained xenomorphic calcite (less than a 1 millimeter grain size) can represent up to 5% volume of the rock unit. Thus, the dolomite to calcite plus dolomite ratio of this unit is

greater than 90% throughout the Bryson area. This silicate-poor unit is observed to contain up to 10% silicate minerals. These silicate minerals include, in order of decreasing abundance, forsterite altered into serpentine nodules, diopside, chondrodite, phlogopite, pyrite, pyrrhotite and finally graphite. The sulfides and graphite are uncommon and occur as traces (less than 1% volume). Silicate minerals are concentrated in centimetric bands. This dominant marble unit ranges from dolomite-pure metric horizons to centimetric bands containing up to 10% of the above listed silicate minerals.

The second marble unit identified in the Bryson area is again a dolomitic marble. However, this unit is rich in silicate minerals. Like the previous unit, the marble is crystalline and coarse-to medium-grained, due in part to the high metamorphic grades that affected the region. But, euhedral to idiomorphic dolomite grains generally represent up to 55% volume of the unit with an average grain size between 3 and 9 millimeters. Interstitial fine-grained (less than 1 millimeter) calcite constitutes up to 5% of the marble unit. The dolomite to calcite plus dolomite ratio is greater than 90% and reflects the strong dolomitic nature of the Bryson marble belt. This silicate-rich marble unit contains up to 40% volume silicate minerals disseminated and concentrated in centimetric to metric bands. This layering represents the primary bedding. Forsterite grains altered in serpentine nodules and diopside grains are the most common calc-silicate minerals found in the unit. Forsterite altered to xenomorphic yellow to dark greenish serpentine nodules can represent up to 25% volume with a grain size between 3 and 8 millimeters. Idiomorphic diopside grains are commonly dark to pale green-colored, have an average grain size of 4 millimeters and represent up to 10% of the rock. The other subordinate common minerals, in decreasing relative abundance, are chondrodite, pyroaurite, phlogopite, apatite, pyrite and pyrrhotite. Pyrite and pyrrhotite are very scarce and are usually spatially associated with phlogopite-diopsidite pluri-centimetric nodules.

Several notable features were observed during the study of the Bryson area marble belt. First of all, the marble belt is exclusively composed of dolomitic marbles, as described in the previous paragraphs. Secondly, a brucite deposit occurs south of the town of Bryson. Finally, the presence of pyroaurite along certain marble outcrops around the town of Bryson is interesting and will be discussed below.

The old Maxwell brucite deposit (12 Million tons of brucitic marble; Osborne, 1939) in the town of Bryson was discussed in our study of the Bryson-Renfrew area. Stratiform xenomorphic coarse-grained brucite nodules are hosted by the silicate-poor dolomitic marble of the Bryson area. This unit contains up to 50% brucite nodules with an average size of 3 to 12 millimeters. The brucite nodules are disseminated and are concentrated in a 3 meter-thick dolomitic marble horizon (Fig. 8.12). Accessory minerals, representing less than 10% of the unit, include white to pale-orange colored chondrotite with a 5 millimeter grain size. A new stratiform brucite occurrence was discovered on the western bank of the Ottawa River, southwest of the town of Bryson (described in chapter 8). Apart from the presence of brucite-rich dolomitic marble horizons, the Bryson area also contains pyroaurite-rich layers (Fig. 10.3). Pyroaurite is observed along the road-cut east of the Bryson bridge and also along a second road-cut near the Cadieux power station to the south. Pyroaurite ($\text{Mg}_6\text{Fe}_2(\text{CO}_3)(\text{OH})_{16} \cdot 4(\text{H}_2\text{O})$) occurs as 3 to 4 millimeter yellowish nodules in the silicate-rich facies of the dolomitic marbles.

Field work show that the Bryson's area marble belt is characterized by a silicate-rich and also a silicate-poor dolomitic marble unit. Brucite and pyroaurite occurrences are reported in this marble belt and their significance will be discussed below. The next section presents our field data results obtained from prospecting for zinc silicates and oxides.

10.4.4 Non-Sulfide Zinc Mineralization

The main objective of our research in the Bryson area is to confirm the presence of non-sulfide zinc mineralization and characterize the host environment. The first step was to visit the Bryson zincian spinel occurrence and then to search the Bryson area for other non-sulfide zinc mineralization. This section presents data collected during the visit of the original discovery site and the general prospecting campaign.

The Bryson zincian magnetite discovery outcrop was successfully located on the field near the bridge between Bryson and the Grand Calumet Island. Investigation and resampling of this outcrop revealed the following features. A stratiform disseminated magnetite horizon is present in a silicate-rich dolomitic marble horizon. Idiomorph magnetite grains are up to 5 millimeters in size and form 25% volume of the marble horizon by volume. Coarse-grained

serpentine nodules averaging 4 millimeters in size are associated with this magnetite bed (Fig. 10.2). The total thickness of the magnetite bed is one meter and has been traced for six meters to the end of the outcrop. Greenish to yellowish pyroaurite is also associated with the horizon. Application of Zinc-Zap on the magnetite bed reveals a strong positive red coloration. Moreover, a second mineral phase in the same horizon also reacts positively with Zinc-Zap. This second phase is the serpentine nodules which are associated with the magnetite bed. Figure 10.3 shows a sample of the Bryson zincian magnetite showing partly sprayed with Zinc-Zap. No sulfides are present on this outcrop and a zinc oxide and silicate are reacting positively with Zinc-Zap. Gauthier et al. (1987) reported analytical results of 1435 ppm of zinc from this outcrop.

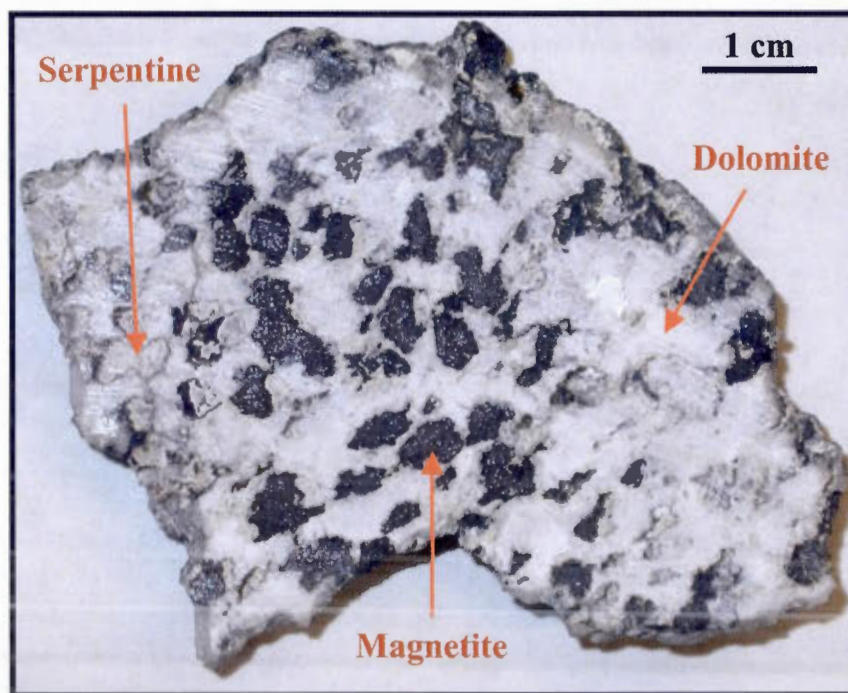


Figure 10.2: Magnetic zinciferous spinel and serpentine nodules from Gauthier's et al. (1987) discovery outcrop. Silicate-rich dolomitic marble sample from the road-cut outcrop near the bridge to Grand-Calumet Island at Bryson.

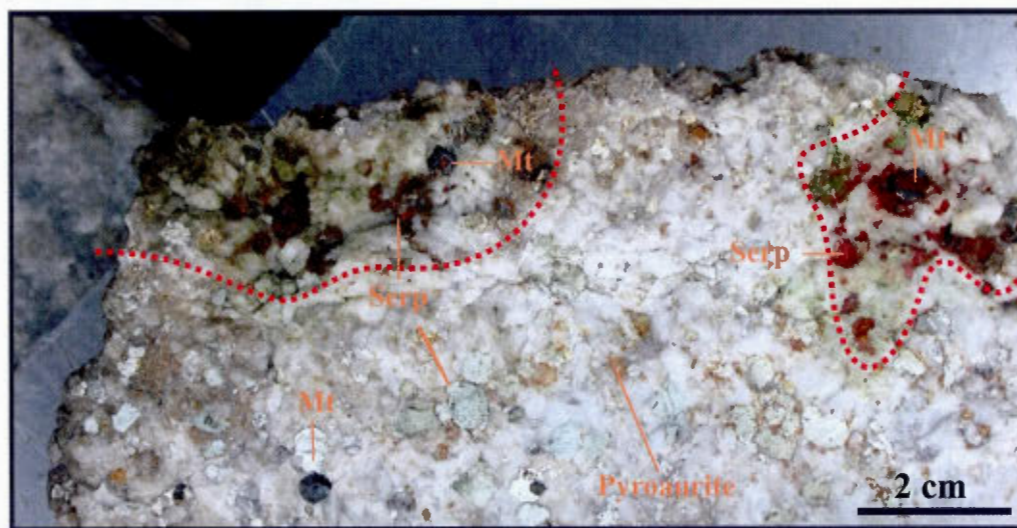


Figure 10.3: Positive Zinc-Zap reaction of the zincian magnetite (Mt) and zinciferous serpentine (Serp) in a pyroaurite-bearing silicate-rich dolomitic marble. Zinc-Zap only applied inside red-dashed lines. Sample from the Bryson bridge to Grand Calumet Island road-cut.

Further prospecting in the Bryson area allowed us to identify several new occurrences of non-sulfide zinc mineralization. The two most significant and characteristic occurrences are the Bryson Hydroelectric Dam and the Bryson Water Treatment Trail showings. Other noteworthy discoveries include the Cadieux Power Station showing.

The Bryson Hydroelectric Dam showing (Fig. 10.1), located in front of Hydro-Quebec's gate on Grand Calumet Island, occurs in a 15-meter wide and 3-meter-high road-side outcrop (Fig. 10.4). The outcrop is characterized by a silicate-rich dolomitic marble unit hosting a one meter-thick magnetite bed. Idiomorphic coarse-grained (average of 5 millimeters) magnetite represents up to 50% of the horizon. Greenish to yellowish serpentine nodules are also present and disseminated throughout the horizon (Fig. 10.5a). The outcrop is devoid of sulfide. The magnetite bed is concordant with the stratigraphic bedding and the outcrop permits us to trace it for more than 10 meters. The horizon strikes 355° north with a dip of 66° . This magnetite bed reacts positively with the Zinc-Zap. Like the Bryson zincian magnetite showing, magnetite and serpentine nodules both react to the Zinc-Zap (Fig. 10.5b). The magnetite bed and its positive Zinc-Zap reaction is stratiform and was sporadically

traced 300 meters further down the hill to the south, behind Hydro-Quebec gate in scattered outcrops (Fig. 10.6). Figure 10.7 shows the outcrop behind Hydro-Quebec's gate. Analytical results from the two occurrences returned respectively 2580 and 942 ppm zinc (Table 10.1) (Chartrand, pers. comm., 2006).

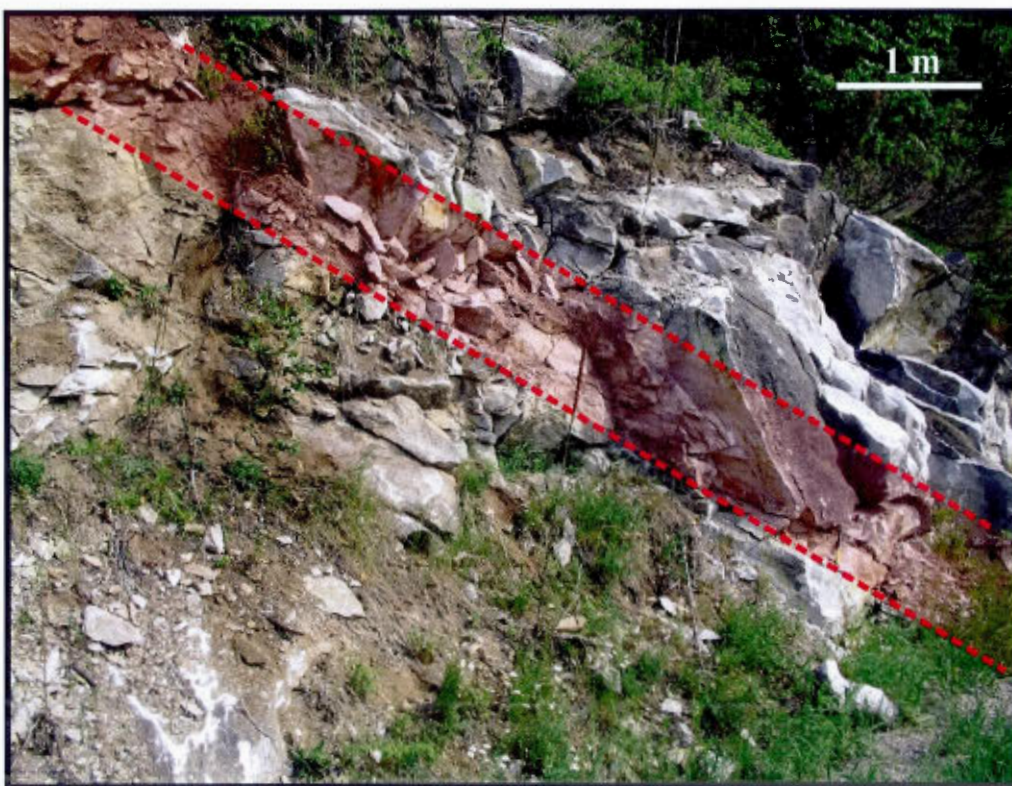


Figure 10.4: Stratiform zincian magnetic spinel and zinciferous serpentine-bearing dolomitic marble. The one-meter thick horizon is represented by the red dashed-line. Showing located at Bryson's hydroelectric dam.

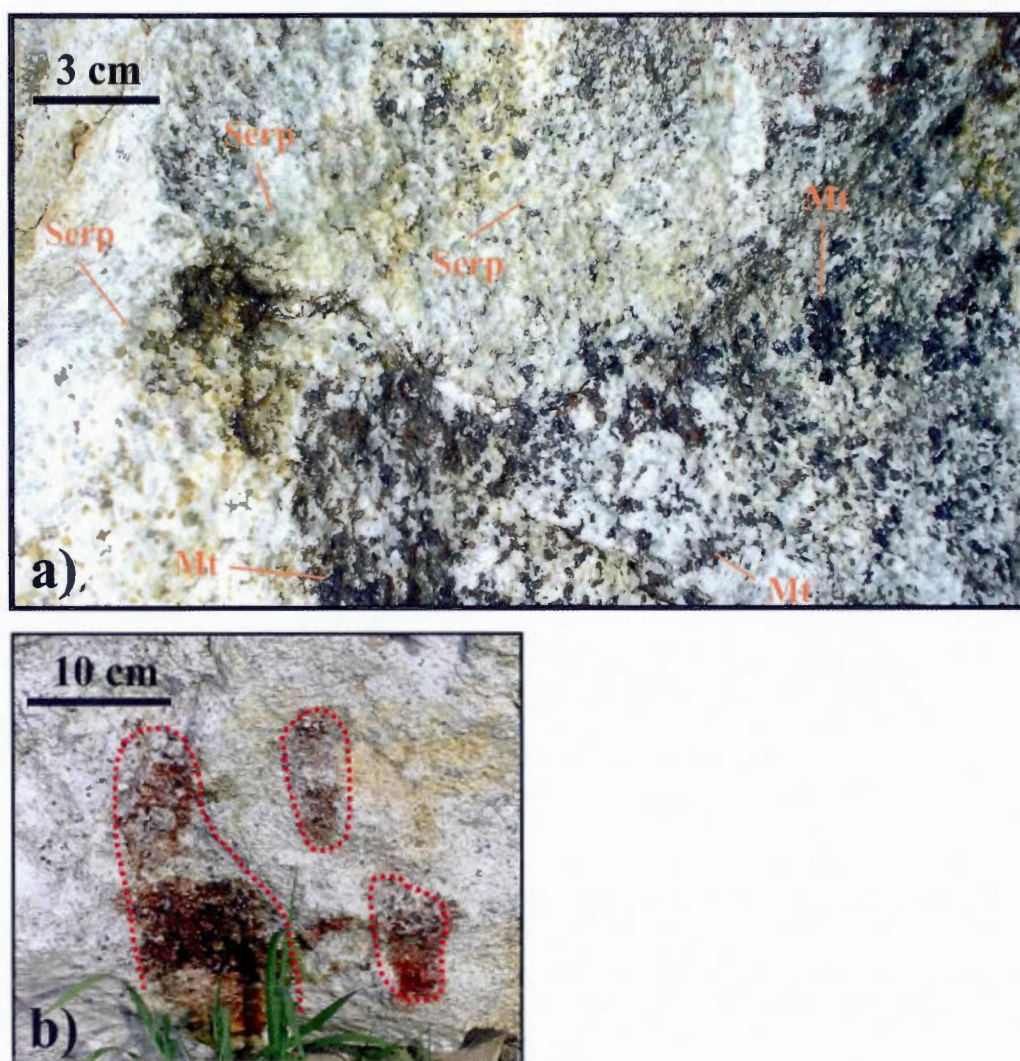


Figure 10.5: a) Bryson hydroelectric dam stratiform zincian magnetic spinel and zinciferous serpentine-bearing dolomitic marble horizon (Sample 065-B1). b) Zinc Zap reaction of this non-sulfide zinc showing inside the red-dashed line.

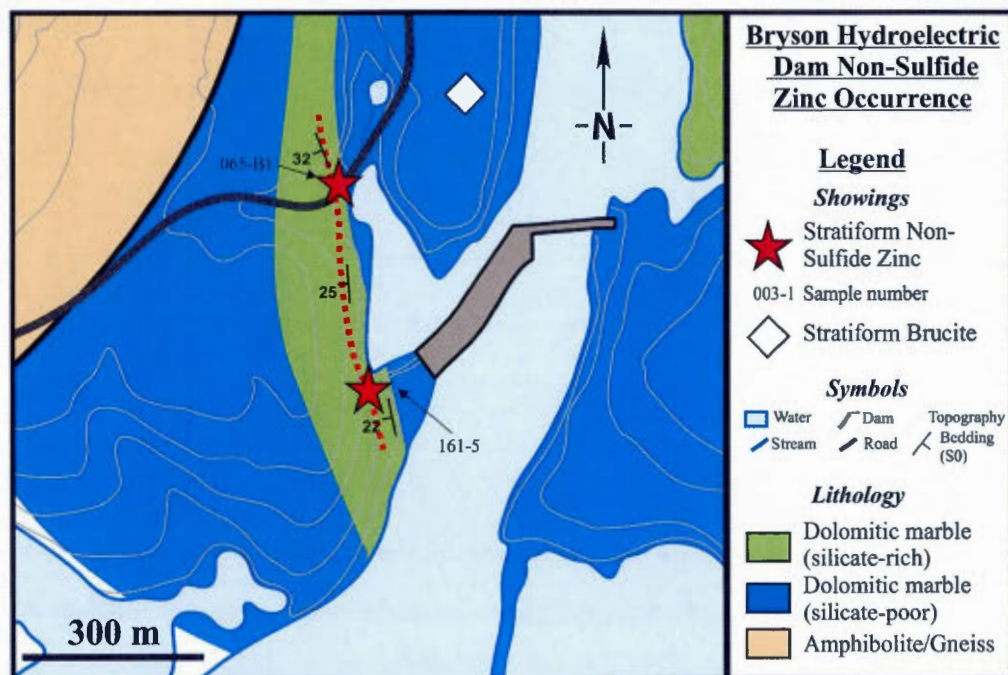


Figure 10.6: Close-up of the area near the Bryson hydroelectric dam stratiform zincian magnetic spinel and zinciferous serpentine dolomitic-marble horizon. The horizon was intercepted, along strike, 300 meters to the south behind Hydro-Quebec's gate near the dam.

Table 10.1: Geochemical Rock Analyses¹

| | | 065-B1 | 161-5 |
|----|---------|--------|-------|
| Mg | percent | 12.25 | 13.55 |
| Mn | ppm | 1355 | 509 |
| Zn | ppm | 2580 | 942 |

¹ Analyses from grab samples from the Bryson hydroelectric dam showing (065-B1) and its extension 300 meters to the south behind Hydro-Quebec's gate (161-5).



Figure 10.7: Stratiform zincian magnetic spinel and zinciferous serpentine-bearing dolomitic marble. Extension along strike of Bryson's hydroelectric dam showing, about 300m behind Hydro-Quebec's gate. The green and/or red colourations is due to application of Zinc Zap (green no zinc red zinc is present).

The Bryson Water Treatment Plant occurrence is located in the southwestern part of the town of Bryson along the trail leading to the water treatment plant. The outcrop is 20 meters long and 1.5 meters high and is characterized by a silicate-rich dolomitic marble. Xenomorphic serpentine nodules (with an average size of 3 to 4 millimeters) form up to 40% of the unit. These serpentine nodules are concentrated in a meter thick band that was only traced for 2 meters due to limited outcrop limitation. The serpentine-rich horizon is concordant with stratigraphic bedding and is thus stratiform. The zinc-bearing horizon strikes to the north (345°) with a dip of 53° . The marble progressively becomes silicate-poor (less than 10% silicate minerals) on either side of this horizon in the rest of the outcrop. The outcrop is devoid of magnetite and sulfide and is similar to common silicate-rich dolomitic

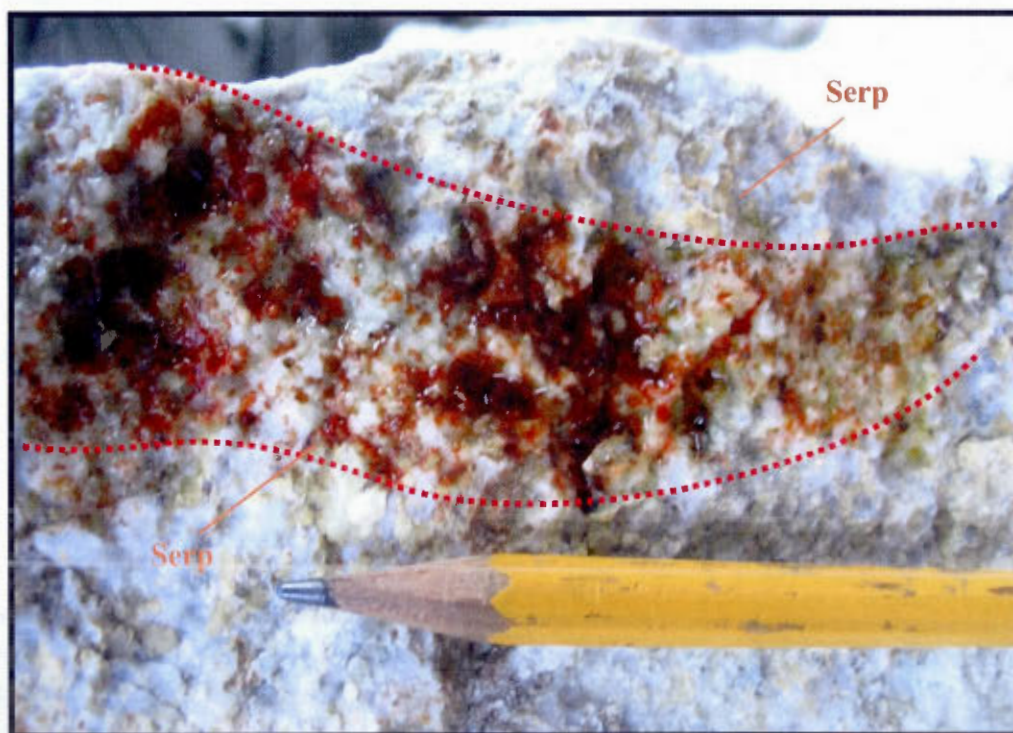


Figure 10.8a: Positive Zinc-Zap reaction of the zinciferous serpentine (Serp) in a silicate-rich dolomitic marble devoid of magnetite from the Bryson water treatment plant showing (Sample 013-8A). Zinc-Zap only applied inside red-dashed lines.

marble bands found throughout the Bryson area. Because we systematically tested all outcrops with Zinc-Zap, we successfully identified this showing following a strong positive red reaction along the one meter-thick serpentine-rich dolomitic marble layer (Fig. 10.8a and b). Macroscopic study of outcrop samples only revealed the presence of serpentine nodules that had reacted to Zinc-Zap.

The Cadieux Power Station showing is located on top of the hill near the Cadieux power station south of the town of Bryson along route 148 (Fig. 10.1). The outcrop is 40 meters long and 3 meters high and is characterized by a silicate-rich dolomitic marble. Xenomorphic serpentine nodules (with an average size of 4 millimeters) form up to 40% of the unit. These serpentine nodules are concentrated along a one meter thick band. The serpentine-rich horizon is concordant with stratigraphic bedding and strikes 360° north with a dip of 46°. Here again, serpentine-type nodules react positively to Zinc Zap (Fig. 10.9).

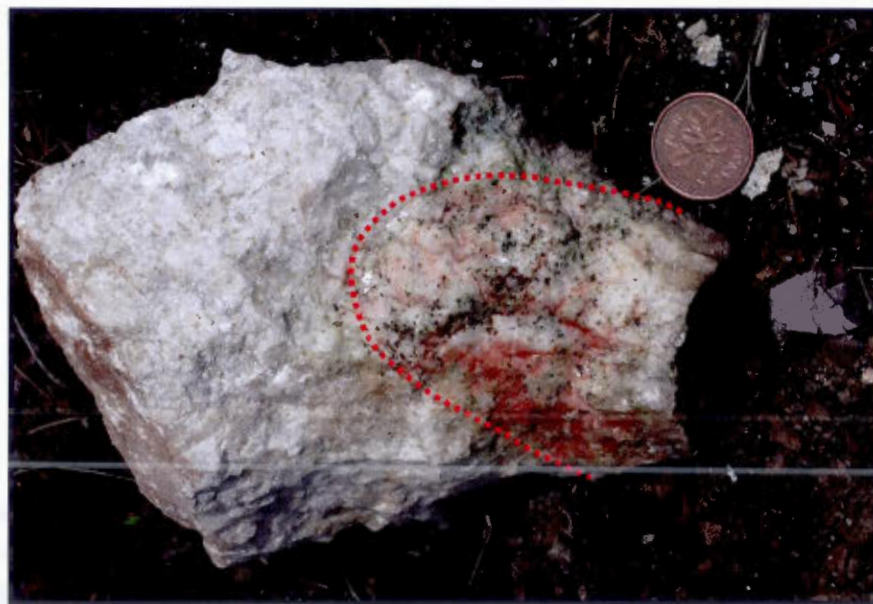


Figure 10.8b: Dolomitic silicate-rich marble horizon from the Bryson water treatment plant showing. A zinc silicate is reacting with Zinc Zap. Sprayed area is outlined in a red dashed line

. Several other non-sulfide zinc occurrences were discovered during our study. Their positions are located on figure 10.1. They are all characterized by the presence of silicate-rich dolomitic marbles where Zinc-Zap identified stratiform zinc-bearing serpentine layers which are less than a meter-thick. They are all similar to the types of occurrences described in the above paragraphs.

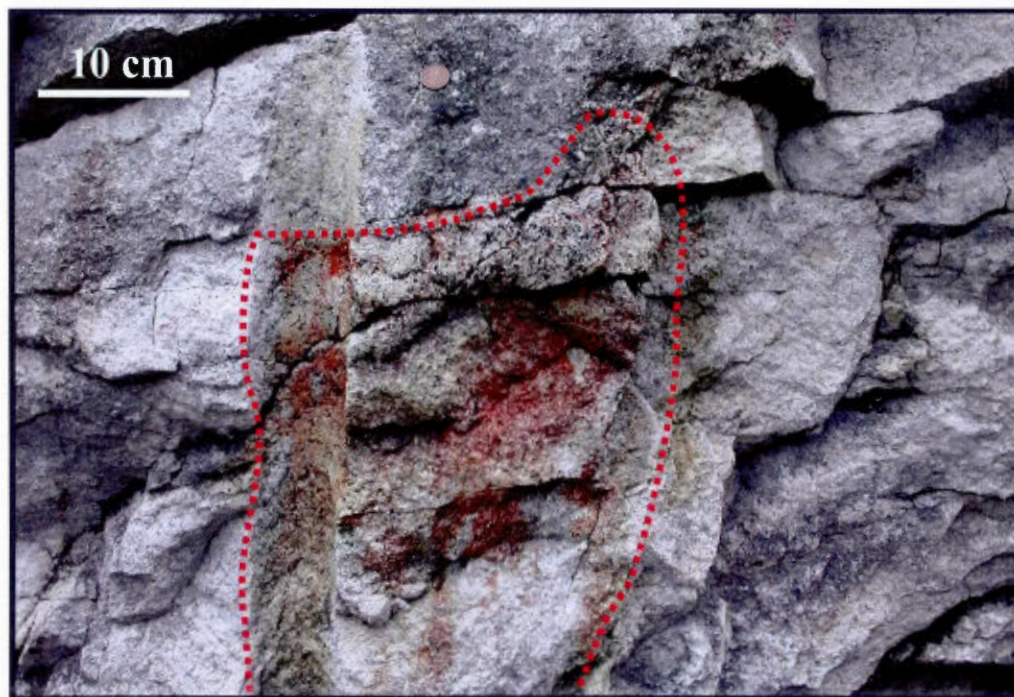


Figure 10.9: Dolomitic silicate and oxide-rich marble horizon from a road-cut outcrop along route 148 near the Bryson's Cadieux power station (Sample 008-9). Zinc Zap sprayed area outlined in a red-dashed line.

10.5 DISCUSSION

The study of the Bryson area was critical in determining if a relationship exists between SEDEX zinc sulfide and non-sulfide zinc deposits. The first step to study such a topic was to confirm the existence of a SEDEX zinc sulfide geological environment. The Bryson-Renfrew region was demonstrated as being one in chapter 8. However, non-sulfide

zinc mineralization also has to be confirmed in the same type of environment in the Bryson-Renfrew region. This is the reason we refined the work of Gauthier et al. (1987) on the Bryson zincian magnetite showing, following their suggestion that it could represent similar to Franklin and Sterling Hill (Franklin-type) non-sulfide zinc mineralization. For the purpose of this thesis, it is a necessary to demonstrate that the Bryson area hosts Franklin-type mineralization.

The results will be discussed in the following order: (1) General geological, structural and marble features used to determine the geological environment, (2) non-sulfide zinc occurrences and their similarities with Franklin-type mineralization, and (3) the consequences of the presence of Franklin-type non-sulfide zinc mineralization in the Bryson-Renfrew region and its spatial relationship with SEDEX zinc sulfide.

10.5.1 The Bryson Geological Environment

The Bryson area is dominated by dolomitic marbles that were affected by high-grade metamorphism (presumed granulite-facies) and polyphase deformation. This assumption is supported by the isoclinal folding observed on the field and by the presence of serpentine nodules in the marbles. During prograde metamorphism, dolomite reacts with quartz to form forsterite at granulite-facies conditions. Retrograde metamorphism is responsible for the alteration of forsterite into serpentine nodules.

Brucite and pyroaurite-rich marble horizons are present in the Bryson area. Pyroaurite is a magnesium and iron-rich carbonate hydroxide that is not commonly observed around the world (Deer et al., 1992). However, pyroaurite is present and associated with willemite-rich layers at Sterling Hill (Dunn, 1995). On the other hand, brucite layers were previously interpreted as meta-evaporites in chapter 8. Therefore, the dominance of dolomite and the presence of brucite (meta-evaporite) and pyroaurite (a magnesium-rich mineral) strongly suggest an evaporitic environment.

Thus, the Bryson area, at a local scale, is characterized by a shallow water evaporitic carbonate platform environment like the Bryson-Renfrew region. Such an environment characterizes the Franklin and Sterling Hill non-sulfide deposits as explained in section 2. We therefore conclude that the geological environment of the Bryson area is similar in many

ways to the one present for Franklin-type SEDEX non-sulfide zinc deposits, which also shares many depositional environment characteristics with Balmat-type SEDEX zinc sulfide deposits.

10.5.2 Non-Sulfide Zinc Mineralization

Reinvestigation of the Bryson zincian magnetite discovery outcrop confirms the presence of zinc oxides in the Bryson area. Furthermore, our study also reveals that on the same outcrop, and along the same horizon, a zinc silicate reacts to Zinc-Zap. This feature was not described by Gauthier et al. (1987). Several new stratiform non-sulfide zinc mineralization were discovered around the Bryson area (summarized in Appendix D). These include magnetic zincian spinels and/or zinciferous serpentine. These showings are reported on figure 10.1 and also on high detail geological maps in Appendix E.

Franklin-type mineralization is characterized by stratiform zinc silicate and oxide hosted in a dolomitic marble. The Bryson area also hosts stratiform zinc silicate and oxide mineralization in a dolomitic marble. To be more specific, the non-sulfide zinc mineralization is hosted by silicate-rich (serpentine) dolomitic marbles. These paragenetic and structural features strongly suggest that the Bryson occurrences are related to Franklin-type mineralization.

10.6 CONCLUSION

The Bryson area non-sulfide zinc mineral paragenesis shows several similarities with Franklin-type mineralization. The Bryson occurrences are located in the Bryson-Renfrew region where several SEDEX zinc sulfide showings were found. In chapter 3, we confirmed the lithologic association of SEDEX zinc sulfide mineralization with silicate-rich dolomitic marbles that was first proposed by Sangster (1970) and Gauthier and Brown (1986). As discovered during our study, non-sulfide zinc occurrences are also associated with silicate-rich dolomitic marble horizons. It follows that the pre-metamorphic host-rock of non-sulfide zinc mineralization is a siliceous dolostone (dolomite).

The presence of SEDEX zinc sulfide occurrences and a volcanogenic polymetallic massive sulfide deposit less than six kilometers away from the Bryson's occurrences is

interesting. Although analytical results from samples of Bryson's non-sulfide zinc mineralization returned uneconomical grades of less than one percent zinc (i.e. compared to Franklin and Sterling Hill district with 20% zinc), the similar mineral paragenesis to Franklin-type mineralization invited more profound mineralogical study. These mineralogical studies will furnish additional evidence for the comparison between the Bryson non-sulfide zinc occurrences and Franklin-type mineralization. Once this has been described and Franklin-type mineralization confirmed in the same marble belt, we will discuss the relationship between both end-member of SEDEX deposits.

CHAPTER XI

MINERALOGICAL PROPERTIES OF ZINC SILICATES AND OXIDES FROM THE BRYSON AREA

11.1 INTRODUCTION

The resemblance between the zinc silicates and oxides encountered during our field work in the Bryson area and those observed at the Franklin and Sterling Hill district led us to conduct more detailed mineralogical studies. The confirmation of Franklin-type non-sulfide zinc mineralization in the same type of geological environment as Balmat-type SEDEX zinc deposits would for the first time permit relationship studies between them to be undertaken.

In chapter 10, we established that the Bryson area is the site of several stratiform non-sulfide zinc occurrences hosted by dolomitic marbles rich in silicates (i.e. serpentine nodules). Two minerals reacted to Zinc-Zap; a zinc oxide and a zinc silicate. This reaction was observed on magnetic spinels and on serpentine nodules occurring in marble units containing magnetic spinels and serpentine, and only serpentine nodules.

In this section we will study the mineralogical properties of the Bryson zincian magnetite showing and also the newly discovered zinc and silicate occurrences. We will discuss petrologic, x-ray diffraction and geochemical data conducted on magnetic spinels and silicates of the Bryson area zinc occurrences. We use these data to identify the zinciferous mineral phases and constrain their metamorphic evolution. We also compare the Bryson occurrences and those observed at Franklin and Sterling Hill deposits to establish if the Bryson paragenesis is related to Franklin-type mineralization as proposed in chapter 10.

11.2 METHODOLOGY

11.2.1 Sample Selection

For the purpose of our mineralogical study, a total of 20 zinc-bearing samples were chosen from the non-sulfide zinc occurrences in the Bryson area. Samples were selected based on their quality (unaltered) and overall representivity of the zinc mineralization. All samples were collected from stratiform non-sulfide zinc mineralizations that were characterized by a clear Zinc-Zap reaction.

11.2.2 Microscope Petrologic Studies

Mineral assemblages were studied under a reflected and transmitted polarized microscope. A total of 18 polished thin sections were prepared and studied. Polished thin sections lack of a glass lamellae cover plate normally found on regular thin sections. They are polished, and thus permit observation under reflected and transmitted light microscopy on the same thin section.

Thin sections were observed at the Metallogenic Laboratory of the Université du Québec à Montréal (Canada). Further research was also conducted at the Mineralogy and Crystallography Laboratory of the Université de Liège (Belgium) under the supervision of professor André-Mathieu Fransolet. Thin sections were studied under a polarized Leica DMLP microscope equipped with the following objectives: 5x, 10x, 20x and 50x. An additional oil immersion objective (125x) was also used when judged necessary to observe smaller mineral phases.

11.2.3 X-Ray Diffraction Studies

X-Ray diffraction was used to identify specific mineral phases and assemblages from the Bryson zinc silicate and oxide occurrences. A total of 20 analyses were conducted on 12 different rock samples. X-Ray diffraction enabled us to identify mineral species and to obtain whole-rock semi-quantitative mineral assemblages. For X-Ray diffraction, samples were manually crushed into a uniform ~10 µm powder.

X-Ray diffraction was carried out at the Mineralogy and Crystallography Laboratory in Liege's (Belgium), operated by professor A.-M. Fransolet on a Philips PW-1730/10 iron anode automated powder diffractometer equipped with a PW3710 computer controlled

goniometer. Single-mineral diffraction patterns were conducted using a Deybe-Scherrer camera mounted on a Philips PW-1729 power generator equipped with an iron anode. Operating conditions for the power generators were 40 kV and 30 mA.

11.2.4 Microprobe Studies

Microprobe analysis was conducted directly on selected thin sections. A total of 40 analyses were obtained on the zinciferous silicates and oxides of the Bryson area to determine their composition and identify mineral phases.

Microprobe study was carried out at McGill University Departement of Earth and Planetary Science microprobe laboratory under the supervision of Shi Leng. Equipment used was a JEOL JXA-8900 electron microprobe with five WDS spectrometers and a fully integrated Si(Li) EDS detector. Each analyzed thin section was coated with approximately 150 Angstroms of carbon and operation conditions were 20kV and 15 to 20 nA. Calibration of the microprobe was done using the laboratory's internal standards.

11.3 RESULTS

The microscopic characteristic of the Bryson area non sulfide- zinc mineralization are going to be presented in two steps. First, we will describe the zincian magnetitic spinel observed at the Bridge showing, at Gauthier et al. (1987) discovery site, and at the Bryson Hydroelectric Dam occurrence. We will then characterize the zincian silicate that is and is not associated with the zinc oxide.

11.3.1 Magnetic Zincian Spinel

Microprobe analysis of the Bryson zincian spinel by Gauthier et al (1987) suggested that the spinel could be an intermediate phase between magnetite and franklinite. However, our microscope observation reveals the presence of dendritic sphalerite and/or wurtzite exsolutions. Sphalerite/wurtzite exsolutions constitute up to 35% by volume of the magnetite and have an average size of 0.01 millimeter (Fig. 11.1). Similar dendritic wurtzite/sphalerite is observed in the serpentine-type nodules associated with the magnetite bed (Fig. 11.2)

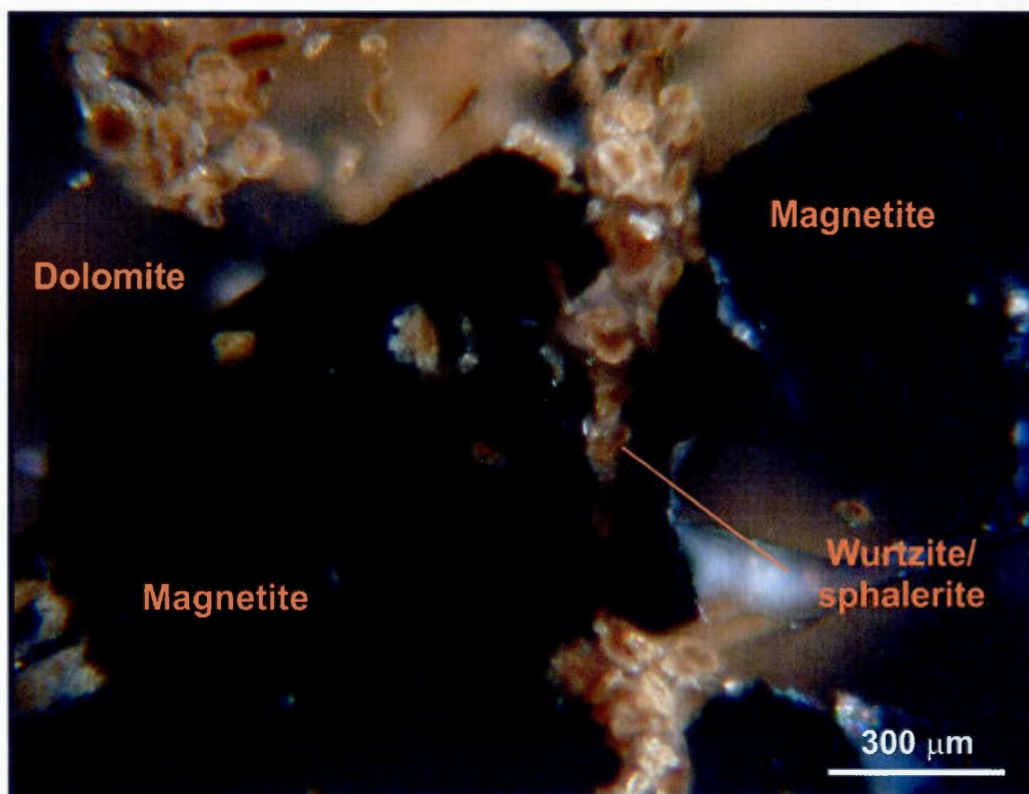


Figure 11.1: Aggregate of fine dendritic wurtzite/sphalerite exsolutions in magnetite from the Bryson hydroelectric dam showing (Sample 065-B1). Photo taken under polarized reflected light.

X-Ray diffraction (XRD) and cell parameter calculations on the magnetic spinels were undertaken to identify the spinel-type and to evaluate its franklinite solid-solution component. XRD confirms the mineralogical structure of magnetite. Figure 11.3 shows the diffractogram obtained from magnetite of the Bryson Hydroelectric Dam showing. The presence of franklinite in solid-solution in magnetite has the effect of increasing the cell parameter “ a ” (magnetite-franklinite crystallizes in the cubic system, therefore the 3 crystallographic axes a , b and c are equal) because of the presence manganese. Cell parameter calculations from the XRD powder diffractograms obtained from samples of the Bridge (sample 003-1) and Hydroelectric Dam (065-B1) showings (Fig. 10.1) returned $a=8.39358$ and $a=8.39316$ respectively (Table 11.1). Pure magnetite has a cell parameter of 8.396 whereas franklinite has a parameter of 8.43 (Deer et al., 1992). This result is consistent

with a strong magnetite component which does not have a considerable franklinite portion in solid-solution.

Microprobe analysis of magnetite confirms the XRD results and indicates that magnetite has manganese (0.00 to 0.12 % MnO) and is zinc-poor (0.00 to 0.22 % ZnO; Table 11.2). Figures 11.4 and 11.5 show dendritic exsolutions of wurtzite/sphalerite inside magnetite grains. Analyses of the dendritic sphalerite/wurtzite intergrowths are shown in table 11.3. These analyses do not enable us to differentiate sphalerite from wurtzite in our sample. There are no significant chemical zinc exchanges observed between magnetite and the sphalerite/wurtzite exsolutions along contacts (Table 11.3).

11.3.2 Zinc Silicate and Oxide

Petrographic observations of the zincian silicate reveal the presence of subrounded fibrous serpentine-talc-type nodules. The alteration process is extensive and no relic mineral is systematically observed inside the serpentine nodules, limiting our petrographic study. The xenomorphic nodules are 3 to 4 millimeter in size. While relics are uncommon in the serpentine nodules, several relic grains of spinel inside serpentine-type nodules were observed on the sample from the Bridge showing (sample 003-1). This spinel is not opaque when observed in transmitted light (Fig. 11.6a and 11.6c) and contains fine exsolutions of a highly reflective mineral (Fig. 11.6b) visible under reflected light. A total of 10% fine exsolutions are present in the relic spinel. XRD and microprobe analysis are needed to identify the different mineral phases.

XRD investigation of the serpentine-type nodules confirms that the mineral is serpentine. Table 11.4 shows the Debye-Scherrer camera results from a serpentine-type nodule of the Water Treatment Plant showing (sample 013-8A) that confirms it is a serpentine. The spinel did not undergo XRD analysis because of the difficulty involved in identifying and isolating the rare spinel from the serpentine nodules. Microprobe analysis of this spinel is required to further study this mineral assemblage.

Microprobe analysis was conducted in serpentine nodules and also on the spinel and its exsolutions. Analysis of the serpentine nodules shows that they contain up to 4.28 % ZnO in their structure. Figure 11.7 shows a back-scatter microprobe image of a typical serpentine

from the Bryson Water Treatment Plant showing (sample 013-8A). Table 11.5 shows the serpentine microprobe analysis results obtained from the Cadieux Power Station and Water Treatment Plant showings while table 11.6 shows the same results but for the Bridge and Hydroelectric Dam showings. Back-scatter microprobe imagery (density-dependent image) of serpentine nodules from the Cadieux Power Plant showing (008-9) locally shows the presence of fine inclusions of a denser mineral, which can represent up to 15% by volume of the nodule (Fig. 11.8). Larger pyrophanite grains are also present and are shown in figures 11.9 and 11.10. The analysis of these fine inclusions identifies them as pyrophanite having an intermediate composition from the pyrophanite-ecandrewsite solid-solution. Pyrophanite (MnTiO_3) is the manganese end-member of the ilmenite group whereas ecandrewsite ($(\text{Mn}, \text{Mg}, \text{Zn})\text{TiO}_3$) is the manganese- magnesium-zinc end-member of the ilmenite group (Deer et al., 1992). These serpentine-hosted pyrophanites are zincian with up to 8.91 % weight zinc oxide (Table 11.7). The composition of the zincian pyrophanites present in the Bryson occurrences varies as follows: $(\text{Fe}_{0.033-0.698}, \text{Mg}_{0.010-0.269}, \text{Zn}_{0-0.215}, \text{Mn}_{0.301-0.928})\text{Ti}_{0.967-1.273}\text{O}_3$.

Microprobe analysis of the spinel relic shows that it has a transitional composition between spinel (MgAl_2O_4) and gahnite (ZnAl_2O_4). The zinc content of this spinel is up to 1.881 % ZnO (Table 11.8). Back-scatter microprobe imagery of the spinel confirms the petrological observation of fine exsolutions (Fig 11.11). Analysis of these exsolutions reveals that they have an intermediate composition between pyrophanite (MnTiO_3) and geikielite (MgTiO_3) (member of the ilmenite group). However, these manganese and magnesium ilmenite exsolutions are devoid of zinc (Table 11.7).

To summarize, mineralogical studies of the zinc silicate at Bryson reveal the presence of zincian serpentine nodules containing inclusions of zincian pyrophanite, and of zincian spinel relic belonging to the spinel-gahnite family which is characterized by non-zincian pyrophanite exsolutions.

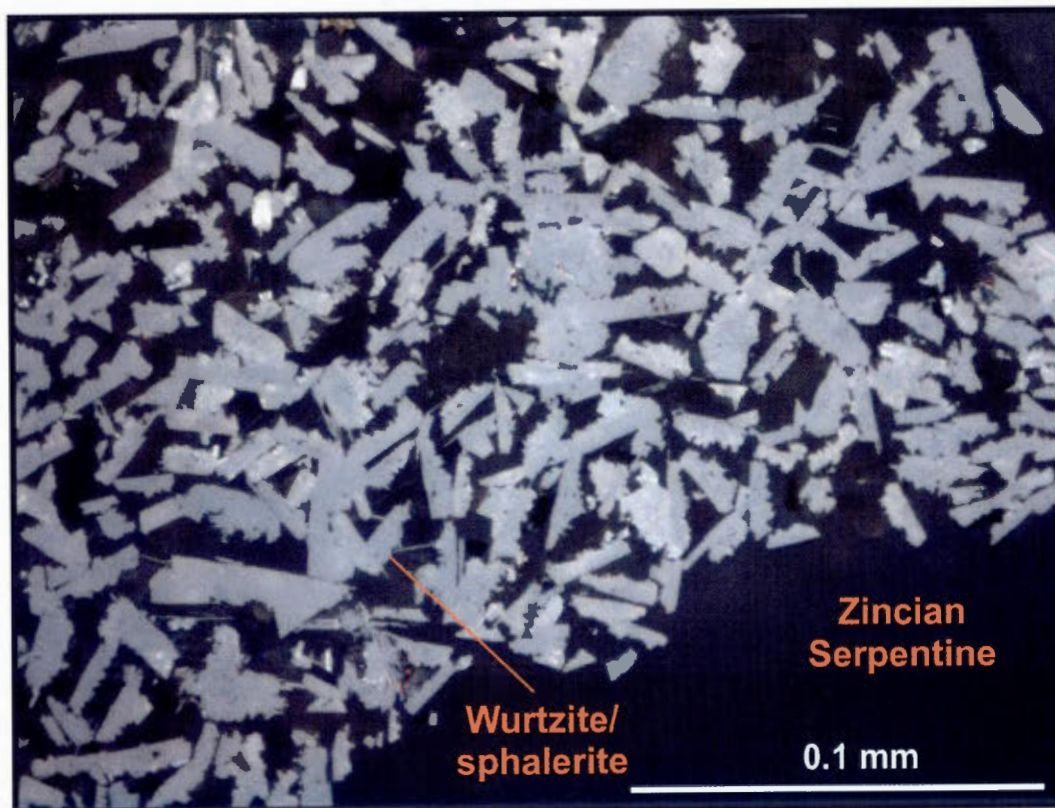


Figure 11.2: Aggregate of fine dendritic wurtzite/sphalerite in a magnetite-bearing dolomitic marble unit from the Bryson hydroelectric dam showing (Sample 065-B1). Photo taken under natural reflected light.

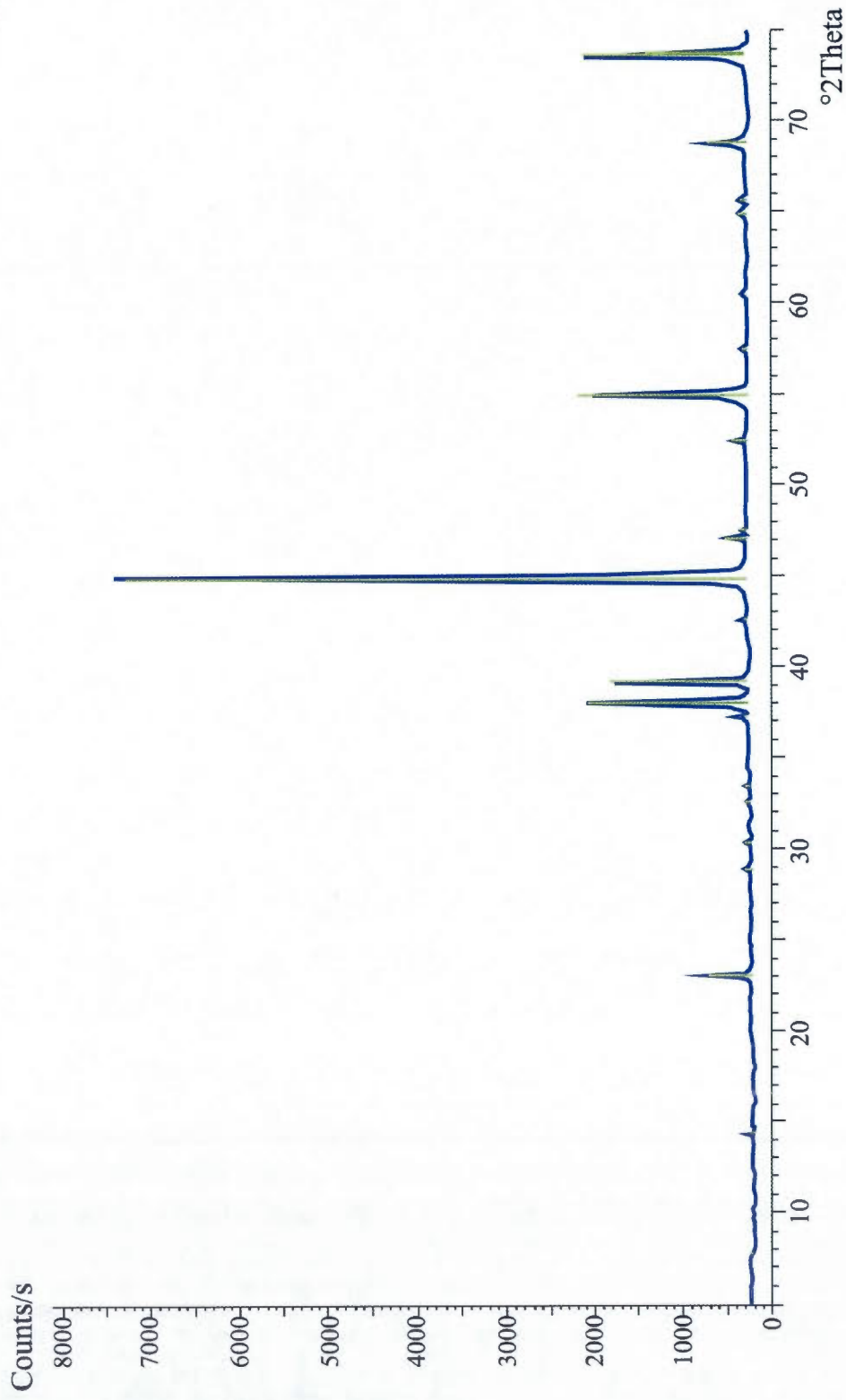


Figure 11.3: X-Ray powder diffractogram of the zincian magnetic spinel from the Bryson hydroelectric dam showing (Sample 065-B1). XRD confirms that the spinel is a magnetite and all the peaks position and intensity relatively match those of the mineralogical database (green lines) (Deer et al., 1992). Data from this diffractogram was used to calculate the cell parameter of this magnetite.

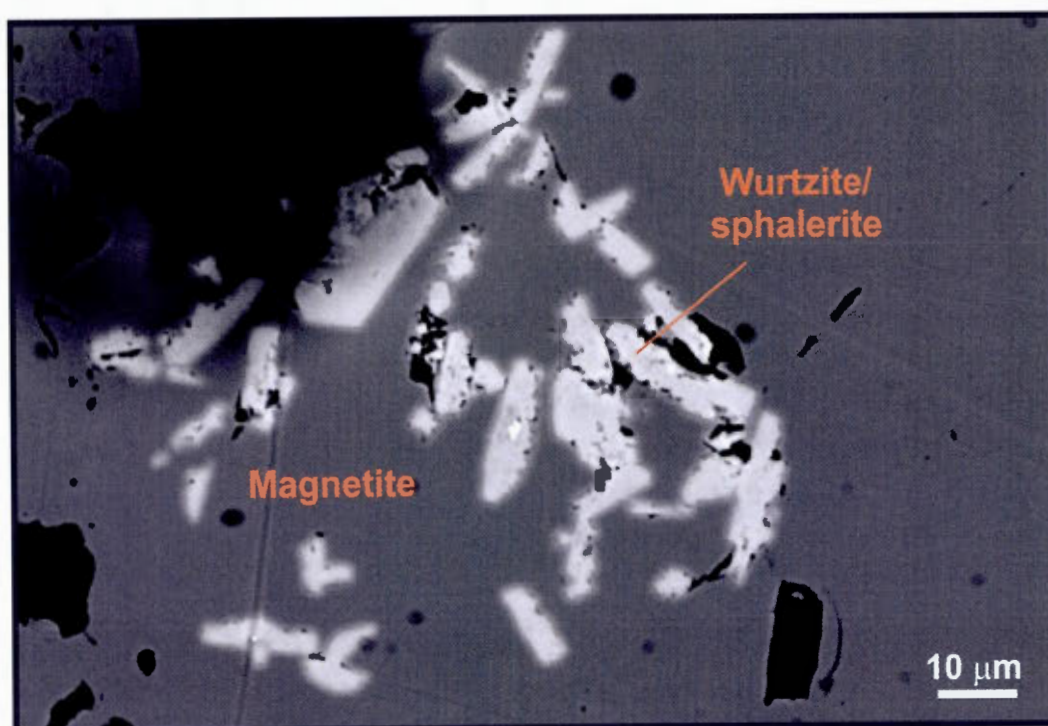


Figure 11.4: Back-scatter microprobe imagery showing dendritic wurtzite/sphalerite exsolutions in a magnetite from the Bryson hydroelectric dam showing (Sample 065-B1).

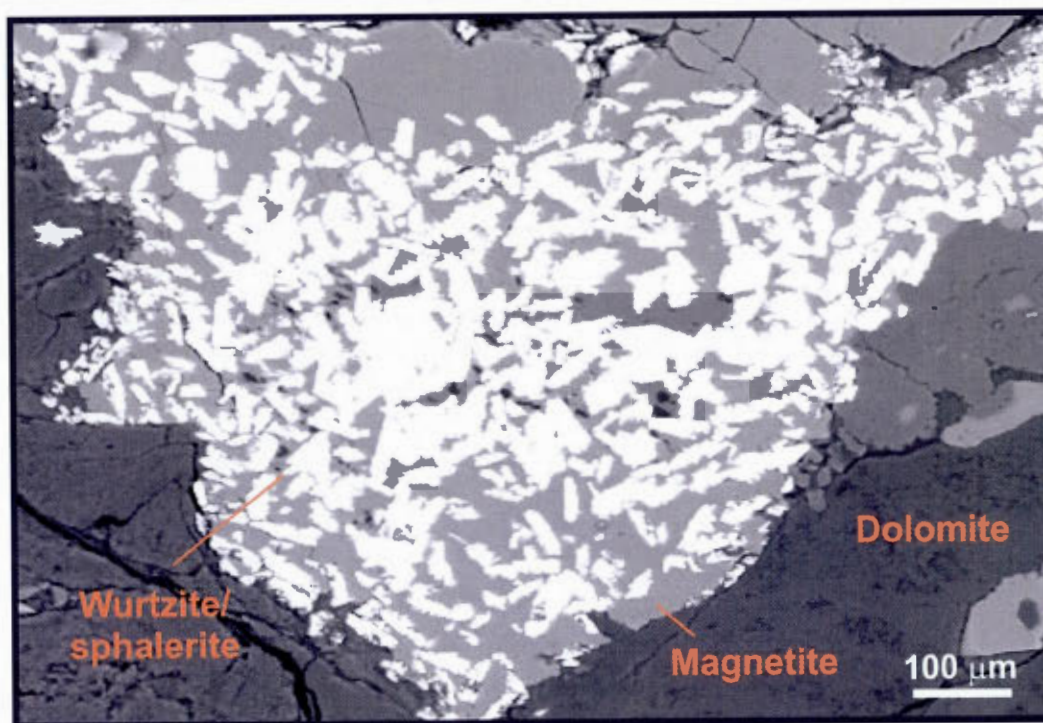


Figure 11.5: Back-scatter microprobe imagery showing a second example of dendritic wurtzite/sphalerite exsolutions in a magnetite from the Bryson hydroelectric dam showing (Sample 065-B1).

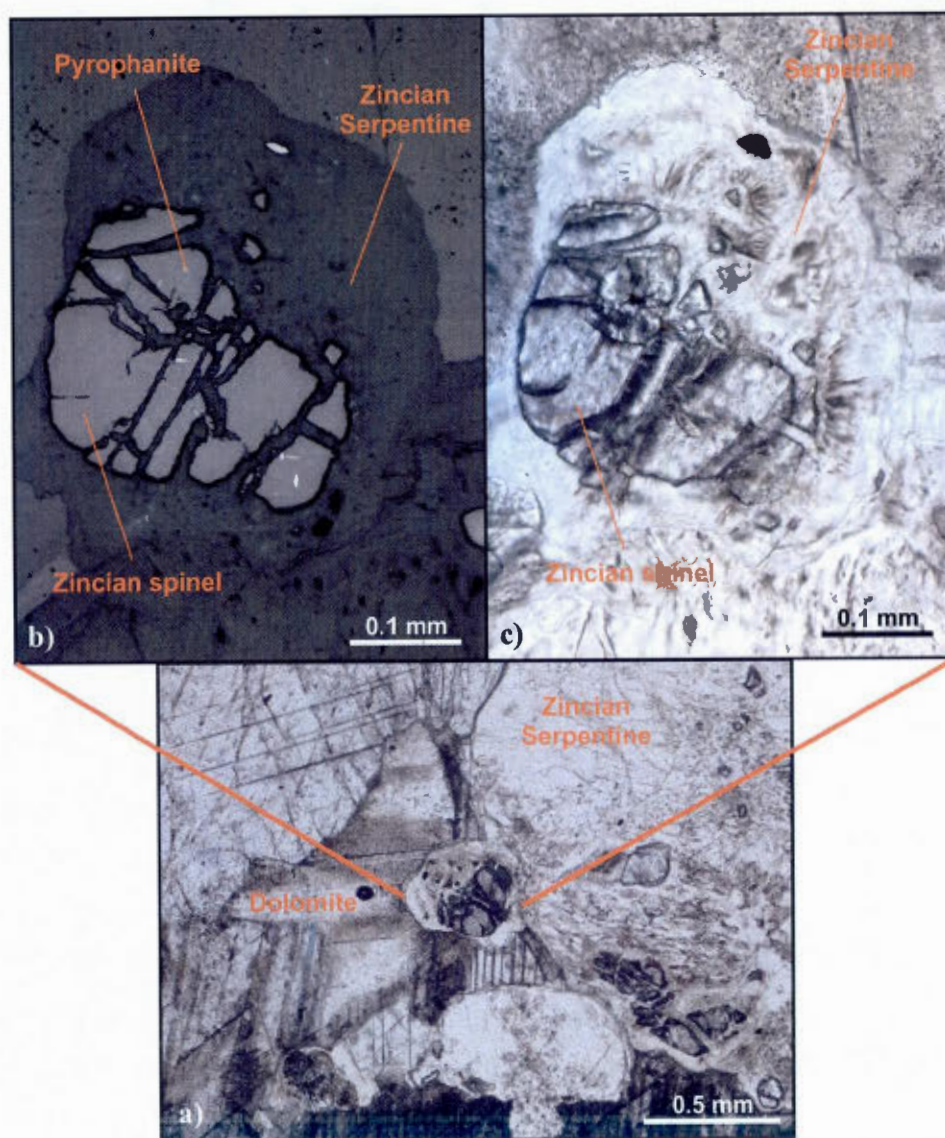


Figure 11.6: a) A relic zincian spinel, of the spinel-gahnite solid-solution, inside a zinciferous serpentine nodule from outcrop 003-1. Observed under natural transmitted light. b) Pyrophanite exsolutions inside the zincian spinel is revealed by observation under natural reflected light. c) Close-up of the zincian spinel relic inside the zinciferous serpentine nodule.

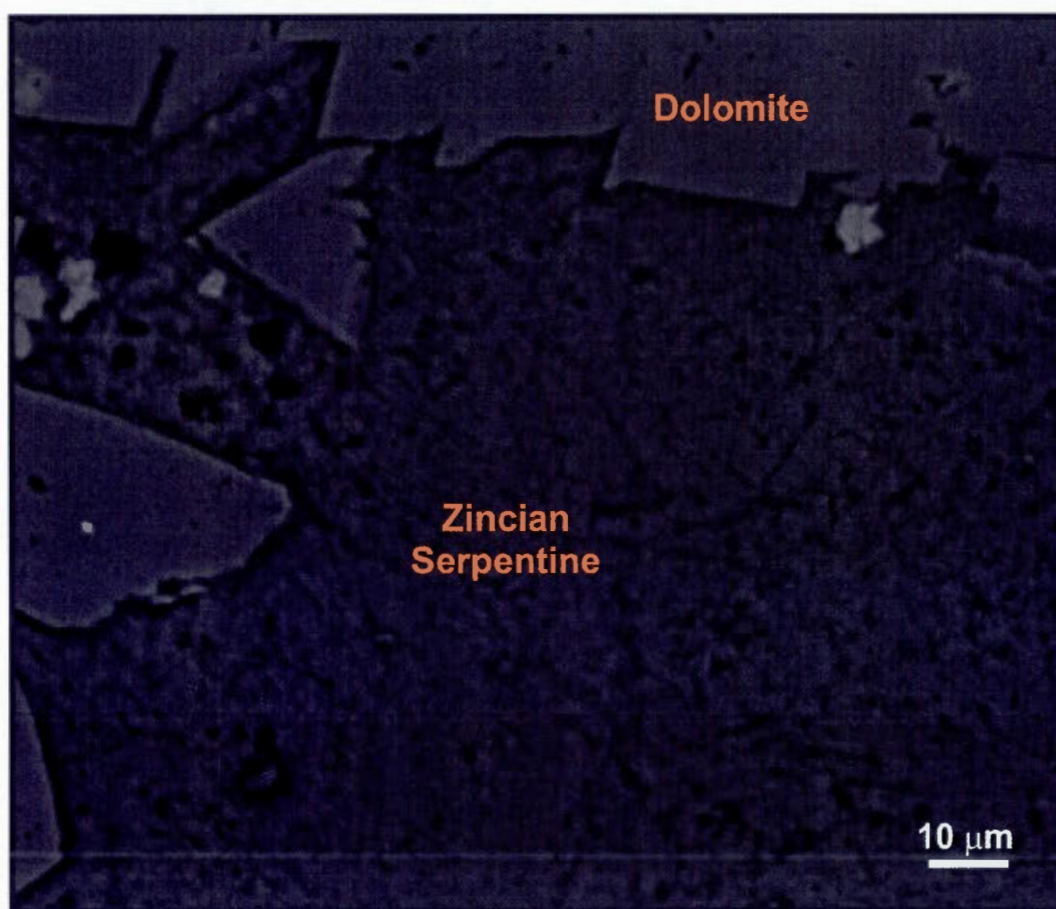


Figure 11.7: Back-scatter microprobe imagery showing zincian serpentine without pyrophanite inclusions from the Bryson water treatment showing (Sample 013-8A).

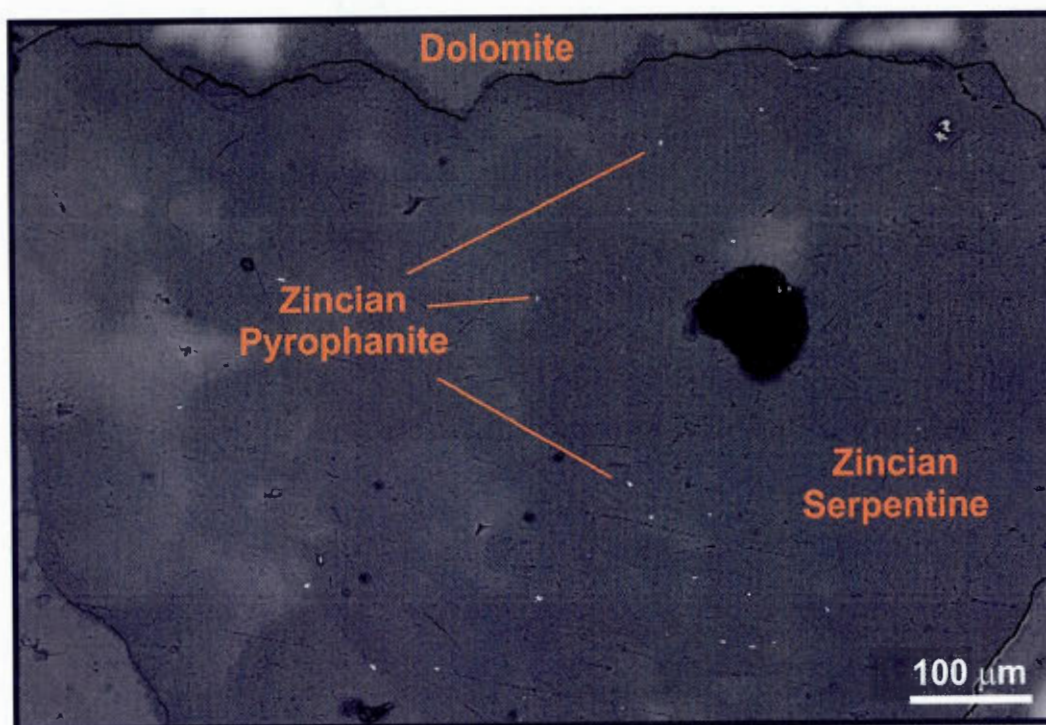


Figure 11.8: Back-scatter microprobe imagery of a zincian serpentine from the road-cut near the Bryson Cadieux power plant (Outcrop 008-9). The serpentine is zinciferous and also contains inclusions of fine zincian pyrophanite (transitory composition between ecandrewsite-pyrophanite solid-solution).

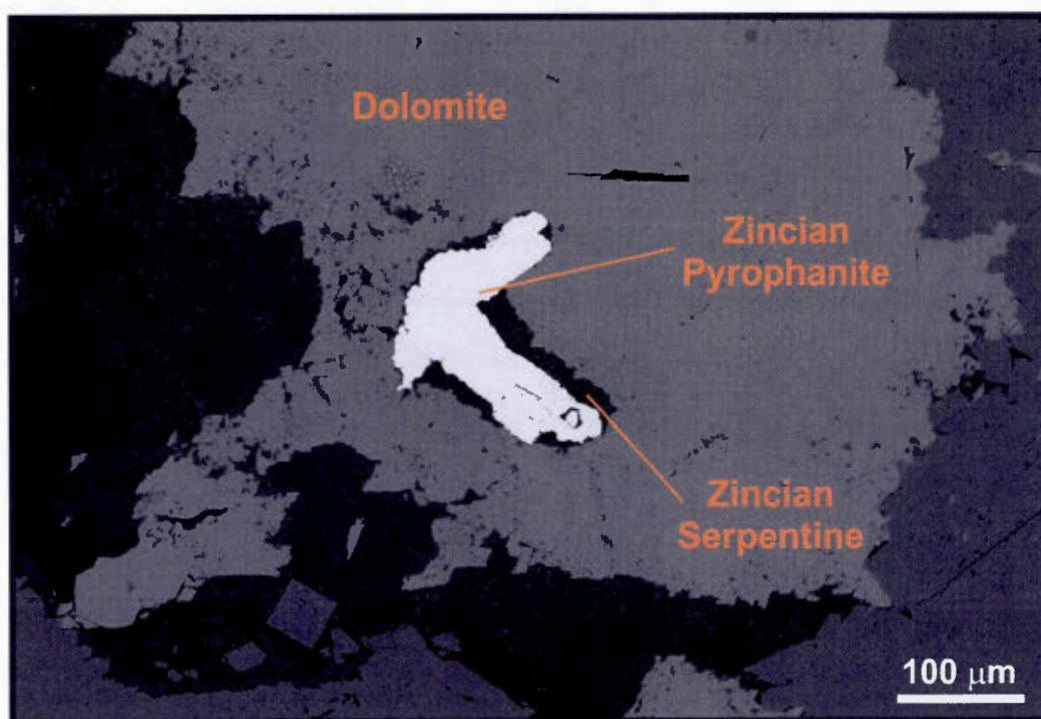


Figure 11.9: Back-scatter microprobe imagery showing a coarser zincian pyrophanite from the road-cut near the Bryson Cadieux power plant (Outcrop 008-9).

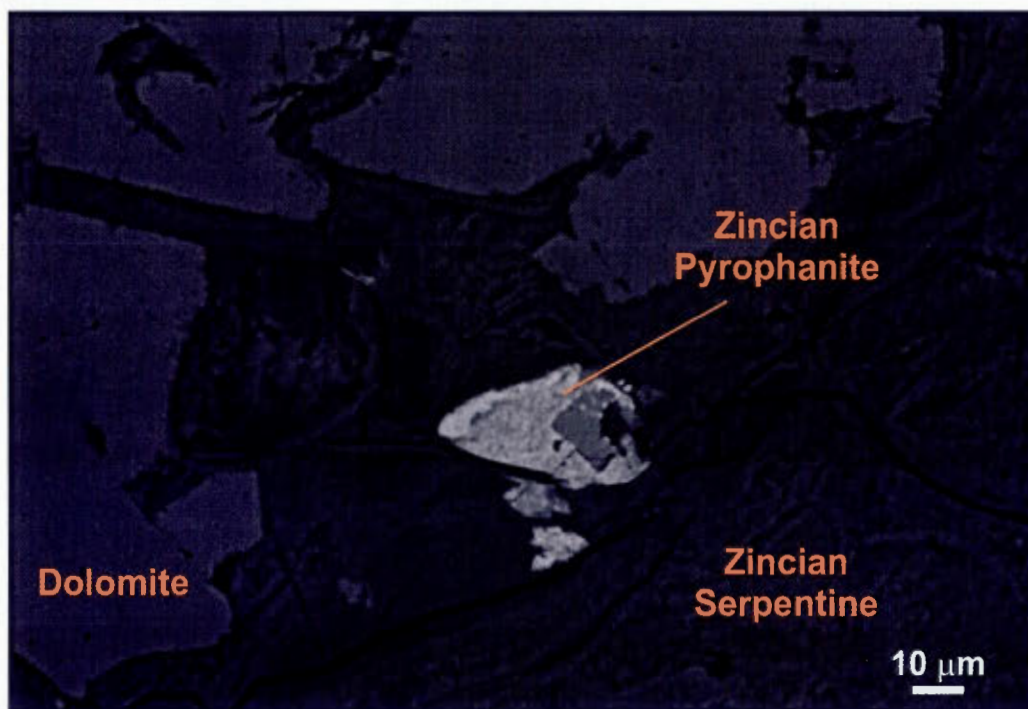


Figure 11.10: Back-scatter microprobe imagery showing a coarser zincian pyrophanite hosted in a zincian serpentine from the road-cut near the Bryson Cadieux power plant (Sample 008-9).

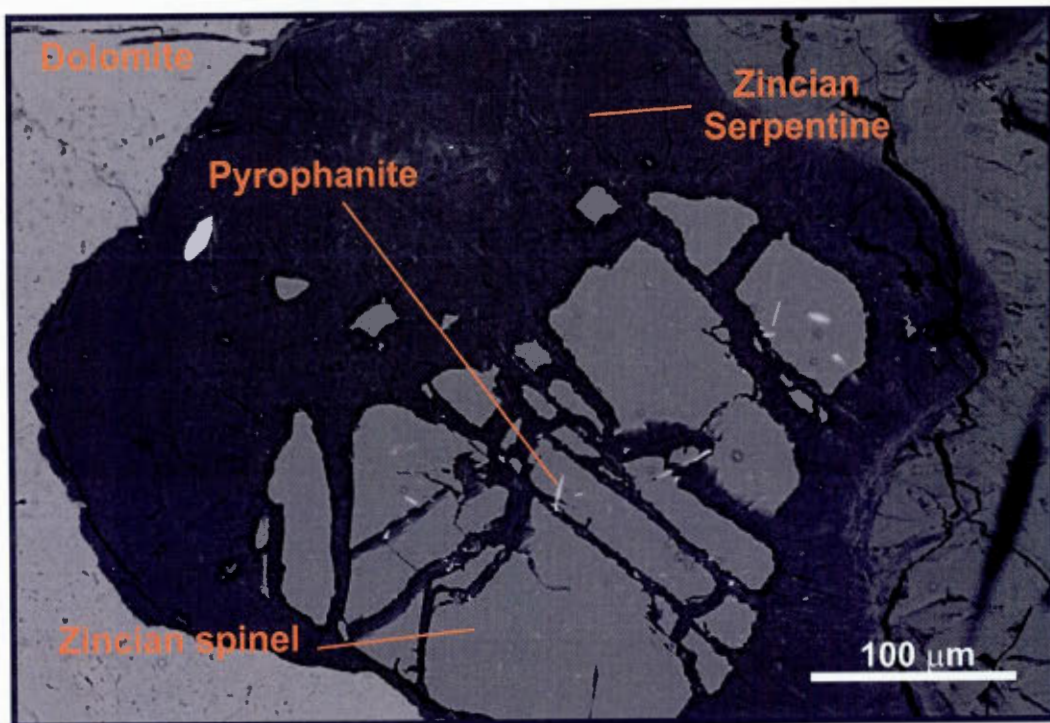


Figure 11.11: Back-scatter microprobe imagery of the zincian spinel (Sample 003-1) confirms the presence of fine pyrophanite exsolutions.

Table 11.1: XRD Data for Lattice Parameter Calculation¹

| Bryson bridge: 003-1 | | Bryson hydroelectric dam: 065-B1 | |
|-----------------------------|---------|----------------------------------|---------|
| $2\theta^2$ | d^3 | $2\theta^2$ | d^3 |
| 7.535 | 14.742 | 7.740 | 14.352 |
| 13.123 | 8.477 | 14.314 | 7.775 |
| 17.294 | 6.443 | 23.029 | 4.853 |
| 23.050 | 4.848 | 28.826 | 3.892 |
| 29.099 | 3.856 | 30.374 | 3.698 |
| 33.573 | 3.354 | 32.579 | 3.453 |
| 37.228 | 3.035 | 33.420 | 3.369 |
| 38.090 | 2.969 | 37.325 | 3.027 |
| 39.218 | 2.886 | 38.094 | 2.968 |
| 44.992 | 2.532 | 39.228 | 2.886 |
| 47.132 | 2.423 | 44.997 | 2.531 |
| 49.585 | 2.310 | 47.592 | 2.401 |
| 52.432 | 2.193 | 52.481 | 2.191 |
| 54.931 | 2.100 | 54.982 | 2.098 |
| 55.112 | 2.094 | 55.112 | 2.094 |
| 57.356 | 2.018 | 57.525 | 2.013 |
| 60.353 | 1.927 | 60.451 | 1.924 |
| 65.750 | 1.785 | 65.726 | 1.785 |
| 68.820 | 1.714 | 68.852 | 1.713 |
| 73.644 | 1.616 | 73.693 | 1.615 |
| 74.336 | 1.603 | 73.865 | 1.612 |
| Lattice calculation results | | | |
| a^4 : | 8.39358 | a^4 : | 8.39316 |

¹ Chemical formulas were calculated by normalizing total cations to 4.² 2θ measured from diffractogram. FeK α : 1.9373 Angstrom.³ d is the spacing between atomic lattice planes of the mineral. d is calculated using Bragg's law ($n\lambda = 2d\sin\theta$).⁴ Lattice a obtained using a computer program (Burnham, 1991).

Table 11.2: Electron Microprobe Analyses of Magnetite¹

| | Bridge showing | | Bryson hydroelectric dam showing | | | | | |
|--------------------------------|----------------|----------|----------------------------------|-----------|-----------|-----------|-----------|-----------|
| | 003-1-C1 | 008-9-C1 | 065-B1-C1 | 065-B1-C2 | 065-B1-C3 | 065-B1-C4 | 065-B1-C5 | 065-B1-C6 |
| SiO ₂ | <0.01 | 0.06 | 0.08 | 0.04 | 0.02 | <0.01 | 0.14 | <0.01 |
| Al ₂ O ₃ | 0.02 | 0.01 | <0.01 | 0.01 | 0.53 | <0.01 | <0.01 | <0.01 |
| ZnO | <0.01 | 0.02 | 0.01 | 0.22 | 0.00 | 0.06 | 0.04 | 0.03 |
| CaO | <0.01 | <0.01 | 0.01 | <0.01 | 0.00 | <0.01 | 0.08 | <0.01 |
| FeO ² | 92.06 | 92.25 | 92.67 | 92.06 | 91.75 | 91.79 | 92.26 | 92.33 |
| MgO | 0.51 | 0.45 | 0.33 | 0.35 | 0.59 | 0.55 | 0.04 | 0.73 |
| TiO ₂ | 0.03 | 0.03 | 0.01 | 0.01 | <0.01 | <0.01 | 0.21 | 0.00 |
| MnO | 0.08 | 0.12 | 0.10 | 0.09 | 0.12 | 0.08 | 0.02 | 0.00 |
| Cr ₂ O ₃ | 0.01 | <0.01 | <0.01 | <0.01 | 0.01 | <0.01 | 0.00 | 0.00 |
| Total | 92.70 | 92.94 | 93.21 | 92.77 | 93.03 | 92.49 | 92.80 | 93.09 |
| Si | 0.000 | 0.003 | 0.004 | 0.002 | 0.001 | 0.000 | 0.007 | 0.000 |
| Al | 0.001 | 0.001 | 0.000 | 0.001 | 0.032 | 0.000 | 0.000 | 0.000 |
| Zn | 0.000 | 0.001 | 0.000 | 0.008 | 0.000 | 0.002 | 0.002 | 0.001 |
| Ca | 0.000 | 0.000 | 0.001 | 0.000 | 0.000 | 0.000 | 0.005 | 0.000 |
| Fe | 3.954 | 3.950 | 3.961 | 3.956 | 3.899 | 3.952 | 3.959 | 3.943 |
| Mg | 0.039 | 0.034 | 0.025 | 0.027 | 0.045 | 0.043 | 0.003 | 0.056 |
| Ti | 0.001 | 0.001 | 0.001 | 0.000 | 0.000 | 0.000 | 0.008 | 0.000 |
| Mn | 0.003 | 0.005 | 0.004 | 0.004 | 0.005 | 0.003 | 0.001 | 0.000 |
| Cr | 0.000 | 0.000 | 0.000 | 0.000 | 0.000 | 0.000 | 0.000 | 0.000 |

¹ Analyses (wt %) from magnetite from the Bryson bridge and hydroelectric dam showings. Chemical formulas were calculated by normalizing total cations to 4.

² Total iron expressed as FeO.

Table 11.3: Electron Microprobe Analyses of Wurtzite/sphalerite¹

| | Dendritic wurtzite/sphalerite exsolutions in magnetite | | | | Centre ² | | Rim ² | | in serpentine nodule | |
|---------------------|--|-----------|-----------|-----------|---------------------|-----------|------------------|-----------|----------------------|-----------|
| | 065-B1-C1 | 065-B1-C2 | 065-B1-C3 | 065-B1-C4 | 065-B1-C5 | 065-B1-C5 | 065-B1-C5 | 065-B1-C5 | 065-B1-C3 | 065-B1-C4 |
| <i>Weight %</i> | | | | | | | | | | |
| Zn | 61.74 | 63.23 | 57.19 | 58.00 | 56.07 | 57.08 | 61.32 | 63.27 | | |
| S | 33.10 | 32.79 | 33.62 | 33.96 | 33.65 | 33.00 | 33.69 | 33.55 | | |
| Fe | 5.84 | 4.92 | 6.48 | 9.61 | 10.75 | 6.57 | 4.10 | 2.40 | | |
| Mn | 0.03 | 0.01 | 0.12 | 0.07 | 0.09 | 0.10 | 0.06 | 0.04 | | |
| Ca | 0.01 | 0.01 | 0.65 | <0.01 | <0.01 | 0.92 | 0.37 | 0.39 | | |
| Total | 100.72 | 100.96 | 98.06 | 101.64 | 100.56 | 97.67 | 99.54 | 99.64 | | |
| <i>Atomic ratio</i> | | | | | | | | | | |
| Zn | 45.360 | 46.535 | 42.511 | 41.854 | 40.820 | 42.697 | 45.262 | 46.812 | | |
| S | 49.583 | 49.208 | 50.954 | 49.967 | 49.942 | 50.339 | 50.706 | 50.614 | | |
| Fe | 5.018 | 4.235 | 5.641 | 8.117 | 9.160 | 5.755 | 3.539 | 2.077 | | |
| Mn | 0.024 | 0.006 | 0.103 | 0.062 | 0.079 | 0.091 | 0.053 | 0.031 | | |
| Ca | 0.016 | 0.015 | 0.792 | 0.000 | 0.000 | 1.119 | 0.440 | 0.465 | | |

¹ Analyses (wt %) of dendritic wurtzite/sphalerite exsolutions inside magnetite and a aggregates inside associated serpentine grains from the Bryson hydroelectric dam showing (065-B1).

² Represents analyses from the center and contact margin with magnetite of a wurtzite/sphalerite exsolution inside a magnetite (Bryson hydroelectric showing 065-B1).

Table 11.4: Debye-Scherrer Camera Data¹

| Bryson water treatment showing (013-8A) | | |
|---|---------------|-------|
| $4\theta^2$ | Intensity | d^3 |
| 23.5 | Medium-strong | 9.50 |
| 49.3 | Weak | 4.54 |
| 66.5 | Weak | 3.39 |
| 72.2 | Medium-strong | 3.13 |
| 75.0 | Very strong | 3.01 |
| 87.5 | Weak | 2.60 |
| 91.7 | Strong | 2.49 |
| 100.5 | Medium | 2.28 |
| 110.5 | Medium | 2.09 |
| 122.1 | Medium | 1.91 |
| 124.7 | Medium | 1.87 |
| 136.5 | Weak | 1.73 |
| 141.7 | Weak | 1.67 |
| 148.7 | Weak | 1.60 |
| 157.7 | Strong | 1.53 |
| 165.0 | Weak | 1.47 |
| 169.1 | Weak | 1.44 |
| 172.1 | Weak | 1.42 |

¹ Analyse (wt %) from a zincian serpentine from the Bryson water treatment plant showing. Peak positions and d spacing corresponds to that of a serpentine-type mineral. Some weak peaks are due to the presence of traces of carbonates.

² Four θ is obtained directly from measuring (in millimeters) the exposed bands on the film.

³ d is calculated using Bragg's law. The X-Ray tube emitting FeK α : 1.9373 Angstrom.

Table 11.5: Electron Microprobe Analyses of Serpentine¹

| | Cadieux power station | | | | | | Water treatment plant | |
|--------------------------------|-----------------------|----------|----------|----------|----------|----------|-----------------------|-----------|
| | 008-9-C1 | 008-9-C2 | 008-9-C3 | 008-9-C4 | 008-9-C5 | 008-9-C6 | 013-8A-C1 | 013-8A-C2 |
| SiO ₂ | 40.20 | 39.72 | 41.28 | 42.45 | 39.19 | 41.49 | 35.01 | 39.71 |
| MgO | 37.40 | 34.98 | 37.92 | 37.01 | 38.41 | 37.34 | 34.96 | 34.40 |
| ZnO | 1.33 | 1.26 | 1.26 | 2.46 | 1.07 | 1.74 | 0.92 | 3.81 |
| CaO | 0.08 | 0.07 | 0.07 | 0.06 | 0.03 | 0.08 | 0.27 | 0.14 |
| FeO ² | 1.40 | 1.43 | 1.45 | 0.70 | 1.52 | 0.79 | 0.68 | 0.83 |
| Al ₂ O ₃ | 3.23 | 2.68 | 3.12 | 0.65 | 2.61 | 0.58 | 2.20 | 0.63 |
| TiO ₂ | 0.02 | 0.04 | 0.03 | 0.02 | <0.01 | 0.02 | 0.22 | 0.05 |
| MnO | 0.02 | 0.01 | 0.01 | 0.02 | <0.01 | 0.01 | 0.02 | 0.02 |
| NiO | <0.01 | 0.02 | <0.01 | <0.01 | 0.00 | <0.01 | <0.01 | 0.02 |
| Total | 83.68 | 80.21 | 85.13 | 83.35 | 82.82 | 82.07 | 74.28 | 79.60 |
| Si | 1.116 | 1.146 | 1.124 | 1.182 | 1.101 | 1.171 | 1.095 | 1.172 |
| Mg | 1.547 | 1.505 | 1.539 | 1.536 | 1.609 | 1.571 | 1.630 | 1.513 |
| Zn | 0.027 | 0.027 | 0.025 | 0.051 | 0.022 | 0.036 | 0.021 | 0.083 |
| Ca | 0.002 | 0.002 | 0.002 | 0.002 | 0.001 | 0.002 | 0.009 | 0.004 |
| Fe | 0.033 | 0.035 | 0.033 | 0.016 | 0.036 | 0.019 | 0.018 | 0.020 |
| Al | 0.106 | 0.091 | 0.100 | 0.021 | 0.086 | 0.019 | 0.081 | 0.022 |
| Ti | 0.000 | 0.001 | 0.001 | 0.000 | 0.000 | 0.001 | 0.005 | 0.001 |
| Mn | 0.001 | 0.000 | 0.000 | 0.000 | 0.000 | 0.000 | 0.001 | 0.001 |
| Ni | 0.000 | 0.000 | 0.000 | 0.000 | 0.000 | 0.000 | 0.000 | 0.001 |

¹ Analyses (wt %) from zincian serpentine from the Bryson area. Chemical formulas were calculated by normalizing total cations to 4.

² Total iron expressed as FeO.

Table 11.6: Electron Microprobe Analyses of Serpentine¹

| | Bryson bridge | | Bryson hydroelectric dam | | | | | |
|--------------------------------|---------------|----------|--------------------------|-----------|-----------|-----------|-----------|-----------|
| | 003-1-C1 | 003-1-C2 | 065-B2-C1 | 065-B2-C2 | 065-B2-C3 | 065-B2-C4 | 065-B2-C5 | 065-B2-C6 |
| SiO ₂ | 39.07 | 38.36 | 27.29 | 30.69 | 31.15 | 32.56 | 37.15 | 38.14 |
| MgO | 36.77 | 32.38 | 22.82 | 25.44 | 25.54 | 26.91 | 31.55 | 32.67 |
| ZnO | 1.15 | 3.93 | 3.61 | 2.07 | 2.31 | 2.80 | 4.28 | 4.31 |
| CaO | 0.09 | 0.10 | 0.00 | 0.09 | 0.16 | 0.11 | 0.09 | 0.13 |
| FeO ² | 0.42 | 0.91 | 3.54 | 23.25 | 22.79 | 19.84 | 0.96 | 0.91 |
| Al ₂ O ₃ | 0.40 | 0.82 | 0.52 | 0.88 | 0.64 | 0.62 | 0.97 | 0.72 |
| TiO ₂ | 0.05 | <0.01 | <0.01 | 0.00 | 0.00 | 0.01 | <0.01 | 0.04 |
| MnO | 0.02 | 0.01 | <0.01 | 0.01 | 0.00 | 0.01 | 0.03 | 0.02 |
| NiO | 0.01 | <0.01 | 0.01 | <0.01 | <0.01 | <0.01 | 0.01 | <0.01 |
| Total | 77.95 | 76.51 | 57.79 | 82.44 | 82.60 | 82.85 | 75.04 | 76.93 |
| Si | 1.157 | 1.178 | 1.147 | 1.007 | 1.018 | 1.041 | 1.169 | 1.170 |
| Mg | 1.624 | 1.483 | 1.430 | 1.244 | 1.244 | 1.282 | 1.480 | 1.494 |
| Zn | 0.025 | 0.089 | 0.112 | 0.050 | 0.056 | 0.066 | 0.100 | 0.098 |
| Ca | 0.003 | 0.003 | 0.000 | 0.003 | 0.006 | 0.004 | 0.003 | 0.004 |
| Fe | 0.010 | 0.023 | 0.125 | 0.638 | 0.623 | 0.530 | 0.025 | 0.023 |
| Al | 0.014 | 0.030 | 0.026 | 0.034 | 0.025 | 0.023 | 0.036 | 0.026 |
| Ti | 0.001 | 0.000 | 0.000 | 0.000 | 0.000 | 0.000 | 0.000 | 0.001 |
| Mn | 0.001 | 0.000 | 0.000 | 0.000 | 0.000 | 0.000 | 0.001 | 0.001 |
| Ni | 0.000 | 0.000 | 0.000 | 0.000 | 0.000 | 0.000 | 0.000 | 0.000 |

¹ Analyses (wt %) from zincian serpentine from the Bryson area. Chemical formulas were calculated by normalizing total cations to 4.

² Total iron expressed as FeO.

Table 11.7: Electron Microprobe Analyses of Pyrophanite¹

| | Exsolution in spinel | | Fine inclusion in zinceferous serpentine | | | | | | | |
|--------------------------------|---------------------------|---------------------------|--|---------------------------|---------------------------|---------------------------|---------------------------|---------------------------|---------------------------|---------------------------|
| | 003-1- C1 ² | 003-1- C2 ² | 008-9- C1 ³ | 008-9- C2 ³ | 008-9- C3 ³ | 008-9- C4 ³ | 008-9- C5 ³ | 008-9- C6 ³ | 008-9- C7 ³ | 008-9- C8 ³ |
| SiO ₂ | 1.01 | 2.53 | 4.10 | 3.32 | 0.73 | 0.36 | <0.01 | 2.52 | 1.20 | 0.86 |
| Al ₂ O ₃ | 0.05 | 0.15 | 0.26 | 0.73 | 0.10 | 0.02 | 0.00 | 1.23 | 0.04 | 0.05 |
| ZnO | <0.01 | <0.01 | 8.91 | 7.40 | 0.24 | 0.99 | 0.02 | 5.31 | 4.58 | 3.80 |
| CaO | 0.07 | 0.05 | 0.06 | 0.03 | <0.01 | <0.01 | <0.01 | <0.01 | <0.01 | <0.01 |
| FeO ⁴ | 1.16 | 1.40 | 4.75 | 3.48 | 23.13 | 25.52 | 32.67 | 3.79 | 10.93 | 16.73 |
| MgO | 1.29 | 3.61 | 3.91 | 5.34 | 0.86 | 0.44 | 0.26 | 4.20 | 1.04 | 0.67 |
| TiO ₂ | 50.75 | 48.17 | 48.33 | 45.67 | 46.89 | 44.40 | 52.96 | 46.64 | 51.98 | 53.11 |
| MnO | 43.12 | 40.94 | 28.95 | 29.91 | 21.08 | 15.74 | 14.14 | 32.35 | 26.88 | 20.65 |
| Cr ₂ O ₃ | 0.02 | <0.01 | 0.01 | <0.01 | <0.01 | <0.01 | <0.01 | <0.01 | <0.01 | <0.01 |
| Total | 97.48 | 96.86 | 99.27 | 95.87 | 93.02 | 87.47 | 100.04 | 96.03 | 96.65 | 95.86 |
| Si | 0.034 | 0.085 | 0.134 | 0.112 | 0.026 | 0.010 | 0.000 | 0.085 | 0.031 | 0.022 |
| Al | 0.002 | 0.006 | 0.010 | 0.029 | 0.004 | 0.001 | 0.000 | 0.049 | 0.001 | 0.002 |
| Zn | 0.000 | 0.000 | 0.215 | 0.185 | 0.006 | 0.021 | 0.000 | 0.133 | 0.086 | 0.072 |
| Ca | 0.003 | 0.002 | 0.002 | 0.001 | 0.000 | 0.000 | 0.000 | 0.000 | 0.000 | 0.000 |
| Fe | 0.033 | 0.039 | 0.130 | 0.099 | 0.698 | 0.618 | 0.687 | 0.107 | 0.233 | 0.359 |
| Mg | 0.065 | 0.181 | 0.191 | 0.269 | 0.046 | 0.019 | 0.010 | 0.212 | 0.040 | 0.026 |
| Ti | 1.294 | 1.217 | 1.189 | 1.161 | 1.273 | 0.967 | 1.001 | 1.188 | 0.998 | 1.024 |
| Mn | 1.239 | 1.165 | 0.802 | 0.857 | 0.645 | 0.386 | 0.301 | 0.928 | 0.581 | 0.449 |
| Cr | 0.001 | 0.000 | 0.000 | 0.000 | 0.000 | 0.000 | 0.000 | 0.000 | 0.000 | 0.000 |

¹ Analyses (wt %) from all pyrophanite occurrences. Chemical formulas were calculated by normalizing total cations to 4.² Analyses of pyrophanite exsolutions inside relic spinels hosted by non-zincian serpentine nodules from Bryson's bridge showing (Sample 003-1).

Table 11.8: Electron Microprobe Analyses of Spinel¹

| | Bryson bridge showing | | |
|--------------------------------|-----------------------|----------|----------|
| | 003-1-C1 | 003-1-C2 | 003-1-C3 |
| SiO ₂ | <0.01 | <0.01 | <0.01 |
| Al ₂ O ₃ | 70.45 | 70.75 | 69.72 |
| ZnO | 1.62 | 1.77 | 1.88 |
| CaO | 0.01 | 0.00 | 0.01 |
| FeO ² | 0.48 | 0.46 | 0.51 |
| MgO | 27.38 | 27.26 | 27.46 |
| TiO ₂ | 0.03 | 0.09 | 0.99 |
| MnO | 0.01 | 0.03 | 0.02 |
| Cr ₂ O ₃ | 0.03 | 0.02 | 0.00 |
| Total | 100.01 | 100.37 | 100.59 |
| Si | 0.000 | 0.000 | 0.000 |
| Al | 1.988 | 1.990 | 1.962 |
| Zn | 0.029 | 0.031 | 0.033 |
| Ca | 0.000 | 0.000 | 0.000 |
| Fe | 0.010 | 0.009 | 0.010 |
| Mg | 0.977 | 0.970 | 0.977 |
| Ti | 0.001 | 0.002 | 0.018 |
| Mn | 0.000 | 0.001 | 0.000 |
| Cr | 0.001 | 0.000 | 0.000 |

¹ Analyses (wt %) from zincian spinel relics inside serpentine nodules from the Bryson bridge showing. Chemical formulas were calculated by normalizing total cations to 3.

² Total iron expressed as FeO.

11.4 DISCUSSION

11.4.1 Magnetic Zincian Spinel

Reinvestigation of the Bryson zincian magnetite showing shows that while a magnetite-franklinite solid-solution exists (Valentino et al., 1990), the magnetite at the Bryson Bridge and Hydroelectric Dam showings has no significant manganese or zinc and does not contain 4% franklinite component. Thus, Gauthier's et al. (1987) conclusion is probably in error which is most likely due to the lower electron beam precision of microprobes used in the early 1980.

Our new observations reveal that the magnetic spinels are magnetite which locally contains dendritic sphalerite/wurtzite exsolutions. Wurtzite (ZnS) is a polymorph of sphalerite which is known to form as a metastable phase in low temperature sulfur deficient environments. Thus, wurtzite has a sulfur deficiency relatively to sphalerite (Deer et al., 1992). Wurtzite and sphalerite usually occur as intergrowths (Ramdohr, 1980) and are therefore difficult to distinguish. Dendritic wurtzite exsolution is an uncommon phenomenon (Ramdohr, 1980), but one of the localities where dendritic wurtzite exsolutions occur is in the Franklin and Sterling Hill district. Here, wurtzite exsolutions were described as the destabilization process of franklinite (Fronde! and Klein, 1965; Squiller and Sclar, 1980; Ramdhor, 1980; Carvalho and Sclar, 1988).

Mineralogical features of magnetite in the stratiform magnetite beds near the bridge and hydroelectric dam of the town of Bryson strongly suggest that they were formed by the destabilization of franklinite, similar to the phenomenon observed at Franklin and Sterling Hill.

11.4.2 Zinc Silicate and Oxide

Investigation of the stratiform zincian silicates associated with and without magnetite reveals a complex assemblage of zincian serpentine nodules, locally containing zincian pyrophanite inclusions. As mentioned above, pyrophanite is a manganese-magnesium-and zinc-bearing mineral belonging to the ilmenite group (Deer et al., 1992). The presence of zincian pyrophanite confirms the metal association of Fe-Mn-Zn observed in Franklin-type

deposits. Pyrophanite is not commonly observed throughout the world but one locality where it is known to occur is at Franklin and Sterling Hill (Valentino et al., 1990).

Our observation of a relic zincian spinel of the gahnite-spinel group has important consequences for our study. The presence of pyrophanite exsolution inside this spinel indicates us that the mineral paragenesis observed in the Bryson area was metamorphosed to granulite-facies conditions. These metamorphic conditions are required to incorporate the manganese and magnesium-ilmenite inside the structure of the spinel in solid-solution (Deer et al., 1992). During retrograde metamorphism, pyrophanite becomes incompatible in the solid-solution and exsolves as fine lamellae inside the spinel.

Willemite (Zn_2SiO_4) is a common zinc silicate at Franklin and Sterling Hill hypogene stratiform non-sulfide zinc deposits. Moreover, it possesses the same chemical formula as olivine ($(\text{Fe,Mg})_2\text{SiO}_4$) although zinc is the main cation rather than iron and/or magnesium. Therefore, the alteration of willemite could form a zincian serpentine, such as the reaction proposed to have occurred at Sterling Hill (Johnson, 1990). Robert Megster, the former Sterling Hill mine geologist, observed these features and confirmed that willemite destabilizes into a serpentine-type product (pers. comm., 2006). These observations strongly suggest that the stratiform zincian serpentine nodules observed in the Bryson area could have had such a protolith.

11.5 INTERPRETATION OF THE BRYSON NON-SULFIDE ZINC PARAGENESIS

The mineralogical study of the non-sulfide zinc occurrences of the Bryson area was successful in providing further evidence towards the determination of their deposit-type. The presence of pyrophanite exsolutions inside a zincian spinel indicates that the Bryson region was metamorphosed to granulite-facies conditions before retrograding into a serpentine assemblage. A retromorphic path also affects the granulite-facies mineral assemblage of Franklin and Sterling Hill (Fron del and Baum, 1974). This retrograde metamorphism renders the recognition of primary facies difficult at the Franklin and Sterling Hill district. Our data enables us to conclude that the Bryson area was affected by a dynamo-metamorphic evolution similar to the one present for Franklin-type deposits. However a notable difference is the stronger retrometamorphic overprint present in the Bryson-Renfrew area compared to

the Franklin and Sterling Hill district. This is explained by presence of the Ottawa-Bonnechere graben and its intensive retrometamorphic fluid circulation that occurs in the Bryson-Renfrew region (Easton, 1992).

Our interpretation of the mineralogical features of the Bryson non-sulfide zinc occurrences is discussed below. The Bryson zincian stratiform magnetite bed paragenesis is interpreted as the product of destabilization of granulite-facies franklinite. In a similar manner, the observed zincian serpentine nodules are interpreted as being the result of the destabilization of granulite-facies willemite. Thus the Bryson non-sulfide zinc mineralization would be a retrograde equivalent of a granulite-facies willemite-franklinite assemblage like the one observed at Franklin and Sterling Hill districts.

Thus, we demonstrated that there are several similarities between the mineralogical assemblage and the dynamo-metamorphic process of the Bryson non-sulfide occurrences and those from Franklin and Sterling Hill. At peak metamorphic conditions reached at the Bryson-Renfrew area, willemite-franklinite solid-solution minerals existed. These similarities lead us to conclude that the Bryson area hosts Franklin-type hypogene stratiform non-sulfide zinc mineralization, comparable to the Franklin and Sterling Hill district. Therefore Franklin and Sterling Hill are no longer the only known examples of non-sulfide zinc mineralization in the Grenville Province.

11.6 CONCLUSION

Our mineralogical study of the zincian silicates and oxides of the Bryson area revealed the presence of zinc-free magnetite containing dendritic exsolutions of sphalerite and/or wurtzite, zincian serpentines locally hosting zincian pyrophanite inclusions, and zincian spinel of the spinel-gahnite group containing non-zincian pyrophanite exsolutions. These features indicated that the Bryson marble belt underwent granulite-facies metamorphism before retrograding to serpentine-rich assemblages. Several of these features are also present at Franklin and Sterling Hill.

The zincian magnetite bed and zincian serpentine nodules are interpreted as being retrograded granulite-facies franklinite and willemite. The Bryson area is thus confirmed to host Franklin-type mineralization, and for the first time, the presence of Franklin-type non-

sulfide zinc mineralization is confirmed outside the New Jersey Highlands. Our study opens up new exploration perspectives for Franklin-type hypogene stratiform non-sulfide zinc mineralization outside of the New Jersey Highlands in the Grenville Supergroup.

SECTION IV

DISCUSSION OF SEDEX ZINC SULFIDE AND NON-SULFIDE MINERALIZATION IN THE BRYSON-RENFREW REGION

CHAPTER XII

GENERAL DISCUSSION

12.1 INTRODUCTION

Our study of the Bryson-Renfrew area marble-hosted SEDEX deposits enabled us to successfully test our hypotheses and bring forward new data for the scientific community. The final discussion is divided into four sections: (1) Conclusion of our non-sulfide zinc study in the Bryson area, (2) conclusions can be made from our study in the Bryson-Renfrew region, (3) Implications of having both SEDEX end-members of deposit in the same marble belt, and (4) Discussion of ideas that could explain the presence of both types of deposits in the same geological environment and their relation with a nearby VMS deposit.

12.2 BRYSON: FRANKLIN-TYPE MINERALIZATION

Three hypotheses were considered in the past for the genetic origin of the Bryson non-sulfide zinc mineralization: (1) It could be linked to the opening of the Ottawa-Bonnechère graben at the end of the Precambrian; (2) it could be related to metasomatism associated with the intrusion of the Chenaux gabbro into the marbles of the Bryson-Renfrew area at about 1100 Ma; (3) it could be syngenetic, stratabound or even epigenetic mineralization within the marbles of the Grenville Supergroup. The observation of a zincian spinel having a transitional composition between spinel and gahnite with pyrophanite exsolutions demonstrate that the Bryson non-sulfide zinc mineralization was brought to granulite-facies metamorphic conditions, like its hosting marbles. The age determination of the exhalative event for the Calumet deposit indicates that the zinc mineralization occurred before the intrusion of the Chenaux gabbro. Moreover, geological mapping and zinc

prospection has shown that the non-sulfide zinc mineralization is stratiform. Thus, the first two hypotheses can be rejected. Bryson's non-sulfide zinc horizons are hypogene and stratiform. Although they could also have been discordant or stratabound at the time of deposition, granulite-facies metamorphism and polyphase deformation obliterated the primary features required to distinguish between these hypotheses. It is also the case for the Balmat-Edwards district and the deposits of the Maniwaki-Gracefield area (deLorraine, 2001; Gauthier and Brown, 1986). Based on the McArthur River unmetamorphosed carbonate-hosted stratiform zinc-lead deposit (Cooke et al., 2000), we believe that the Grenville Supergroup marble-hosted zinc deposits are also stratiform.

Although the Bryson non-sulfide zinc horizons contains a sub-economic quantity of zinc, the similarities of their dynamo-metamorphic evolution and their mineralogical features with Franklin and Sterling Hill enables us to conclude that they are Franklin-type mineralizations (i.e. formation of high temperature assemblage of willemite-franklinite; the presence of pyroaurite, pyrophanite, etc.). Franklin-type mineralization is thus confirmed outside the New Jersey Highlands for the first time in Mesoproterozoic Grenville Supergroup marbles of Quebec and Ontario. Franklin-type SEDEX deposits are therefore not exceptionally anomalous in the Grenville Province and our study suggests that there is a potential for finding others.

12.3 BRYSON-RENFREW: BALMAT-TYPE SEDEX GEOLOGICAL ENVIRONMENT

The detailed geological mapping survey conducted from the town of Bryson to the north, to Renfrew to the south, had two objectives: (1) To determine the geological environment of deposition of the marble belt and its SEDEX zinc sulfide deposits, and (2) to trace the primary facies variations that could explain the gradation of non-sulfide zinc mineralization to disseminated/semi-massive sphalerite horizons such as those of the Cadieux deposit.

The mapping program was successful in permitting us to define the geological environment. For the first time, the Bryson-Renfrew area is defined as a shallow-water, evaporitic and oxidized, carbonate platform environment. This hypothesis is supported by the abundance of magnesium in the marble belt (i.e. dominance of pure dolomitic marbles) and

the presence of meta-evaporites (i.e. stratiform anhydrite and brucitic horizons). We were also successful in identifying several new SEDEX zinc sulfide occurrences throughout the Bryson-Renfrew region. Some of these occurrences are located much closer to the town of Bryson than the Cadieux deposit. We successfully traced these disseminated sphalerite silicate-rich dolomitic marble horizons from Grand-Calumet Island to the town of Bryson, a distance of 4 to 5 kilometers. These SEDEX zinc sulfide occurrences are found along a stratigraphic continuity linking the Bryson non-sulfide mineralization to these SEDEX zinc sulfide occurrences. This spatial relationship is discussed in the next section.

In our review of the Balmat-type marble-hosted SEDEX zinc sulfide deposits (i.e. Balmat-Edwards district) we pointed out that this type of deposit is deposited in a shallow-water evaporitic and oxidized carbonate platform environment. This geological depositional environment is characteristic of McArthur-subtype SEDEX deposits (Cooke et al., 2000). Therefore, we proposed in section 1 that Balmat-type SEDEX zinc sulfide deposits are McArthur-subtype SEDEX deposits metamorphosed to granulite-facies. The same geological environment and same zinc sulfide mineralization characterizes the Bryson-Renfrew region.

The Bryson-Renfrew area is therefore also typical Balmat-type geological environment, like those present throughout the Grenville Supergroup of Quebec, Ontario and New York State (i.e. Balmat-Edwards district, Cadieux and Maniwaki-Gracefield). It should then be possible to find other Balmat-type sphalerite-rich deposits in the Bryson-Renfrew area.

12.4 BRYSON: THE MISSING LINK BETWEEN SEDEX SULFIDE AND NON-SULFIDE DEPOSITS

Our identification of Franklin-type mineralization in the Mesoproterozoic Grenville Supergroup marbles of the Bryson-Renfrew area further refines our understanding of the formation of these deposits. For the first time, Franklin-type mineralization is confirmed to exist inside a continuous marble belt also hosting Balmat-type mineralization in the Bryson-Renfrew area. Because the Bryson-Renfrew area is characterized by a typical Balmat-type SEDEX environment, we can conclude that Franklin-type SEDEX non-sulfide deposits also occur in such an environment. Our review of the most important examples for Franklin-type deposits (i.e. Franklin and Sterling Hill) in section 2 showed that these SEDEX deposits were

deposited in a shallow-water carbonate platform environment. However, Franklin and Sterling Hill, the most important examples of non-sulfide mineralization were considered unique and restricted to the New Jersey Highlands (Fron del et Baum, 1974, Johnson, 1990). However, our work demonstrate that Franklin-type mineralization does occur in the more widely distributed Balmat-type SEDEX zinc sulfide environment. Because this environment is recognized throughout the world and is well understood, it is possible to study the genetic differences between both end-member of marble-hosted SEDEX deposits.

The less than 2 kilometer long lateral variation from SEDEX disseminated zinc sulfide mineralization on Grand Calumet Island to SEDEX non-sulfide zinc mineralization at Bryson is similar to a facies variation observed by Gauthier and Brown (1986) in the Maniwaki-Gracefield area, 90 kilometers to the northeast of Bryson. Here, we observe the lateral facies change is from massive to semi-massive SEDEX zinc sulfide deposits to stratiform magnetite-breunnerite (iron magnesite)-graphite horizon with traces of sphalerite (Gauthier et al., 2004; Gauthier et al., 1987; Gauthier and Brown, 1986). This particular mineral assemblage is interpreted as the prograde metamorphic dissociation of a magnesian siderite-rich horizon (Gauthier and Brown, 1986). In fact, the presence of a siderite halo is one of the features of McArthur subtype SEDEX deposits (Cooke et al., 2000) as discussed in section 1. This subtype of deposit is deposited by oxidized, neutral and warm hydrothermal brines.

The non-sulfide zinc horizon in the Bryson area is also characterized by the abundance of iron (i.e. magnetite) and magnesium (i.e. pyroaurite). However, silica is much more abundant in the dolomitic marbles (silicate-rich dolomitic horizon hosts non-sulfide zinc mineralization) and is expressed by the presence magnesium-rich silicates (i.e. magnesium-rich olivine: forsterite). With prograde metamorphism and locally present zinc, zincian olivine from the forsterite-willemite solid-solution formed at Bryson. The Maxwell brucite quarry is less than fifty meters way from the Bryson Water Treatment non-sulfide zinc occurrence. This nearby presence of brucitic marble shows that the abundance of silicate is not a regional feature of these dolomitic marbles, but rather seems associated with the appearance of zinc mineralization. Such a phenomenon is already well described by Sangster (1970) and Gauthier and Brown (1986) respectively for the SEDEX zinc deposits of

southeast Ontario and the Maniwaki-Gracefield region. A new fact outlined by our study is that SEDEX zinc sulfide and non-sulfide zinc mineralization are both associated with the deposition of a siliceous dolostone.

The objective of this thesis was to determine if a relationship exists between marble-hosted SEDEX zinc sulfide and non-sulfide zinc deposits (i.e. Balmat-Edwards and Franklin-Sterling Hill). Our studies successfully established this by demonstrating that both end-members of SEDEX deposits exist in the same continuous marble belt in the Bryson-Renfrew area and that they occur in a similar geological environment (the better understood geological environment for Balmat-type SEDEX deposits). Therefore, Bryson (Qc) is proposed to be the "missing link" between SEDEX zinc sulfide and non-sulfide deposits, as conventional SEDEX zinc-sulfide and unconventional stratiform non-sulfide zinc mineralization are believed to form in the same environment.

12.5 RELATIONSHIP BETWEEN BOTH END-MEMBERS OF SEDEX DEPOSITS

A question arises: what is the relationship between Balmat-type and Franklin-type SEDEX deposits? Mineral assemblage comparisons between both types of SEDEX deposit raises the possibility that the following dichotomy exists: a magnetite-sphalerite association for Balmat-type SEDEX deposits and a willemite-magnetite (magnetite-franklinite solid-solution) association for Franklin-type deposits. For example, the Bryson zincian serpentine, without inclusions of pyrophanite, is interpreted as the retromorphic destabilization of willemite (which has the same chemical formula as olivine and where complete substitution of magnesium by zinc is possible). Moreover willemite-franklinite are the main ore minerals for the Franklin and Sterling Hill deposits.

The explanation for the first mineral association (sphalerite-magnetite) may come from the recent research on the SEDEX deposit-type. Has mentioned in section 1, the genetic model and exploration guidelines established for the Grenville Supergroup Balmat-type mineralization (i.e. Balmat-Edwards district, Maniwaki-Gracefield, Cadieux) was based on shale-hosted SEDEX deposits such as those of the Selwyn Basin in Canada and Rammelsburg in Germany (Large, 1980; deLorraine and Dill, 1982; Gauthier and Brown, 1986). Research during the 80's has shown that this genetic model was not perfect for the

Grenville Supergroup SEDEX zinc sulfide deposits. For example, isotopic study of sulfur and lead by Whelan et al. (1984) on the zinc ore from the Balmat-Edwards district has shown that the mineralization fluids for the synsedimentary zinc ore was chemically similar to the fluids responsible for Mississippi Valley-Type (MVT) deposits rather than those forming the Selwyn Basin SEDEX deposits. For this reason and those presented in section 1, we proposed that the Grenville Supergroup SEDEX deposits rather belong to the McArthur-subtype of SEDEX deposits, as defined by Cooke et al. (2000). McArthur-subtype SEDEX are characterized by moderate to low temperature oxidized ($\text{SO}_4^{2-} > \text{H}_2\text{S}$) hydrothermal brines operating in a broad carbonate-evaporite platform. Zinc deposition under its sulfide form is due to the mixing of this hydrothermal fluid with a second fluid such as H_2S -rich anoxic seawater in sub-basins (Cooke et al., 2000). A link to tectonism (extensional regime) with sub-basins is then required to form the anoxic trap environment and control bacterial sulfate reduction (Whelan et al., 1990) and to control the release of hydrothermal brines into the hydrosphere and on the sea-floor. Such relation to sub-basin is mentioned at the Balmat-Edwards district (de Lorraine, 2001) and Maniwaki-Gracefield area (Gauthier and Brown, 1986).

Similar to McArthur-subtype hydrothermal ore fluids also characterize (1) the Irish-type stratabound carbonate-hosted zinc-lead deposits (Hitzman and Beaty, 1996), and (2) some Mississippi Valley-Type zinc-lead deposits (Cooke et al., 2000). McArthur SEDEX, Irish-type and some MVT deposits share these characteristics: (1) They are carbonate-hosted, (2) deposited by similar oxidized hydrothermal brines, and (3) metal deposition occurs because of fluid mixing (Hitzman and Beaty, 1996; Cooke et al., 2000; Hitzman et al., 2003). For example, the Irish-type orebodies in Ireland share chemically analogue hydrothermal brines and were formed in a carbonate sequence which overlies an oxidized clastic sequence, the Old Red Sandstone Formation which is very similar to the environment present at the McArthur River basin in Australia (Cooke et al., 2000). The presence of colloform textured sphalerite in unmetamorphosed environments of these deposits suggest rapid deposition and fluid mixing is the simplest means of inducing rapid mineral precipitation (Hitzman et al., 2003). The fluid mixing with the oxidized hydrothermal fluid could be seawater, reduced anoxic H_2S -rich basinal brines, reduced ground water or basinal fluid which equilibrated with an oxidized or reduced rock mass such as a red-bed sequence or graphite-bearing sediments

(Hitzman et al., 2003). Although they are morphologically and genetically distinct (i.e. McArthur SEDEX are syngenetic while Irish-type and MVT are epigenetic), this difference has mainly to do with where fluid mixing actually occurred. If the zinc-bearing oxidized hydrothermal fluid mixes with a reduced H_2S -bearing fluid before reaching the surface, it would form an epigenetic stratabound zinc-lead deposit with replacement mineralization for example. However, if fluid mixing occurs with reduced H_2S basinal seawater brines in an anoxic sub-basin, syngenetic zinc sulfide precipitation occurs forming McArthur SEDEX subtype deposits.

Oxidized McArthur SEDEX-subtype hydrothermal fluids are capable of depositing sphalerite and magnetite (Cooke et al., 2000) such as it is observed for example in the Maniwaki and Bryson area. The recent research advances in the SEDEX deposit-type can thus explain the sphalerite-magnetite mineral association observed with the Grenville Supergroup SEDEX zinc deposits. But what can explain the willemite-magnetite mineral association?

Willemite is the main constituent of hypogene (structurally-controlled and stratiform) non-sulfide zinc deposits and can be thought as the defining mineral for these types (Hitzman et al., 2003). While hypogene structurally-controlled and stratiform non-sulfide zinc deposits are morphologically distinct, they seem similar in many ways and their difference could have to do with where mineralization occurred and the fact that the biggest example for stratiform deposit-type (i.e. Franklin and Sterling Hill) has been metamorphosed to granulite-facies (Hitzman et al., 2003). Willemite has been considered a metamorphic mineral by several authors because of its abundant presence in the highly metamorphosed Franklin and Sterling deposits (Hitzman et al., 2003). Moreover, the high temperature stability of willemite is well documented and supported by its presence in slags from zinc smelters, in alkaline intrusions, in ceramic glazes and even lunar fragments (Hitzman et al., 2003 and reference therein). At the Franklin and Sterling Hill district, Squiller and Sclar (1980), Johnson et al. (1990) and Johnson and Skinner (2003) suggests that willemite is formed by prograde metamorphic dissociation of a zincian dolomite or a carbonate zinc hydroxide mud (section 2). However, hypogene willemite is present in the unmetamorphosed deposits of Vazante in Brazil and Beltana in Australia (Monteiro et al., 1999; Brugger et al., 2003; Hitzman et al., 2003).

Franklinite is also present and associated with willemite at the Vazante mine (Monteiro et al., 1999). The presence of willemite at these deposits clearly indicates that willemite did not form under extreme high temperature conditions and raises the possibility that primary precipitation of willemite, and even franklinite, from hydrothermal fluids is possible.

So, another question arises: Is this willemite formed by prograde metamorphic dissociation of a zincian dolomite reacting with available silica, as proposed by Squiller and Sclar (1980) for Franklin and Sterling Hill deposits, or is it rather primary and contemporaneous to the exhalative system?

Recent experimental research on willemite stability in hydrothermal environments suggests the latter possibility and could help explain the existing dichotomy between Balmat-type and Franklin-type deposits. According to Brugger et al. (2003), willemite is more stable than sphalerite and will precipitate in neutral and oxidized (sulfate stable) conditions. Balmat and Franklin-type SEDEX deposits are characterized by a shallow-water oxidized evaporitic carbonate platform environment where such conditions exist. Moreover, willemite is more stable than sphalerite at high temperatures ($>300^{\circ}\text{C}$) and can coexist with magnetite (Brugger et al., 2003). Therefore, willemite will precipitate in a hot environment whereas sphalerite will precipitate when the environment is warm ($<300^{\circ}\text{C}$). The mineral association of willemite and magnetite is thus possible in hydrothermal unmetamorphosed environments. The hydrothermal fluid capable of precipitating hypogene hydrothermal willemite (Brugger et al., 2003) share several features with the one for depositing McArthur SEDEX Zinc sulfide deposits (Cooke et al., 2000). The similarities include (1) a carbonate platform environment, a (2) sulfate-stable oxidized hydrothermal brines, and (3) deposition by fluid mixing. Therefore, the differences between SEDEX sulfide zinc and Franklin-type non-sulfide zinc deposits could be an indication of a hot exhalative system rather than a warm one operating in an evaporitic carbonate platform environment. Both deposits could be primary and hydrothermal in origin and therefore be found in the same districts as sphalerite-rich SEDEX, Irish-type and MVT deposits.

Such scenario exists in Brazil in the unmetamorphosed carbonate platform hosting the Vazante hypogene non-sulfide zinc deposit. The Morro Agudo zinc-lead sulfide deposit is located approximately 100 kilometers north of the Vazante deposits. The Morro Agudo

deposit is interpreted as a classic Irish-type deposit and occurs in rocks equivalent and stratigraphically above those hosting the Vazante mineralization (Monteiro et al., 1999; Hitzman et al., 1995; Hitzman et al., 2003). Both deposits thus occur in the same carbonate belt and in the same district. Thus, the mixing of hot ($< 300^{\circ}\text{C}$) zinc-bearing oxidized (sulfate stable) hydrothermal brines with oxidized sulfur-poor seawater would precipitate willemite and the mixing of a similar fluid with basinal H_2S -rich anoxic brine pools on the ocean floor would form sphalerite. The existence of co-precipitation of willemite and sphalerite at the Vazante deposit (Monteiro et al., 1999) also confirms that temperature control on the brine is an efficient way to precipitate willemite and sphalerite (Brugger et al., 2003).

It is then possible to consider that Franklin and Sterling Hill willemite-franklinite mineralization could be deposited as a primary assemblage by hydrothermal brines and later metamorphosed to granulite facies. Such metamorphism would not change the mineral assemblage because of the high range of stability for willemite (Hitzman et al., 2003). Such an interpretation could also apply to the Bryson-Renfrew area with primary hydrothermal precipitation of stratiform hypogene willemite locally associated with magnetite. This genetic model explains the existing dichotomy between both end-member of SEDEX zinc deposits. A continuum is therefore possible between carbonate-hosted SEDEX non-sulfide and sulfide zinc deposits. Franklin-type SEDEX mineralization could be typical of a hot hydrothermal system operating in a shallow-water evaporitic and oxidized carbonate platform environment with the direct precipitation of willemite and franklinite. As the hydrothermal brines cool down, by distance from the hydrothermal source, Balmat-type mineralization precipitates. Thus, Franklin-type mineralization could indicate the nearby presence of Balmat-type mineralization, and vice versa.

Our age determination for the Calumet exhalative volcanogenic polymetallic (Zn-Pb-Au-Ag) sulfide deposit, located west of the Bryson non-sulfide zinc occurrence, enables us to surpass the objectives of this thesis. As mentioned earlier, the Calumet deposit has been extensively studied but never but in a regional context (Sangster, 1967; Sangster, 1970; Jourdain, 1993). Shown to be comparable to the Montauban deposit which was historically dated, the Calumet deposit was thought to be older than the Grenville Supergroup, like Montauban, and to represent a basement of some kind (Gauthier et al., 2004). However, our

radiometric datation of the Calumet deposit indicates that it belongs to the metallogenic epoch of the Grenville Supergroup rather than the one of the Montauban Group. This conclusion forced us to consider the exhalative event associated with the deposition of the Calumet deposit as being contemporary with the deposition of SEDEX non-sulfide and sulfide zinc deposits in the Grenville Supergroup of the Bryson-Renfrew area.

Putting the Calumet deposit in the regional context of the Bryson-Renfrew area for the first time reveals new insights for the region's zinc mineralization and geological environment. Volcanogenic polymetallic massive sulfide (VMS) activity can form distal SEDEX-type mineralization (Goodfellow et al., 1993; Lydon, 1996). During the deposition of Grenville Supergroup carbonates there is simultaneous deposition of volcanic rocks. During the volcanogenic exhalative event forming the Calumet Zn-Pb-Au-Ag massive sulfide deposit, there is contemporaneous distal deposition of zinc-dominant sedimentary exhalites. A mineral zonation can be established from the volcanogenic polymetallic (Zn-Pb-Au-Ag) massive sulfide mineralization which then regionally grades to distal zinc dominant sedimentary exhalative deposits away from the center of hydrothermal activity. This zonation is well documented for VMS deposits and mostly results in temperature decrease (Goodfellow et al., 1993; Lydon, 1996). The observed mineralization zonation in the Bryson-Renfrew basin reflects that the Calumet volcanogenic exhalative event is contemporaneous. The hydrothermal brines, that are regionally exhaled in the carbonate platform gradually, cool down as the distance from the VMS deposit raises. This temperature cool-down as a direct implication for the type of SEDEX mineralization deposited. We propose that close to the VMS deposit, hotter SEDEX hydrothermal brines would precipitate willemite and magnetite while further away, with brine cooling, sphalerite and magnetite mineral association becomes stable and precipitates. This model also explains why sub-economic values were obtained for the Bryson non-sulfide zinc occurrences and why disseminated sphalerite mineralization was encountered throughout the Bryson-Renfrew area (0.2% zinc). We propose that the SEDEX mineralizations discovered in the Bryson area are distal exhalites from the Calumet deposit. Exhalites usually contains sub-economic metals (Goodfellow et al., 1993). Therefore, hypogene non-sulfide zinc mineralization could also indicate the presence of a hot volcanogenic massive sulfide deposit in the area.

Not only do we propose that a continuum exists between SEDEX non-sulfide and sulfide zinc deposits, but we also propose that such mineral association can also be linked to a geological environment hosting a volcanogenic exhalative deposit.

CONCLUSION

Our studies show the existence of Franklin-type non-sulfide zinc occurrences in the marbles of the Bryson-Renfrew region. We show that Franklin-type non-sulfide zinc deposits occur in the same environment as SEDEX zinc sulfide deposits providing clues on the relationship between both end-members of hypogene zinc deposits. Moreover, both end-members of zinc deposits are hosted by metamorphosed siliceous dolostone units.

So SEDEX deposits could then present themselves as chameleons: sometimes under the form of stratiform sulfide beds and more rarely under the appearance of disseminated non-sulfide zinc mineralizations. This difference in mineralogy could be explained by the operation of a hot exhalative system (willemite) rather than a warm one (sphalerite). The results of our study reveal new exploration perspectives which were unsuspected until-now and confirm that Franklin-type deposits are not an exceptional anomaly in the Grenville Province. Franklin-type deposits are to be sought throughout the Mesoproterozoic Grenville Supergroup marbles of Canada. Such mineralization can also indicate the presence of a nearby polymetallic volcanogenic massive sulfide deposit.

APPENDIX A

GEOLOGICAL FEATURES OF BALMAT-TYPE AND FRANKLIN-TYPE SEDEX DEPOSITS

Table: Comparaison of the major geologic features of marble-hosted Grenville Supergroup zinc deposits (Balmat-type and Franklin-type)¹

| | Balmat-Edwards | Franklin and Sterling Hill | Maniwaki-Gracefield | Cadieux | Bryson |
|------------------------------------|-------------------------------------|--|--|-------------------------------------|-------------------------------------|
| Basin stratigraphy | Broad carbonate evaporite platforms | Broad carbonate platforms | Broad carbonate evaporite platforms | Broad carbonate evaporite platforms | Broad carbonate evaporite platforms |
| Depositional environment | Shallow marine to lacustrine | Shallow marine | Shallow marine to lacustrine | Shallow marine to lacustrine | Shallow marine to lacustrine |
| Carbonates | Dolomitic carbonate | Calcitic and locally dolomitic carbonate | Dolomitic carbonate | Dolomitic carbonate | Dolomitic carbonate |
| Evaporites | Anhydrite and boron-rich layers | Boron-rich layers are present | Boron of evaporitic marine environment | Anhydrite | Anhydrite, magnesium and boron |
| Mineralization | Stratiform zinc sulfide | Stratiform zinc silicate and oxide | Stratiform zinc sulfide | Stratiform zinc sulfide | Stratiform zinc silicate and oxide |
| Unit hosting zinc mineralization | Siliceous dolomitic marble | Calcitic and dolomitic siliceous marble | Siliceous dolomitic marble | Siliceous dolomitic marble | Siliceous dolomitic marble |
| Fe carbonate halo (i.e. magnetite) | Present | Present | Present | Present | Present |

¹ Compilation from the following references: deLorraine (2001); Gauthier and Brown (1986); Johnson and Skinner (2003); Peck et al. (2009) and references cited in section 2.

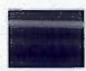

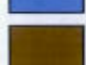

APPENDIX B

LOCATION OF DIAMOND DRILLING HOLES USED FOR THE U-PB GEOCHRONOLOGY OF THE NEW CALUMET MINE

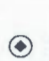




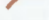


LEGEND


LITHOLOGY

-  MAFIC TO ULTRAMAFIC
INTRUSIVE ROCKS
INTRUSIVE CONTACT
-  M01 DOLOMITIC
MARBLE
-  AMPHIBOLITE BIOTITE
GNEISS
-  AMPHIBOLITIC GNEISS

SYMBOLS

-  Diamond drilling hole
UTM coordinates :
369 301mE/5 062 134mN
-  Geological contact
-  Road
-  River/Lake
-  Stream
-  Topographic
contour

METALLOGENY

-  New Calumet Mine
Volcanogenic exhalative polymetallic
(Zn-Pb-Au-Ag) massive sulfide
deposit of Mesoproterozoic age

NEW CALUMET MINE, DRILL HOLE LOCATION

Geology by
Jean-François Larivière

Topographic data :
© Department of Natural Resources Canada. All rights
reserved.

APPENDIX C

U-PB GEOCHRONOLOGY OF A SAMPLE FROM THE NEW CALUMET MINE

GÉOCHRONOLOGIE U-PB D'UN ÉCHANTILLON PROVENANT DE LA MINE CALUMET – MAI 2009

TEL QUE SOUMIS PAR

JEAN DAVID (2009)

Un échantillon (#GT080605-1) de roche de composition intermédiaire présentant une bonne foliation a été traité afin d'en établir l'âge de mise en place par la technique de datation utilisant le géochronomètre U-Pb sur zircon. L'échantillon constitué de morceaux de carotte de forage provenant de la mine Calumet semble relativement homogène.

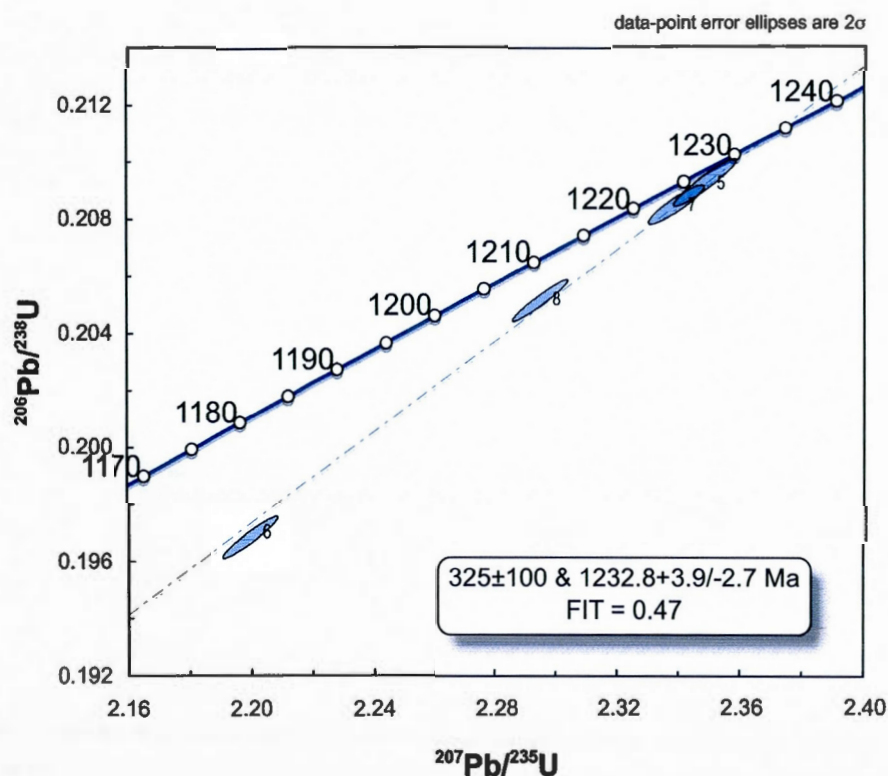
RÉSULTATS

Les zircons récupérés de l'échantillon sont de dimension moyenne avec quelques grains pouvant atteindre près de 220 μm de longueur. On retrouve 2 types de cristaux soit des zircons à section prismatique courte et à terminaisons pyramidales asymétriques, soit des cristaux équidimensionnels à multifacettes. Les cristaux sont généralement incolores avec quelques spécimens ayant une coloration brune dorée. Ils ne contiennent généralement pas d'inclusion.



Grossissement ca. 100X

Quatre fractions analytiques, chacune constituée de 1 à 2 cristaux, ont été analysées en mode solution (ID-TIMS). Les résultats indiquent qu'il s'agit de zircon ayant des concentrations en uranium relativement élevées jusqu'à 1400 ppm pour la fraction constitué de cristaux brun doré et des rapports Th/U faible variant entre 0.193 et 0.284. Les résultats sont tous considérés comme étant discordant et ont livré des âges $^{207}\text{Pb}/^{206}\text{Pb}$ qui varient entre 1231.5 ± 1.1 Ma (discordance de 0.6%) et 1221.1 ± 1 Ma (discordance de 5.5%). Les quatre résultats se répartissent sur une même droite qui peut être établie par un calcul de régression linéaire. L'intersection supérieure de la droite avec la courbe Concordia représente un âge de $1232.8 \pm 3.9 / -2.7$ Ma (probabilité de concordance de 47%).



MÉTHODOLOGIE

Récupération des minéraux lourds et sélection des zircons

Les échantillons sont préalablement nettoyés sous l'eau et avec une brosse pour éviter toute contamination. Tous les appareils sont rigoureusement nettoyés encore une fois afin d'éviter une contamination des poudres d'un échantillon précédemment traité.

L'échantillon est réduit à l'aide d'un broyeur à mâchoire puis d'un pulvérisateur à disques pour obtenir une poudre ayant la granulométrie d'un sable fin à très fin. Une première étape de concentration des minéraux lourds est effectuée en utilisant une table à secousse de type Wilfley. La fraction la plus lourde, après avoir été asséchée, est tamisée pour n'en conserver que le matériel inférieur à 200 μm . La deuxième étape est effectuée en utilisant une liqueur dense à base d'iodure de méthylène ($d=3.3$). Finalement les minéraux lourds sont séparés en fonction de leur susceptibilité magnétique en utilisant un séparateur isodynamique Frantz. Les zircons se caractérisant par des propriétés diamagnétiques sont examinés à la loupe binoculaire et sélectionnés sur la base de leur qualité (absence de micro-fractures, d'évidences d'altération et d'inclusions) pour ensuite être classés en fonction de critères typologiques: morphologie, développement des faces cristallines et couleur.

Analyse par dilution isotopique et spectrométrie de masse à ionisation thermique (ID-TIMS)

Les analyses effectuées par mise en solution du zircon exigent que les surfaces des zircons sélectionnés soient préalablement enlevées par abrasion dans une chambre à pression d'air (Krogh, 1982) afin de retirer la portion métamictite souvent affectée par une perte en Pb. Après avoir nettoyé les zircons à l'acide nitrique (HNO_3 4N) dans un bain ultrasonique, les cristaux choisis sont placés dans des capsules en téflon dans lesquelles on ajoute de l'acide fluorhydrique concentré (HF) et quelques milligrammes d'un étalon isotopique de ^{205}Pb et $^{233-235}\text{U}$, pour être mis au four à 220°C . Les produits de décomposition sont traités avec de l'acide chlorhydrique (HCl) pour assurer une dissolution complète. Les solutions sont subséquemment purifiées pour le plomb et l'uranium grâce à l'utilisation de colonnes chromatographiques utilisant des résines d'échange anionique en mode chlorydrique. Cette méthode présentée par Krogh (1973) a été modifiée pour des capsules de dissolution et des colonnes de taille réduite afin de minimiser la contamination.

Le plomb et l'uranium, pour être ionisés, sont déposés sur un même filament de rhénium dans un mélange de gel de silice et d'acide phosphorique. Les analyses sont effectuées en mode dynamique en utilisant le compteur d'ions du détecteur Daly d'un spectromètre de masse VG Sector54. Les facteurs de correction, prenant en considération à la fois la discrimination thermique des masses et celle du détecteur, sont de 0,15 %/AMU pour

le plomb et 0,16-0,18 %/AMU pour l'uranium. Ces corrections sont déterminées grâce à l'analyse répétée d'une solution standard de plomb (SRM981) et des isotopes ^{233}U - ^{235}U contenus dans l'étalon isotopique.

Les "droites discordia" sont établies en utilisant un calcul de régression linéaire (Davis 1982). Il s'agit d'un calcul qui prend en considération, 1) les erreurs corrélées des rapports Pb/U et Pb/Pb; 2) la discordance des points par rapport à l'intersection supérieure de la droite avec la 'courbe concordia'. Lorsque les données se distribuent à proximité ou sur la "courbe concordia" l'intercept supérieur est calculé en forçant l'extrémité inférieure de la droite de régression vers un âge de 0 Ma. La validité statistique de la droite obtenue par le calcul de régression linéaire s'exprime par un indice de probabilité de coïncidence ("probability of fit") qui devrait normalement être de ca. 0.50. On considère qu'une valeur de 0.10-0.15 est statistiquement acceptable (cf Ludwig 2003 pour une discussion sur ces considérations). Les incertitudes sur les rapports sont présentées à 1 sigma (intervalle de confiance de 65%) alors que les incertitudes sur les âges sont présentées à 2 sigma (intervalle de confiance de 95%).

RÉFÉRENCES

- Davis, D.W. 1982. Optimum linear regression and errors estimation applied to U-Pb data. *Canadian Journal of Earth Sciences*, 19 :2124-2149.
- Krogh, T.E. 1973. A low contamination method for hydrothermal decomposition of zircon and extraction of U and Pb for isotopic age determinations. *Geochimica et Cosmochimica Acta* 37: 485-494.
- Krogh, T.E. 1982. Improved accuracy of U-Pb ages by the creation of more concordant systems using an air abrasion technique. *Geochimica et Cosmochimica Acta* 46: 637-649.
- Ludwig, K.R. 2003. Isoplot 3.0, A geochronological Toolkit for Microsoft Excel. Berkeley Geochronological Center, Special Publication No.4.

APPENDIX D

GEOLOGICAL CHARACTERISTICS OF THE BRYSON-RENFREW REGION SEDEX ZINC SHOWINGS

Table: Characteristics of the SEDEX zinc sulfide showings of the Bryson-Renfrew region

| | Cadieux | Renfrew North | Portage-du-Fort | Calumet Trench | Calumet South |
|---------------------------------------|--|--|--|---|--|
| Location (<i>UTM zone 18 NAD83</i>) | 366300 mE/ 5030610 mN | 369090 mE/ 5033550 mN | 369090 mE/ 5051130 mN | 369200 mE/ 5059600 mN | 368750 mE/ 5058440 mN |
| Hosting rock unit | Siliceous dolomitic marble unit (M06) | Siliceous dolomitic marble unit (M06) | Siliceous dolomitic marble unit (M06) | Siliceous dolomitic marble unit (M06) | Siliceous dolomitic marble unit (M06) |
| Zinc ore mineral | Sphalerite | Sphalerite | Sphalerite | Sphalerite | Sphalerite |
| Mineralization | Semi-massive (up to 60% Sp ¹) | Disseminated (1- 2% Sp ¹) | Disseminated (3% Sp ¹) | Semi-massive to disseminated (up to 40% Sp ¹) | Disseminated (6% Sp ¹) |
| Evaporites | Anhydrite (drill core) | no drill core available | no core available | Anhydrite (drill core) | no drill core available |
| Morphology | Stratiform | Stratiform | Stratiform | Stratiform | Stratiform |
| Pre-metamorphic origin | Quartz-rich dolostone beds with sphalerite | Quartz-rich dolostone beds with sphalerite | Quartz-rich dolostone beds with sphalerite | Quartz-rich dolostone beds with sphalerite | Quartz-rich dolostone beds with sphalerite |

¹ Sp: Sphalerite

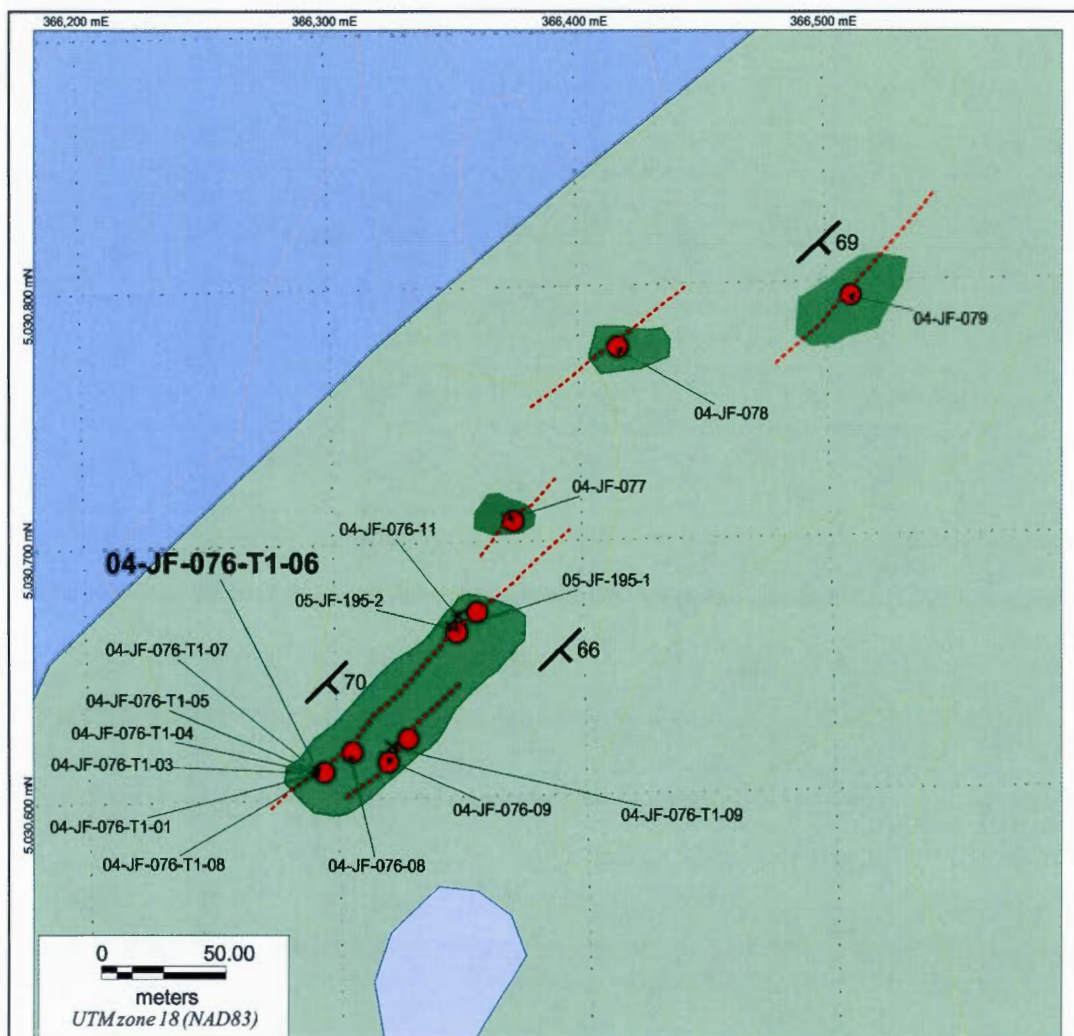
Table: Characteristics of the SEDEX non-sulfide zinc showings of the Bryson region

| | Bryson Bridge | Bryson Hydroelectric Dam | Bryson Water Treatment Plant | Cadieux Power Station |
|------------------------|---------------------------------------|---------------------------------------|---------------------------------------|---------------------------------------|
| Location ¹ | 373670 mE/ 5059080 mN | 372750 mE/ 5057900 mN | 373650 mE/ 5058890 mN | 373740 mE/ 5057310 mN |
| Hosting rock unit | Siliceous dolomitic marble unit (M06) | Siliceous dolomitic marble unit (M06) | Siliceous dolomitic marble unit (M06) | Siliceous dolomitic marble unit (M06) |
| Zinc ore mineral | Zinciferous magnetite and serpentine | Zinciferous magnetite and serpentine | Zinciferous serpentine | Zinciferous serpentine |
| Mineralization | Disseminated | Disseminated | Disseminated | Disseminated |
| Evaporites | Pyroaurite (boron) + dolomite | Brucite + dolomite | Brucite + dolomite | Pyroaurite (boron) + dolomite |
| Morphology | Stratiform | Stratiform | Stratiform | Stratiform |
| Pre-metamorphic origin | Quartz-rich dolostone beds | Quartz-rich dolostone beds | Quartz-rich dolostone beds | Quartz-rich dolostone beds |

¹ UTM zone 18 NAD83

APPENDIX E

DETAILED GEOLOGICAL MAPS OF THE BRYSON-RENFREW SHOWINGS



LEGEND

LITHOLOGY

- CHENAUX GABBRO INTRUSIVE
- M06 SILICEOUS DOLOMITIC MARBLE
- M01 DOLOMITIC MARBLE

INTRUSIVE CONTACT

SYMBOLS

- Outcrop / Trench or quarry
- Sample number and location
- Geological contact
- Strike and dip of bedding
- Road
- River / Lake
- Stream
- Dam
- Topographic contour

METALLOGENY

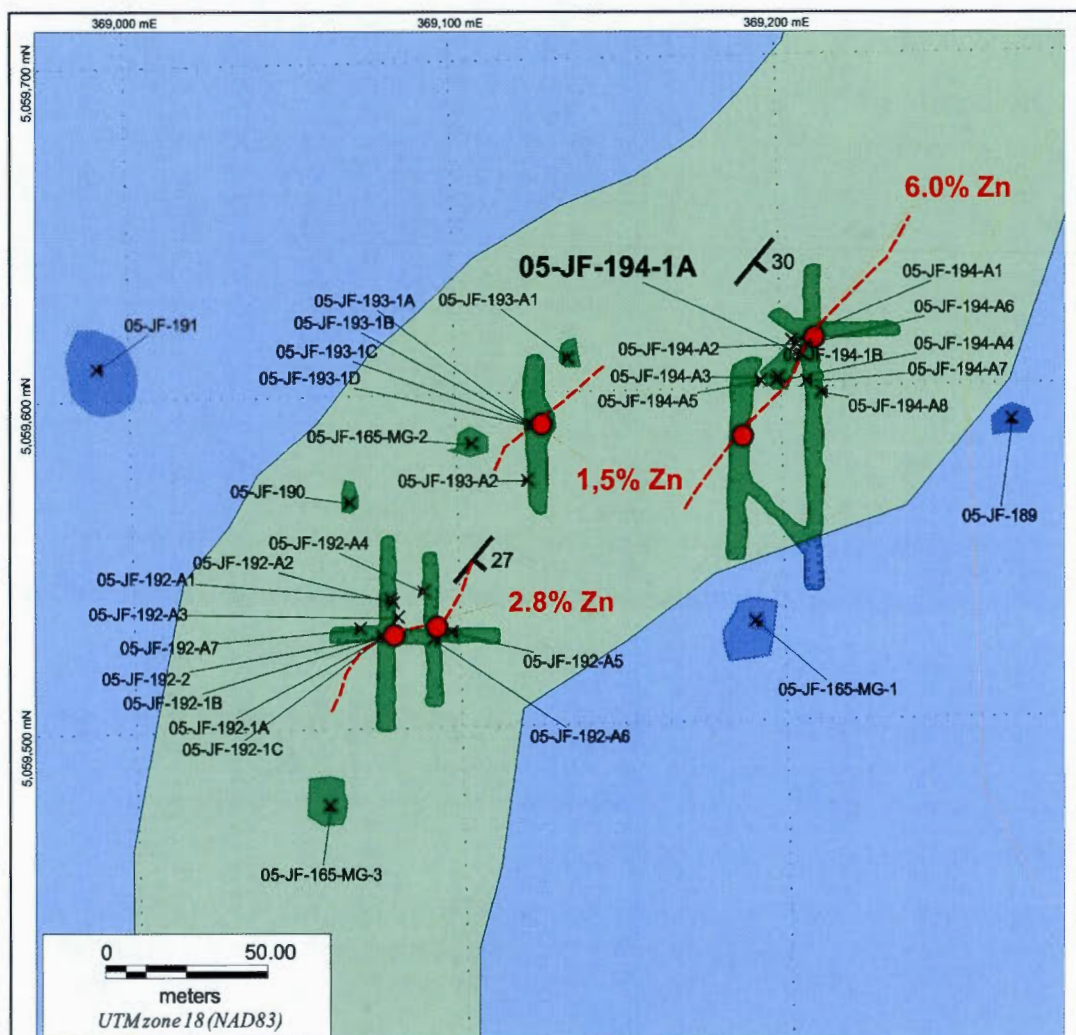
- SEDEX zinc silicate and oxide
- SEDEX zinc sulfide
- Stratiform magnesium mineralization (pure dolomite)
- Industrial mineral deposit (dolomitic marble)
- Stratiform brucite-rich horizon

* Lithologies or symbols may not occur on this sheet

Topographic data :
 @ Department of Natural Resources Canada. All rights reserved.

CADIEUX DEPOSIT, RENFREW

Geology by
 Jean-François Larivière



LEGEND

LITHOLOGY

- CHENAUX GABBRO INTRUSIVE
- INTRUSIVE CONTACT
- M06 SILICEOUS DOLOMITIC MARBLE
- M01 DOLOMITIC MARBLE

* Lithologies or symbols may not occur on this sheet

Topographic data :
© Department of Natural Resources Canada. All rights reserved.

SYMBOLS

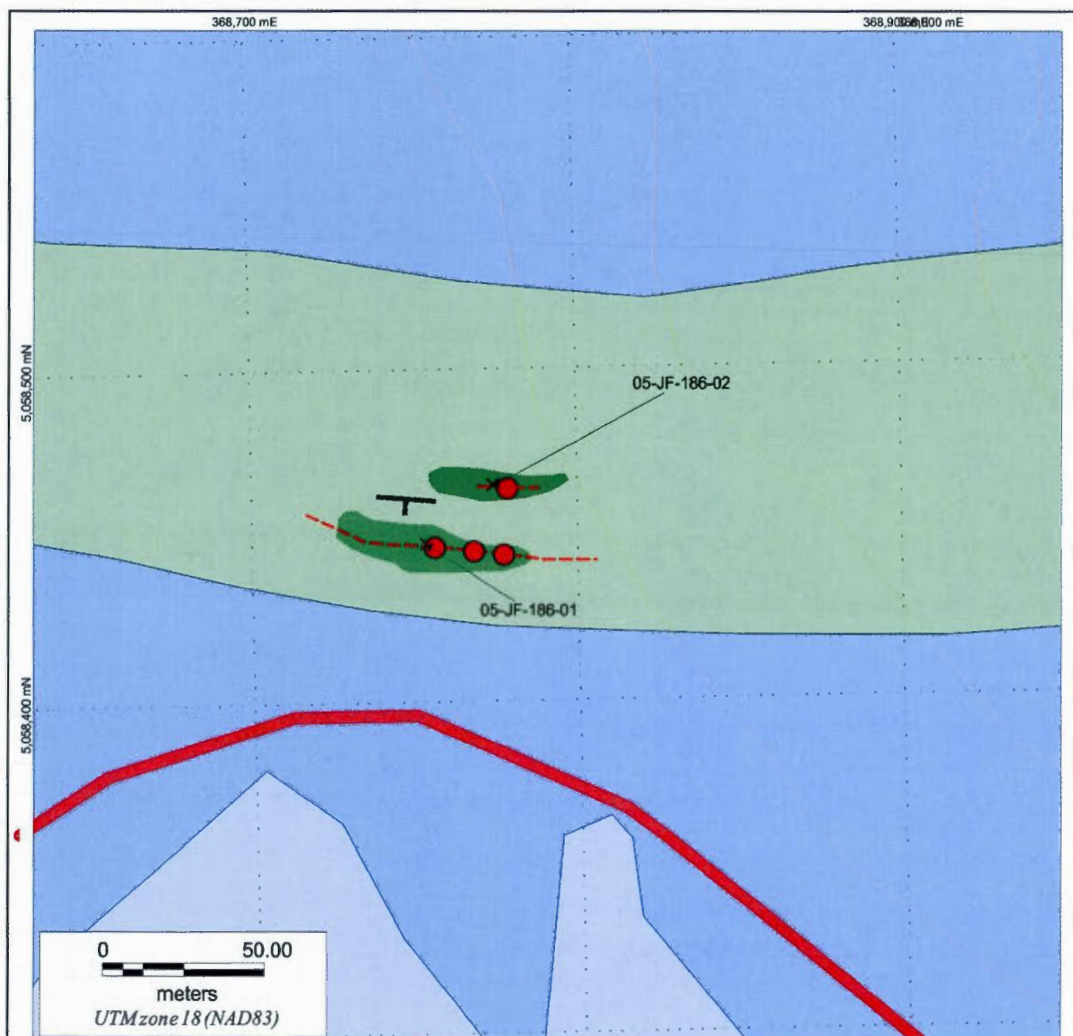
- Outcrop / Trench or quarry
- Sample number and location
- Geological contact
- Strike and dip of bedding
- Road
- River / Lake
- Stream
- Dam
- Topographic contour

METALLOGENY

- SEDEX zinc silicate and oxide
- SEDEX zinc sulfide
- Stratiform magnesium mineralization (pure dolomite)
- Industrial mineral deposit (dolomitic marble)
- Stratiform brucite-rich horizon

CALUMET TRENCH SHOWING

Geology by
Jean-François Larivière



LEGEND

LITHOLOGY

- CHENAUX GABBRO INTRUSIVE
- INTRUSIVE CONTACT
- M06 SILICEOUS DOLOMITIC MARBLE
- M01 DOLOMITIC MARBLE

* Lithologies or symbols may not occur on this sheet

Topographic data :
 @ Department of Natural Resources Canada. All rights reserved.

SYMBOLS

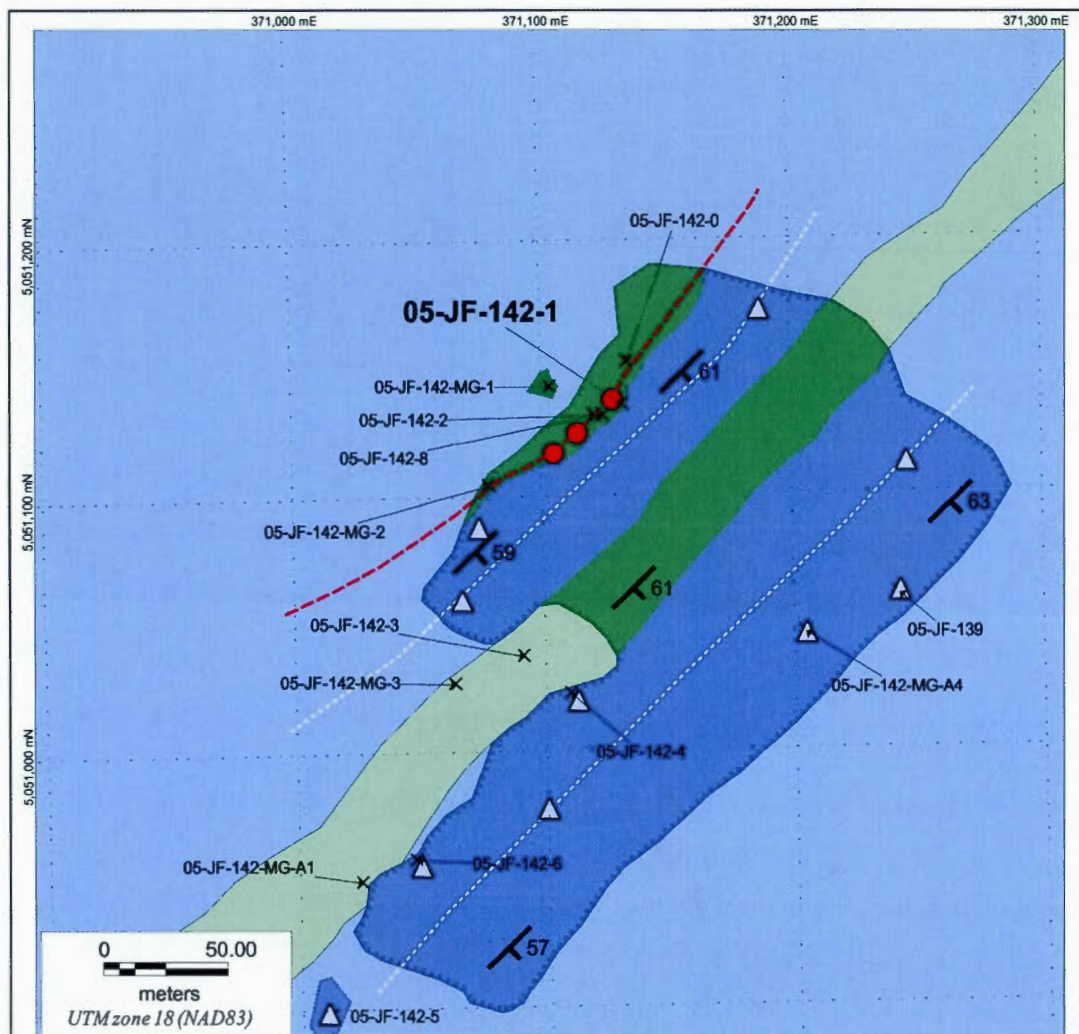
- Outcrop
- Sample number and location
- Geological contact
- Strike and dip of bedding
- Road
- River/Lake
- Stream
- Dam
- Topographic contour

METALLOGENY

- SEDEX zinc silicate and oxide
- SEDEX zinc sulfide
- Stratiform magnesium mineralization (pure dolomite)
- Industrial mineral deposit (dolomitic marble)
- Stratiform brucite-rich horizon

CALUMET SOUTH SHOWING

Geology by
 Jean-François Larivière



LEGEND

LITHOLOGY

- CHENAUX GABBRO INTRUSIVE
- M06 SILICEOUS DOLOMITIC MARBLE
- M01 DOLOMITIC MARBLE

INTRUSIVE CONTACT

SYMBOLS

- Outcrop / Trench or quarry
- Sample number and location
- Geological contact
- Strike and dip of bedding
- Road
- River / Lake
- Stream
- Dam
- Topographic contour

METALLOGENY

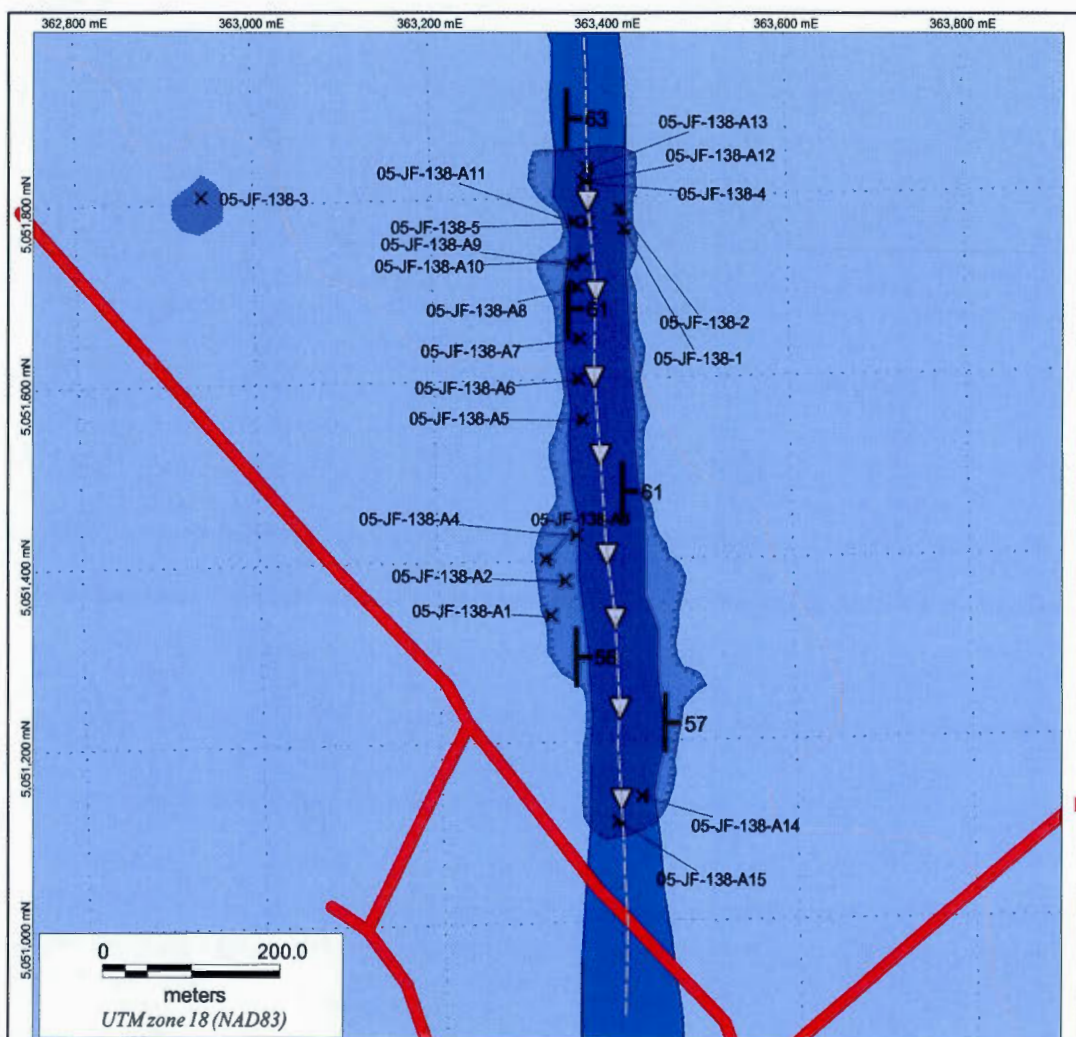
- SEDEX zinc silicate and oxide
- SEDEX zinc sulfide
- Stratiform magnesium mineralization (pure dolomite)
- Industrial mineral deposit (dolomitic marble)
- Stratiform brucite-rich horizon

* Lithologies or symbols may not occur on this sheet

Topographic data :
© Department of Natural Resources Canada. All rights reserved.

DOLOMEX DOLOMITE QUARRY, PORTAGE-DU-FORT

Geology by
Jean-François Larivière



LEGEND

LITHOLOGY

- CHENAUX GABBRO INTRUSIVE
- INTRUSIVE CONTACT
- M06 SILICEOUS DOLOMITIC MARBLE
- M01 DOLOMITIC MARBLE/ PURE DOLOMITIC MARBLE

* Lithologies or symbols may not occur on this sheet

Topographic data :
© Department of Natural Resources Canada. All rights reserved.

SYMBOLS

- Outcrop / Trench or quarry
- Sample number and location
- Geological contact
- Strike and dip of bedding
- Road
- River / Lake
- Stream
- Dam
- Topographic contour

METALLOGENY

- SEDEX zinc silicate and oxide
- SEDEX zinc sulfide
- Stratiform magnesium mineralization (pure dolomite)
- Industrial mineral deposit (dolomitic marble)
- Stratiform brucite-rich horizon


TIMMINCO DOLOMITE QUARRY, HALEY STATION

Geology by
Jean-François Larivière

LITHOLOGY

CHENAUX GABBRO
INTRUSIVE

INTRUSIVE CONTACT

 **M06 SILICEOUS
DOLOMITIC MARBLE**

M01 DOLOMITIC MARBLE

SYMBOLS

- Outcrop
- X Sample number and location
- Geological contact
- └ Strike and dip of bedding
- Road
- River/Lake
- Stream
- Dam
- Topographic contour

METALLOGENY

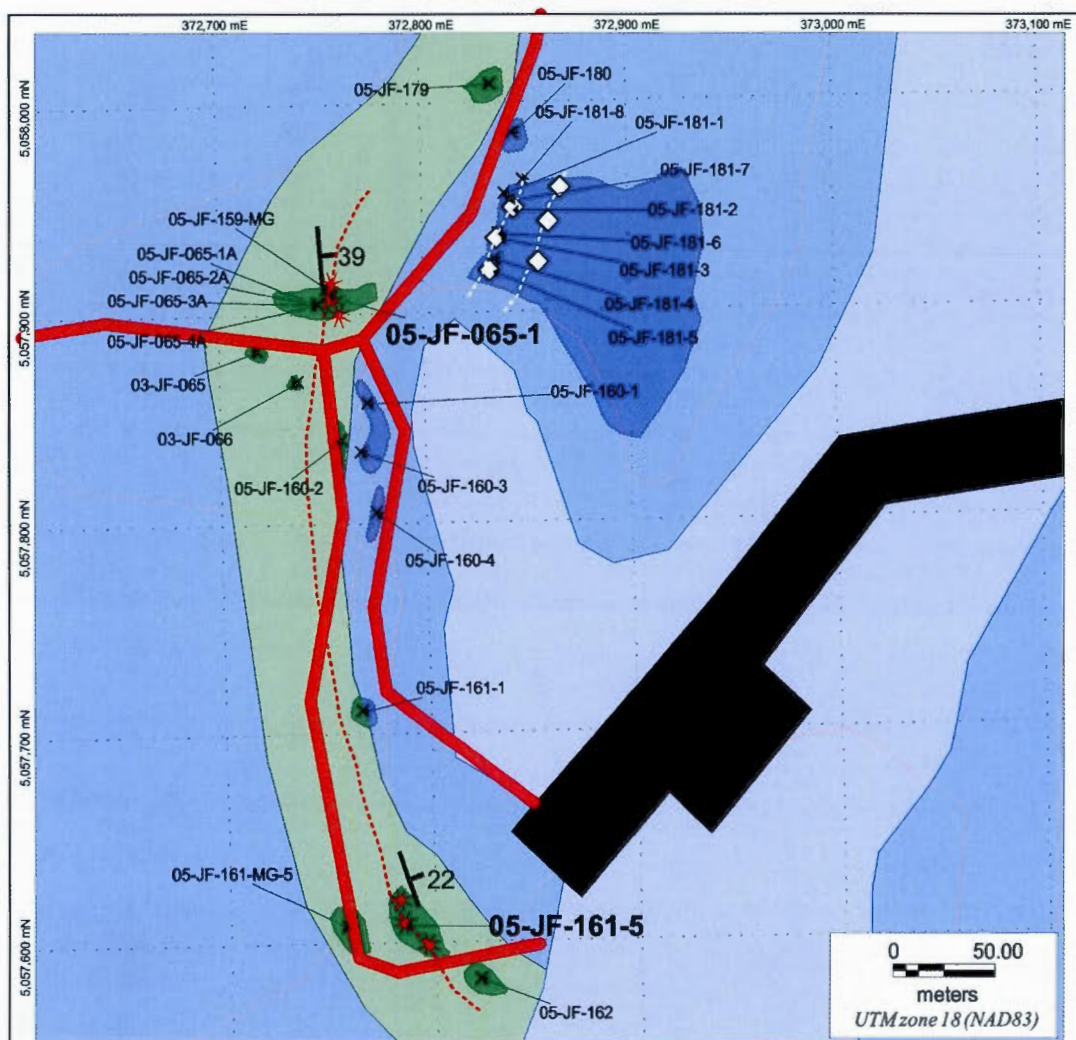
- ✱ SEDEX zinc silicate and oxide
- SEDEX zinc sulfide
- ▼ Stratiform magnesium mineralization (pure dolomite)
- ▲ Industrial mineral deposit (dolomitic marble)
- ◇ Stratiform brucite-rich horizon

* Lithologies or symbols may not occur on this sheet

Topographic data :
 @ Department of Natural Resources Canada. All rights reserved.

BRYSON BRIDGE SHOWING

Geology by
Jean-François Larivière



LEGEND

LITHOLOGY

- CHENAUX GABBRO INTRUSIVE
- INTRUSIVE CONTACT
- M06 SILICEOUS DOLOMITIC MARBLE
- M01 DOLOMITIC MARBLE

SYMBOLS

- Outcrop
- Sample number and location
- Geological contact
- Strike and dip of bedding
- Road
- River/Lake
- Stream
- Dam
- Topographic contour

METALLOGENY

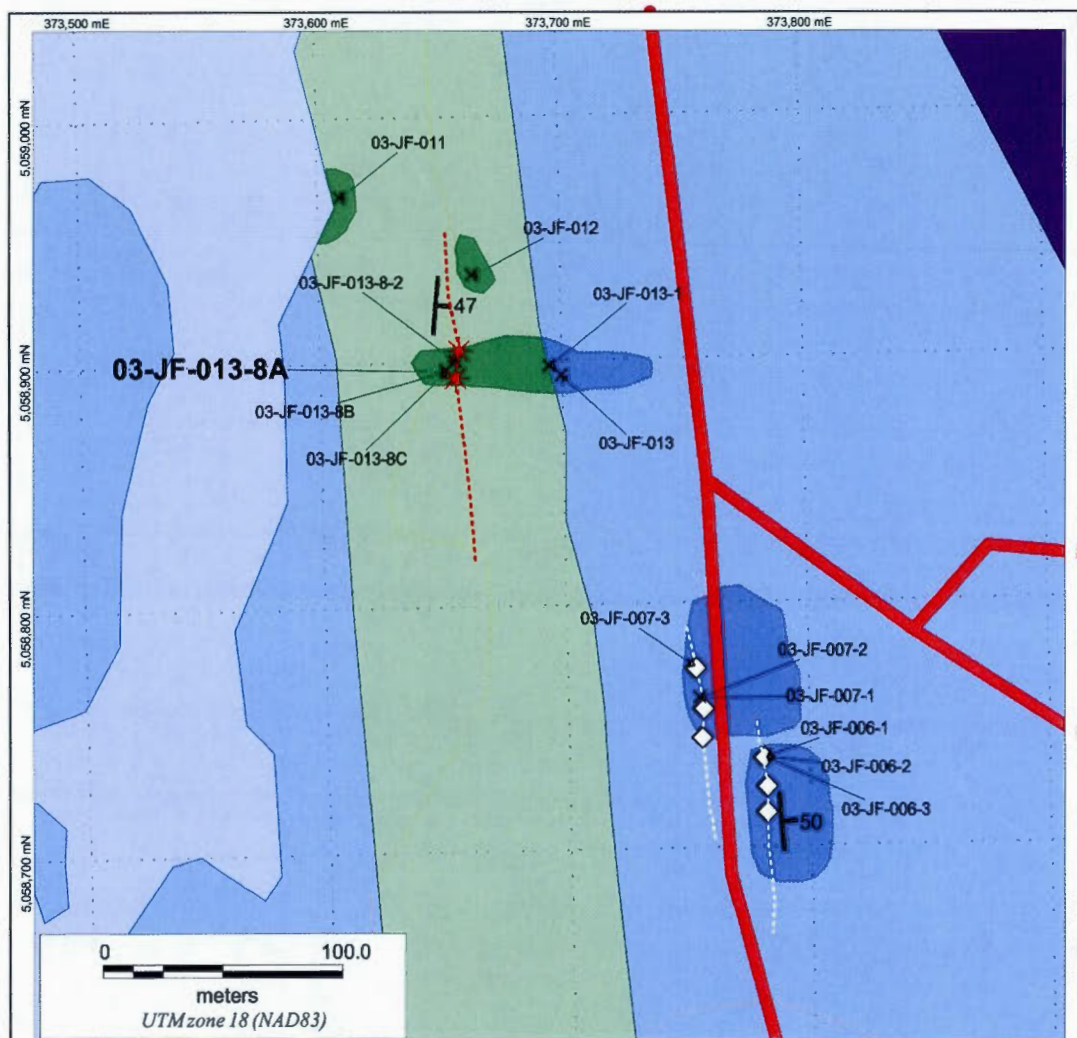
- SEDEX zinc silicate and oxide
- SEDEX zinc sulfide
- Stratiform magnesium mineralization (pure dolomite)
- Industrial mineral deposit (dolomitic marble)
- Stratiform brucite-rich horizon

* Lithologies or symbols may not occur on this sheet

Topographic data :
© Department of Natural Resources Canada. All rights reserved.

BRYSON HYDROELECTRIC DAM SHOWING

Geology by
Jean-François Larivière



LEGEND

LITHOLOGY

- CHENAUX GABBRO INTRUSIVE
- INTRUSIVE CONTACT
- M06 SILICEOUS DOLOMITIC MARBLE
- M01 DOLOMITIC MARBLE

* Lithologies or symbols may not occur on this sheet

Topographic data :
© Department of Natural Resources Canada. All rights reserved.

SYMBOLS

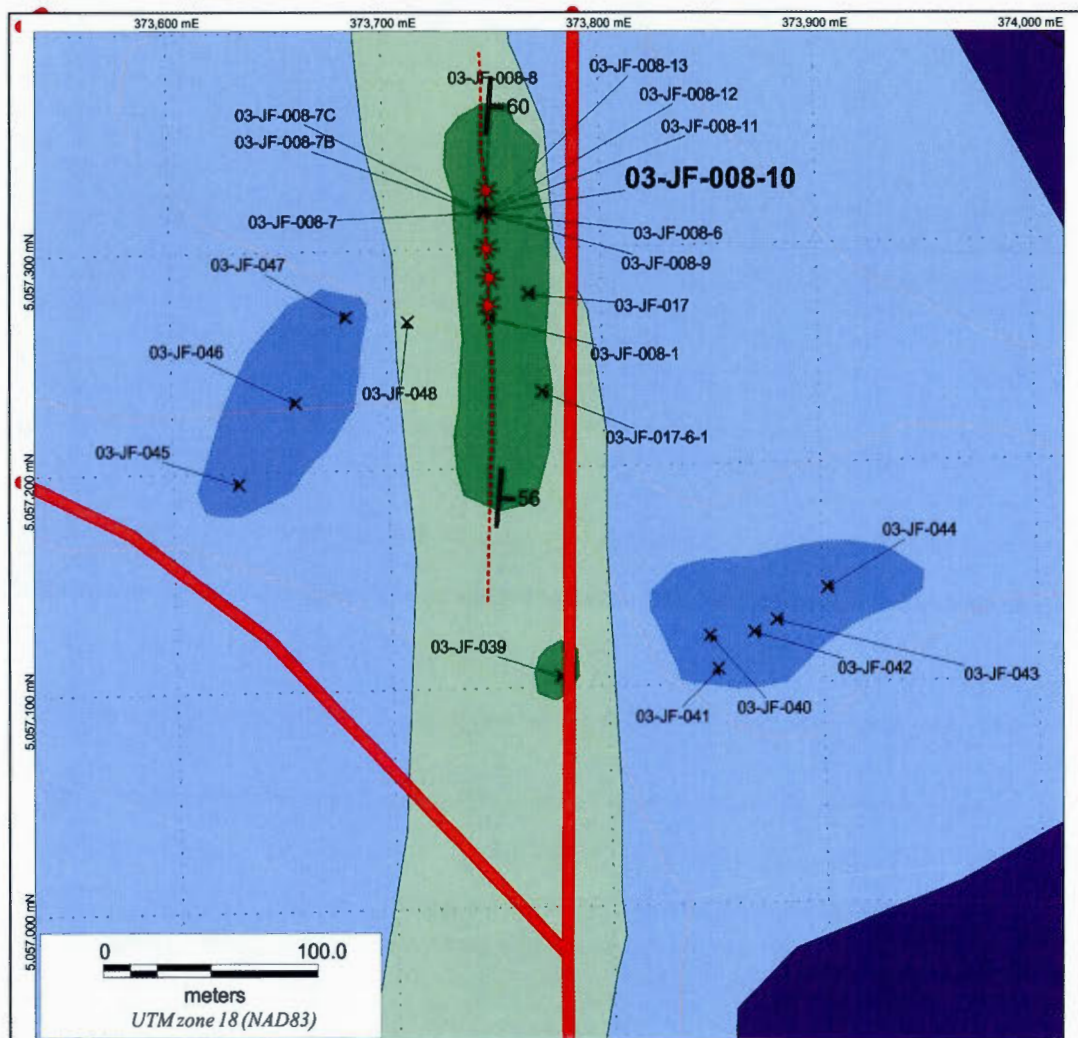
- Outcrop
- Sample number and location
- Geological contact
- Strike and dip of bedding
- Road
- River/Lake
- Stream
- Dam
- Topographic contour

METALLOGENY

- SEDEX zinc silicate and oxide
- SEDEX zinc sulfide
- Stratiform magnesium mineralization (pure dolomite)
- Industrial mineral deposit (dolomitic marble)
- Stratiform brucite-rich horizon

BRYSON WATER TREATMENT PLANT SHOWING

Geology by
Jean-François Larivière



LEGEND

LITHOLOGY

- CHENAUX GABBRO INTRUSIVE**
- INTRUSIVE CONTACT
- M06 SILICEOUS DOLOMITIC MARBLE**
- M01 DOLOMITIC MARBLE**

SYMBOLS

- Outcrop
- × Sample number and location
- Geological contact
- Strike and dip of bedding
- Road
- River / Lake
- Stream
- Dam
- Topographic contour

METALLOGENY

- ✱ SEDEX zinc silicate and oxide
- SEDEX zinc sulfide
- ▽ Stratiform magnesium mineralization (pure dolomite)
- ▲ Industrial mineral deposit (dolomitic marble)
- ◇ Stratiform brucite-rich horizon

* Lithologies or symbols may not occur on this sheet

Topographic data :
© Department of Natural Resources Canada. All rights reserved.

BRYSON CADIEUX POWER STATION SHOWING

Geology by
Jean-François Larivière

APPENDIX F

OUTCROP LOCATION AND DESCRIPTION DATABASE

Table: Outcrop description summary

| Station | UTM E | UTM N | Lithology | Zinc Mineral | Pure Dolomite | Bedding Strike/dip | Foliation Strike/dip |
|----------------|--------|---------|---|-----------------------------|---------------|--------------------|----------------------|
| 03-JF-001 | | | Marbre dolomitique ~ pur (< 10% silicates) | | | 65/65 | |
| 03-JF-002 | | | Marbre dolomitique à diopside-forstérite (21-40%Si) | Silicates et oxydes de zinc | | | |
| 03-JF-003-1 | 373652 | 5059922 | Marbre dolomitique à diopside-forstérite (10-20%Si) | Sulfures de zinc | | 325/60 | |
| 03-JF-003-10 | 373723 | 5059964 | Marbre dolomitique à diopside-forstérite (21-40%Si) | | | | |
| 03-JF-003-11 | 373713 | 5059943 | Marbre dolomitique à diopside-forstérite (21-40%Si) | | | 355/80 | |
| 03-JF-003-12 | 373704 | 5059955 | Marbre dolomitique ~ pur (< 10% silicates) | Sulfures de zinc | | | |
| 03-JF-003-12-B | 373713 | 5059943 | Marbre dolomitique ~ pur (< 10% silicates) | | | | |
| 03-JF-003-12C | 373713 | 5059943 | Marbre dolomitique ~ pur (< 10% silicates) | | | | |
| 03-JF-003-13 | 373723 | 5059949 | Marbre dolomitique ~ pur (< 10% silicates) | | | | |
| 03-JF-003-2 | 373647 | 5060017 | Marbre dolomitique à diopside-forstérite (21-40%Si) | | | 325/60 | |
| 03-JF-003-3 | 373649 | 5060010 | Marbre dolomitique à diopside-forstérite (10-20%Si) | Silicates et oxydes de zinc | | 325/60 | |
| 03-JF-003-4 | 373659 | 5060000 | Marbre dolomitique à diopside-forstérite (21-40%Si) | Sulfures de zinc | | 325/60 | |
| 03-JF-003-5 | 373660 | 5059991 | Marbre dolomitique à diopside-forstérite (21-40%Si) | Silicates et oxydes de zinc | | 355/64 | |
| 03-JF-003-5.5 | 373677 | 5059979 | Dyke de diabase (gabbro) | | | | |
| 03-JF-003-5.6 | 373680 | 5059979 | Dyke de diabase (gabbro) | | | | |
| 03-JF-003-6 | 373677 | 5059981 | Marbre dolomitique à diopside-forstérite (21-40%Si) | Sulfures de zinc | | | |
| 03-JF-003-7 | 373691 | 5059974 | Marbre dolomitique à diopside-forstérite (21-40%Si) | Sulfures de zinc | | | |
| 03-JF-003-8A | 373714 | 5059966 | Marbre dolomitique à diopside-forstérite (21-40%Si) | Sulfures de zinc | | 28/78 | |
| 03-JF-003-8B | 373714 | 5059966 | Marbre dolomitique à diopside-forstérite (21-40%Si) | Sulfures de zinc | | | |
| 03-JF-003-8C | 373714 | 5059966 | Marbre dolomitique à diopside-forstérite (21-40%Si) | Sulfures de zinc | | | |
| 03-JF-003-8D | 373714 | 5059966 | Marbre dolomitique à diopside-forstérite (21-40%Si) | Sulfures de zinc | | 235/15 | |
| 03-JF-003-8E | 373714 | 5059966 | Marbre dolomitique à diopside-forstérite (21-40%Si) | Silicates et oxydes de zinc | | | |
| 03-JF-003-9 | 373709 | 5059960 | Marbre dolomitique ~ pur (< 10% silicates) | Sulfures de zinc | | 12/68 | |
| 03-JF-003-W | 373718 | 5059956 | Marbre dolomitique à diopside-forstérite (21-40%Si) | | | | |
| 03-JF-004-1 | 373697 | 5059255 | Marbre dolomitique à diopside-forstérite (21-40%Si) | Sulfures de zinc | | 20/85 | |
| 03-JF-004-2 | 373706 | 5059249 | Marbre dolomitique à diopside-forstérite (21-40%Si) | | | | |
| 03-JF-004-3 | 373698 | 5059232 | Marbre dolomitique à diopside-forstérite (21-40%Si) | | | | |
| 03-JF-004-4 | 373726 | 5059187 | Marbre dolomitique à diopside-forstérite (21-40%Si) | | | | |
| 03-JF-005 | 373709 | 5059173 | Marbre dolomitique à diopside-forstérite (21-40%Si) | | | | |
| 03-JF-006-1 | 373782 | 5058736 | Marbre dolomitique brucitique (> 20%) | | | 30/46 | |

Table: Outcrop description summary

| Station | UTM E | UTM N | Lithology | Zinc Mineral | Pure Dolomite | Bedding Strike/dip | Foliation Strike/dip |
|--------------|--------|---------|---|-----------------------------|---------------|--------------------|----------------------|
| 03-JF-006-2 | 373782 | 5058736 | Marbre dolomitique brucitique (> 20%) | | | 20/36 | |
| 03-JF-006-3 | 373782 | 5058736 | Marbre dolomitique brucitique (> 20%) | | | 15/36 | |
| 03-JF-007-1 | 373755 | 5058761 | Marbre dolomitique à diopside-forstérite (21-40%Si) | | | 5/47 | |
| 03-JF-007-2 | 373755 | 5058761 | Marbre dolomitique à brucite (< 20%) | | | 10/52 | |
| 03-JF-007-3 | 373752 | 5058774 | Marbre dolomitique à brucite (< 20%) | | | | |
| 03-JF-008-1 | 373748 | 5057268 | Marbre dolomitique ~ pur (< 10% silicates) | | | 12/88 | |
| 03-JF-008-10 | 373746 | 5057316 | Marbre dolomitique à diopside-forstérite (21-40%Si) | Silicates et oxydes de zinc | | 5/56 | |
| 03-JF-008-11 | 373746 | 5057316 | Marbre dolomitique à diopside-forstérite (21-40%Si) | | | 5/56 | |
| 03-JF-008-12 | 373746 | 5057316 | Marbre dolomitique à diopside-forstérite (21-40%Si) | | | 5/56 | |
| 03-JF-008-13 | 373746 | 5057316 | Marbre dolomitique à diopside-forstérite (21-40%Si) | | | 5/56 | |
| 03-JF-008-2 | | | Marbre dolomitique ~ pur (< 10% silicates) | Silicates et oxydes de zinc | | | |
| 03-JF-008-3 | | | Marbre dolomitique ~ pur (< 10% silicates) | Silicates et oxydes de zinc | | | |
| 03-JF-008-4 | | | Marbre dolomitique à diopside-forstérite (21-40%Si) | Silicates et oxydes de zinc | | 353/88 | |
| 03-JF-008-5 | | | Marbre dolomitique à diopside-forstérite (21-40%Si) | Silicates et oxydes de zinc | | 5/56 | |
| 03-JF-008-6 | 373746 | 5057316 | Marbre dolomitique à diopside-forstérite (21-40%Si) | Silicates et oxydes de zinc | | 5/56 | |
| 03-JF-008-7 | 373746 | 5057316 | Marbre dolomitique à diopside-forstérite (21-40%Si) | Silicates et oxydes de zinc | | 5/56 | |
| 03-JF-008-7B | 373746 | 5057316 | Marbre dolomitique à diopside-forstérite (21-40%Si) | Silicates et oxydes de zinc | | 5/56 | |
| 03-JF-008-7C | 373746 | 5057316 | Marbre dolomitique à diopside-forstérite (21-40%Si) | Silicates et oxydes de zinc | | 5/56 | |
| 03-JF-008-8 | 373746 | 5057316 | Marbre dolomitique à diopside-forstérite (21-40%Si) | Silicates et oxydes de zinc | | 5/56 | |
| 03-JF-008-9 | 373746 | 5057316 | Marbre dolomitique à diopside-forstérite (21-40%Si) | Silicates et oxydes de zinc | | 5/56 | |
| 03-JF-009 | 373557 | 5059189 | Marbre dolomitique à diopside-forstérite (21-40%Si) | Silicates et oxydes de zinc | | 340/76 | |
| 03-JF-010 | 373672 | 5059138 | Marbre dolomitique à diopside-forstérite (21-40%Si) | | | 25/64 | |
| 03-JF-011 | 373610 | 5058967 | Marbre dolomitique à diopside-forstérite (21-40%Si) | | | | |
| 03-JF-012 | 373664 | 5058935 | Marbre dolomitique à diopside-forstérite (21-40%Si) | | | | |
| 03-JF-013 | 373700 | 5058893 | Marbre dolomitique à brucite (< 20%) | | | | |
| 03-JF-013-1 | 373695 | 5058897 | Marbre dolomitique à diopside-forstérite (21-40%Si) | Silicates et oxydes de zinc | | 345/53 | |
| 03-JF-013-2 | | | Marbre dolomitique à diopside-forstérite (21-40%Si) | Silicates et oxydes de zinc | | | |
| 03-JF-013-3 | | | Marbre dolomitique à diopside-forstérite (21-40%Si) | Silicates et oxydes de zinc | | | |
| 03-JF-013-4 | | | Marbre dolomitique ~ pur (< 10% silicates) | Silicates et oxydes de zinc | | 345/53 | |
| 03-JF-013-5 | | | Marbre dolomitique à diopside-forstérite (10-20%Si) | Silicates et oxydes de zinc | | | |

Table: Outcrop description summary

| Station | UTM E | UTM N | Lithology | Zinc Mineral | Pure Dolomite | Bedding Strike/dip | Foliation Strike/dip |
|---------------|--------|---------|---|-----------------------------|---------------|--------------------|----------------------|
| 03-JF-013-6 | | | Marbre dolomitique à diopside-forst rite (21-40%Si) | Silicates et oxydes de zinc | | | |
| 03-JF-013-7 | | | Marbre dolomitique   diopside-forst rite (21-40%Si) | | | | |
| 03-JF-013-7-1 | | | Marbre dolomitique   diopside-forst rite (21-40%Si) | | | | |
| 03-JF-013-7-2 | | | Marbre dolomitique   diopside-forst rite (21-40%Si) | | | | |
| 03-JF-013-8-1 | | | Marbre dolomitique   diopside-forst rite (21-40%Si) | | | | |
| 03-JF-013-8-2 | 373656 | 5058900 | Marbre dolomitique   diopside-forst rite (21-40%Si) | Silicates et oxydes de zinc | 345/53 | | |
| 03-JF-013-8A | 373652 | 5058896 | Marbre dolomitique   diopside-forst rite (21-40%Si) | Silicates et oxydes de zinc | 345/53 | | |
| 03-JF-013-8B | 373652 | 5058896 | Marbre dolomitique   diopside-forst rite (21-40%Si) | Silicates et oxydes de zinc | | | |
| 03-JF-013-8C | 373652 | 5058896 | Marbre dolomitique   diopside-forst rite (21-40%Si) | Silicates et oxydes de zinc | | | |
| 03-JF-014 | 373719 | 5060054 | Marbre calcitique gris (< 10% silicates-graphite) | | | | |
| 03-JF-015 | 373719 | 5060116 | Marbre dolomitique   diopside-forst rite (21-40%Si) | | 10/65 | | |
| 03-JF-016 | 373727 | 5060128 | Marbre dolomitique   diopside-forst rite (21-40%Si) | | | | |
| 03-JF-017 | 373766 | 5057279 | Marbre dolomitique   diopside-forst rite (21-40%Si) | | | | |
| 03-JF-017-1 | | | Marbre dolomitique   diopside-forst rite (21-40%Si) | Silicates et oxydes de zinc | 325/45 | | |
| 03-JF-017-1-1 | | | Marbre dolomitique   diopside-forst rite (21-40%Si) | | | | |
| 03-JF-017-1-2 | | | Diopsidite (> 80% Diopside) | | | | |
| 03-JF-017-1-3 | | | Marbre dolomitique   diopside-forst rite (21-40%Si) | | | | |
| 03-JF-017-2 | | | Marbre dolomitique   diopside-forst rite (21-40%Si) | Silicates et oxydes de zinc | 10/53 | | |
| 03-JF-017-3 | | | Marbre dolomitique   diopside-forst rite (21-40%Si) | | | | |
| 03-JF-017-3-1 | | | Marbre dolomitique   diopside-forst rite (21-40%Si) | | | | |
| 03-JF-017-3-2 | | | Marbre dolomitique   diopside-forst rite (21-40%Si) | | | | |
| 03-JF-017-4A | | | Marbre dolomitique   diopside-forst rite (21-40%Si) | Silicates et oxydes de zinc | | | |
| 03-JF-017-4B | | | Marbre dolomitique   diopside-forst rite (21-40%Si) | | | | |
| 03-JF-017-5 | | | Marbre dolomitique   diopside-forst rite (21-40%Si) | Sulfures de zinc | | | |
| 03-JF-017-5-1 | | | Marbre dolomitique   diopside-forst rite (21-40%Si) | Silicates et oxydes de zinc | 355/57 | | |
| 03-JF-017-5-2 | | | Marbre dolomitique   diopside-forst rite (21-40%Si) | | | | |
| 03-JF-017-6-1 | 373772 | 5057234 | Marbre dolomitique   diopside-forst rite (21-40%Si) | | | | |
| 03-JF-017-6A | | | Marbre dolomitique calcosilicat  quartzeux (Di + > 20% Qtz) | | | | |
| 03-JF-017-6B | | | Quartzite grise (> 90% Quartz) | | | | |
| 03-JF-018 | 373778 | 5057738 | M tagabbro m lanocrate | | | | 65/65 |

Table: Outcrop description summary

| Station | UTM E | UTM N | Lithology | Zinc Mineral | Pure Dolomite | Bedding Strike/dip | Foliation Strike/dip |
|-------------|--------|---------|--|-----------------------------|---------------|--------------------|----------------------|
| 03-JF-019 | 373127 | 5057955 | Marbre dolomitique à diopside-forstérite (21-40%Si) | Silicates et oxydes de zinc | | | |
| 03-JF-020 | 373350 | 5058022 | Marbre dolomitique ~ pur (< 10% silicates) | Silicates et oxydes de zinc | | | |
| 03-JF-021 | 373365 | 5058065 | Marbre dolomitique à diopside-forstérite (21-40%Si) | | 25/35 | | |
| 03-JF-022 | 373444 | 5058250 | Marbre dolomitique à diopside-forstérite (10-20%Si) | | | | |
| 03-JF-023 | 373237 | 5057693 | Marbre dolomitique à diopside-forstérite (21-40%Si) | | | | |
| 03-JF-024 | 373240 | 5057597 | Marbre dolomitique à diopside-forstérite (21-40%Si) | Silicates et oxydes de zinc | 50/ | | |
| 03-JF-025 | 373238 | 5057434 | Quartzite grise (> 90% Quartz) | | | | |
| 03-JF-026 | 373502 | 5059407 | Marbre dolomitique à diopside-forstérite (10-20%Si) | | | | |
| 03-JF-027 | 373486 | 5059348 | Marbre dolomitique à diopside-forstérite (10-20%Si) | | | | |
| 03-JF-028 | 373387 | 5059278 | Amphibolite à hornblende-biotite | | | | |
| 03-JF-029 | 373338 | 5059266 | Amphibolite à hornblende-biotite | | | | 25/90 |
| 03-JF-030 | 373328 | 5059225 | Amphibolite à hornblende-biotite | | | | |
| 03-JF-031 | 373285 | 5059232 | Amphibolite à hornblende-biotite | | | | |
| 03-JF-032 | 373357 | 5059375 | Amphibolite à hornblende-biotite | | | | |
| 03-JF-033 | 373389 | 5059344 | Amphibolite à hornblende-biotite | | | | |
| 03-JF-034 | 373419 | 5059309 | Amphibolite à hornblende-biotite | | | | 20/68 |
| 03-JF-035-1 | 373593 | 5059405 | Marbre dolomitique à diopside-forstérite (21-40%Si) | Sulfures de zinc | | | |
| 03-JF-035-2 | | | Marbre dolomitique à diopside-forstérite (10-20%Si) | | 355/70 | | |
| 03-JF-035-3 | | | Marbre dolomitique à diopside-forstérite (10-20%Si) | | | | |
| 03-JF-035-4 | | | Marbre dolomitique à diopside-forstérite (21-40%Si) | | | | |
| 03-JF-035-5 | | | Marbre dolomitique à diopside-forstérite (21-40%Si) | | | | |
| 03-JF-035-6 | 373594 | 5059427 | Marbre dolomitique à diopside-forstérite (21-40%Si) | | | | |
| 03-JF-036 | 373725 | 5059132 | Marbre dolomitique ~ pur (< 10% silicates) | | | | |
| 03-JF-037 | 373709 | 5059130 | Marbre dolomitique à diopside-forstérite (21-40%Si) | | | | |
| 03-JF-038 | 373696 | 5059132 | Marbre dolomitique à diopside-forstérite (21-40%Si) | | | | |
| 03-JF-039 | 373778 | 5057104 | Marbre dolomitique à diopside-trémolite (10-20%Si) | | | | |
| 03-JF-040 | 373848 | 5057121 | Marbre dolomitique à diopside-forstérite (41-60%Si) | | | | |
| 03-JF-041 | 373851 | 5057106 | Marbre dolomitique à diopside-forstérite (10-20%Si) | | | | |
| 03-JF-042 | 373868 | 5057123 | Marbre calcarodolomitique à diopside-forstérite (10-20%Si) | | | | |
| 03-JF-043 | 373879 | 5057128 | Marbre calcarodolomitique à diopside-forstérite (21-40%Si) | | | | |

Table: Outcrop description summary

| Station | UTM E | UTM N | Lithology | Zinc Mineral | Pure Dolomite | Bedding Strike/dip | Foliation Strike/dip |
|---------------|--------|---------|--|-----------------------------|---------------|--------------------|----------------------|
| 03-JF-044 | 373903 | 5057143 | Marbre calcaire dolomitique à diopside-forstérite (21-40%Si) | | | 320/75 | |
| 03-JF-045 | 373631 | 5057194 | Marbre dolomitique à diopside-forstérite (21-40%Si) | Silicates et oxydes de zinc | | 28/58 | |
| 03-JF-046 | 373658 | 5057231 | Marbre dolomitique à diopside-forstérite (10-20%Si) | | | | |
| 03-JF-047 | 373682 | 5057269 | Marbre dolomitique à diopside-forstérite (10-20%Si) | | | | |
| 03-JF-048 | 373710 | 5057267 | Marbre dolomitique pur | | Oui | 0/46 | |
| 03-JF-049-1 | 373946 | 5060324 | Métagabbro mélanocrate | | | | |
| 03-JF-049-10 | 373794 | 5059223 | Métagabbro mélanocrate | | | | |
| 03-JF-049-11 | 373789 | 5059232 | Métagabbro mélanocrate | | | | |
| 03-JF-049-12 | 373785 | 5059247 | Métagabbro mélanocrate | | | | |
| 03-JF-049-13 | 373786 | 5059275 | Métagabbro mélanocrate | | | | |
| 03-JF-049-14 | 373741 | 5059354 | Métagabbro mélanocrate | | | | |
| 03-JF-049-2 | 373997 | 5060416 | Métagabbro mélanocrate | | | | |
| 03-JF-049-3 | 374156 | 5060496 | Métagabbro mélanocrate | | | | |
| 03-JF-049-4 | 374295 | 5060549 | Métagabbro mélanocrate | | | | |
| 03-JF-049-5 | 374339 | 5060681 | Métagabbro mélanocrate | | | | |
| 03-JF-049-6 | 375262 | 5061066 | Métagabbro mélanocrate | | | | |
| 03-JF-049-7 | 373843 | 5059155 | Métagabbro mélanocrate | | | | |
| 03-JF-049-8 | 373824 | 5059176 | Métagabbro mélanocrate | | | | |
| 03-JF-049-9 | 373813 | 5059195 | Métagabbro mélanocrate | | | | |
| 03-JF-050-0-0 | 373360 | 5060230 | Marbre dolomitique à diopside-forstérite (10-20%Si) | | | | |
| 03-JF-050-0-1 | | | Marbre dolomitique à diopside-forstérite (10-20%Si) | | | | |
| 03-JF-050-0-2 | | | Marbre dolomitique ~ pur (< 10% silicates) | | | 355/68 | |
| 03-JF-050-0-3 | | | Marbre dolomitique à diopside-forstérite (21-40%Si) | | | | |
| 03-JF-050-0-4 | | | Marbre dolomitique à diopside-forstérite (21-40%Si) | | | 355/68 | |
| 03-JF-050-0-5 | | | Marbre dolomitique à diopside-forstérite (21-40%Si) | | | | |
| 03-JF-050-0-6 | | | Marbre dolomitique à diopside-forstérite (21-40%Si) | | | | |
| 03-JF-050-0-7 | | | Marbre dolomitique à diopside-forstérite (21-40%Si) | | | | |
| 03-JF-050-1 | | | Marbre dolomitique à diopside-forstérite (21-40%Si) | Silicates et oxydes de zinc | | | |
| 03-JF-050-10 | 373921 | 5061714 | Amphibolite à hornblende-biotite | | | | |
| 03-JF-050-1-1 | 373413 | 5060261 | Marbre dolomitique à diopside-forstérite (21-40%Si) | | | | |

Table: Outcrop description summary

| Station | UTME | UTM N | Lithology | Zinc Mineral | Pure Dolomite | Bedding Strike/dip | Foliation Strike/dip |
|---------------|--------|---------|---|-----------------------------|---------------|--------------------|----------------------|
| 03-JF-050-1-2 | 373395 | 5060293 | Marbre dolomitique à diopside-forst rite (21-40%Si) | | | | |
| 03-JF-050-2 | 373395 | 5060293 | Amphibolite   homblende-biotite | | | | |
| 03-JF-050-3 | 373418 | 5060263 | Amphibolite   homblende-biotite | | | | |
| 03-JF-050-4 | 373302 | 5060396 | Amphibolite   homblende-biotite | | | | |
| 03-JF-050-5 | 373182 | 5060540 | Amphibolite   homblende-biotite | | | | |
| 03-JF-050-6 | 373098 | 5061019 | Amphibolite   homblende-biotite | | | | |
| 03-JF-050-7 | 373231 | 5061087 | Amphibolite   homblende-biotite | | | | |
| 03-JF-050-8 | 373592 | 5061359 | Amphibolite   homblende-biotite | | | | |
| 03-JF-050-9 | 373784 | 5061569 | Amphibolite   homblende-biotite | | | | |
| 03-JF-051 | 373395 | 5060294 | Marbre dolomitique   diopside-forst rite (10-20%Si) | | | | |
| 03-JF-052-1 | 373255 | 5060047 | Marbre dolomitique   diopside-forst rite (21-40%Si) | | | 35/57 | |
| 03-JF-052-2 | 373287 | 5060097 | Marbre dolomitique   diopside-forst rite (21-40%Si) | | | 35/57 | |
| 03-JF-053 | 372979 | 5059892 | M tagabbro m lanocrate | | | | 270/30 |
| 03-JF-054 | 372814 | 5059686 | Amphibolite   homblende-biotite | | | | |
| 03-JF-055 | 372697 | 5059601 | Marbre dolomitique   diopside-forst rite (10-20%Si) | | | | |
| 03-JF-056 | 372658 | 5059491 | Marbre dolomitique   diopside-forst rite (21-40%Si) | | | | |
| 03-JF-057 | 372625 | 5059486 | Quartzite grise (> 90% Quartz) | | | | |
| 03-JF-058 | 372609 | 5059058 | Marbre dolomitique   diopside-forst rite (10-20%Si) | | | | |
| 03-JF-059 | 372651 | 5058854 | Quartzite grise (> 90% Quartz) | | | | |
| 03-JF-060-A | 372699 | 5058752 | Marbre dolomitique   diopside-forst rite (21-40%Si) | Silicates et oxydes de zinc | | 340/52 | |
| 03-JF-060-B | 372699 | 5058752 | Marbre dolomitique   diopside-forst rite (21-40%Si) | Silicates et oxydes de zinc | | 340/52 | |
| 03-JF-061 | 372715 | 5058699 | Marbre dolomitique   diopside-forst rite (21-40%Si) | Silicates et oxydes de zinc | | 330/40 | |
| 03-JF-062 | | | Marbre dolomitique   diopside-forst rite (21-40%Si) | Silicates et oxydes de zinc | | | |
| 03-JF-063 | | | Marbre dolomitique calcosilicat  quartzeux (Di + > 20% Qtz) | | | | |
| 03-JF-064 | | | Marbre dolomitique   diopside-forst rite (10-20%Si) | | | | |
| 03-JF-065 | 372719 | 5057883 | Marbre dolomitique   diopside-forst rite (21-40%Si) | Silicates et oxydes de zinc | | 260/30 | |
| 03-JF-066 | 372738 | 5057868 | Marbre dolomitique   diopside-forst rite (10-20%Si) | Silicates et oxydes de zinc | | | |
| 03-JF-067 | 372284 | 5057724 | Amphibolite   homblende-biotite | | | | |
| 04-JF-008-8B | | | Marbre dolomitique   diopside-forst rite (21-40%Si) | Silicates et oxydes de zinc | | | |
| 04-JF-008-9B | | | Marbre dolomitique   diopside-forst rite (21-40%Si) | Silicates et oxydes de zinc | | | |

Table: Outcrop description summary

| Station | UTM E | UTM N | Lithology | Zinc Mineral | Pure Dolomite | Bedding Strike/dip | Foliation Strike/dip |
|-----------------|--------|---------|---|-----------------------------|---------------|--------------------|----------------------|
| 04-JF-008-9C | | | Marbre dolomitique à diopside-forstérite (21-40%Si) | Silicates et oxydes de zinc | | | |
| 04-JF-073 | 366607 | 5029922 | Paragneiss quartzofeldspathique à biotite | | | | |
| 04-JF-074 | 366607 | 5029922 | Paragneiss quartzofeldspathique à biotite | | | | |
| 04-JF-075-01 | 366111 | 5030579 | Marbre dolomitique pur | | Oui | | |
| 04-JF-075-02 | | | Marbre dolomitique ~ pur (< 10% silicates) | | | | |
| 04-JF-075-03 | | | Marbre dolomitique pur | | Oui | | |
| 04-JF-075-04 | | | Marbre dolomitique pur | | Oui | | |
| 04-JF-075-05 | | | Marbre dolomitique ~ pur (< 10% silicates) | | | | |
| 04-JF-075-06 | | | Marbre dolomitique ~ pur (< 10% silicates) | | | | |
| 04-JF-075-07 | | | Marbre dolomitique pur | | Oui | | |
| 04-JF-075-08 | | | Marbre dolomitique ~ pur (< 10% silicates) | | | | |
| 04-JF-075-09 | | | Marbre dolomitique pur | | | | |
| 04-JF-075-10 | | | Marbre dolomitique ~ pur (< 10% silicates) | | | | |
| 04-JF-075-11 | | | Marbre dolomitique pur | | Oui | | |
| 04-JF-076-08 | 366305 | 5030617 | Marbre dolomitique à diopside-trémolite (10-20%Si) | Sulfures de zinc | | 226/70 | |
| 04-JF-076-09 | 366320 | 5030615 | Marbre dolomitique à diopside-trémolite (10-20%Si) | Sulfures de zinc | | 226/70 | |
| 04-JF-076-10A | 366331 | 5030101 | Marbre dolomitique à diopside-trémolite (10-20%Si) | Sulfures de zinc | | 226/70 | |
| 04-JF-076-10B | 366331 | 5030101 | Marbre dolomitique à diopside-trémolite (10-20%Si) | Sulfures de zinc | | 226/70 | |
| 04-JF-076-11 | 366350 | 5030670 | Marbre dolomitique à diopside-trémolite (10-20%Si) | Sulfures de zinc | | 226/70 | |
| 04-JF-076-T1-01 | 366292 | 5030610 | Diopsidite quartzreuse (50% Di - 50% Qtz) | | | | 226/70 |
| 04-JF-076-T1-02 | | | Marbre dolomitique pur | | Oui | 226/70 | |
| 04-JF-076-T1-03 | 366292 | 5030610 | Marbre dolomitique à diopside-trémolite (10-20%Si) | | | 226/70 | |
| 04-JF-076-T1-04 | 366292 | 5030610 | Marbre dolomitique à diopside-trémolite (21-40%Si) | Sulfures de zinc | | 226/70 | |
| 04-JF-076-T1-05 | 366292 | 5030610 | Marbre dolomitique à diopside-trémolite (21-40%Si) | Sulfures de zinc | | 226/70 | |
| 04-JF-076-T1-06 | 366292 | 5030610 | Marbre dolomitique à diopside-trémolite (21-40%Si) | Sulfures de zinc | | 226/70 | |
| 04-JF-076-T1-07 | 366292 | 5030610 | Marbre dolomitique à diopside-trémolite (21-40%Si) | Sulfures de zinc | | 226/70 | |
| 04-JF-076-T1-08 | 366292 | 5030610 | Marbre dolomitique à diopside-trémolite (21-40%Si) | Sulfures de zinc | | 226/70 | |
| 04-JF-076-T1-09 | 366322 | 5030620 | Paragneiss quartzofeldspathique à biotite | | | | 226/70 |
| 04-JF-077 | 366370 | 5030709 | Marbre dolomitique à diopside-trémolite (10-20%Si) | Sulfures de zinc | | 226/70 | |
| 04-JF-078 | 366416 | 5030774 | Marbre dolomitique à diopside-trémolite (21-40%Si) | Sulfures de zinc | | 226/70 | |

Table: Outcrop description summary

| Station | UTM E | UTM N | Lithology | Zinc Mineral | Pure Dolomite | Bedding Strike/dip | Foliation Strike/dip |
|--------------|--------|---------|---|------------------|---------------|--------------------|----------------------|
| 04-JF-079 | 366509 | 5030794 | Marbre dolomitique à diopside-trémolite (21-40%Si) | Sulfures de zinc | | 226/70 | |
| 04-JF-080 | 366730 | 5030031 | Paragneiss quartzofeldspatique à biotite | | | | |
| 04-JF-081 | 366864 | 5030146 | Paragneiss quartzofeldspatique à biotite | | | | |
| 04-JF-082 | 367072 | 5030323 | Paragneiss quartzofeldspatique à biotite | | | | |
| 04-JF-083 | 367185 | 5030420 | Paragneiss quartzofeldspatique à biotite | | | | |
| 04-JF-084 | 367799 | 5030365 | Paragneiss quartzofeldspatique à biotite | | | | |
| 04-JF-085 | 367882 | 5030149 | Paragneiss quartzofeldspatique à biotite | | | | |
| 04-JF-086 | 367937 | 5029887 | Paragneiss quartzofeldspatique à biotite | | | | |
| 04-JF-087 | 368177 | 5029432 | Paragneiss quartzofeldspatique à biotite | | | | |
| 04-JF-088 | 367830 | 5030306 | Paragneiss quartzofeldspatique à biotite | | | | |
| 04-JF-089 | 367138 | 5031419 | Paragneiss quartzofeldspatique à biotite | | | | |
| 04-JF-090 | 367192 | 5031345 | Paragneiss quartzofeldspatique à biotite | | | | |
| 04-JF-090-01 | | | Marbre dolomitique ~ pur (< 10% silicates) | | | | |
| 04-JF-091 | 367055 | 5031487 | Marbre dolomitique à diopside-trémolite (10-20%Si) | | | | |
| 04-JF-092 | 366911 | 5031692 | Paragneiss quartzofeldspatique à biotite | | | | |
| 04-JF-093 | 366778 | 5031878 | Paragneiss quartzofeldspatique à biotite | | | | |
| 04-JF-094 | 366590 | 5032094 | Paragneiss quartzofeldspatique à biotite | | | | |
| 04-JF-095 | 366496 | 5032214 | Paragneiss quartzofeldspatique à biotite | | | | |
| 04-JF-096 | 366475 | 5032227 | Paragneiss quartzofeldspatique à biotite | | | | |
| 04-JF-097-01 | 370506 | 5034171 | Marbre dolomitique à diopside-forstérite (10-20%Si) | | | 53/36 | 65/46 |
| 04-JF-097-02 | 370468 | 5034174 | Paragneiss quartzofeldspatique à biotite | | | | |
| 04-JF-097-03 | 370468 | 5034174 | Marbre dolomitique à diopside-forstérite (21-40%Si) | | | 53/36 | |
| 04-JF-097-04 | 370464 | 5034220 | Marbre dolomitique à diopside-forstérite (41-60%Si) | | | | |
| 04-JF-097-05 | 370464 | 5034220 | Paragneiss quartzofeldspatique à biotite | | | | |
| 04-JF-097-06 | 370441 | 5034246 | Marbre dolomitique à diopside-forstérite (21-40%Si) | | | | |
| 04-JF-098 | 373204 | 5036376 | Marbre dolomitique ~ pur (< 10% silicates) | | | 312/11 | 228/73 |
| 04-JF-099 | 373105 | 5036424 | Marbre dolomitique à diopside-trémolite (10-20%Si) | | | | |
| 04-JF-100 | 375075 | 5041419 | Paragneiss quartzofeldspatique à biotite | | | 212/32 | |
| 04-JF-101-01 | 374959 | 5041382 | Marbre dolomitique à diopside-trémolite (41-60%Si) | | | | |
| 04-JF-101-02 | 374936 | 5041375 | Marbre dolomitique à diopside-trémolite (41-60%Si) | | | | |

Table: Outcrop description summary

| Station | UTM E | UTM N | Lithology | Zinc Mineral | Pure Dolomite | Bedding Strike/dip | Foliation Strike/dip |
|--------------|--------|---------|---|--------------|---------------|--------------------|----------------------|
| 04-JF-102 | 374270 | 5041180 | Marbre dolomitique à diopside-trémolite (21-40%Si) | | | 54/54 | |
| 04-JF-103 | 374637 | 5039814 | Paragneiss quartzofeldspatique à biotite | | | | |
| 04-JF-104 | 374611 | 5039879 | Paragneiss quartzofeldspatique à biotite | | | | |
| 04-JF-105 | 374372 | 5039990 | Paragneiss quartzofeldspatique à biotite | | | | |
| 04-JF-106 | 374305 | 5040078 | Paragneiss quartzofeldspatique à biotite | | | | |
| 04-JF-107 | 374278 | 5040169 | Paragneiss quartzofeldspatique à biotite | | | | |
| 04-JF-108 | 374156 | 5040367 | Paragneiss quartzofeldspatique à biotite | | | | |
| 04-JF-109 | 374043 | 5040532 | Paragneiss quartzofeldspatique à biotite | | | | |
| 04-JF-110 | 373440 | 5040601 | Marbre dolomitique à diopside-forstérite (10-20%Si) | | | | |
| 04-JF-111 | 373117 | 5040556 | Marbre dolomitique à diopside-forstérite (21-40%Si) | | 46/-99 | | |
| 04-JF-112 | 373046 | 5040502 | Marbre dolomitique à diopside-forstérite (10-20%Si) | | 55/65 | | |
| 04-JF-113 | 372990 | 5040503 | Marbre dolomitique à diopside-forstérite (21-40%Si) | | | | |
| 04-JF-114 | 372949 | 5040471 | Marbre dolomitique à diopside-forstérite (21-40%Si) | | | | |
| 04-JF-115 | 372796 | 5040352 | Marbre dolomitique à diopside-forstérite (10-20%Si) | | | | |
| 04-JF-116 | 371526 | 5039968 | Marbre dolomitique à diopside-forstérite (10-20%Si) | | | | |
| 04-JF-117 | 370933 | 5040168 | Marbre dolomitique à diopside-forstérite (10-20%Si) | | | | |
| 04-JF-118 | 370245 | 5040789 | Marbre dolomitique à diopside-forstérite (21-40%Si) | | | | |
| 04-JF-119 | 369842 | 5041293 | Marbre dolomitique à diopside-forstérite (21-40%Si) | | | | |
| 04-JF-120 | 370995 | 5042541 | Marbre dolomitique à diopside-forstérite (10-20%Si) | | | | |
| 04-JF-121 | 372376 | 5043713 | Paragneiss quartzofeldspatique à biotite | Oui | 236/39 | | |
| 04-JF-122 | 374422 | 5048702 | Marbre dolomitique pur | Oui | | | |
| 04-JF-123 | 373995 | 5048501 | Marbre dolomitique pur | Oui | | | |
| 04-JF-124 | 373934 | 5048477 | Marbre dolomitique pur | Oui | | | |
| 04-JF-125 | 374990 | 5049298 | Paragneiss quartzofeldspatique à biotite | | | | |
| 04-JF-126 | 370532 | 5053284 | Marbre dolomitique à diopside-forstérite (10-20%Si) | | | | |
| 04-JF-127 | 370967 | 5051344 | Marbre dolomitique pur | | | | |
| 05-JF-003-20 | 373685 | 5060001 | Marbre dolomitique à diopside-forstérite (21-40%Si) | Oui | 355/65 | | |
| 05-JF-003-21 | 373685 | 5059998 | Marbre dolomitique à diopside-forstérite (21-40%Si) | | 355/67 | | |
| 05-JF-003-22 | 373685 | 5060001 | Marbre dolomitique à diopside-forstérite (10-20%Si) | | | | |
| 05-JF-003-23 | 373730 | 5059971 | Marbre dolomitique ~ pur (< 10% silicates) | | | | |

Table: Outcrop description summary

| Station | UTM E | UTM N | Lithology | Zinc Mineral | Pure Dolomite | Bedding Strike/dip | Foliation Strike/dip |
|---------------|--------|---------|--|-----------------------------|---------------|--------------------|----------------------|
| 05-JF-065-1 | 372755 | 5057909 | Marbre dolomitique à diopside-forstérite (21-40%Si) | Silicates et oxydes de zinc | | 260/29 | |
| 05-JF-065-1A | 372749 | 5057904 | Marbre dolomitique à diopside-forstérite (21-40%Si) | Silicates et oxydes de zinc | | 333/28 | |
| 05-JF-065-2A | 372749 | 5057904 | Marbre dolomitique à diopside-forstérite (21-40%Si) | Silicates et oxydes de zinc | | 330/24 | |
| 05-JF-065-3A | 372749 | 5057904 | Marbre dolomitique à diopside-forstérite (21-40%Si) | Silicates et oxydes de zinc | | 330/24 | |
| 05-JF-065-4A | 372749 | 5057904 | Marbre dolomitique à diopside-forstérite (21-40%Si) | Silicates et oxydes de zinc | | 333/28 | |
| 05-JF-065-R01 | | | Marbre dolomitique à diopside-forstérite (21-40%Si) | Silicates et oxydes de zinc | | | |
| 05-JF-065-R02 | | | Marbre dolomitique à diopside-forstérite (21-40%Si) | | | | |
| 05-JF-065-R03 | | | Marbre dolomitique à diopside-forstérite (21-40%Si) | | | | |
| 05-JF-065-R04 | | | Marbre dolomitique à diopside-forstérite (21-40%Si) | | | | |
| 05-JF-065-R05 | | | Marbre dolomitique à diopside-forstérite (21-40%Si) | | | | |
| 05-JF-065-R06 | | | Marbre dolomitique à diopside-forstérite (21-40%Si) | | | | |
| 05-JF-065-R07 | | | Marbre dolomitique à diopside-forstérite (21-40%Si) | Silicates et oxydes de zinc | | | |
| 05-JF-065-R08 | | | Marbre dolomitique à diopside-forstérite (21-40%Si) | Silicates et oxydes de zinc | | | |
| 05-JF-065-R09 | | | Marbre dolomitique à diopside-forstérite (21-40%Si) | Silicates et oxydes de zinc | | | |
| 05-JF-065-R10 | | | Marbre dolomitique à diopside-forstérite (21-40%Si) | Silicates et oxydes de zinc | | | |
| 05-JF-065-R11 | | | Marbre dolomitique à diopside-forstérite (21-40%Si) | Silicates et oxydes de zinc | | | |
| 05-JF-065-R12 | | | Marbre dolomitique à diopside-forstérite (21-40%Si) | Silicates et oxydes de zinc | | | |
| 05-JF-065-R13 | | | Marbre dolomitique à diopside-forstérite (21-40%Si) | Silicates et oxydes de zinc | | | |
| 05-JF-065-R14 | | | Marbre dolomitique à diopside-forstérite (21-40%Si) | Silicates et oxydes de zinc | | | |
| 05-JF-065-R15 | | | Marbre dolomitique à diopside-forstérite (21-40%Si) | Silicates et oxydes de zinc | | | |
| 05-JF-073-1 | 366611 | 5029899 | Paragneiss quartzofeldspathique à biotite | | | | 30/84 |
| 05-JF-096-1 | 366474 | 5032227 | Paragneiss quartzofeldspathique à biotite | | | 56/26 | |
| 05-JF-097 | 370470 | 5034207 | Marbre dolomitique ~ pur (< 10% silicates) | | | 58/29 | |
| 05-JF-097-A | 370497 | 5034178 | Marbre dolomitique à diopside-forstérite (10-20%Si) | | | 58/29 | |
| 05-JF-097-B | 370454 | 5034215 | Marbre dolomitique à diopside-trémolite (10-20%Si) | | | 340/18 | |
| 05-JF-099-01 | 373082 | 5036450 | Marbre calcarodolomitique à diopside-forstérite (10-20%Si) | | | | |
| 05-JF-099-02 | 373058 | 5036478 | Marbre calcarodolomitique à diopside-forstérite (10-20%Si) | | | | |
| 05-JF-099-03 | 373172 | 5036362 | Marbre calcarodolomitique à diopside-forstérite (10-20%Si) | | | | |
| 05-JF-099-04 | 373229 | 5036417 | Marbre calcarodolomitique à diopside-forstérite (10-20%Si) | | | | |
| 05-JF-128 | 369754 | 5058441 | Marbre dolomitique à diopside-forstérite (21-40%Si) | | | 262/50 | |

Table: Outcrop description summary

| Station | UTM E | UTM N | Lithology | Zinc Mineral | Pure Dolomite | Bedding Strike/dip | Foliation Strike/dip |
|---------------|--------|---------|---|--------------|---------------|--------------------|----------------------|
| 05-JF-129 | 369744 | 5058390 | Marbre dolomitique à diopside-forstérite (10-20%Si) | | | 260/60 | |
| 05-JF-130 | 370685 | 5058048 | Marbre dolomitique ~ pur (< 10% silicates) | | | | |
| 05-JF-131 | 372279 | 5057715 | Amphibolite à hornblende-biotite | | | | |
| 05-JF-132 | 369790 | 5049659 | Marbre calcitique gris (< 10% silicates-graphite) | | | 22/51 | |
| 05-JF-133 | 369656 | 5046244 | Marbre dolomitique ~ pur (< 10% silicates) | | | | |
| 05-JF-134 | 369588 | 5046632 | Métagabbro mélanocrate | | | | |
| 05-JF-135 | 369178 | 5046969 | Métagabbro mélanocrate | | | | |
| 05-JF-136 | 368834 | 5047212 | Métagabbro mélanocrate | | | | |
| 05-JF-137 | 368642 | 5047365 | Métagabbro mélanocrate | | | | |
| 05-JF-138-1 | 363418 | 5051764 | Brèche calcitique hématisée à nodules de quartzites | | | | |
| 05-JF-138-2 | 363414 | 5051785 | Marbre dolomitique à diopside-forstérite (21-40%Si) | | | | |
| 05-JF-138-3 | 362943 | 5051806 | Marbre dolomitique graphiteux | | | | |
| 05-JF-138-4 | 363376 | 5051816 | Marbre dolomitique pur | Oui | | 4/57 | |
| 05-JF-138-5 | 363378 | 5051771 | Marbre dolomitique pur | Oui | | | |
| 05-JF-138-A1 | 363327 | 5051338 | Marbre dolomitique pur | Oui | | 352/61 | |
| 05-JF-138-A10 | 363372 | 5051730 | Marbre dolomitique pur | Oui | | 4/57 | |
| 05-JF-138-A11 | 363362 | 5051772 | Marbre dolomitique pur | Oui | | 350/56 | |
| 05-JF-138-A12 | 363374 | 5051816 | Marbre dolomitique pur | Oui | | 350/56 | |
| 05-JF-138-A13 | 363378 | 5051830 | Marbre dolomitique pur | Oui | | 4/57 | |
| 05-JF-138-A14 | 363426 | 5051137 | Marbre dolomitique pur | Oui | | 4/57 | |
| 05-JF-138-A15 | 363399 | 5051109 | Marbre dolomitique pur | Oui | | 4/57 | |
| 05-JF-138-A16 | 371241 | 5051420 | Brèche calcitique hématisée à nodules de quartzites | | | | 4/57 |
| 05-JF-138-A2 | 363344 | 5051376 | Marbre dolomitique pur | Oui | | | |
| 05-JF-138-A3 | 363322 | 5051400 | Marbre dolomitique pur | Oui | | 352/61 | |
| 05-JF-138-A4 | 363358 | 5051426 | Marbre dolomitique pur | Oui | | | |
| 05-JF-138-A5 | 363368 | 5051554 | Marbre dolomitique pur | Oui | | | |
| 05-JF-138-A6 | 363364 | 5051598 | Marbre dolomitique pur | Oui | | | |
| 05-JF-138-A7 | 363366 | 5051643 | Marbre dolomitique pur | Oui | | | |
| 05-JF-138-A8 | 363365 | 5051700 | Marbre dolomitique pur | Oui | | 4/57 | |
| 05-JF-138-A9 | 363359 | 5051725 | Marbre dolomitique pur | Oui | | | |

Table: Outcrop description summary

| Station | UTM E | UTM N | Lithology | Zinc Mineral | Pure Dolomite | Bedding Strike/dip | Foliation Strike/dip |
|-----------------|--------|---------|---|------------------|---------------|--------------------|----------------------|
| 05-JF-139 | 371243 | 5051060 | Marbre dolomitique pur | | Oui | 0/-99 | |
| 05-JF-140-1 | 369620 | 5049304 | Marbre calcaire dolomitique ~ pur (< 10% silicates) | | | 175/70 | |
| 05-JF-140-2 | 369681 | 5049435 | Marbre calcaire dolomitique ~ pur (< 10% silicates) | | | 135/90 | |
| 05-JF-141-1 | 369689 | 5049102 | Marbre calcitique gris (< 10% silicates-graphite) | | | | |
| 05-JF-141-2 | 369689 | 5049102 | Marbre calcitique métagabbro rose | | | | |
| 05-JF-141-3 | 369689 | 5049102 | Métagabbro mélanocrate | | | | |
| 05-JF-141-4 | 369728 | 5048973 | Métagabbro mélanocrate | | | | |
| 05-JF-141-5 | 369704 | 5048954 | Métagabbro mélanocrate | | | | |
| 05-JF-141-6 | 369644 | 5048867 | Métagabbro mélanocrate | | | | |
| 05-JF-142-0 | 371135 | 5051152 | Marbre dolomitique à diopside-forstérite (10-20%Si) | | | | |
| 05-JF-142-1 | 371133 | 5051135 | Marbre dolomitique à diopside-forstérite (10-20%Si) | Sulfures de zinc | | 34/59 | |
| 05-JF-142-2 | 371125 | 5051131 | Marbre dolomitique pur | Sulfures de zinc | Oui | 34/59 | |
| 05-JF-142-3 | 371092 | 5051037 | Marbre dolomitique à diopside-forstérite (21-40%Si) | | | | |
| 05-JF-142-4 | 371110 | 5051022 | Marbre dolomitique pur | | Oui | 34/59 | |
| 05-JF-142-5 | 371011 | 5050898 | Marbre dolomitique pur | | Oui | 34/59 | |
| 05-JF-142-6 | 371047 | 5050958 | Marbre dolomitique pur | | Oui | | |
| 05-JF-142-7 | 371009 | 5050879 | Marbre dolomitique pur | | Oui | | |
| 05-JF-142-8 | 371122 | 5051131 | Métagabbro mélanocrate | | | | |
| 05-JF-142-MG-1 | 371104 | 5051143 | Marbre dolomitique à diopside-forstérite (10-20%Si) | Sulfures de zinc | | | |
| 05-JF-142-MG-2 | 371079 | 5051104 | Marbre dolomitique pur | | Oui | 60/80 | |
| 05-JF-142-MG-3 | 371064 | 5051027 | Marbre dolomitique pur | | Oui | 46/61 | |
| 05-JF-142-MG-A1 | 371025 | 5050950 | Marbre dolomitique pur | | Oui | | |
| 05-JF-142-MG-A2 | 370995 | 5050838 | Marbre dolomitique ~ pur (< 10% silicates) | | | | |
| 05-JF-142-MG-A3 | 371061 | 5050871 | Marbre dolomitique pur | | Oui | | |
| 05-JF-142-MG-A4 | 371205 | 5051045 | Marbre dolomitique pur | | Oui | | |
| 05-JF-143-1 | 369574 | 5039258 | Marbre calcitique à diopside-forstérite (21-40%Si) | | | 300/46 | |
| 05-JF-143-2 | 369573 | 5039198 | Marbre calcitique à diopside-forstérite (21-40%Si) | | | 302/32 | |

Table: Outcrop description summary

| Station | UTM E | UTM N | Lithology | Zinc Mineral | Pure Dolomite | Bedding Strike/dip | Foliation Strike/dip |
|--------------|--------|---------|--|------------------|---------------|--------------------|----------------------|
| 05-JF-143-3 | 369656 | 5039096 | Marbre calcitique à diopside-forst rite (10-20%Si) | | | 275/30 | |
| 05-JF-143-4 | 369640 | 5039144 | Marbre calcitique gris (< 10% silicates-graphite) | | | 286/28 | |
| 05-JF-143-5 | 369618 | 5039149 | Marbre calcitique gris (< 10% silicates-graphite) | | | 249/53 | |
| 05-JF-143-6 | 369625 | 5039108 | Dyke felsique | | | | 81/-99 |
| 05-JF-143-7 | 369633 | 5039103 | Marbre calcitique gris (< 10% silicates-graphite) | | | 259/53 | |
| 05-JF-143-A1 | 369574 | 5039235 | Marbre calcitique à diopside-forst rite (10-20%Si) | | | | |
| 05-JF-144 | 370073 | 5036839 | Marbre calcarodolomitique à diopside-forst rite (10-20%Si) | | | 325/37 | |
| 05-JF-145-1 | 367664 | 5043083 | Paragneiss quartzofeldspatique à biotite | | | | 268/52 |
| 05-JF-145-2 | 367562 | 5043203 | Paragneiss quartzofeldspatique à biotite | | | | 268/42 |
| 05-JF-145-3 | 367552 | 5043209 | Paragneiss quartzofeldspatique à biotite | | | | 42/60 |
| 05-JF-145-4 | 367536 | 5043230 | Paragneiss quartzofeldspatique à biotite | | | | 250/70 |
| 05-JF-146-1 | 365866 | 5044451 | M tagabbro m lanocrate | | | | |
| 05-JF-146-2 | 365777 | 5044475 | M tagabbro m lanocrate | | | | |
| 05-JF-146-A1 | 365773 | 5044485 | M tagabbro m lanocrate | | | | |
| 05-JF-146-A2 | 366149 | 5044351 | M tagabbro m lanocrate | | | | |
| 05-JF-147-A1 | 365316 | 5044728 | M tagabbro m lanocrate | | | | |
| 05-JF-147-A2 | 365361 | 5044695 | M tagabbro m lanocrate | | | | |
| 05-JF-148 | 365275 | 5044764 | M tagabbro m lanocrate | | | | |
| 05-JF-149 | 365127 | 5044952 | M tagabbro m lanocrate | | | | |
| 05-JF-150-1 | 365024 | 5045105 | Marbre calcitique gris (< 10% silicates-graphite) | | | | |
| 05-JF-150-2 | 365033 | 5045076 | M tagabbro m lanocrate | | | | |
| 05-JF-150-3 | 365023 | 5045103 | M tagabbro m lanocrate | | | | |
| 05-JF-151-A1 | 364936 | 5045295 | M tagabbro m lanocrate | | | | |
| 05-JF-151-A2 | 364918 | 5045286 | M tagabbro m lanocrate | | | | |
| 05-JF-151-A3 | 364901 | 5045314 | M tagabbro m lanocrate | | | | |
| 05-JF-151-A4 | 364891 | 5045363 | M tagabbro m lanocrate | | | | |
| 05-JF-152-1 | 369103 | 5062214 | Amphibolite   homblende mafique | | | | |
| 05-JF-152-2 | 369268 | 5061795 | Amphibolite   homblende mafique | | | | |
| 05-JF-152-3 | 368894 | 5062102 | Amphibolite   homblende et calcite | | | | |
| 05-JF-153-1 | 364578 | 5045854 | Marbre calcitique gris (< 10% silicates-graphite) | Sulfures de zinc | | 14/56 | |

Table: Outcrop description summary

| Station | UTM E | UTM N | Lithology | Zinc Mineral | Pure Dolomite | Bedding Strike/dip | Foliation Strike/dip |
|---------------|--------|---------|---|-----------------------------|---------------|--------------------|----------------------|
| 05-JF-153-2 | 364618 | 5045819 | Marbre calcitique graphiteux (~ 30% graphite) | | | 20/-99 | |
| 05-JF-153-3 | 364625 | 5045815 | Marbre calcitique gris (< 10% silicates-graphite) | | | | |
| 05-JF-153-4 | 364638 | 5045820 | Marbre calcitique gris (< 10% silicates-graphite) | | | 35/43 | |
| 05-JF-153-5 | 364643 | 5045799 | Marbre calcitique gris (< 10% silicates-graphite) | | | 347/16 | |
| 05-JF-154-1 | 362943 | 5047231 | Marbre dolomitique calcosilicaté quartzeux (Di + > 20% Qtz) | | | 18/55 | |
| 05-JF-154-2 | 362962 | 5047224 | Diopsidite pure | | | | 25/26 |
| 05-JF-154-3 | 362976 | 5047213 | Marbre dolomitique calcosilicaté quartzeux (Di + > 20% Qtz) | | | | |
| 05-JF-154-4 | 362976 | 5047213 | Diopsidite quartzreuse (50% Di - 50% Qtz) | | | | |
| 05-JF-154-5 | 362991 | 5047203 | Diopsidite pure | | | | |
| 05-JF-154-6 | 363022 | 5047180 | Diopsidite quartzreuse (50% Di - 50% Qtz) | | | | |
| 05-JF-155-1 | 362988 | 5047856 | Marbre calcitique gris (< 10% silicates-graphite) | | | | |
| 05-JF-155-2 | 363017 | 5047851 | Marbre calcitique à diopside-forstérite (10-20%Si) | | | | |
| 05-JF-155-3 | 363026 | 5047861 | Marbre calcitique gris (< 10% silicates-graphite) | | | 340/32 | |
| 05-JF-156 | 369717 | 5049539 | Marbre calcitique gris (< 10% silicates-graphite) | | | 20/50 | |
| 05-JF-157-1 | 369787 | 5049652 | Marbre calcarodolomitique ~ pur (< 10% silicates) | Sulfures de zinc | | | |
| 05-JF-157-2 | 369792 | 5049656 | Métagabbro mélanocrate | | | | |
| 05-JF-157-3 | 369788 | 5049649 | Métagabbro mélanocrate | | | | |
| 05-JF-158-1 | 370735 | 5051311 | Marbre dolomitique pur | | Oui | | |
| 05-JF-158-2 | 370746 | 5051363 | Marbre dolomitique pur | | Oui | | |
| 05-JF-159-MG | 372754 | 5057912 | Marbre dolomitique à diopside-forstérite (21-40%Si) | Silicates et oxydes de zinc | | 348/22 | |
| 05-JF-160-1 | 372772 | 5057857 | Marbre calcarodolomitique pur | | | 334/32 | |
| 05-JF-160-2 | 372759 | 5057840 | Marbre calcarodolomitique pur | | | 348/22 | |
| 05-JF-160-3 | 372769 | 5057834 | Marbre calcarodolomitique pur | | | | |
| 05-JF-160-4 | 372776 | 5057805 | Marbre calcarodolomitique pur | | | | |
| 05-JF-161-1 | 372767 | 5057711 | Marbre calcarodolomitique pur | | | 348/25 | |
| 05-JF-161-105 | | | Marbre dolomitique à diopside-forstérite (21-40%Si) | Silicates et oxydes de zinc | | | |
| 05-JF-161-115 | | | Marbre dolomitique à diopside-forstérite (21-40%Si) | Silicates et oxydes de zinc | | | |
| 05-JF-161-125 | | | Marbre dolomitique à diopside-forstérite (21-40%Si) | Silicates et oxydes de zinc | | | |
| 05-JF-161-155 | | | Marbre dolomitique à diopside-forstérite (21-40%Si) | Silicates et oxydes de zinc | | | |
| 05-JF-161-185 | | | Marbre dolomitique à diopside-forstérite (21-40%Si) | Silicates et oxydes de zinc | | | |

Table: Outcrop description summary

| Station | UTM E | UTM N | Lithology | Zinc Mineral | Pure Dolomite | Bedding Strike/dip | Foliation Strike/dip |
|----------------|--------|---------|---|-----------------------------|---------------|--------------------|----------------------|
| 05-JF-161-35 | | | Marbre dolomitique à diopside-forstérite (21-40%Si) | Silicates et oxydes de zinc | | | |
| 05-JF-161-45 | | | Marbre dolomitique à diopside-forstérite (21-40%Si) | Silicates et oxydes de zinc | | | |
| 05-JF-161-5 | 372786 | 5057608 | Marbre dolomitique à diopside-forstérite (21-40%Si) | Silicates et oxydes de zinc | | 340/22 | |
| 05-JF-161-55 | | | Marbre dolomitique à diopside-forstérite (21-40%Si) | Silicates et oxydes de zinc | | | |
| 05-JF-161-5-5 | | | Marbre dolomitique à diopside-forstérite (21-40%Si) | Silicates et oxydes de zinc | | 348/22 | |
| 05-JF-161-65 | | | Marbre dolomitique à diopside-forstérite (21-40%Si) | Silicates et oxydes de zinc | | | |
| 05-JF-161-75 | | | Marbre dolomitique à diopside-forstérite (21-40%Si) | Silicates et oxydes de zinc | | | |
| 05-JF-161-85 | | | Marbre dolomitique à diopside-forstérite (21-40%Si) | Silicates et oxydes de zinc | | | |
| 05-JF-161-95 | | | Marbre dolomitique à diopside-forstérite (21-40%Si) | Silicates et oxydes de zinc | | | |
| 05-JF-161-MG-5 | 372758 | 5057607 | | | | | |
| 05-JF-162 | 372822 | 5057582 | Marbre dolomitique à diopside-forstérite (21-40%Si) | Silicates et oxydes de zinc | | | |
| 05-JF-163-1 | 368323 | 5062122 | Marbre dolomitique pur | | Oui | | |
| 05-JF-163-2 | 368307 | 5062008 | Marbre dolomitique pur | | Oui | | |
| 05-JF-163-3 | 368370 | 5061753 | Marbre dolomitique pur | | Oui | | |
| 05-JF-163-4 | 368404 | 5061670 | Marbre calcaire dolomitique pur | | | | |
| 05-JF-163-5 | 368454 | 5061694 | Marbre dolomitique pur | | | 25/25 | |
| 05-JF-164-MG-1 | 368443 | 5061832 | Amphibolite à hornblende et calcite | | | | 303/39 |
| 05-JF-164-MG-2 | 368418 | 5061721 | Marbre dolomitique à diopside-forstérite (21-40%Si) | | | 350/47 | |
| 05-JF-164-MG-3 | 368368 | 5061750 | Marbre dolomitique à diopside-forstérite (10-20%Si) | | | 14/38 | |
| 05-JF-164-MG-4 | 368463 | 5061747 | Amphibolite à hornblende et calcite | | | | |
| 05-JF-165-MG-1 | 369191 | 5059530 | Marbre dolomitique ~ pur (< 10% silicates) | | | | |
| 05-JF-165-MG-2 | 369105 | 5059585 | Marbre dolomitique à diopside-forstérite (10-20%Si) | | | | |
| 05-JF-165-MG-3 | 369059 | 5059477 | Marbre dolomitique à diopside-forstérite (10-20%Si) | | | 47/27 | |
| 05-JF-166 | 371947 | 5052709 | Métagabbro mélanocrate | | | | |
| 05-JF-167 | 372566 | 5052121 | Granite rose | | | | |
| 05-JF-168 | 372546 | 5052114 | Granite rose | | | | |
| 05-JF-169 | 372528 | 5052116 | Granite rose | | | | |
| 05-JF-170 | 372514 | 5052101 | Granite rose | | | | |
| 05-JF-171 | 372526 | 5052090 | Granite rose | | | | |
| 05-JF-172 | 373146 | 5051602 | Marbre dolomitique ~ pur (< 10% silicates) | | | | |

Table: Outcrop description summary

| Station | UTM E | UTM N | Lithology | Zinc Mineral | Pure Dolomite | Bedding Strike/dip | Foliation Strike/dip |
|--------------|--------|---------|--|------------------|---------------|--------------------|----------------------|
| 05-JF-172-1 | 373139 | 5051603 | Marbre dolomitique ~ pur (< 10% silicates) | | | | |
| 05-JF-172-2 | 373123 | 5051596 | Marbre dolomitique ~ pur (< 10% silicates) | | | | |
| 05-JF-172-3 | 373122 | 5051567 | Marbre dolomitique ~ pur (< 10% silicates) | | | | |
| 05-JF-172-4 | 373144 | 5051591 | Marbre dolomitique ~ pur (< 10% silicates) | | | | |
| 05-JF-172-5 | 373141 | 5051596 | Marbre dolomitique ~ pur (< 10% silicates) | | | | |
| 05-JF-172-6 | 373149 | 5051605 | Marbre dolomitique ~ pur (< 10% silicates) | | | | |
| 05-JF-173 | 373537 | 5051152 | Paragneiss quartzofeldspatique à biotite | | | | |
| 05-JF-174 | 374134 | 5050373 | Métagabbro mélanocrate | | | | |
| 05-JF-175 | 374414 | 5050323 | Métagabbro mélanocrate | | | | |
| 05-JF-175-1 | 374393 | 5050321 | Métagabbro mélanocrate | | | | |
| 05-JF-175-2 | 374397 | 5050315 | Métagabbro mélanocrate | | | | |
| 05-JF-175-3 | 374390 | 5050312 | Métagabbro mélanocrate | | | | |
| 05-JF-176 | 374867 | 5050261 | Paragneiss quartzofeldspatique à biotite | | | | |
| 05-JF-176-A1 | 374837 | 5050223 | Paragneiss quartzofeldspatique à biotite | | | | |
| 05-JF-177 | 374421 | 5051812 | Métagabbro mélanocrate | | | | |
| 05-JF-178 | 374728 | 5051561 | Paragneiss quartzofeldspatique à biotite | | | | |
| 05-JF-179 | 372835 | 5058008 | Marbre dolomitique à diopside-forstérite (21-40%Si) | | | | |
| 05-JF-180 | 372845 | 5057985 | Marbre dolomitique à diopside-forstérite (21-40%Si) | | | | |
| 05-JF-181-1 | 372840 | 5057956 | Marbre calcarodolomitique ~ pur (< 10% silicates) | | | | |
| 05-JF-181-2 | 372844 | 5057948 | Marbre calcarodolomitique ~ pur (< 10% silicates) | | | | |
| 05-JF-181-3 | 372838 | 5057935 | Marbre calcarodolomitique ~ pur (< 10% silicates) | | | | |
| 05-JF-181-4 | 372835 | 5057925 | Marbre calcarodolomitique à diopside-forstérite (10-20%Si) | | | | |
| 05-JF-181-5 | 372834 | 5057919 | Marbre calcarodolomitique ~ pur (< 10% silicates) | | | | |
| 05-JF-181-6 | 372837 | 5057937 | Marbre calcarodolomitique ~ pur (< 10% silicates) | | | | |
| 05-JF-181-7 | 372843 | 5057952 | Marbre calcarodolomitique ~ pur (< 10% silicates) | | | | |
| 05-JF-181-8 | 372849 | 5057962 | Marbre calcarodolomitique ~ pur (< 10% silicates) | | | | |
| 05-JF-182 | 369317 | 5058194 | Marbre dolomitique à diopside-forstérite (21-40%Si) | | | | |
| 05-JF-183 | 369354 | 5058209 | Marbre dolomitique ~ pur (< 10% silicates) | | Oui | 50/25 | |
| 05-JF-184 | 369398 | 5058260 | Marbre dolomitique pur | | | 67/24 | |
| 05-JF-185 | 368944 | 5058273 | Marbre dolomitique à diopside-forstérite (21-40%Si) | Sulfures de zinc | | 58/28 | |

Table: Outcrop description summary

| Station | UTM E | UTM N | Lithology | Zinc Mineral | Pure Dolomite | Bedding Strike/dip | Foliation Strike/dip |
|--------------|--------|---------|--|------------------|---------------|--------------------|----------------------|
| 05-JF-186-01 | 368754 | 5058447 | Marbre dolomitique à diopside-forst rite (21-40%Si) | | | 90/15 | |
| 05-JF-186-02 | 368774 | 5058465 | Marbre dolomitique à diopside-forst rite (10-20%Si) | Sulfures de zinc | | Dec-65 | |
| 05-JF-186-03 | | | Marbre dolomitique à diopside-forst rite (21-40%Si) | | | | |
| 05-JF-187 | 369076 | 5058219 | Marbre calcaire dolomitique à diopside-forst rite (10-20%Si) | | | 307/49 | |
| 05-JF-188 | 369804 | 5059308 | Amphibolite à hornblende mafique | | Oui | 345/-99 | 345/51 |
| 05-JF-189 | 369271 | 5059589 | Marbre dolomitique pur | | | 345/10 | |
| 05-JF-190 | 369067 | 5059568 | Marbre dolomitique à diopside-forst rite (10-20%Si) | | | 112/48 | |
| 05-JF-191 | 368990 | 5059609 | Marbre dolomitique à diopside-forst rite (10-20%Si) | | | 110/18 | |
| 05-JF-192-1A | 369077 | 5059527 | Marbre dolomitique ~ pur (< 10% silicates) | | | 110/18 | |
| 05-JF-192-1B | 369077 | 5059527 | Marbre dolomitique à diopside-forst rite (10-20%Si) | Sulfures de zinc | | 110/18 | |
| 05-JF-192-1C | 369077 | 5059527 | Marbre dolomitique ~ pur (< 10% silicates) | | | 110/18 | |
| 05-JF-192-2 | 369077 | 5059527 | Marbre dolomitique à diopside-forst rite (10-20%Si) | Sulfures de zinc | | 47/27 | |
| 05-JF-192-A1 | 369079 | 5059539 | Marbre dolomitique ~ pur (< 10% silicates) | | | | |
| 05-JF-192-A2 | 369080 | 5059537 | Marbre dolomitique ~ pur (< 10% silicates) | | | | |
| 05-JF-192-A3 | 369081 | 5059533 | Marbre dolomitique ~ pur (< 10% silicates) | | | | |
| 05-JF-192-A4 | 369089 | 5059541 | Marbre dolomitique ~ pur (< 10% silicates) | | | | |
| 05-JF-192-A5 | 369098 | 5059528 | Marbre dolomitique ~ pur (< 10% silicates) | | | | |
| 05-JF-192-A6 | 369092 | 5059526 | Marbre dolomitique ~ pur (< 10% silicates) | | | | |
| 05-JF-192-A7 | 369070 | 5059530 | Marbre dolomitique ~ pur (< 10% silicates) | | | | |
| 05-JF-193-1A | 369124 | 5059590 | Marbre dolomitique à diopside-forst rite (10-20%Si) | Sulfures de zinc | | 118/26 | |
| 05-JF-193-1B | 369124 | 5059590 | Marbre dolomitique ~ pur (< 10% silicates) | Sulfures de zinc | | 118/26 | |
| 05-JF-193-1C | 369124 | 5059590 | Marbre dolomitique ~ pur (< 10% silicates) | Sulfures de zinc | | 118/26 | |
| 05-JF-193-1D | 369124 | 5059590 | Marbre dolomitique ~ pur (< 10% silicates) | | | 118/26 | |
| 05-JF-193-A1 | 369135 | 5059610 | Marbre dolomitique ~ pur (< 10% silicates) | | | | |
| 05-JF-193-A2 | 369122 | 5059573 | Marbre dolomitique ~ pur (< 10% silicates) | | | | |
| 05-JF-194-1A | 369207 | 5059609 | Marbre dolomitique à diopside-forst rite (10-20%Si) | Sulfures de zinc | | 77/16 | |
| 05-JF-194-1B | 369207 | 5059609 | Marbre dolomitique ~ pur (< 10% silicates) | | | 77/16 | |
| 05-JF-194-A1 | 369204 | 5059614 | Marbre dolomitique ~ pur (< 10% silicates) | | | | |
| 05-JF-194-A2 | 369205 | 5059613 | Marbre dolomitique ~ pur (< 10% silicates) | | | | |
| 05-JF-194-A3 | 369200 | 5059603 | Marbre dolomitique ~ pur (< 10% silicates) | | | | |

Table: Outcrop description summary

| Station | UTM E | UTM N | Lithology | Zinc Mineral | Pure Dolomite | Bedding Strike/dip | Foliation Strike/dip |
|---------------|--------|---------|---|------------------|---------------|--------------------|----------------------|
| 05-JF-194-A4 | 369199 | 5059602 | Marbre dolomitique ~ pur (< 10% silicates) | | | | |
| 05-JF-194-A5 | 369194 | 5059602 | Marbre dolomitique ~ pur (< 10% silicates) | | | | |
| 05-JF-194-A6 | 369208 | 5059613 | Marbre dolomitique ~ pur (< 10% silicates) | | | | |
| 05-JF-194-A7 | 369208 | 5059601 | Marbre dolomitique ~ pur (< 10% silicates) | | | | |
| 05-JF-194-A8 | 369213 | 5059598 | Marbre dolomitique ~ pur (< 10% silicates) | | | | |
| 05-JF-195-1 | 366348 | 5030666 | Marbre dolomitique à diopside-trémolite (21-40%Si) | Sulfures de zinc | 240/77 | | 340/17 |
| 05-JF-195-2 | 366348 | 5030666 | Marbre dolomitique à diopside-trémolite (21-40%Si) | | 240/77 | | 20/29 |
| 05-JF-196 | 366605 | 5032303 | Paragneiss quartzofeldspatique à biotite | | | | 9/44 |
| 05-JF-197 | 366696 | 5032375 | Paragneiss quartzofeldspatique à biotite | | | | 135/38 |
| 05-JF-198 | 366747 | 5032428 | Paragneiss quartzofeldspatique à biotite | | | | 19/34 |
| 05-JF-199 | 366868 | 5032528 | Paragneiss quartzofeldspatique à biotite | | | | 23/29 |
| 05-JF-200 | 367196 | 5032805 | Paragneiss quartzofeldspatique à biotite | | | | 33/35 |
| 05-JF-201 | 367415 | 5033003 | Paragneiss quartzofeldspatique à biotite | | | | 75/60 |
| 05-JF-202 | 368155 | 5033674 | Paragneiss quartzofeldspatique à biotite | | | | 52/49 |
| 05-JF-203 | 368740 | 5033931 | Paragneiss quartzofeldspatique à biotite | | | | |
| 05-JF-204 | 369045 | 5033620 | Paragneiss quartzofeldspatique à biotite | | | | |
| 05-JF-205-01A | 369085 | 5033559 | Marbre dolomitique ~ pur (< 10% silicates) | Sulfures de zinc | 54/63 | | |
| 05-JF-205-01B | 369085 | 5033559 | Marbre dolomitique ~ pur (< 10% silicates) | Sulfures de zinc | 54/63 | | |
| 05-JF-205-01C | 369085 | 5033559 | Marbre dolomitique ~ pur (< 10% silicates) | Sulfures de zinc | 54/63 | | |
| 05-JF-205-02 | 369082 | 5033564 | Paragneiss quartzofeldspatique à biotite | | | | |
| 05-JF-205-03 | 369073 | 5033571 | Paragneiss quartzofeldspatique à biotite | | | | |
| 05-JF-205-04 | 369091 | 5033547 | Marbre dolomitique ~ pur (< 10% silicates) | | | | |
| 05-JF-205-05 | 369091 | 5033550 | Marbre dolomitique ~ pur (< 10% silicates) | | | | |
| 05-JF-205-06 | 369086 | 5033556 | Marbre dolomitique ~ pur (< 10% silicates) | | | | |
| 05-JF-206 | 369123 | 5033499 | Marbre dolomitique à diopside-forstérite (10-20%Si) | | 64/77 | | 65/56 |
| 05-JF-207 | 369130 | 5033473 | Paragneiss quartzofeldspatique à biotite | | | | |
| 05-JF-208 | 368822 | 5034158 | Paragneiss quartzofeldspatique à biotite | | | | |
| 05-JF-209 | 369257 | 5034547 | Paragneiss quartzofeldspatique à biotite | | | | |
| 05-JF-210 | 371941 | 5032457 | Paragneiss quartzofeldspatique à biotite | | | | 50/81 |
| 05-JF-211 | 371695 | 5032755 | Paragneiss quartzofeldspatique à biotite | | | | 40/65 |

Table: Outcrop description summary

| Station | UTM E | UTM N | Lithology | Zinc Mineral | Pure Dolomite | Bedding Strike/dip | Foliation Strike/dip |
|--------------|--------|---------|--|--------------|---------------|--------------------|----------------------|
| 05-JF-212 | 371459 | 5033026 | Paragneiss quartzofeldspathique à biotite | | | | 45/34 |
| 05-JF-213-01 | 371408 | 5035278 | Marbre calcitique à diopside-forstérite (10-20%Si) | | | | |
| 05-JF-213-02 | 371390 | 5035293 | Marbre calcarodolomitique à diopside-forstérite (10-20%Si) | | | 322/33 | |
| 05-JF-213-03 | 371379 | 5035306 | Marbre calcitique à diopside-forstérite (10-20%Si) | | | 350/24 | |
| 05-JF-213-04 | 371347 | 5035333 | Marbre calcitique à diopside-forstérite (10-20%Si) | | | | |
| 05-JF-214-01 | 370142 | 5036802 | Marbre dolomitique ~ pur (< 10% silicates) | | | 295/24 | |
| 05-JF-214-02 | 370130 | 5036851 | Marbre dolomitique ~ pur (< 10% silicates) | | | | |
| 05-JF-214-03 | 370123 | 5036810 | Marbre dolomitique ~ pur (< 10% silicates) | | | | |
| 05-JF-214-04 | 373070 | 5036746 | Marbre dolomitique à diopside-forstérite (10-20%Si) | | | | |
| 05-JF-215 | 370484 | 5036405 | Marbre calcarodolomitique ~ pur (< 10% silicates) | | | 310/44 | |
| 05-JF-216-01 | 373063 | 5036408 | Marbre calcarodolomitique à diopside-forstérite (10-20%Si) | | | 125/56 | |
| 05-JF-216-02 | 373086 | 5036397 | Marbre calcarodolomitique à diopside-forstérite (10-20%Si) | | | | |
| 05-JF-216-03 | 373021 | 5036479 | Marbre calcarodolomitique à diopside-forstérite (10-20%Si) | | | | |
| 05-JF-217 | 369601 | 5035280 | Paragneiss quartzofeldspathique à biotite | | | | |

REFERENCES

- Barrow, G., 1893, On an intrusion of muscovite-biotite gneiss in the east Jighlands of Scotland, and its accompanying metamorphism., *Quarterly Journal Geological Society of London*, v. 49, p. 330-358
- Bernier, L., Pouliot, G., and MacLean, W.H., 1987, Geology and metamorphism of the Montauban North gold zone: A metamorphosed polymetallic exhalative deposit, Grenville Province, Quebec., *Economic Geology*, v. 82, p. 2076-2090
- Bishop, C., 1987, Preliminary report on phase II diamond drilling, spring 1987, Calumet Island gold Project, Internal report, Lacana Mining Corporation, 236 pp.
- Bishop, C., and Jourdain, V., 1987, Grenville Polymetallics., *The Northern Miner*, V 2 No 12, 15-17
- Bishop, C., and Villeneuve, D., 1987, Report on the New Calumet Mine gold property., Lacana Mining Corp., Statuary reports, GM-44397, 367 p.
- Brown, J.S., 1973, Sulfur isotope of Precambrian sulfates and sulfides in the Grenville of New York and Ontario., *Economic Geology*, v. 68, p. 362-370
- Brown, J.S., and Engel, A.E.J., 1956, Revision of Grenville stratigraphy and structure in the Balmat-Edward district, northwest Adirondacks, N.Y., *Bulletin of the Geological Society of America*, v. 67, p. 1599-1622
- Brugger, J., McPhail, D.C., Wallace, M. and Waters, J., 2003, Formation of willemite in hydrothermal environments., *Economic Geology*, v. 98, p. 819-835
- Burnham, C.W., 1991, LCLSQ; lattice parameter refinement using correction terms for systematic errors., *American Mineralogist*, v. 76, p. 663-664
- Callahan, W.H., 1966, Genesis of the Franklin-Sterling Hill, New Jersey orebodies., *Economic Geology*, v. 61, p. 1140-1141
- Carl, J.D., 1988, Popple Hill Gneiss as dacite colcanic: A geochemical study of mesosome and leucosome, northwest Adirondacks, New York., *Geological Society of America, Bulletin*, v. 100, p. 841-849
- Carne, R.C. and Cathro, R.J., 1982, Sedimentary exhalative (SEDEX) zinc-lead deposits, northern Canadian Cordillera., *The Canadian Mining and Metallurgy Bulletin*, v. 75, p.66-78

- Cartwright, I., and Oliver, H.D., 2000, Metamorphic Fluids and Their Relationship to the Formation of Metamorphosed and Metamorphogenic Ore Deposits., In, *Metamorphosed and Metamorphogenic Ore Deposits*, Edited by Spry, P.G., Marshall, B., and Vokes, F.M., *Reviews in Economic Geology*, v. 11, p. 81-96
- Carvalho, A. V., III, and Sclar, C. B., 1988, Experimental Determination of the ZnFe_2O_4 - ZnAl_2O_4 Miscibility gap With Application to Franklinite-Gahnite exsolution intergrowths from the Sterling Hill Zinc Deposit, New Jersey., *Economic Geology*, Vol 83, p. 1447-1452
- Chouteau, M., Giroux, B. and Gauthier, M., 2005, Minéralogie et propriétés des gîtes de zinc disséminé dans les marbres du Supergroupe de Grenville - Volet géophysique., Final Report, DIVEX, 14 p.
- Cooke, D.R., Bull, S.W., Large, R.R. and McGoldrick, P.J., 2000, The Importance of Oxidized Brines for the Formation of Australian Proterozoic Stratiform Sediment-Hosted Pb-Zn (Sedex) Deposits, *Economic Geology*, v. 95, p. 1-18
- Davidson, A., 1998, Survol de la géologie de la Province de Grenville, Bouclier Canadien. In Lucas, F.B. et St-Onge, M.R., *Géologie des Provinces Précambriennes du lac Supérieur et de Grenville et fossils du Précambrien en Amérique du Nord.*, Commission Géologique du Canada, *Géologie du Canada*, no 7, 426 p.
- Deer, W.A., Howie, R.A., and Zussman, J., 1992, An introduction to the rock-forming minerals., Second edition, Prentice Hall, 549 p.
- Dickson, J.A.D., 1965, A modified technique for carbonate thin section., *Nature*, v.205, no. 4971, p. 587
- deLorraine, W.F., 2001, Metamorphism, polydeformation, and extensive remobilization of the Balmat zinc ore bodies, northwest Adirondacks, New York., *Society of Economic Geologists Guidebook Series*, v. 35, p. 25-54
- deLorraine, W.F., and Dill, D.B., 1982, Structure, stratigraphic controls, and genesis of the Balmat-Edwards zinc deposits, northwest Adirondacks, New York. In *Precambrian sulphide deposits*. Edited by R.W. Hutchinson, C.D. Spence, and J.M. Franklin. Geological Association of Canada, Special Paper 25, pp. 571-596
- Dunn, P.J., 1995, Franklin and Sterling Hill, New Jersey: The world's most magnificent mineral deposits., *Franklin-Ogdensburg Mineral Society*, 977 p.
- Easton, R.M., 1992, The Grenville Province and the Proterozoic History of Central and Southern Ontario.; In *Geology of Ontario.*, Editors P.C. Thurston, H.R. Williams, R.H. Stutcliffe and G.M. Scott., Ontario Geological Survey, Special Volume 4, Part 2, p. 715-906
- Easton, R.M., and Fyon, J.A., 1992, Metallogeny of the Grenville Province. In *Geology of Ontario.* Edited by Thurston, P.C., Williams, H.R., Stutcliffe, R.H. and Scott, G.M., Ontario Geological Survey, Special volume 4, p. 1217-1254

- Evamy, B.D., 1983, The application of a chemical staining technique to a study of dedolomitisation., *Sedimentology*, v. 2, p. 176-170
- Frondel, C. and Baum, J.L., 1974, Structure and mineralogy of the Franklin zinc-iron-manganese deposit, New Jersey., *Economic Geology*, v. 69, p. 157-180
- Frondel, C. and Klein, C., 1965, Exsolution in franklinite., *American Mineralogist*, v. 50, p. 1270-1280
- Gauthier, M. and Brown, A.C., 1986, Zinc and iron metallogeny in the Maniwaki-Gracefield district, southwestern Quebec., *Economic Geology*, v. 81, p. 89-112
- Gauthier, M. and Chartrand, F., 2005, Metallogeny of the Grenville Province Revisited., *Canadian Journal of Earth Sciences*, v. 42, pp. 1719-1734
- Gauthier, M., Brown, A. C. and Morin, G., 1987, Small Iron-Formations as a Guide to Base and Precious-Metal Deposits in the Grenville Province of Southern Quebec, *In* P.W.U. Appel et G.L. Laberge editors., *Precambrian Iron-Formation: Athènes.*, Theophrastus Publication, p. 297-327
- Gauthier, M., Corriveau, L. and Chouteau, M., 2004, Metamorphosed and metamorphogenic ore deposits of the Central Metasedimentary Belt, southwestern Québec and southeastern Ontario Grenville Province. *Field Trip Guidebook.*, DIVEX Research Group, 39 p.
- Goodfellow, W.D., Lydon, J.W. and Turner, R.J.W., 1993, Geology and Genesis of Stratiform Sediment-Hosted (sedex) Zinc-Lead-Silver sulphide deposits., *In*, *Mineral Deposits Modelling*, Edited by Kirkham, R.V., Sinclair, W.D., Thorpe, R.I. and Duke, J.M., Geological Association of Canada, Special Paper 40, 770 pp.
- Groves, I.A., Carman, C.E., and James Dunlap, W., 2003, Geology of the Beltana Willemite Deposit, Flinders Ranges, South Australia., *Economic Geology*, v. 98, p.797-818.
- Hague, J.M., Baum, J.L., Herrmann, L.A., and Pickering, R.J., 1956, Geology and structure of the Franklin-Sterling area, New Jersey., *Geological Society of America Bulletin*, v. 67, p. 435-474
- Hanmer, S., Corrigan, D., Pehrsson, S., and Nadeau, L., 2000, SW Grenville Province, Canada: The case against post-1.4 Ga accretionary tectonics., *Tectonophysics*, v. 319, p. 33-51
- Heffernan, V., 2006, Hot market has juniors eyeing zinc oxides., *The Northern Miner*, No. June 2-8, pp. B1 and B8
- Hitzman, M.W., Reynolds, N.A., Sangster, D.F., Allen, C.R. and Carman, C.E., 2003, Classification, Genesis and Exploration Guides for Nonsulfide Zinc Deposits, *Economic Geology*, v. 98, p. 685-714

- Hitzman, M.W., Thorman, C.H., Romagna, G., Olivera, T.F., Dardenne, M.A., and Drew, L.J., 1995, The Morro Agudo Zn-Pb deposit, Minas Gerais, Brazil: A Proterozoic Irish-type carbonate hosted sedex-replacement deposit [abs]., Geological Society of America Abstracts with Programs, v.27, p. A408
- Indares, A. and Martignole, J., 1984, Evolution of P-T conditions during a high-grade metamorphic event in the Maniwaki area (Grenville Province)., Canadian Journal of Earth Sciences, v. 21, p. 852-863
- Isachsen, Y. and Landing, E., 1983, First Proterozoic stromatolites from the Adirondack massif: Stratigraphic, structural and depositional implications., Geological Society of America Abstracts with Programs, v. 15, p. 601
- Johnson, C.A. and Skinner, B.J., 2003, Geochemistry of the Furnace Magnetite Bed, Franklin, New Jersey, and the relationship between stratiform iron oxide ores and stratiform zinc oxide-cilicate ores in the New Jersey Highlands., Economic Geology, v. 98, p.837-854.
- Johnson, C.A., 1990, Petrologic and Stable Isotope studies of the Metamorphosed zinc-iron-manganese deposit at Sterling Hill, New Jersey, Ph. D. dissertation Yale University, 108 p.
- Johnson, C.A., Rye, D.M. and Skinner, B.J., 1990, Petrology and stable isotope geochemistry of the metamorphosed zinc-iron-manganese deposit at Sterling Hill, New Jersey., Economic Geology, v. 85, p. 1133-1161
- Jourdain, V., 1993, Géologie des amas sulfurés aurifères de la Province de Grenville., Université du Québec à Montréal, Ph.D. Thesis.
- Katz, M.B., 1976, Région Portage-du-fort et Lac Saint Patrice, Ministère de l'énergie et des ressources, Québec, R.G. 170, 122 p.
- Kearns, L.E., 1975, Fluoborite, a new locality., Mineral Record, v. 6, p. 174-175
- Kearns, L.E., 1977, The mineralogy of the Franklin marble, Orange County, New York., Unpublished Ph.D. dissertation, Newark, University of Delaware, 211 p.
- Landry, B., Pageau, J.G., Gauthier, M., Bernard, J., Beaudin, J., et Duplessis, D., 1995, Prospection minière., Modulo, Montréal, 232 p.
- Large, D.E., 1980, Geological parameters associated with sediment-hosted submarine exhalative Pb-Zn deposits: An empirical model for mineral exploration. Geologische Jahrbuch, v.40, p.59-129
- Large, R., Bodon, S., Davidson, G., and Cooke, D., 1996, The chemistry of BHT ore formation – one of the keys to understanding the differences between SEDEX and BHT deposits, In New developments in Broken Hill-type deposits: Hobart, Tasmania, Australia, Edited by Pongratz, J., and Davidson, G.J., Centre for Ore Deposits and Exploration Studies Special Publication 1, p.105-112

- Logan, W.E., 1863, Report on the geology of Canada., Ottawa, Ontario, Report of progress from the commencement to 1863., Geological Survey of Canada, 983 p.
- Lumbers, S.B., 1982, Summary of Metallogeny Renfrew County Area., Ontario Geological Survey, OGS Report 212, 58 p.
- Lydon, J.W., 1996, Gîtes de sulfures exhalatifs dans des roches sédimentaires (gîtes sedex); In *Géologie des types de gîtes minéraux du Canada*, edited by O.R. Eckstrand, W.D. Sinclair and R.I. Thorpe, Commission géologique du Canada, *Géologie du Canada*, N. 8 p.142-167
- McLelland, J., Chiarenzell, J. and Perham, A., 1992, Age, field, and petrologic relationships of the Hyde School Gneiss, Adirondack Lowlands, New York: Criteria for an intrusive igneous origin., *Journal of Geology*, v. 100, p. 69-90
- Megster, R.W., 2001, Evolution of the Sterling Hill Zinc Deposit, Ogdensburg, Sussex County, New Jersey., *Society of Economic Geologists Guidebook Series*, v. 35, p. 75-87
- Megster, R.W., Skinner, B.J. and Barton, B.P., 1969, Structural interpretation of the Sterling Hill ore body, Ogdensburg, N.J. [abs], *Geological Society of America Abstracts with Programs*, v. 7, p. 150
- Megster, R.W., Tennant, C.B. and Rodda, J.L., 1958, Geochimistry of the Sterling Hill zinc deposit, Sussex Co., N.J., *Bulletin of the Geological Society of America*, v. 69, p. 775-788
- Montiero, L.V.S., Bettencourt J.S., Juliani C., and Oliveira, T.F., 2006, Geology, petrography, and mineral chemistry of the Vazante non-sulfide and Ambro' sia and Fagundes sulfide-rich carbonate-hosted Zn-(Pb) deposits, Minas Gerais, Brazil., *Ore Geology Reviews*, v. 28, p.201-234
- Monteiro, L.V.S., Bettencourt, J.S., Spiro, B., Graça, R. and De Oloveira, T.F., 1999, The Vazante zinc mine, Minas Gerais, Brazil: Constraints on willemitic mineralization and fluid evolution., *Exploration and Mining Geology*, v. 8, p. 21-42
- Nadeau, L., and van Breemen, O., 1994, Do the 1.45-1.39 Ga Montauban Group and La Bostonnais complex constitute a Grenvillian accreted terrane? GAC-MAC Meeting, Program with abstract., v. 19, p. A81
- Nantel, S., 1994, Les tourmalinites et les roches riches en tourmaline dans la partie sud de la Province de Grenville, Québec, et leur association avec des minéralisations en Zn et en Cu-Co plus ou moins Au., *Ministère des Ressources Naturelles du Québec*, 26 p.
- Nawab, Z.A., 1994, Atlantis II Deep, In *Mineral resources of Saudi Arabia, not including oil, natural gas, and sulfur.*, Edited by Collenette, P., and Grainger, D.J., Directorate General of Mineral Ressources Special Publication SP-2: Jiddah, Kingdom of Saudi Arabia Ministry of Petroleum and Mineral Ressources, p. 297-301

- Nesbitt, B.E., and Kelly, W.C., 1980, Metamorphic zonation of sulfides, oxides, and graphite in and around the orebodies at Ducktown, Tennessee., *Economic Geology*, v. 75, p. 1010-1021
- Osborne, F.F., 1939, Brucite, Rapport préliminaire., Ministère de l'énergie et des ressources, Québec, no. 139
- Osborne, F.F., 1941, Anhydrite and gypsum at Calumet Mines, Calumet Island, Que., *University of Toronto Studies.*, v. 46, p. 75-82
- Osborne, F.F., 1944, Région de l'île Calumet, Ministère de l'énergie et des ressources, Québec, RG-18
- Palache, C., 1935, The Minerals of Franklin and Sterling Hill., U.S. Geological Survey, Prof. Paper 180, 135 p.
- Palmer, M.R. et Slack, J.F., 1989, Boron isotopic composition of tourmaline from massive sulfide deposits and tourmalinites. *Contributions to mineralogy and petrology*; v. 103, pp. 434-451
- Peck, W.H., Volkert, R.A., Mansur, A.T. and Doverspike, B.A., 2009, Stable isotope and petrologic evidence of the origin of regional marble-hosted magnetite deposits and the zinc deposits at Franklin and Sterling Hill, New Jersey Highlands, United States., *Economic Geology*, v. 104, p. 1037-1054
- Pietsch, B.A., Rawlings, D.J., Creaser, P.M., Kruse, P.D., Ahmad, M., Fernenczi, P.A., and Findhammer, T.L.R., 1991, Bauhinia Downs SE53-3. 1:250,000 geological map series, explanatory notes: Government Printer of the Northern Territory, 76 pp.
- Pinger, A.W., 1950, Geology of the Franklin-Sterling Hill area, Sussex County, New Jersey., *International Geological Congress, London, 1948 Rept. V. 7*, p. 77-87
- Pomerol, C., Lagabrielle, Y., and Renard, M., 2000, *Éléments de géologie.*, 12e édition, Dunod, 746 p.
- Pottorf, R.J., and Barnes, H.L., 1983, Mineralogy, geochemistry, and ore genesis of hydrothermal sediments from the Atlantis II Deep, Red Sea., *Economic Geology Monograph* 5, p.198-223
- Puffer, J.H., and Volkert, R.A., 1991, Generation of trondhjemite from partial melting of dacite under granulite facies conditions: An example from the New Jersey Highlands, USA., *Precambrian Research*, v. 51, p. 115-125
- Ramdohr, P., 1980, The ore minerals and their intergrowths, 2nd edition., Pergamon Press, Oxford, v. 2, 941 p.
- Ridge, J.D., 1952, The geochemistry of the ores of Franklin, New Jersey., *Economic Geology*, v. 47, p. 180-192

- Ries, H. and Bowen, W.C., 1922, Origin of the zinc ores of Sussex County, New Jersey., *Economic Geology*, v. 17, p. 517-571
- Rivers, T., 1997, Lithotectonic elements of the Grenville Province: Review and tectonic implications., *Precambrian Research*, v. 86, p. 117-154
- Rivers, T., and Corrigan, D., 1999, Convergent margin on southeastern Laurentia during Mesoproterozoic: Tectonic implications., *Canadian Journal of Earth Sciences*, v. 37, p. 359-383
- Rivers, T., Ketchum, J., Indares, A., and Hynes, A., 2002, The High Pressure belt in the Grenville Province: architecture, timing, and exhumation., *Canadian Journal of Earth Sciences*, v. 39, p. 867-893
- Roger, G. and Lapointe, S., 1998, Report of Field Work - 1998, Cadieux Property, Admaston Township, Ontario, Noranda Mining and Exploration Inc., October 1998
- Rogers, H.B., 1836, Report on the geological survey of the State of New Jersey., Second edition, Philadelphia, Desilver, Thomas, 188 p.
- Rollinson, H.R., 1993, Using geochemical data: Evaluation, presentation, interpretation., Longman Publishing Group, 352 p.
- Sangster, A.L., 1967, Metamorphism of the New Calumet sulphide deposit, Quebec., M.Sc. Thesis, Carleton University, Ottawa, Ont.
- Sangster, A.L., 1970, Metallogeny of base metal, gold, and iron deposits of the Grenville Province ou southeastern Ontario., Ph. D. thesis, Queen's University, Kingston, Ontario, 355 p.
- Sangster, D.F., 2003, A special issue devoted to nonsulfide zinc deposits: A new look., Preface, *Economic Geology*, v. 98, p. 683-684.
- Scholten, J.C., Stoffers, P., Garbe-Schönberg, D., and Moammar, M., 2000, Hydrothermal mineralization in the Red Sea, In *Handbook of marine mineral deposits*, Edited by Cronan D.S., Boca Raton, Florida, CRC Press, p.369-395
- Soever, A. and Meusy, G., 1987, The Cadieux (Renprior) zinc deposit. In *livret-guide de l'excursion sur gîtes métallifères dans le sud du Grenville québécois*, 25-26-27 mai 1987. Édité by A. Vallières and M. Gauthier., Ministère de l'énergie et des ressources naturelles, Québec, p. 45-47
- Spencer, A.C., Kummel, H.B., Wolf, J.E., Salisbury, R.D. and Palache, C., 1908, Franklin Furnace folio., U.S. Geological Survey, Atlas 161, 27 p.
- Squiller, S.F. and Sclar, C.B., 1980, Genesis of the Sterling Hill zinc deposit, Sussex County, New Jersey, In *Proceedings of the 5th International Association on the Genesis of Ore Deposits (IAGOD) Symposium*. Edited by Ridge, J.D., Stuttgart, Germany, E. Schweizerbart'sche Verlagsbuch Handlung., p. 759-766

- Swihart, G.H. et Moore, P.B., 1989, A reconnaissance of boron isotopic composition of tourmaline. *Geochimica et Cosmochimica Acta*; v. 53, pp. 911-916
- Tarr, W.A., 1929, Origin of the zinc deposits at Franklin and Sterling Hill, New Jersey., *American Mineralogist*, v. 14, p. 207-221
- Valentino, A. J., Carvalho III, A. V. and Sclar, C., 1990, Franklinite-Magnetite-Pyrophanite Intergrowths in the Sterling Hill Zinc Deposit, New Jersey., *Economic Geology*, Vol 85, 1941-1946
- Veizer, J. and Hoefs, J., 1976, The nature of $^{18}\text{O}/^{16}\text{O}$ and $^{13}\text{C}/^{12}\text{C}$ secular trends in sedimentary carbonate rocks., *Geochimica et Cosmochimica Acta*, v. 40, p. 1387-1395
- Villeneuve, D., 1987, The Calumet project. In *Livret-guide de l'excursion sur les gîtes métallifères dans le sud du Grenville québécois.*, 25-26-27 may 1987. Edited by A. Valières et M. Gauthier. Ministère de l'Énergie et des Ressources du Québec: 35-41
- Vokes, F.M., 2000, Ores and Metamorphism: Introduction and Historical Perspective., In, *Metamorphosed and Metamorphogenic Ore Deposits*, Edited by Spry, P.G., Marshall, B., and Vokes, F.M., *Reviews in Economic Geology*, v. 11, p.1-18.
- Volkert, R.A., 2001, Geologic setting of Proterozoic iron, zinc, and graphite deposits, New Jersey Highlands., *Society of Economic Geologists Guidebook Series*, v. 35, p. 59-73
- Volkert, R.A., 2004, Meseoproterozoic rocks of the New Jersey Highlands, north-central Appalachians: Petrogenesis and tectonic history., *Geological Society of America, Memoir 197*, p. 697-728
- Volkert, R.A., and Drake, A.A., Jr., 1999, Geochemistry and stratigraphic relations of Middle Proterozoic rocks of the New Jersey Highlands., *U.S. Geological Survey*, 1565-C, 77 p.
- Whelan, J.F., Rye, R.O., and deLorraine, W.F., 1984, The Balmat-Edwards Zinc-Lead Deposits - Synsedimentary Ore from Mississippi Valley-Type Fluids., *Economic Geology*, v. 79, p. 239-265
- Whelan, J.F., Rye, R.O., deLorraine, W.F. And Ohmoto, H., 1990, Isotopic geochemistry of a mid-Proterozoic evaporite basin: Balmat, New York., *American Journal of Science*, v. 290, p. 396-424
- Winter, J.D., 2001, *An introduction to igneous and metamorphic petrology.*, Prentice Hall, 699 p.
- Wolff, J.E., 1903, Zinc and manganese deposits of Franklin Furnace, N.J., *U.S.G.S. Bulletin*, v. 213, p. 214-217
- Wynne-Edwards, H.R., 1972, The Grenville Province; in *Variations in Tectonic Styles in Canada.*, Editors R.A. Price and R.J.W. Douglas., *Geological Association of Canada, Special Paper 11*, p. 263-334